DELHI COLLEGE OF ENGINEERING

LIBRARY
Kashmiri Gate, Delhi-110006

Accession No. 18654

Class No. 620.1

Book No. CRE

Borrower is requisted to check the book and get the signatures on the torned pages, if any.

DELHI COLLEGE OF ENGINEERING
Kashmiri Gate, Delhi-110006
LIBRARY

DATE DUE

For each day's delay after the due date a fine of 10 Paise per Vol. shall be charged for the first week, and 50 Paise per Vol. per day for subsequent days.

Borrower's No.	Date Due	Borrower's No.	Date Due

VIBRATION and SHOCK ISOLATION

Charles E. Crede
CHIEF ENGINEER
THE BARRY CORPORATION

JOHN WILEY & SONS, INC., NEW YORK
CHAPMAN & HALL, LIMITED, LONDON

Copyright, 1951
by
John Wiley & Sons, Inc.

All Rights Reserved

This book or any part thereof must not
be reproduced in any form without
the written permission of the publisher.

Printed in the United States of America

To my wife
EDNA
whose assistance and encouragement
contributed greatly to the
writing of this book

Preface

This book has been written primarily to provide the practicing engineer with a rigorous, yet practical, reference on the design and application of resilient mountings. It includes little that I claim to be original. On the contrary, I have attempted to produce a convenient and comprehensive reference book from the information available in the technical literature and in commercial brochures, supplemented by experience gained from engineering practice.

In popular language, resilient mountings are often designated as "shock mounts." This is a misnomer in many instances. A more descriptive term is "isolators," a generic designation which can be prefixed by vibration, shock, or sound, where necessary to define characteristics that are associated with particular applications of isolators. The function performed by all isolators is isolation. This book is concerned with the basic mechanics of isolation and includes practical discussions on the design and application of isolators. Although the book has been written primarily for the practicing engineer, the analytical treatment of certain problems may be of value to students having special interests.

The book includes six chapters. Chapter 1 is introductory, devoted to a discussion of several mathematical and physical concepts used in succeeding chapters. Chapters 2 and 3 are comprised primarily of basic discussions of fundamental principles of vibration and shock isolation. Chapter 4, supplementary to the two preceding chapters, includes a discussion of non-linear and damped systems, practical aspects of damper design, and sound isolation. Chapter 5 is devoted to the properties of materials used in isolators, and to the design of isolators that employ these materials. Finally, Chapter 6 discusses many specific applications of isolators, both industrial and military. This last chapter is largely descriptive and points out the significance and application of much of the basic theory developed in preceding chapters.

I have made every effort to assure that the information included in this book is authoritative. Practically all portions of the manuscript have been reviewed by persons eminently qualified by experience to criticize the presentation. Their suggestions and constructive criticisms were an important factor in shaping the manuscript into its final form, and their encouragement has given me confidence in pursuing this work to a conclusion.

CHARLES E. CREDE

Watertown, Mass.
May, 1951

Acknowledgments

I extend my sincere thanks to the many individuals and organizations who have helped with the writing of this volume. My associates at The Barry Corporation, Mr. Ervin Pietz, Mr. Frank Lambert, Jr., and Mr. M. C. Junger, in making many constructive suggestions for its improvement, in reviewing sections pertinent to their interests, and in checking many mathematical details, have rendered invaluable assistance.

In addition, many chapters and sections were reviewed constructively by the following persons, to whom I am truly indebted for thoughtful advice and suggestions: Mr. C. D. Pengelley, Southwest Research Institute; Mr. F. E. Reed, Arthur D. Little, Inc.; Mr. V. F. Sepavich and Mr. R. A. Huey, Crompton and Knowles Loom Works; Mr. W. H. Lehmberg, American Felt Company; Mr. J. H. Widmyer, Armstrong Cork Company; Mr. J. H. Best, Bendix Aviation Corporation; Mr. J. S. Parkinson, Johns-Manville Corporation; Dr. C. T. Morrow, Sperry Gyroscope Company; Dr. P. H. Geiger, University of Michigan; Mr. F. Mintz, Armour Research Foundation; Mr. K. W. Johnson and Mr. H. A. Magrath, Air Materiel Command, U.S.A.F.; Mr. J. P. Walsh, Naval Research Laboratory; Mr. F. K. Priebe and Mr. N. E. Lee, Signal Corps Engineering Laboratories; Mr. C. D. Montgomery, Aberdeen Proving Ground; the technical staffs of United States Rubber Company and The Felters Company; and many others too numerous to list.

Several organizations and individuals have provided me with detailed information, drawings, and data. The United States Rubber Company granted permission to reproduce certain copyrighted material; Dr. R. D. Mindlin, Columbia University and Bell Telephone Laboratories, loaned original drawings and furnished certain tabular data from his files; and the Armstrong Cork Company made available hitherto unpublished technical information.

I am particularly grateful for the help given by Mr. W. P. Welch, Westinghouse Electric Corporation, and Mr. S. E. Young, The Barry Corporation. Mr. Welch's painstaking and constructive review of a portion of the manuscript was of inestimable value; Mr. Young read the entire manuscript carefully and critically and made many con-

structive suggestions. Finally, I sincerely appreciate the friendly and helpful assistance of the publisher, John Wiley and Sons, Inc., in many matters relating to the writing and publication of this book.

Contents

1. Introduction

1·1 Nature of Isolation 1

1·2 Vector Representation of Sinusoids 5

1·3 Characteristics of Harmonic Motion 12

1·4 Moment of Inertia and Principal Axes of Inertia 12

1·5 Properties of Rigid Bodies Determined Experimentally 16

1·6 Elastic Properties of Isolators 23

1·7 Dynamics of Rigid Bodies 28

2. Isolation of Vibration

2·1 Single-Degree-of-Freedom System Excited by Force 32

2·2 Single-Degree-of-Freedom System Excited by Motion 37

2·3 Modes of Vibration 41

2·4 Multi-Degree-of-Freedom System Excited by Force—Two Planes of Symmetry 43

2·5 Multi-Degree-of-Freedom System Excited by Motion—Two Planes of Symmetry 50

2·6 Natural Frequencies—Two Planes of Symmetry 53

2·7 Problems in Isolator Application 58

2·8 Natural Frequencies—One Plane of Symmetry 68

2·9 Inclined Isolators 73

2·10 Decoupling of Modes 83

3. Isolation of Shock

A. Isolation of Shock Motions of Large Displacement

3·1 Velocity Shock 89

3·2 Isolation of Velocity Shock—Inelastic Impact 94

3·3 Effectiveness of Isolators—Inelastic Impact 98

3·4 Magnitude of Shock Transmitted by Isolators—Inelastic Impact 101

3·5 Isolation of Velocity Shock—Elastic Impact 106

3·6 Effect of Snubbing 112

3·7 Preloaded Isolators 115

B. Isolation of Shock Forces That Cause Displacements of Large Magnitude

3·8 Shock Severity with Rigidly Supported Machines 122

3·9 Isolation of Shock 128
3·10 Effectiveness of Isolators 132

C. Isolation of Shock Forces That Cause Displacements of Small Magnitude

3·11 Machines of Conservative Momentum 135
3·12 Isolation of Shock 142
3·13 Positioning Means 143

D. Isolation of Shock Motions of Small Displacement

3·14 Shock Severity 145
3·15 Isolation of Shock 148

4. Further Considerations in Vibration and Shock Isolation

4·1 Vibration Characteristics of System with Non-Linear Isolators 151
4·2 Natural Frequency of System with Non-Linear Isolators 154
4·3 Shock Isolation with Non-Linear Isolators—Analytical Treatment 158
4·4 Shock Isolation with Non-Linear Isolators—Numerical Treatment 162
4·5 Free Vibration with Viscous Damping 170
4·6 Forced Vibration with Viscous Damping 176
4·7 Velocity Shock with Viscous Damping 186
4·8 Damper Design 190
4·9 Damping from Internal Hysteresis 193
4·10 Applications Involving Superimposed Loads and Non-Uniform Weight Distribution 195
4·11 Lack of Stiffness in Equipment 201
4·12 Sound Isolation 203

5. Properties of Materials and Design of Isolators

A. Natural and Synthetic Rubbers

5·1 General Properties 216
5·2 Methods of Use 219
5·3 Rubber Stiffness 220
5·4 Compression Pad 222
5·5 Shear Sandwich 227
5·6 Bushing 229
5·7 Application of Stiffness Data 232
5·8 Maximum Loads 234
5·9 Minimum Natural Frequencies 235
5·10 Damping 238
5·11 Effect of Temperature 240
5·12 Practical Design Considerations 241

B. Metal Springs

5·13 General Properties 242
5·14 Stiffness of Helical Compression Springs 243
5·15 Stability of Helical Compression Springs 247
5·16 Stiffness of Helical Tension Springs 249
5·17 Constant Frequency Springs 251

C. Other Materials

5·18 Felt 252
5·19 Cork 255
5·20 Sponge Rubber 259

6. Particular Applications of Isolators

6·1 Low-Speed Machinery 262
6·2 Kinematics of Reciprocating Machines 267
6·3 Application of Isolators to Reciprocating Machines 273
6·4 Punch Presses 277
6·5 Looms 284
6·6 Electric Motors 289
6·7 Miscellaneous Industrial Equipment 291
6·8 Train and Road-Vehicle Installations 299
6·9 Military Equipment—General 302
6·10 Military Equipment—Aircraft 304
6·11 Military Equipment—Vehicles 310
6·12 Military Equipment—Naval Vessels 314
6·13 Military Equipment—Portable 320

Index 325

Notation

The principal symbols used throughout this book are listed below. Important subscripts are included where usage is general. Subscripts employed for special purposes, and special interpretations which apply to general symbols, are not listed here but are appropriately explained in the text or on the figures.

A, B = undetermined coefficients.
a, b, c, d = distance to isolator from coordinate axis, in.
$a,'$ b' = distance to any point from coordinate axis, in.
c = coefficient of viscous damping, lb sec/in.
c_c = coefficient of viscous damping for a critically damped system, lb sec/in.
D, d = diameter, in.
E = Young's modulus, psi.
e = base of Naperian logarithms.
F = force, lb.
f = forcing frequency, cps.
f_n = natural frequency, cps.
G = modulus of elasticity in shear, psi.
g = acceleration due to gravity, in./sec.^{2}
H_E = dimensionless amplification factor for linear isolator, elastic impact.
H_I = dimensionless amplification factor for linear isolator, inelastic impact.
H_p = dimensionless amplification factor for preloaded isolator, elastic impact.
h_f = height of free fall, in.
h_t = thickness of isolator, in.
I = moment of inertia, lb sec^2/in.
j = $\sqrt{-1}$.
k = linear stiffness, lb/in. (The subscripts x, y, z are used extensively with the symbol k. In a single-mass system, the axis for which the stiffness applies is indicated by the subscript. In the type of two-mass system considered here, freedom of motion is restricted to a single direction, and the subscript refers to the designation of the particular mass with which the elastic member is associated.)
k_α = torsional stiffness, in. lb/rad.
L, l = lengths, in.

M = moment or couple, in. lb.
m = total mass of rigid body, lb sec^2/in.
n = a number.
P = sound energy.
p, q = principal elastic axes.
Q = impulse, lb sec.
q = damped natural frequency, rad/sec.
R = specific acoustical impedance, gm/cm^2 sec.
r = radius, in.
S = cross-sectional area, in.^{2}
s = displacement of support in direction of Y axis, in.
T = transmissibility, dimensionless.
t = time, sec.
u = displacement of support in direction of X axis, in.
V = velocity of a rigid body, in./sec.
v = velocity of sound, cm/sec.
W = total weight of a rigid body, lb.
X, Y, Z = coordinate axes.
x, y, z = in a single-mass system, displacement of rigid body in direction of X, Y, Z axes, respectively, in. In a two-mass system, y is the displacement of mass m_y and z is the displacement of mass m_z, in the direction of the Y axis.
α, β = angular displacement of a rigid body, rad.
γ = dimensionless ratio of forces on non-linear isolator.
Δ = logarithmic decrement. Also small incremental quantity.
δ = deflection of isolator or elastic member, in. (A single subscript indicates displacement of a body relative to a fixed support. A double subscript indicates relative displacement of two bodies.)
δ_c = clearance to snubber, in.
δ_{st} = static deflection, in.
ϵ = distance from coordinate axis to unbalanced mass, or to point of application of force, in.
ζ = dimensionless ratio of maximum accelerations transmitted by non-linear and linear isolators.
η = k_x/k_y = dimensionless stiffness ratio (also k/k_y in Section 2·6).
θ = an angle, particularly the angle of inclination of principal elastic axes of an isolator, rad.
Λ = acceleration of a rigid body, in./sec.^{2}

λ = dimensionless ratio of height to width of a rigid body. Also wavelength of vibration, cm, and dimensionless ratio of uncoupled natural frequencies.

μ = mass per unit length, lb $\text{sec}^2/\text{in.}^2$, or mass per unit volume, lb $\text{sec}^2/\text{in.}^4$

ξ = dimensionless ratio of deflection to thickness of isolator.

ρ = radius of gyration, in.

σ = dimensionless ratio of vertical to horizontal force components acting on mounted body.

τ = period of vibration, sec.

ϕ = an angle, particularly the angle of a crank, rad.

ψ = phase angle, rad.

Ω = natural frequency, rad/sec.

ω = forcing frequency, rad/sec.

The subscript 0 is used to designate the maximum value of a variable. One dot over a variable indicates differentiation with respect to time; two dots indicate double differentiation with respect to time.

CHAPTER ONE

Introduction

1·1 Nature of Isolation

This treatise deals with the mechanics of vibration and shock isolation, and with the design of vibration and shock isolators. The meaning of these terms as used here is defined in the following paragraphs.

Vibration is a continuing condition in which an oscillatory force or motion exists at a constant frequency, or combination of frequencies. This condition is designated steady-state, because the identical pattern of vibration amplitude is repeated during each cycle. It is also referred to as forced vibration, inasmuch as energy is supplied in sufficient quantity to compensate for any lost as a result of damping in the system. Forced or steady-state vibration at a single frequency is illustrated in Figure 1.1(*a*).

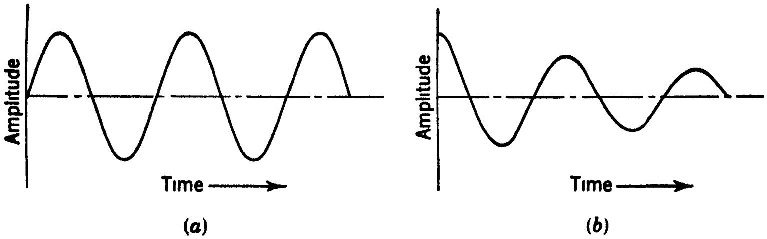

FIGURE 1.1. Typical steady-state and damped transient vibrations at a single frequency.

Shock, as contrasted to vibration, is a transient condition. The equilibrium of a system is disrupted by a suddenly applied force or increment of force, or by a sudden change in the direction or magnitude of a velocity vector. This disruption, and the ensuing reaction of the system in restoring equilibrium, constitute a condition of shock. A typical example is the sudden displacement and ensuing damped vibration illustrated in Figure 1.1(*b*).

Isolation of vibration or shock signifies the temporary storage of energy, and its subsequent release substantially in its entirety but in a different time relation. Isolation is thus distinct from the absorption or dissipation of energy. The effectiveness of an isolator is sometimes enhanced by limited dissipation of energy, but this is a secondary consideration in its function.

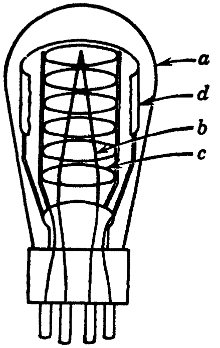

FIGURE 1.2.

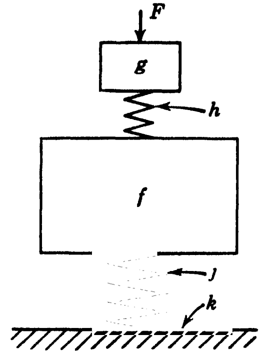

FIGURE 1.3.

FIGURE 1.2. Schematic illustration of a typical vacuum tube. This illustration shows the elements, whose relative displacement as a result of vibration or shock would interfere with proper functioning of the tube. (From *The Radio Amateur's Handbook*, 1950 edition, by permission.)

FIGURE 1.3. Idealized representation of vacuum tube supported by isolator. This system may also represent engine and engine support, with isolator interposed therebetween, as shown in Figure 1.4.

There are two aspects to the principle of isolation: (1) isolation of a motion and (2) isolation of a force. Isolation of a motion applies to the reduction of the stresses and deflections of members whose support experiences motion resulting from shock or vibration. This may be illustrated by reference to the typical vacuum tube shown schematically in Figure 1.2. A vacuum tube is usually a glass or metal envelope *a* containing a filament *b*, grid *c*, and plate *d* accurately positioned relative one to another. The tube is considered to be attached to a support which experiences shock or vibration; if there is a resultant change in the relative positions of the elements *b*, *c*, *d*, deterioration in the operation of the vacuum tube occurs. An isolator may be employed to reduce the relative motion of these elements.

The mechanics of isolating the vacuum tube from the motion of its support is analyzed by creating the hypothetical system shown in Figure 1.3. The large mass *f* represents the base and envelope of the vacuum tube. A system comprised of the smaller mass *g* and spring *h*, taken together, is made to represent any one of the vacuum-tube elements *b*, *c*, *d* by setting its natural frequency equal to the natural frequency of the element being represented. The isolator, represented by the spring *j*, is inserted between the mass *f* and support *k* and is designed so that it brings about a reduction in the motion of the mass *g* relative to the mass *f*. This indicates that the elements *b*, *c*, *d* of the vacuum tube have less motion relative to the envelope *a*, and therefore generally less motion relative to one another. The operation of the vacuum tube is thus correspondingly improved. The necessary characteristics of the isolator *j*, for various types of equipment to be protected and for various disturbing motions, are discussed in detail in ensuing chapters.

The second aspect of isolation involves the forces created by the operation of machinery. In the internal combustion engine illustrated in Figure 1.4, for example, forces are generated by the firing of the explosive mixture. Additional forces result from the inertia of unbalanced rotating and reciprocating members. All these forces are transmitted to the support for the engine. The support thus experiences a motion that depends on the nature of the forces and on the characteristics of the support. In some instances, the stress in the support may become so great as to endanger its integrity; in other instances, the motion of the support constitutes an annoyance to personnel or disrupts the operation of other equipment that shares the support. The forces created by operation of the engine are isolated from the support by mounting the engine upon properly designed isolators.

The nature of the problem is illustrated in an idealized form by the system shown in Figure 1.3. The engine is simulated by the mass *g*. The support for the engine, often in the form of a beam-like structure, is simulated by the system comprised of the mass *f* and the spring *j*. A force originates within the engine, due to gas pressure and inertia force, and acts on the mass *g*. If the engine is secured directly to the support, both engine and support experience a common deflection in response to this force. By inserting a properly designed isolator *h* between the engine and its support, the motion of the mass *f* may be reduced. This has the beneficial result of decreasing the stress in the spring *j*, and of reducing the disturbance experienced by personnel and equipment supported by the mass *f*. Subsequent chapters discuss in detail the nature of the force associated with different types of machines, and the necessary characteristics of the isolator j for bringing about a reduction in motion of the mass f.

The motion experienced by the support or the force created by operation of the machine may embody the characteristics of either vibration or shock, as described above. The analytical treatment for the condition of steady-state vibration is fundamentally different from that for the condition of shock. Vibration is considered to be a continuing condition which repeats itself periodically. All parts of the system are assumed to partake of motion at the frequency of the actuating force or motion. Vibration at any other frequency is assumed to be non-existent, for the reason that no energy is being supplied to the system at such other frequency, and the natural dissipation of energy within a structure will eventually cause the random or transient vibration to die out. A relation exists which defines the rela-

FIGURE 1.4. Typical application of isolators to reduce transmission of vibratory force from an automobile-type internal combustion engine The isolators and associated brackets are shown darker (Buick Motor Division, General Motors Corporation.)

tive values of the various forces and motions, and this relation applies at each cycle of vibration after the transient has been eliminated.

In a system subjected to shock, the internal equilibrium of the system is disrupted by a suddenly applied force or increment of force, or by a sudden change in the direction or magnitude of a velocity vector. This differs from vibration in that energy is impulsively supplied to the system in a non-repetitive manner, in contrast to the periodically supplied energy of forced vibration. The most severe conditions thus occur almost immediately, before the transient vibration has been eliminated by internal damping. A transient vibration inherently occurs at a natural frequency of the system, but the system also responds at a frequency that is forced by the addition of energy during application of the shock. The analysis of a system subjected to shock requires that this combination of transient and forced components be evaluated.

The mechanics of isolation is treated in detail in subsequent chapters, taking into consideration various types of equipment and different service conditions. The remainder of this chapter is devoted to a discussion of several somewhat unrelated topics of a mathematical and mechanical nature. These topics are presented in such a manner that their relation to the subject matter of subsequent chapters is emphasized.

1·2 Vector Representation of Sinusoids

The predominance of harmonic functions in the analysis of vibration and shock makes it desirable to discuss in detail the properties of sine functions, both singly and in combination. A sine function may be indicated by a rotating vector, as shown in Figure 1.5. The coordinate axes X, Y define a plane which includes the circle whose center coincides with the intersection of the axes. Let the point P move on the circle in the direction indicated by the arrow. A vector, which is defined as a quantity having both magnitude and direction, is drawn from the center of coordinates to the point P. The length of the vector is taken as $OP = A$, and its angular velocity as ω. The angular velocity ω is commonly expressed in radians per second, where a radian is the angle that intercepts a length of peripheral arc equal to the radius. Rotation is counterclockwise, and angles are considered positive if measured in a counterclockwise direction from the positive end of the X axis.

The physical meaning of the rotating vector becomes apparent by referring to Figure 1.6. The heights of the curves at the right of Figure 1.6 are the projections upon the Y axis of the rotating vectors at the left, and the distance along the horizontal axis corresponds to the peripheral distance on the vector circle. A particle whose path is defined by the projection of a rotating vector is said to describe harmonic motion. Such motion is defined analytically by sine and cosine functions.

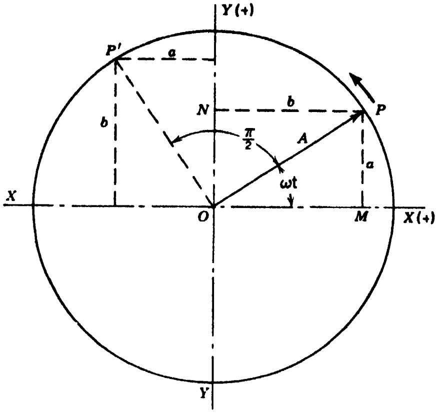

FIGURE 1.5. Vector representation of a sine function.

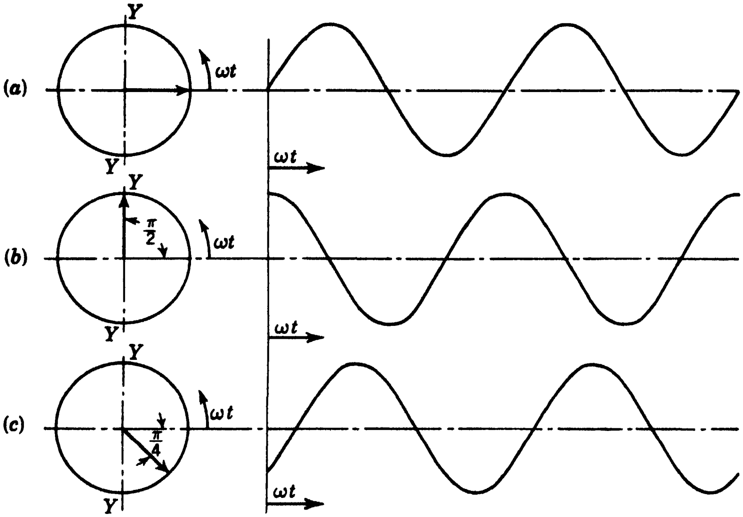

FIGURE 1.6. Displacement-time diagrams of sine functions having different phase relations.

There are 2π radians for each revolution of the vector OP, and the number of complete revolutions or cycles per second f is thus given by

$$f = \frac{\omega}{2\pi}, \tag{1.1}$$

The period τ, or time in seconds required for a complete revolution of the vector OP, is the reciprocal of the rotational frequency:

$$\tau = \frac{1}{f} = \frac{2\pi}{\omega}. \tag{1.2}$$

The length A of the vector OP in Figure 1.5 is commonly termed the amplitude of the harmonic motion. This is a source of some confusion, inasmuch as the total observable motion of a vibrating body is $2A$. The difficulty is sometimes resolved by referring to $2A$ as total travel, peak-to-peak amplitude, or double amplitude; and referring to A as half total travel, or single amplitude.

A phase shift of a particle describing harmonic motion constitutes a displacement along the time axis. In Figure 1.6(*b*), for example, the equation of the displacement-time curve is

$$y = A \sin\left(\omega t + \frac{\pi}{2}\right), \tag{1.3}$$

whereas in Figure 1.6(*c*), the corresponding equation is

$$y = A \sin\left(\omega t - \frac{\pi}{4}\right). \tag{1.4}$$

Phase shift is of little significance where only one rotating vector is involved, because the phase angle can be eliminated by appropriate selection of the zero time reference. Where two or more vectors are rotating at the same frequency, the phase angle is important in determining the relation between the vectors.

The simplest example of the addition of two sine functions occurs when the two functions are of equal frequency with a phase difference of 90°, or $\pi/2$ radians. Such a pair of functions can be expressed by

$$\begin{aligned} y_1 &= b \sin \omega t, \\ y_2 &= a \sin\left(\omega t + \frac{\pi}{2}\right). \end{aligned} \tag{1.5}$$

The following relations are evident from the geometry of Figure 1.5:

$$\begin{aligned} \sin \omega t &= \frac{ON}{OP} = \frac{a}{\sqrt{a^2 + b^2}}, \\ \cos \omega t &= \frac{OM}{OP} = \frac{b}{\sqrt{a^2 + b^2}}, \end{aligned} \tag{1.6}$$

where a and b are the projections of A upon the Y and X axes, respectively. If the vector OP is rotated 90°, or $\pi/2$ radians, to the position OP', the following relations apply:

$$\begin{aligned} \sin\left(\omega t + \frac{\pi}{2}\right) &= \frac{b}{\sqrt{a^2 + b^2}} = \cos \omega t, \\ \cos\left(\omega t + \frac{\pi}{2}\right) &= \frac{-a}{\sqrt{a^2 + b^2}} = -\sin \omega t. \end{aligned} \tag{1.7}$$

Another important trigonometric relation, whose derivation will not be given here, but which can be found in any standard reference is*

$$\sin(\phi_1 + \phi_2) = \sin \phi_1 \cos \phi_2 + \cos \phi_1 \sin \phi_2. \tag{1.8}$$

The sum of the trigonometric functions given by equation 1.5 is written $y = y_1 + y_2$. Substituting for $\sin(\omega t + \pi/2)$ from equation 1.7 and dividing both sides of the resulting equation by $\sqrt{a^2 + b^2}$:

$$\frac{y}{\sqrt{a^2 + b^2}} = \frac{a}{\sqrt{a^2 + b^2}} \cos \omega t + \frac{b}{\sqrt{a^2 + b^2}} \sin \omega t. \tag{1.9}$$

From equation 1.6 it is evident that an angle ψ can always be found such that

$$\sin \psi = \frac{a}{\sqrt{a^2 + b^2}}; \quad \cos \psi = \frac{b}{\sqrt{a^2 + b^2}}. \tag{1.10}$$

Substituting from equation 1.10 in equation 1.9:

$$y = \sqrt{a^2 + b^2}\,(\sin \psi \cos \omega t + \cos \psi \sin \omega t). \tag{1.11}$$

This is expressed as a single sine function by employing the relation of equation 1.8:

$$y = \sqrt{a^2 + b^2} \sin(\omega t + \psi), \tag{1.12}$$

where the phase angle ψ is determined from equation 1.10 as follows:

$$\tan \psi = \frac{\sin \psi}{\cos \psi} = \frac{a}{b}. \tag{1.13}$$

Thus the wave form resulting from the addition of sine and cosine functions of equal frequency is sinusoidal and has the same frequency as the component functions. The physical significance of equation 1.12 may perhaps be envisioned more readily from the vector representation shown in Figure 1.7. The vector sum of y_1 and y_2 is obtained by completing the vector diagram to obtain the resultant of magnitude $\sqrt{a^2 + b^2}$. The phase angle ψ is readily determined from the lengths of the vectors a and b.

---

* See, for example, B. O. Pierce, *A Short Table of Integrals*, Ginn and Company, Boston, 1929, page 75.

The more general case of two sine functions of the same frequency with any phase angle is readily solved by the same vector method.

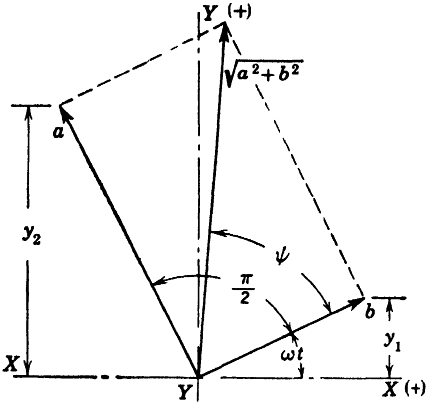

FIGURE 1.7.

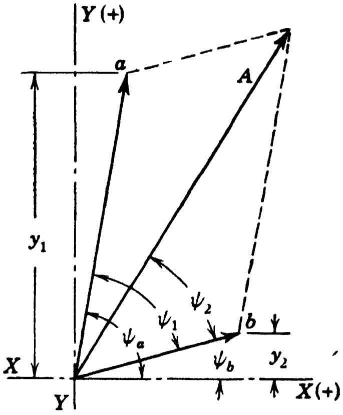

FIGURE 1.8.

FIGURE 1.7. Vector addition of sine and cosine functions of the same frequency but of different amplitudes. This diagram also represents vector addition of two sine functions having a phase difference of $\pi/2$ radians.

FIGURE 1.8. Vector addition of two sine functions of same frequency and different amplitudes, and of any phase difference.

The two functions are represented by

$$\begin{aligned} y_1 &= a \sin (\omega t + \psi_a), \\ y_2 &= b \sin (\omega t + \psi_b), \end{aligned} \tag{1.14}$$

and the applicable vector diagram is shown in Figure 1.8 for the time $t = 0$. The magnitude of the resultant A is found by completing the vector diagram. It is expressed analytically by the cosine rule for an oblique triangle:

$$A = \sqrt{a^2 + b^2 + 2ab \cos (\psi_a - \psi_b)}. \tag{1.15}$$

An expression for the phase angle ψ_2 between the resultant A and the vector b is obtained by first writing an expression for the tangent of $(\psi_2 + \psi_b)$:

$$\tan (\psi_2 + \psi_b) = \frac{b \sin \psi_b + a \sin \psi_a}{b \cos \psi_b + a \cos \psi_a}. \tag{1.16}$$

When $\psi_b = 0$, $\psi_a = \psi_1$. Then

$$\tan \psi_2 = \frac{a \sin \psi_1}{b + a \cos \psi_1}. \tag{1.17}$$

The vector method of representing sine or cosine functions is extended to the complex plane by introducing real and imaginary axes. The horizontal axis is commonly taken as the real axis, and the vertical axis as the imaginary axis. The projection of the rotating vector upon the real axis represents the tangible physical aspect of a vibratory phenomenon, as illustrated by Figure 1.9. The projections on the real and imaginary axes are:

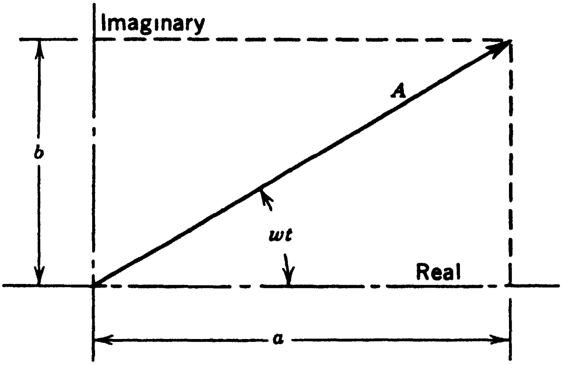

FIGURE 1.9. Vector representation of a cosine function in the complex plane.

$$\begin{aligned} a &= A \cos \omega t, \\ b &= A \sin \omega t. \end{aligned} \tag{1.18}$$

The complex notation for the vector A in Figure 1.9 is

$$\mathbf{A} = a + jb. \tag{1.19}$$

Substituting from equations 1.18, equation 1.19 is written

$$\mathbf{A} = A(\cos \omega t + j \sin \omega t), \tag{1.20}$$

where $A = \sqrt{a^2 + b^2}$ and $\tan \omega t = b/a$.

The advantage of the complex plane in carrying out analyses of vibrating systems is that the real and imaginary parts of the solution may be maintained separate throughout the analysis, and subsequently combined in the final expression to obtain numerical results. Equation 1.20 is conveniently written in exponential rather than trigonometric terms by applying Euler's formula as follows:*

$$e^{j\phi} = \cos\phi + j\sin\phi. \tag{1.21}$$

The angle ϕ in equation 1.21 can be a time function ωt having a phase angle ψ to establish its relation to the time reference. Euler's formula then takes the following form:

$$Ae^{j(\omega t+\psi)} = A[\cos(\omega t+\psi) + j\sin(\omega t+\psi)]. \tag{1.22}$$

The left side of the above equation may be written as the product of two exponentials:

$$Ae^{j(\omega t+\psi)} = (Ae^{j\psi})e^{j\omega t}. \tag{1.23}$$

The first factor $Ae^{j\psi}$ in equation 1.23 indicates the length of the vector and is usually represented by $\mathbf{A}$. The second factor $e^{j\omega t}$ defines the rotation of the vector as a linear function of time. Equation 1.23 and the first and second derivatives thereof with respect to time now become:

$$\begin{aligned} Ae^{j(\omega t+\psi)} &= \mathbf{A}e^{j\omega t}, \\ \frac{d}{dt}(\mathbf{A}e^{j\omega t}) &= j\omega(\mathbf{A}e^{j\omega t}), \\ \frac{d^2}{dt^2}(\mathbf{A}e^{j\omega t}) &= -\omega^2(\mathbf{A}e^{j\omega t}). \end{aligned} \tag{1.24}$$

It is thus evident that single differentiation is equivalent to multiplication by $j\omega$, and double differentiation is equivalent to multiplication by $-\omega^2$.

Complex notation is conveniently applied to the solution of vibration problems by taking sinusoidal functions of force and displacement to be the real components of the complex expression given by equation 1.22. A force defined by $F = F_0\cos\omega t$ may therefore be written:

$$F_0\cos\omega t = F_0e^{j\omega t}, \tag{1.25}$$

and a displacement y having a phase angle ψ with the force F may be written

$$y_0\cos(\omega t+\psi) = y_0e^{j(\omega t+\psi)}. \tag{1.26}$$

The above expressions are very useful in analyzing the performance of viscously damped systems, and are applied in Chapter 4.

---

* See W. C. Johnson, *Mathematical and Physical Principles of Engineering Analysis*, McGraw-Hill Book Co., New York, 1944, page 102.

1·3 Characteristics of Harmonic Motion

A body that experiences simple harmonic motion, as described in the preceding section, follows a displacement pattern defined by the following equation:

$$y = y_0 \sin \omega t. \tag{1.27}$$

The velocity and the displacement of the body are found from first and second differentiation, respectively, of equation 1.27:

$$\dot{y} = y_0 \omega \cos \omega t, \qquad (1.28)^*$$

$$\ddot{y} = -y_0 \omega^2 \sin \omega t. \qquad (1.29)^*$$

The maximum absolute values of the displacement, velocity, and acceleration of a body undergoing harmonic motion occur when the trigonometric factors in equations 1.27, 1.28, and 1.29 are numerically equal to unity. These maxima are given by the following relations:

$$y_0 = y_0; \quad \dot{y}_0 = y_0 \omega; \quad \ddot{y}_0 = y_0 \omega^2. \tag{1.30}$$

Equations 1.30 are more conveniently written with the frequency expressed in units of cycles per second. Substituting $\omega = 2\pi f$, equations 1.30 become

$$y_0 = y_0; \quad \dot{y}_0 = 2\pi y_0 f; \quad \ddot{y}_0 = 4\pi^2 y_0 f^2. \tag{1.31}$$

Equations 1.31 are shown graphically in Figure 1.10 for ready reference. The acceleration is expressed as a multiple of the acceleration due to gravity by dividing the expression for $\ddot{y}_0$ by g.

1·4 Moment of Inertia and Principal Axes of Inertia

The mass and moment of inertia of a rigid body are of particular significance to the subject matter discussed in this book. If the masses and the moments of inertia of two bodies are equivalent, they behave in an equivalent manner dynamically. The center of gravity of a body constitutes a convenient center of coordinates and is used in that manner throughout this book unless otherwise noted.

The moment of inertia of a particle about any axis is defined as $\Delta I = (\Delta m)r^2$, where Δm is the mass of the particle and r is its distance from the axis, measured along a line perpendicular to the axis. The moment of inertia of a rigid body comprised of a number of discrete particles is the summation of the moments of inertia of the separate

---

* The short notation $\dot{y}$ and $\ddot{y}$ is used for the first and second derivatives, respectively, of y with respect to time; i.e., $\dot{y} = dy/dt$ and $\ddot{y} = d^2y/dt^2$. These symbols are used generally throughout this book.

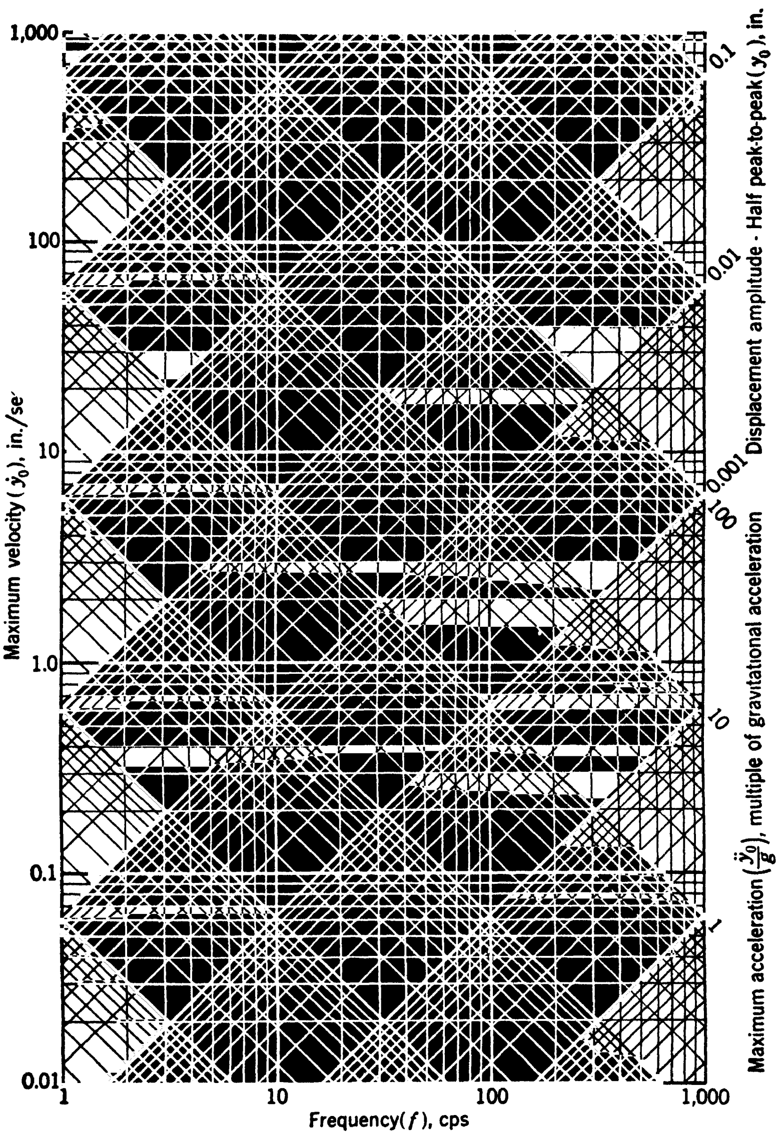

FIGURE 1.10. Diagram showing the relation between frequency and maximum values of displacement, velocity, and acceleration in harmonic motion. (Courtesy General Electric Company.)

particles. Thus,

$$I = \sum_{i=1}^{i=n} (\Delta m)_i r_i^2 \tag{1.32}$$

is the moment of inertia of a rigid body consisting of n particles of masses Δm_1, Δm_2, $\cdots$ Δm_n, situated at distances r_1, r_2, $\cdots$ r_n from the axis about which the moment of inertia is taken. It is thus evident that the moment of inertia of a body with respect to a given axis is the sum of the moments of inertia of its parts with respect to the *same* axis.

It is convenient to define a length ρ, designated the radius of gyration of the body. If a body of total mass m has a moment of inertia I, the radius of gyration ρ is defined by the equation

$$I = m\rho^2. \tag{1.33}$$

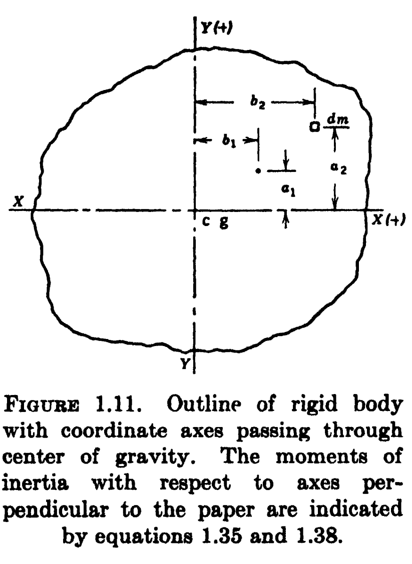

FIGURE 1.11. Outline of rigid body with coordinate axes passing through center of gravity. The moments of inertia with respect to axes perpendicular to the paper are indicated by equations 1.35 and 1.38.

When the body consists of a single particle, it is evident that the radius of gyration of the body about any axis is simply the distance from the particle to the axis.

When the mass of the body is distributed, in contrast to a body comprised of discrete particles, the definition expressed by equation 1.32 becomes

$$I = \int r^2 \, dm, \tag{1.34}$$

where the integral sign indicates the limit of a process in which the body is divided into a great number of infinitesimal elements and the summation taken. Constructing coordinate axes X, Y, Z through the center of gravity of the body, as illustrated in Figure 1.11, the moment of inertia with respect to the Z axis (normal to the plane of the paper) is then found from equation 1.34:

$$I_z = \int (a_2^2 + b_2^2) \, dm. \tag{1.35}$$

The moment of inertia with respect to any parallel axis Z', which intersects the XY plane at the coordinate point a_1, b_1 is

$$I_{z'} = \int [(b_2 - b_1)^2 + (a_2 - a_1)^2] \, dm. \tag{1.36}$$

Equation 1.36 expands to

$$I_{z'} = \int[(a_2^2 + b_2^2) + (a_1^2 + b_1^2) - 2b_1b_2 - 2a_1a_2]\,dm. \quad (1.37)$$

The first term in equation 1.37 is identical to equation 1.35, and the second term is equal to $(a_1^2 + b_1^2)m$. The last two terms are equal to zero because $\int b_2\,dm = \int a_2\,dm = 0$ by definition of the center of gravity. The moment of inertia with respect to the Z' axis is therefore

$$I_{z'} = I_z + m(a_1^2 + b_1^2). \quad (1.38)$$

The moment of inertia of a body with respect to any axis is thus the sum of its moment of inertia with respect to a parallel axis through the center of gravity, and the product of the mass of the body and the square of the distance between axes.

The radius of gyration with respect to any axis Z' may be readily determined with relation to the radius of gyration about a parallel axis through the center of gravity. Designating the distance between Z and Z' by $r = \sqrt{a_1^2 + b_1^2}$, equation 1.38 becomes

$$m\rho_{z'}^2 = m\rho_z^2 + mr^2.$$

Dividing both sides of the equation by m and solving for $\rho_{z'}$:

$$\rho_{z'} = \sqrt{\rho_z^2 + r^2}. \quad (1.39)$$

The orientation of the coordinate axes with respect to the body is arbitrary and may assume any one of an infinite number of positions, always keeping the center of coordinates coincident with the center of gravity. If the moment of inertia about each axis, for every possible orientation of the coordinate system, is laid off to scale from the center of gravity along the respective axes, the locus of points thus determined is an ellipsoid. This is called the momental ellipsoid. Each momental ellipsoid has three mutually perpendicular axes which represent the principal inertia axes of the body, and three principal planes mutually perpendicular to the principal axes. The moment of inertia is a maximum about one of the principal axes, and a minimum about another principal axis. The following criteria determine the location of the principal axes and planes:

(*a*) Any axis about which the ellipsoid may be rotated less than 360° and become identical with its initial configuration in space is a principal axis.

(*b*) Any plane which reflects an identical half of the ellipsoid is a principal plane.

Many types of structures possess such symmetry that the principal axes and planes of inertia, as determined by the above criteria, are parallel with or perpendicular to established geometrical lines of the structures. This condition is illustrated by the following examples:

(*a*) In a solid rectangular cuboid of homogeneous material, the principal axes through the center of gravity are respectively parallel with the edges of the body. This may be readily determined by the fact that rotation of the body through 180° about any one of the principal axes will produce an identical momental ellipsoid.

(*b*) In a solid circular cylinder, one of the principal axes extends through the center of gravity parallel with the length of the cylinder. The other two principal axes are any two axes passing through the center of gravity of the cylinder, perpendicular to the first-mentioned axis. Any rotation of the body about the first axis produces an identical ellipsoid, whereas rotation of 180° about either of the two latter axes will produce the equivalent momental ellipsoid.

(*c*) In a solid elliptical cylinder, one of the principal axes extends through the center of gravity parallel with the length of the cylinder. The other two principal axes extend perpendicular to this first axis, and respectively parallel with the long and the short diameters of the ellipse.

1·5 *Properties of Rigid Bodies Determined Experimentally*

The location of the center of gravity of a rigid body may be determined experimentally by several different methods. A very simple and convenient procedure is to balance the equipment upon a small round or triangular rod. The center of gravity is thus known to lie directly above this rod at some point along its length. The rod is then rotated about a vertical axis so that, in its new position, it will intersect its previous position. The equipment is again balanced upon the rod. It is thus determined that the intersection of these two positions represents the projection of the center of gravity upon the horizontal plane. This method requires careful experimental work when applied to tall bodies because the moment of the center of gravity with respect to the rod tends to make the condition of balance relatively unstable. If the equipment is then turned on one of its sides and the procedure repeated, the elevation of the center of gravity above the base may be determined. Inasmuch as the projection of the center of gravity upon a horizontal plane had been determined previously, its location is now fully defined.

Another convenient method of determining the location of the center of gravity is to weigh the equipment on three scales arbitrarily positioned in any convenient triangular arrangement. By taking static moments with respect to a line through any two scales, the moment of the center of gravity is equated to the moment of the force applied by the third scale. This procedure determines a plane through the center of gravity and parallel to the line through the first two scales. The operation may be repeated by taking moments with respect to a line through a different pair of scales and a second plane through the center of gravity is determined. The intersection of these planes defines a vertical line through the center of gravity. The height of the center of gravity may be found by turning the equipment on its side and repeating the process.

It should be noted that the method described in the above paragraph is conveniently adapted only to the use of three scales. If two scales are used, the problem is susceptible to solution but is impractical because of balancing difficulties. If four scales are used, the problem is complex because the loaded heights of the various scales become factors in the solution. This is indicated by the analysis of a rigid body on four resilient supports in Section 4·10 of Chapter 4. The difficulties that are encountered in such an arrangement may be envisioned by slightly raising the base of one scale. This will modify the load distribution on the respective scales, although there obviously has been no change in the location of the center of gravity of the body being investigated. In contrast, the load carried by the respective scales in the three-scale arrangement cannot be changed by elevating one scale unless the magnitude of the elevation becomes so great that the weight of the body, because of the height of its center of gravity, is shifted toward one or two scales.

The moment of inertia of a body may be obtained either by calculation, using the relation given by equation 1.32, or by experiment using one of the methods described in the following paragraphs. An accurate calculation of moment of inertia becomes quite laborious for complex equipment and may involve errors of considerable magnitude unless good judgment is shown. An experimental determination of moment of inertia usually will be found to be more satisfactory for small and medium-sized equipment. This may be accomplished by supporting the equipment from an overhead structure by means of wires to form either a torsional or a compound pendulum.

The arrangement for performing the experiment by the torsional pendulum method is shown schematically in Figure 1.12. The body is suspended by three long parallel wires so that the axis about which the moment of inertia is to be determined extends in a vertical direction. The moment of inertia of the suspended body is determined by displacing the system torsionally about a vertical axis and measuring the period of the free vibration. For a small angular displacement α,

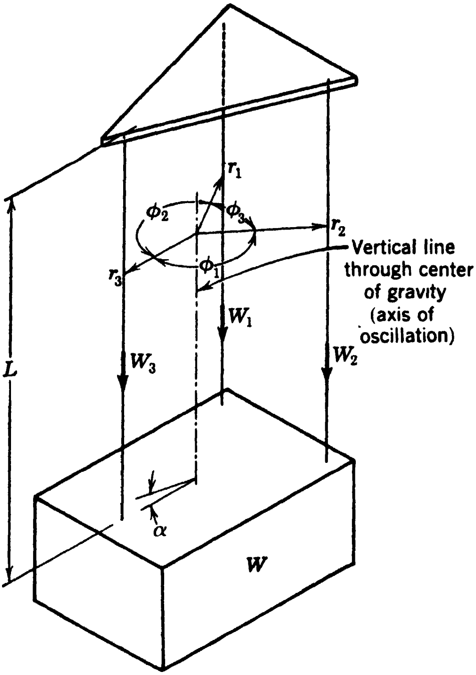

FIGURE 1.12. Torsional pendulum method for determining moment of inertia. The axis, with respect to which the moment of inertia is determined, extends vertically.

the tangential restoring force F_n at the attachment of any wire is

$$F_n = \frac{W_n r_n \alpha}{L}, \tag{1.40}$$

where F_n = tangential restoring force at nth wire, lb.
W_n = portion of weight carried by nth wire, lb.
r_n = distance to nth wire from axis of oscillation, in.
L = length of wire, in.
α = angle of displacement about axis of oscillation, rad.

The torsional stiffness of the entire system is therefore

$$k_\alpha = \sum \frac{F_n r_n}{\alpha} = \sum \frac{W_n r_n}{L}. \tag{1.41}$$

The portion of the weight carried by each of the suspension wires is obtained from the condition of static equilibrium by taking moments successively with respect to lines through two of the wires. The resultant weights are:

$$W_1 = \frac{Wr_2r_3 \sin \phi_1}{r_2r_3 \sin \phi_1 + r_1r_3 \sin \phi_2 + r_1r_2 \sin \phi_3}, \tag{1.42}$$

$$W_2 = \frac{Wr_1r_3 \sin \phi_2}{r_2r_3 \sin \phi_1 + r_1r_3 \sin \phi_2 + r_1r_2 \sin \phi_3}, \tag{1.43}$$

$$W_3 = \frac{Wr_1r_2 \sin \phi_3}{r_2r_3 \sin \phi_1 + r_1r_3 \sin \phi_2 + r_1r_2 \sin \phi_3}. \tag{1.44}$$

The natural period τ of a torsional system is given by

$$\tau = 2\pi\sqrt{\frac{I}{k_\alpha}}; \quad \therefore I = \frac{\tau^2 k_\alpha}{4\pi^2}. \tag{1.45*}$$

Substituting for k_α in equation 1.45 from equation 1.41, and using the expressions for W_1, W_2, and W_3 from equations 1.42, 1.43, and 1.44, the moment of inertia is

$$I = \frac{Wr_1r_2r_3\tau^2}{4\pi^2 L}\left[\frac{r_1 \sin \phi_1 + r_2 \sin \phi_2 + r_3 \sin \phi_3}{r_2r_3 \sin \phi_1 + r_1r_3 \sin \phi_2 + r_1r_2 \sin \phi_3}\right]. \tag{1.46}$$

For small and medium-sized equipment, particularly where values for moment of inertia must be determined repeatedly, it is convenient to construct a light platform supported by three long vertical wires.† The equipment to be evaluated is then set upon the platform. If the wires are equally spaced and the equipment is set in such a manner that its center of gravity is aligned vertically with a point midway between the wires, the various values of r_n and ϕ_n in equation 1.46 become respectively equal. Then:

$$I = \frac{Wr^2\tau^2}{4\pi^2 L}. \tag{1.47}$$

For any particular platform, r and L are constant, and a very simple equation gives a value for I upon substitution of W and τ. The value for W is obtained by adding the platform weight to the equipment weight; the resultant value of I then includes the known I of the platform which must be subtracted to obtain the net I of the equipment.

---

* See F. B. Seely and N. E. Ensign, *Analytical Mechanics for Engineers*, John Wiley and Sons, Inc., New York, 1941, page 347.

† See C. E. Crede, "Determining Moment of Inertia," *Machine Design*, Vol. 20, No. 8, August, 1948, page 138.

The moment of inertia may also be determined by the compound pendulum method, using the arrangement illustrated in Figure 1.13. This method will be found of particular value for large equipment which cannot be conveniently oriented so that its axis of oscillation is vertical. The axis about which the moment of inertia is to be determined is a horizontal axis C-C through the center of gravity and parallel with the axis of oscillation O-O. The expression for the moment of inertia of a compound pendulum is

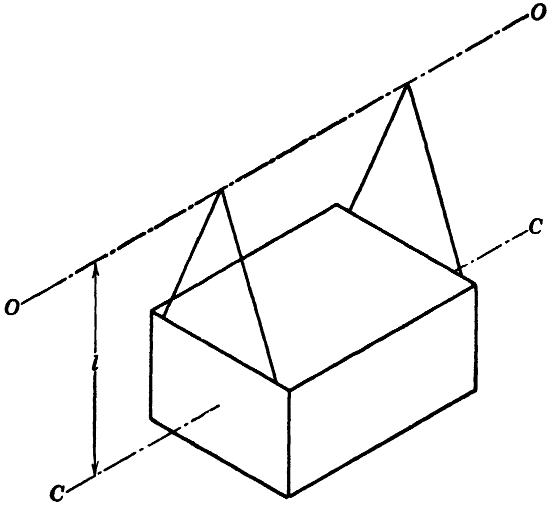

FIGURE 1.13. Compound pendulum method for determining moment of inertia. The fulcrum O-O of the pendulum is parallel to the axis C-C through the center of gravity.

$$I_0 = \frac{Wl\tau^2}{4\pi^2}, \tag{1.48*}$$

where I_0 = moment of inertia with respect to axis O-O, lb in. sec.^{2}
W = weight of equipment, lb.
l = distance from axis of oscillation to center of gravity of equipment, in.
τ = natural period, sec.

It is evident that the moment of inertia can be determined with reasonable accuracy from equation 1.48 only if the distance l is ac-

---

[*] See N. C. Riggs, *Applied Mechanics*, The Macmillan Co., New York, 1930, page 268.

curately known. This is often impracticable, because of difficulty in determining the exact location of the center of gravity of the equipment. The distance l can be computed, however, by selecting a second distance $(l + \Delta l)$ and comparing the natural periods obtained with the distances l and $(l + \Delta l)$.*

An expression that relates the moment of inertia I_C with respect to axis C-C through the center of gravity to the moment of inertia with respect to axis of oscillation O-O is derived from equation 1.38 as follows:

$$I_C = I_0 - \frac{W}{g} l^2 = I_0' - \frac{W}{g}(l + \Delta l)^2, \tag{1.49}$$

where I_0 designates the moment of inertia about axis O-O for the distance l, and I_0' designates the moment of inertia about axis O'-O' for the distance $(l + \Delta l)$. The natural period of the pendulum whose distance is l will be designated as τ_1, and that whose distance is $(l + \Delta l)$ as τ_2. The following equation is now obtained by substituting in equation 1.49 the expressions obtained from equation 1.48 for I_0 and I_0':

$$l = \Delta l \left[\frac{\tau_2^2 g - 4\pi^2 \Delta l}{(\tau_1^2 - \tau_2^2) g + 8\pi^2 \Delta l} \right]. \tag{1.50}$$

The value of l can be computed from equation 1.50, using the two experimentally determined natural periods τ_1, τ_2, and the readily known differential distance Δl. The value of l thus determined can be used with equation 1.48 to determine I_0; the moment of inertia I_C with respect to axis C-C through the center of gravity is then determined from equation 1.49.

The need to determine the moment of inertia frequently arises under conditions that make both its measurement and calculation impracticable. It is necessary then to resort to an estimating method. The radius of gyration, being a simple linear quantity, lends itself more readily to visualizing its physical significance than does the composite moment of inertia. The radius of gyration is essentially a measure of mass distribution within the body. Its meaning is best illustrated by reference to the several typical bodies shown in Figure 1.14.†

---

* This method is suggested by Wm. Gracey, "The Experimental Determination of the Moments of Inertia of Airplanes by a Simplified Compound-Pendulum Method," *NACA Technical Note* No. 1629, June 1948.

† Formulae for calculation of moments of inertia of various bodies are given by L. S. Marks, *Mechanical Engineers' Handbook*, McGraw-Hill Book Co., New York, 4th edition, 1941, page 212.

In the thin-walled cylinder whose end view is shown in Figure 1.14(*a*), the mass is concentrated at the radius r from the axis of symmetry. The radius of gyration with respect to an axis normal to the paper is therefore equal to the radius. The mass is distributed, however, in the solid homogeneous cylinder shown in Figure 1.14(*b*); and the radius of gyration is less than the radius, $\rho = 0.71r$. If the mass distribution were non-uniform with the preponderant portion being adjacent the center, the radius of gyration would be still smaller.

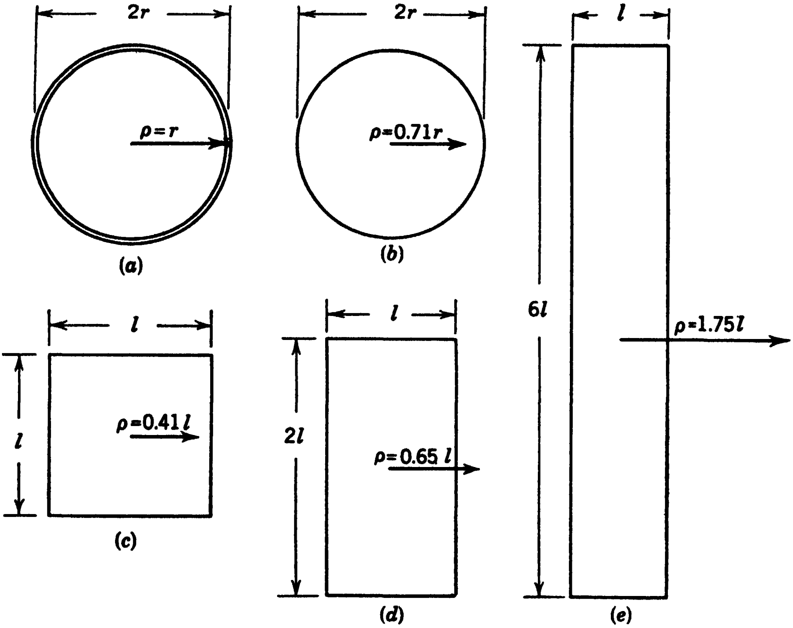

FIGURE 1.14. Outlines of representative bodies. The arrows indicate radii of gyration with respect to axes perpendicular to the paper and passing through the centers of gravity of the respective bodies.

Several rectangular prisms with various form factors are illustrated in Figure 1.14(*c*), (*d*), and (*e*). The radius of gyration for each is indicated with reference to the length of the short side. It should be noted that, when the outline of the body has the general form of a circle or square, the radius of gyration cannot exceed one-half the distance across the body, regardless of the mass distribution. Where the length exceeds the width to a substantial degree, however, the radius of gyration tends to be greater than the width but must always be less than the length. These general theorems may be applied in estimating radius of gyration by visualizing the body under consideration as having a mass distribution equivalent to that of some regular body whose radius of gyration is known or can be determined.

1·6 Elastic Properties of Isolators

The stiffness, or spring rate, of an isolator whose force-deflection characteristic is represented by a straight line is defined by

$$k = \frac{F}{\delta}, \tag{1.51}$$

where F = force applied to isolator, lb.
δ = deflection of isolator in response to force F, in.
k = stiffness or spring rate of isolator, lb/in.

When the force-deflection characteristic is not a straight line, the isolator is said to be non-linear and equation 1.51 does not apply. The stiffness then has a different value for each value of deflection, and is determined from the slope of the force-deflection curve. This phase of isolator stiffness is considered in more detail in Sections 4·1 and 4·2 of Chapter 4.

The general relation defined by equation 1.51 must be qualified by adding that the relation holds only if the force F is applied along a principal elastic axis of the isolator. Deflection of the isolator then takes place along a line that extends in the same direction as the applied force F. If a force is applied in an arbitrary direction to any given isolator, the magnitude and direction of the resultant deflection depends on the nature of the isolator and the type of restraints which act upon it. In the following discussion of an isolator subjected to an obliquely applied force, the directions of its principal elastic axes are presumed to be known. A subsequent discussion considers the physical significance of these axes in greater detail.

Consider first an elastic element, symmetrical with respect to the plane of the paper, as shown by the outline in Figure 1.15. The principal elastic axes p-p and q-q are inclined with respect to the coordinate axes X and Y, as indicated by the angle θ. The only external force acting on the elastic element is the force F directed along the Y axis. To determine the deflection of the elastic element in response to the force F, it is convenient first to write expressions for the components of F along the principal axes p-p and q-q:

$$\begin{aligned} &\text{Along } p\text{-}p \text{ axis: } F \sin\theta, \\ &\text{Along } q\text{-}q \text{ axis: } F \cos\theta. \end{aligned} \tag{1.52}$$

Indicating the stiffnesses along the principal axes *p-p* and *q-q* by k_p and k_q, respectively, the deflections along the principal axes are

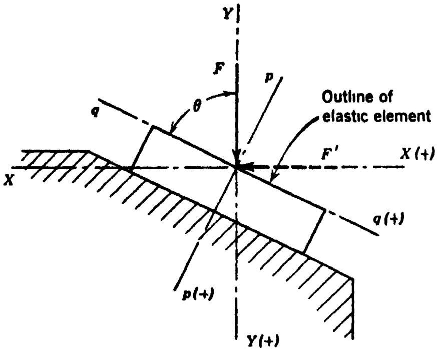

FIGURE 1.15. Diagram of element whose principal elastic axes *p*, *q* are inclined with respect to the coordinate axes *X*, *Y*.

determined by dividing the force components, equation 1.52, by the respective stiffnesses:

$$\delta_p = \frac{F \sin \theta}{k_p}, \qquad \delta_q = \frac{F \cos \theta}{k_q}. \tag{1.53}$$

These deflections along the principal elastic axes may now be resolved into deflections δ_x, δ_y along the coordinate axes *X* and *Y*, as follows:

$$\delta_y = \frac{F \sin \theta}{k_p} \sin \theta + \frac{F \cos \theta}{k_q} \cos \theta = F\left(\frac{1}{k_p} \sin^2 \theta + \frac{1}{k_q} \cos^2 \theta\right), \tag{1.54}$$

$$\delta_x = -\frac{F \sin \theta}{k_p} \cos \theta + \frac{F \cos \theta}{k_q} \sin \theta = F\left(\frac{1}{k_q} - \frac{1}{k_p}\right) \sin \theta \cos \theta. \tag{1.55}$$

The stiffness along the *Y* axis is the force *F* divided by the component δ_y of the deflection:

$$k_y = \frac{F}{\delta_y} = \frac{1}{(1/k_p) \sin^2 \theta + (1/k_q) \cos^2 \theta}, \tag{1.56}$$

It is important to note that the deflection along the *Y* axis is accompanied by a deflection in the *X* direction, even though no force is applied in this direction. When the elastic element is constrained to prevent deflection in the *X* direction, the stiffness in the *Y* direction is not k_y as indicated by equation 1.56 but a different stiffness which will be derived in the following paragraph.

Consider now an elastic element arranged as shown in Figure 1.15 and subjected to the same force F along the Y axis. However, because of a rigid lateral restraint or symmetry of elastic supports, deflection can take place only in the Y direction. It thus becomes evident that a force designated by F' acts upon the element in the X direction to provide the constraint necessary to assure that deflection occurs only in the Y direction. The components of F along the principal axes are given by equation 1.52; the components of F' along the principal axes p-p and q-q are:

$$\begin{aligned} &\text{Along } p\text{-}p \text{ axis: } F' \cos \theta, \\ &\text{Along } q\text{-}q \text{ axis: } F' \sin \theta. \end{aligned} \tag{1.57}$$

The total deflection components δ_p, δ_q of the elastic element along the principal axes p-p and q-q are then the sums of the deflections resulting from F and F', as indicated by the following equations:

$$\delta_p = \frac{F \sin \theta}{k_p} + \frac{F' \cos \theta}{k_p}, \tag{1.58}$$

$$\delta_q = \frac{F \cos \theta}{k_q} - \frac{F' \sin \theta}{k_q}. \tag{1.59}$$

The component δ_x of these deflections is

$$\delta_x = -\left(\frac{F \sin \theta + F' \cos \theta}{k_p}\right) \cos \theta + \left(\frac{F \cos \theta - F' \sin \theta}{k_q}\right) \sin \theta. \tag{1.60}$$

Setting the deflection δ_x in the X direction equal to zero, the magnitude of the restraining force F' is determined by solving equation 1.60 as follows:

$$F' = \frac{F(k_p - k_q) \sin \theta \cos \theta}{k_p \sin^2 \theta + k_q \cos^2 \theta}. \tag{1.61}$$

The component δ_y of the deflections δ_p, δ_q, as determined from equations 1.58 and 1.59, is as follows:

$$\delta_y = \left(\frac{F \sin \theta + F' \cos \theta}{k_p}\right) \sin \theta + \left(\frac{F \cos \theta - F' \sin \theta}{k_q}\right) \cos \theta. \tag{1.62}$$

Substituting in equation 1.62 the expression for F' given by equatior 1.61, an expression is obtained for the deflection δ_y as follows:

$$\delta_y = F\left(\frac{1}{k_p}\sin^2\theta + \frac{1}{k_q}\cos^2\theta\right) + F\left(\frac{1}{k_p} - \frac{1}{k_q}\right)\left(\frac{(k_p - k_q)\sin^2\theta\cos^2\theta}{k_p\sin^2\theta + k_q\cos^2\theta}\right). \quad (1.63)$$

The stiffness k_y' in the direction of the Y axis is the quotient obtained from dividing the force F by the deflection δ_y. Substituting δ_y from equation 1.63 and rearranging terms:

$$k_y' = \frac{F}{\delta_y} = k_p\sin^2\theta + k_q\cos^2\theta. \quad (1.64)$$

The relative stiffness of the isolator when free to deflect laterally and when constrained to move only in the Y direction may be found from a comparison of equations 1.56 and 1.64. It may be noted that the stiffness k_y' given by equation 1.64 is greater than k_y given by equation 1.56 for all values of k_p/k_q except unity. When $k_p/k_q = 1$, all axes are principal axes and the isolator does not deflect laterally when subjected to a vertical load.

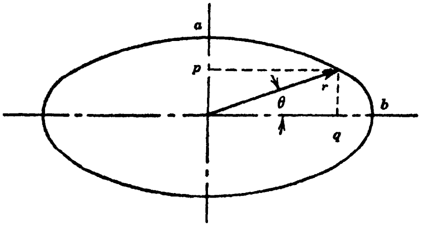

FIGURE 1.16. Ellipse of stiffness, which indicates stiffness of isolator in direction of an inclined axis.

Equation 1.64 for the stiffness k_y' of an isolator constrained against lateral movement is the equation of an ellipse. If the radius to any point on the ellipse is designated by r and the projections of this radius upon the principal axes are designated by p and q, the ellipse may be drawn as illustrated in Figure 1.16. Its equation is derived from equation 1.64 by substituting $\sin\theta = p/r$ and $\cos\theta = q/r$:

$$k_y' = k_p\left(\frac{p^2}{r^2}\right) + k_q\left(\frac{q^2}{r^2}\right). \quad (1.65)$$

The intercepts a and b on the principal axes are determined by setting $p = a$ when $q = 0$; then, independently, setting $p = 0$ when $q = b$. The following expressions are thus obtained for the stiffnesses along the principal axes p-p and q-q:

$$k_p = k_y'\left(\frac{r^2}{a^2}\right); \quad k_q = k_y'\left(\frac{r^2}{b^2}\right). \quad (1.66)$$

Substitution of these expressions for the principal stiffnesses in equation 1.65 gives the following equation:

$$1 = \frac{p^2}{a^2} + \frac{q^2}{b^2}. \tag{1.67}$$

Dividing both sides of the above equation by $r^2 = p^2 + q^2$, and noting that $p/r = \sin\theta$, $q/r = \cos\theta$, the following equation is obtained:

$$\frac{1}{r^2} = \frac{1}{a^2}\sin^2\theta + \frac{1}{b^2}\cos^2\theta. \tag{1.68}$$

This equation is similar to equation 1.64. It thus becomes evident that, if an ellipse be drawn with principal radii $a = 1/\sqrt{k_p}$ and $b = 1/\sqrt{k_q}$, the stiffness k along any axis may be found from the relation $r = 1/\sqrt{k}$. This relation holds, as indicated above, only when the elastic element is constrained to deflect colinearly with the force which causes the deflection.

The stiffness of an elastic element along any axis in space may be determined by writing the equation for an ellipsoid, analogous to equation 1.68:

$$\frac{1}{r^2} = \frac{1}{a^2}\cos^2\theta_a + \frac{1}{b^2}\cos^2\theta_b + \frac{1}{c^2}\cos^2\theta_c, \tag{1.69}$$

where θ_a, θ_b, θ_c represent the angles between the principal axes and any line r through the coordinate center. If the intercepts a, b, c of the ellipsoid on the principal axes follow the relation

$$a = \frac{1}{\sqrt{k_a}};\quad b = \frac{1}{\sqrt{k_b}};\quad c = \frac{1}{\sqrt{k_c}}, \tag{1.70}$$

the stiffness k along line r is given by the relation

$$r = \frac{1}{\sqrt{k}}. \tag{1.71}$$

If any two principal stiffnesses are equal, the ellipsoid becomes an ellipsoid of revolution. If the three principal stiffnesses are equal, the ellipsoid becomes a sphere.

It is usually possible to determine principal elastic axes from conditions of symmetry. An axis of symmetry is a principal axis, and the elastic ellipsoid becomes an ellipsoid of revolution about this axis.

Any plane of symmetry contains a principal elastic axis. The line of intersection of two planes of symmetry therefore defines a principal elastic axis. It may be taken as a general rule that geometric symmetry always produces elastic symmetry, but the reverse is not always true. If two lines are not orthogonal but are known from symmetry or otherwise to be principal elastic axes, it follows that every line in the plane defined by these two lines is, therefore, a principal elastic axis because the necessary condition that the principal elastic axes be orthogonal cannot be attained otherwise.

1·7 *Dynamics of Rigid Bodies*

This section includes a brief discussion of certain aspects of the dynamics of rigid bodies which are useful in analyzing the motion of a body mounted upon resilient supports. It is necessary to consider here only plane motion of a body. Plane motion occurs if the plane of the motion is a plane of symmetry, or if the body and its supports are otherwise arranged so that movement in the plane does not create forces having components normal to the plane. These conditions are discussed in greater detail in Chapter 2.

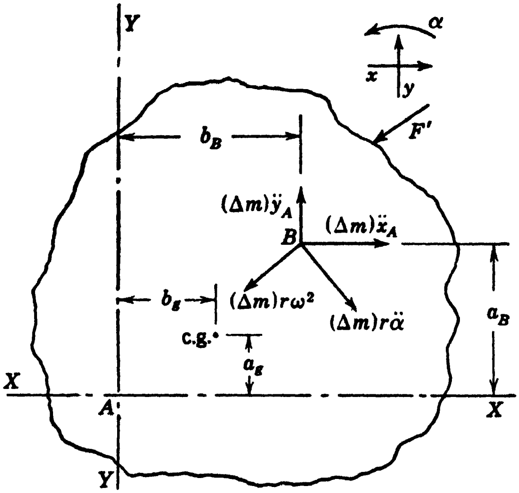

FIGURE 1.17. Rigid body acted on by an external force system whose resultant is indicated by the force vector F'. Inertia or body forces of the infinitesimal mass particle Δm are indicated by force vectors at point B.

Plane motion of the body shown in outline in Figure 1.17 is investigated by projecting the body upon the coordinate plane defined by the axes X and Y. Translation of a body is motion such that no straight line in the body changes direction; i.e., it remains parallel with itself. All points of the body therefore move along parallel paths and have equal velocities and accelerations. Rotation of the body is motion such that one line normal to the plane of the paper remains at least momentarily fixed in space while all points of the body not on the line describe circular paths having centers on the fixed line. Plane motion is, in general, a combination of translatory and rotational components. The instantaneous motion of the body shown in Figure 1.17 in the plane of the X and the Y axes may be resolved into the following components:

(*a*) Pure rotation of the body, with respect to an axis perpendicular to the XY plane and passing through any point A in the body. This rotation embodies the instantaneous angular velocity and acceleration which are representative of the motion of the body.

(*b*) Pure translation of the body, which gives to each point of the body the instantaneous linear velocity and acceleration of point A.

The body shown in Figure 1.17 is considered to be acted upon by a series of unbalanced external forces and couples whose resultant is represented by F'. The body has at any instant an angular velocity ω and an angular acceleration $\ddot{\alpha}$. In accordance with the principle outlined above, this may be considered as pure rotation of the body about any point A and translation of the body with a motion identical to that of point A. The motion of any point B at a distance r from A is comprised of (1) a rotational component about the point A as a center and (2) a translatory component having vertical and horizontal displacements y_A, x_A identical to those at A.

The inertia forces associated with the motion of the particle Δm located at B are indicated on Figure 1.17. The inertia forces resulting from vertical and horizontal translation are $(\Delta m)\ddot{y}_A$ and $(\Delta m)\ddot{x}_A$, respectively. As a result of the rotational motion, the radial acceleration $(\Delta m)r\omega^2$ is directed toward the center of rotation A, and the acceleration $(\Delta m)r\ddot{\alpha}$ has a tangential direction.

The resultant of the external forces has a magnitude equal to the product of the mass of the body and the acceleration of its center of gravity. This resultant force is in a direction parallel with the acceleration of the center of gravity, though it is not in general directed along a line passing through the center of gravity. Since every point on the body has the same translatory motion as point A, it is proper to equate the resultant of external forces to the inertia force of the body derived from the translatory acceleration of point, A. Taking components in the directions of the Y and X axes:

$$\Sigma F_y = \Sigma(\Delta m)\ddot{y}_A = m\ddot{y}_A, \tag{1.72}$$

$$\Sigma F_x = \Sigma(\Delta m)\ddot{x}_A = m\ddot{x}_A. \tag{1.73}$$

External and inertia couples are now equated. The resultant inertia couple is the summation of the moments of the several inertia forces with respect to an axis through point A, and the external couple is a component of the resultant F':

$$\Sigma M = \Sigma(\Delta m)r\ddot{\alpha}r - \Sigma(\Delta m)\ddot{x}_A a_B + \Sigma(\Delta m)\ddot{y}_A b_B. \tag{1.74}$$

In the first term on the right side of equation 1.74, the expression $\Sigma(\Delta m)r^2$ is the moment of inertia of the body with respect to the axis through A, designated I_A. The second term on the right side includes the expression $\Sigma(\Delta m)a_B$. This expression is, by definition, equal to ma_g where a_g is the distance from the coordinate axis X to the center of gravity of the body. In a similar manner, $\Sigma(\Delta m)b_B = mb_g$. Equation 1.74 now becomes:

$$\Sigma M = I_A\ddot{\alpha} - ma_g\ddot{x}_A + mb_g\ddot{y}_A. \tag{1.75}$$

If the coordinate axes are taken through the center of gravity of the body, $a_g = b_g = 0$. Then

$$\Sigma M = I_g\ddot{\alpha}, \tag{1.76}$$

where I_g indicates moment of inertia with respect to an axis through the center of gravity.

The above equations are basic in determining the motion of a rigid body mounted upon flexible supports in such a manner as to have several degrees of freedom in coupled modes. In many of the cases considered, the principal elastic axes of the isolators are respectively parallel to the principal inertia axes of the body and it is convenient to take the center of coordinates at the center of gravity. The applicable equations are then 1.72, 1.73, and 1.76, of which two or more sometimes must be solved simultaneously, depending on the coupling between various modes of vibration. Where the principal elastic axes of the isolators are inclined with respect to the principal inertia axes of the body, it is convenient to take the center of coordinates at the elastic axis of the system. The applicable equations of the motion of the body are then 1.72, 1.73, and 1.75.

BIBLIOGRAPHY

Crede, C. E., "Determining Moment of Inertia," *Mach. Des.*, Vol. 20, No. 8, August 1948.

GRACEY, WM., "The Experimental Determination of the Moments of Inertia of Airplanes by a Simplified Compound-Pendulum Method," *NACA Tech. Note* 1629, June 1948.

JOHNSON, W. C., *Mathematical and Physical Principles of Engineering Analysis*, McGraw-Hill Book Co., New York, 1944.

MANLEY, R. G., *Fundamentals of Vibration Study*, John Wiley and Sons, Inc., New York, 1944.

PIERCE, B. O., *A Short Table of Integrals*, Ginn and Company, Boston, 1929.

RIGGS, N. C., *Applied Mechanics*, The Macmillan Co., New York, 1930.

SEELY, F. B., and N. E. Ensign, *Analytical Mechanics for Engineers*, John Wiley and Sons, Inc., New York, 1941.

CHAPTER TWO

Isolation of Vibration

There are two aspects to the problem of vibration isolation: first, the isolation of forces of the type created by rotating and reciprocating machinery, such as fans, compressors, electric motors, and diesel engines; and second, the isolation of motions such as occur in airplanes, ships, and vehicles. The principal objective in the first mentioned aspect is the reduction in the magnitude of the force transmitted to the support for the machinery. In the second aspect, the principal objective is a reduction in vibration amplitude so that the mounted equipment will be subjected to vibration of less severity than the supporting structure. Although the ultimate objectives and the test for effectiveness of isolation are different in the two cases, the same engineering principle applies to both. This principle, in general terms, is to mount the equipment upon resilient supports or isolators in such a manner that the natural frequency of the equipment-and-isolator system is substantially lower than the frequency of the vibration to be isolated. A detailed discussion of the principle is set forth in this chapter.

2·1 Single-Degree-of-Freedom System Excited by Force

Isolation of the force created by the operation of machinery is discussed by referring to the system shown in Figure 2.1. This system consists of the concentrated mass m_y supported by the massless, linear spring k_y and constrained by frictionless guides to move only in the vertical direction. The mass is acted upon by a vertically directed force whose magnitude varies with time according to the expression $F = F_0 \sin \omega t$. The differential equation of motion of the mass m_y is obtained from equation 1.72 of Chapter 1. The summation of external forces ΣF_y acting upon the mass includes the force F and the force $-k_y y$ resulting from deflection of the isolator:

$$m_y \ddot{y} = F_0 \sin \omega t - k_y y. \tag{2.1}$$

The above equation neglects gravitational forces which can be shown to influence the average position of the mass m_y but not the effectiveness of vibration isolation. The complete solution of the equation is

$$y = A \sin \sqrt{\frac{k_y}{m_y}}\, t + B \cos \sqrt{\frac{k_y}{m_y}}\, t + \frac{F_0/m_y}{(k_y/m_y) - \omega^2} \sin \omega t. \tag{2.2}$$

The expression for the displacement y, equation 2.2, is the sum of vibration at two different frequencies. One of the frequencies is the forcing frequency ω associated with the force F acting on the mass m_y. The other is the natural frequency of the mass-spring system, $\Omega_y = \sqrt{k_y/m_y}$, which is transient in nature. The values of the coefficients A and B depend on the manner in which the force F is initially applied. Equation 2.2 refers to an undamped system, and the transient vibration consequently is considered to continue indefinitely without diminution. Every practical system embodies damping to some extent, however, and it is proper in the consideration of steady-state vibration to neglect the transient terms. Deleting transient terms from equation 2.2, and dividing both numerator and denominator of the remaining forced term by k_y/m_y:

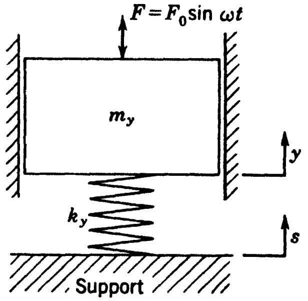

FIGURE 2.1. Undamped single-degree-of-freedom system excited by harmonic force applied to mounted body. The system may also be excited by harmonic motion s of support when $F_0 = 0$.

$$y = \frac{F_0/k_y}{1 - [\omega^2/(k_y/m_y)]} \sin \omega t = \frac{F_0/k_y}{1 - (\omega^2/\Omega_y^2)} \sin \omega t. \tag{2.3}$$

The numerator of equation 2.3 is the static deflection which would be experienced by the mass m_y under the influence of a steadily applied force of magnitude F_0. The denominator is a function only of the ratio of forcing frequency ω to natural frequency Ω_y.

The applied force in a system of this type often is the result of unbalanced rotating or reciprocating members, and its magnitude then tends to vary directly as the square of the frequency. The force resulting from an unbalanced mass m_ϵ at an effective radius ϵ is $F_0 = m_\epsilon \epsilon \omega^2$. Substituting this expression for the force F_0 in equation 2.2 and neglecting the transients as in the above solution, the following expression is obtained:

$$y = \frac{\epsilon(m_\epsilon/m_y)(\omega^2/\Omega_y^2)}{1 - (\omega^2/\Omega_y^2)} \sin \omega t. \tag{2.4}$$

The displacement y of the mass m_y is directly proportional to the magnitude of the unbalanced mass m_ϵ and to the radius ϵ of the unbalance. At the higher operating speeds, $\omega^2/\Omega_y^2 \gg 1$, and the maximum value of y as given by equation 2.4 is

$$\frac{y_0}{\epsilon} \approx -\frac{m_\epsilon}{m_y}, \qquad \left[\frac{\omega^2}{\Omega_y^2} \gg 1\right]. \tag{2.5}$$

The maximum displacement y_0 of the mass m_y and the radius ϵ of the unbalanced rotating mass m_ϵ are thus in the inverse ratio of the respective masses. The negative sign indicates 180° phase difference.

An alternative method can be used to solve the differential equation of motion, equation 2.1. Since the inevitable damping in any practical system will ultimately cause the disappearance of transient vibration, the displacement of the mass m_y may be assumed a sinusoid at the forcing frequency:

$$\begin{aligned} y &= y_0 \sin \omega t, \\ \ddot{y} &= -y_0\omega^2 \sin \omega t. \end{aligned} \tag{2.6}$$

Substituting in equation 2.1 the expressions for the displacement y and its second derivative $\ddot{y}$ given by equations 2.6, dividing both sides of the resulting equation by $\sin \omega t$, and solving for y_0:

$$y_0 = \frac{F_0}{k_y - m_y\omega^2} = \frac{F_0/k_y}{1 - (\omega^2/\Omega_y^2)}. \tag{2.7}$$

Substituting this expression for y_0 in equation 2.6:

$$y = \frac{F_0/k_y}{1 - (\omega^2/\Omega_y^2)} \sin \omega t. \tag{2.8}$$

Equation 2.8 is identical to previously derived equation 2.3.

The purpose in providing a vibration isolator for a system of the type illustrated in Figure 2.1 is to attain a condition wherein the force transmitted to the support is less than the force F applied to the mass. This force is transmitted only by the isolator, and its magnitude in an undamped system is the product of the isolator stiffness k_y and the displacement y of the mass from its neutral position. Defining force transmissibility T_F as the ratio of the force transmitted by the isolator to the force applied to the mass, the following expression is obtained:

$$T_F = \frac{k_y y}{F} = \frac{\dfrac{F_0 \sin \omega t}{1 - (\omega^2/\Omega_y^2)}}{F_0 \sin \omega t} = \frac{1}{1 - (\omega^2/\Omega_y^2)}. \tag{2.9}$$

A similar analysis can be applied to a system in which the vibration is caused by a torque $M_0 \sin \omega t$ acting on a flexibly supported body constrained to move only in rotation with respect to an axis through its center of gravity. The differential equation of motion is then obtained from equation 1.76 of Chapter 1:

$$I\ddot{\alpha} = M_0 \sin \omega t - k_\alpha \alpha. \tag{2.10}$$

This equation is similar in form to equation 2.1, and its solution may be written simply by analogy with equation 2.3:

$$\alpha = \frac{M_0/k_\alpha}{1 - (\omega^2/\Omega_\alpha^2)} \sin \omega t, \tag{2.11}$$

where k_α = stiffness of isolator, in. lb/rad.

$\Omega_\alpha = \sqrt{k_\alpha/I}$* = natural frequency of system in rotation, rad/sec.

I = moment of inertia with respect to axis through center of gravity, lb in. sec^2.

The torque transmissibility T_F is the ratio of the torque $k_\alpha \alpha$ transmitted by the isolator to the applied torque $M_0 \sin \omega t$. The resulting equation is similar to equation 2.9:

$$T_F = \frac{k_\alpha \alpha}{M_0 \sin \omega t} = \frac{\dfrac{M_0 \sin \omega t}{1 - (\omega^2/\Omega_\alpha^2)}}{M_0 \sin \omega t} = \frac{1}{1 - (\omega^2/\Omega_\alpha^2)}. \tag{2.12}$$

It should be noted that the transmissibility T_F, as indicated by equations 2.9 and 2.12, becomes negative when the frequency ratio ω/Ω_y is greater than unity. The significance of this is a change in phase. For $\omega/\Omega_y < 1$, the mass m_y moves downward as the force F is directed downward. The maximum downward force experienced by the support therefore occurs simultaneously with the maximum downward force applied to the mass. For $\omega/\Omega_y > 1$, the mass m_y moves downward as the force F is directed upward. The force experienced by the support is therefore out of phase with the force applied to the mass; i.e., the maximum downward force on the support occurs simultaneously with the maximum upward force on the mass. The transmissibility T_F is shown graphically in Figure 2.2, neglecting the phase relations and indicating only the maximum values of the respective forces.

---

* See equation 1.45 of Chapter 1.

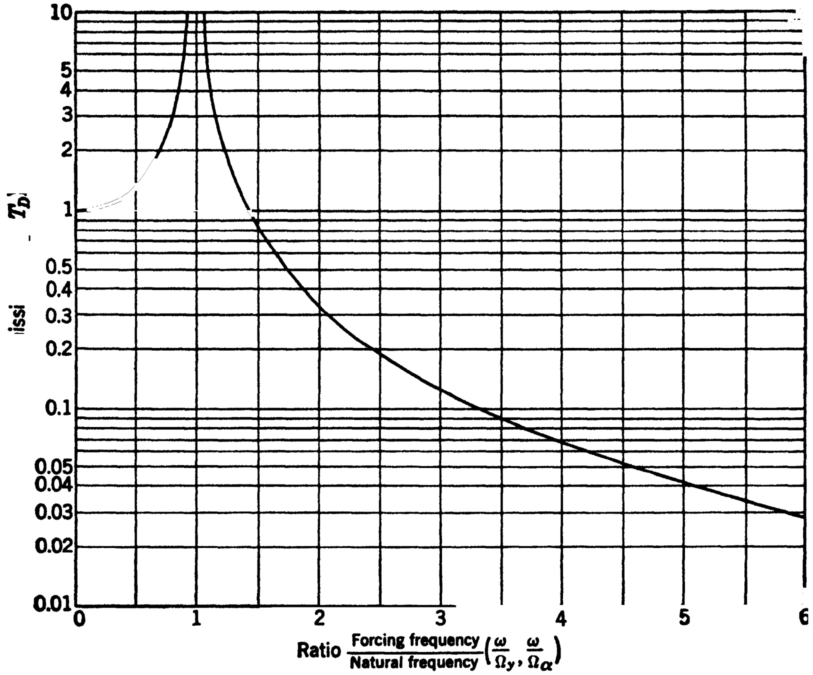

FIGURE 2.2. Transmissibility of an undamped, single-degree-of-freedom system. Force transmissibility T_F and displacement transmissibility T_D are defined by identical mathematical expressions.

A transmissibility of unity occurs at a frequency defined by $\omega/\Omega_y = \sqrt{2}$. When the forcing frequency ω is greater than 1.41 times the natural frequency Ω_y, the transmitted force is less than the applied force and becomes increasingly less as the forcing frequency increases. When the forcing frequency is less than 1.41 times the natural frequency, the transmitted force is always greater than the applied force. The transmissibility becomes infinitely great in an undamped system when the forcing and the natural frequencies are equal. This condition can exist only theoretically, since all practical systems embody some damping. Forced vibration of a damped system is considered in Chapter 4.

2·2 Single-Degree-of-Freedom System Excited by Motion

The system shown in Figure 2.1 may also be excited by vertical motion of the support, where the force F applied to the mass m_y is zero. Defining the vertical motion of the support by $s = s_0 \sin \omega t$, the motion of the mass m_y can be determined by writing its differential equation of motion. The only external force acting on the mass is that transmitted by the isolator; the magnitude of the force is equal to the product of the isolator stiffness and the relative displacement between the mass and the support:

$$m_y \ddot{y} = k_y(s - y). \tag{2.13}$$

This equation may be solved by applying the principles developed in the preceding section. Neglecting the transient terms which would ultimately disappear in steady-state vibration, the assumed expression for the sinusoidal displacement of the mass m_y is $y = y_0 \sin \omega t$. Substituting the expressions for s, y, and $\ddot{y}$ in equation 2.13, solving for y_0, dividing numerator and denominator by k_y, and writing $k_y/m_y = \Omega_y^2$:

$$y_0 = \frac{s_0}{1 - (\omega^2/\Omega_y^2)}. \tag{2.14}$$

The displacement transmissibility T_D is defined as the ratio of the maximum displacement of the mass m_y to the maximum displacement of the support. An expression for T_D is obtained directly from equation 2.14:

$$T_D = \frac{y_0}{s_0} = \frac{1}{1 - (\omega^2/\Omega_y^2)}. \tag{2.15}$$

The expression for displacement transmissibility is thus identical with the expression for force transmissibility, equation 2.9. The same phase relations apply, the displacement of the mass being in phase with the displacement of the support when $\omega/\Omega_y < 1$, and out of phase when $\omega/\Omega_y > 1$. Transmissibility is less than unity when $\omega/\Omega_y > 1.41$.

It has become popular in specifying transmissibility to use the term isolation, the complement of transmissibility. Transmissibility of 0.30 is thus isolation of 70 percent. The meaning of this concept is quite clear when the transmissibility is less than unity. When the transmissibility becomes greater than unity, the concept of isolation *becomes confused and leads to a mathematically untenable position.* The meaning of transmissibility is entirely clear and is suitable under all circumstances. It is used exclusively in this book.

The expression given on page 33 for the natural frequency of a single-degree-of-freedom system, $\Omega_y = \sqrt{k_y/m_y}$, takes the following form when the right side of the equation is multiplied by g^2/g^2:

$$\Omega_y = \sqrt{\frac{k_y}{m_y}} = \sqrt{\frac{k_y g}{W}}, \tag{2.16}$$

where Ω_y = natural frequency, rad/sec.
W = weight of mounted body, lb.
g = acceleration due to gravity, in./sec^2.
k_y = stiffness of isolator, lb/in.

The natural frequency may be obtained in units of cycles per second by dividing equation 2.16 by 2π. The result is expressed more conveniently by substituting the constant $g = 386$ in./sec^2:

$$f_n = \frac{\Omega_y}{2\pi} = 3.13 \sqrt{\frac{k_y}{W}}. \tag{2.17}$$

The relation expressed by equation 2.17 is shown graphically in Figure 2.3 for ready reference when isolators for an application are being selected.

If the force-deflection characteristic of the isolator is linear, the stiffness k_y is constant. The static deflection of the isolator; i.e., its deflection when acted upon by the weight W of the mounted body, is given by $\delta_{st} = W/k_y$. Substituting this expression in equation 2.17, the following expression for natural frequency is obtained:

$$f_n = 3.13 \sqrt{\frac{1}{\delta_{st}}}, \tag{2.18}$$

where f_n = natural frequency, cps.
δ_{st} = static deflection, in.

The natural frequency of a linear isolator is thus a function only of its static deflection. The relation indicated by equation 2.18 is shown graphically in Figure 2.4.

The expression for transmissibility, equations 2.9 and 2.15, may be written in terms of forcing frequency f, expressed in cycles per second,

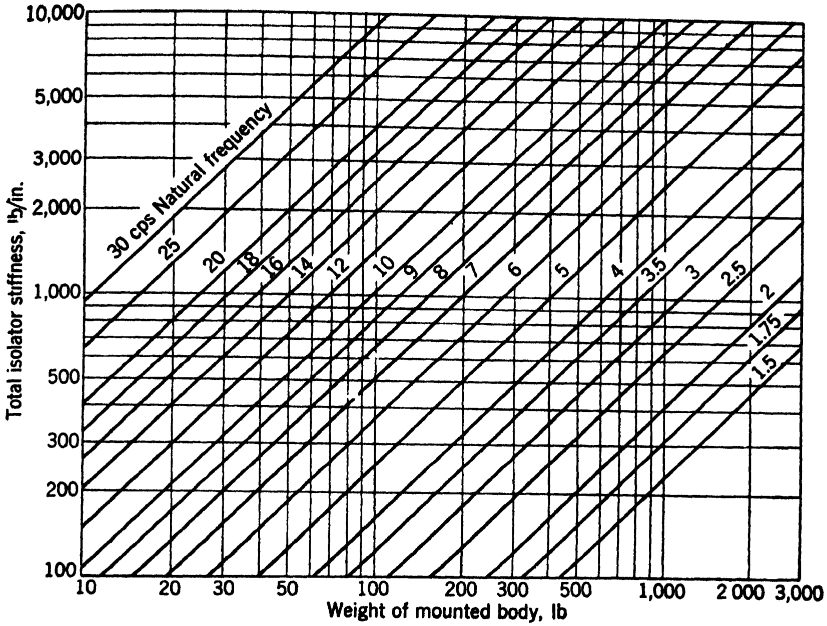

FIGURE 2.3. Natural frequency of a single-degree-of-freedom system as a function of weight of mounted body and total isolator stiffness.

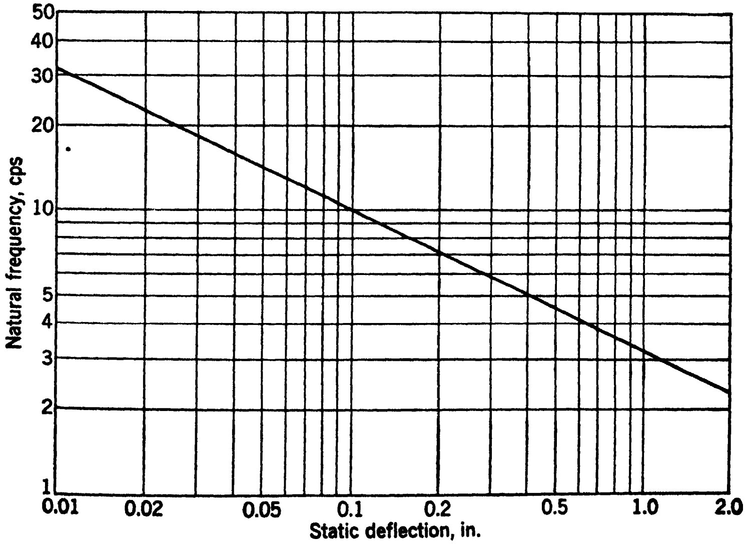

FIGURE 2.4. Relation between natural frequency and static deflection for a linear, single-degree-of-freedom system.

and static deflection δ_{st}, expressed in inches, by substituting $\omega = 2\pi f$ and $\Omega_y = \sqrt{g/\delta_{st}}$. Then:

$$T_F = T_D = \frac{1}{1 - (4\pi^2/g)f^2\delta_{st}}. \tag{2.19}$$

The relation defined by equation 2.19 is shown graphically in Figure 2.5. This widely known family of curves is included here, at the risk of oversimplifying the problem, for the purpose of emphasizing certain fundamental facts in vibration isolation. It should be pointed out that Figure 2.5 is applicable only when the motion of the mounted body is along a vertical line, and when the exciting force or motion acts in the direction of motion of the mounted body. Furthermore, it applies only to isolators with linear force-deflection characteristics; isolators with non-linear characteristics are discussed in Chapter 4. It is important to recognize, however, that Figure 2.5 does indicate in most applications the minimum static deflection required to provide vibration isolation. It becomes evident, for example, that a linear isolator having a static deflection of $\frac{1}{16}$ inch is of no use for isolating vibration having a frequency of 10 cps. In general, it is a necessary but not sufficient condition that isolators have the static deflection indicated by Figure 2.5. Additional necessary conditions are considered in subsequent sections.

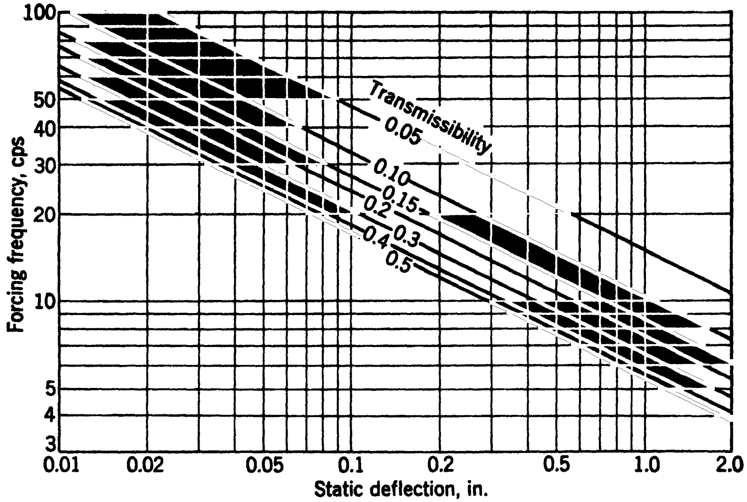

FIGURE 2.5. Transmissibility of a linear, single-degree-of-freedom system in terms of forcing frequency and static deflection.

2·3 Modes of Vibration

The preceding analysis of a single-degree-of-freedom system illustrates the fundamental principles of vibration isolation. This analysis is applicable to practical problems only where the resiliently supported body is constrained to move in translation along a fixed line or in rotation about a fixed axis, or where the symmetry of the system is such that only one mode of vibration is excited. In general, more than one mode of vibration must be considered.

A resiliently supported rigid body may have from one to six natural modes of vibration, depending on the mounting arrangement. If a rigid body is supported by a massless, resilient support and constrained by rigid guides to move only in a vertical direction, as shown in Figure 2.6(a), it constitutes a single-degree-of-freedom system; i.e., its position is determined at any time by one coordinate. It has one natural frequency, in a vertical translatory mode y. If it has additional freedom to rotate about a vertical axis, it constitutes a two-degree-of-freedom system in which the position of the body at any time is determined by its vertical height and by its angular orientation when viewed from above. It has two natural frequencies, one in the vertical translatory mode y and the other in a rotational mode with respect to a vertical axis.

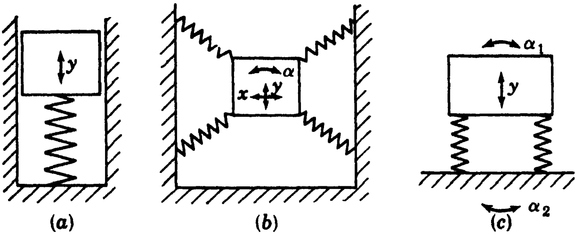

FIGURE 2.6. Modes of vibration of (a) single-degree-of-freedom system, (b) multi-degree-of-freedom system having decoupled natural modes of vibration, and (c) multi-degree-of-freedom system having coupled natural modes of vibration.

Consider now a symmetrical body supported by identical flexible supports at each of the eight corners and unrestrained by rigid guides, as shown in Figure 2.6(b). This is a six-degree-of-freedom system. It is free to move vertically y and horizontally x in the plane of the paper; and rotationally α with respect to an axis normal to the paper. Furthermore, when viewed in a vertical plane normal to the plane of the paper, it has similar freedom of motion horizontally and rotationally (the vertical mode is the y previously considered). When viewed from above, it is free to rotate with respect to a vertical axis. The system has a natural frequency in each of these six natural modes of vibration: three in translatory modes along three mutually perpendicular axes, and three in rotational modes with respect to the same three mutually perpendicular axes. Any vibration may be resolved into components in these modes.

When the resilient supports are located unsymmetrically with respect to the center of gravity of the body, certain translatory and rotational modes of vibration may become coupled. A coupled mode of vibration may be comprised, for example, of a translatory component and a rotational component about an axis through the center of gravity of the body. This may appear as a rotational component about an axis which does not pass through the center of gravity. If the supports are placed at the bottom, as shown in Figure 2.6(*c*), the vibration x in the horizontal translatory mode degenerates to the coupled mode α_1 in which the body vibrates in rotation with respect to an axis below the center of gravity of the body. Furthermore, the rotational vibration α in Figure 2.6(*b*) degenerates to the coupled vibration α_2 with respect to an axis above the center of gravity.

A body on resilient supports may vibrate in a natural mode simultaneously with but independently of its vibration in other natural modes if the respective modes are decoupled. If the modes are coupled, vibration in one coupled mode cannot occur independently of vibration in another coupled mode. Coupling depends on the stiffness and location of the resilient supports and on the mass distribution of the supported body. The following test may be applied to a body on flexible supports: If it is desired to determine whether translatory vibration in a particular direction is decoupled, apply a steady force to the body through its center of gravity and in the specified direction; if the body moves in the direction of the force, *without rotation*, translatory vibration in the direction of the force is decoupled from vibration in other modes. A similar test may be applied to rotational modes. If a couple is applied to the body, with respect to the specified axis through the center of gravity, the body will rotate about the specified axis *without translation* when the rotational mode is decoupled from translatory modes. The meaning of these tests can be illustrated by reference to Figure 2.6(*c*). When a vertical force is applied to the body along a line extending through the center of gravity, the body moves vertically without rotation. The vertical translatory mode is thus decoupled. A horizontal force through the center of gravity, however, not only displaces the body horizontally but causes it to rotate about an axis below the body. The horizontal and rotational modes are thus coupled, and vibration in one of these modes cannot exist independently of vibration in the other mode.

The complete analysis of the performance of an undamped single-degree-of-freedom system, as shown in Figure 2.1, requires knowledge of only the mass of the mounted body, the stiffness of the isolators, and the magnitude and frequency of the excitation acting in the direction of freedom of motion. This simplified condition seldom occurs in practice. In most installations of resiliently mounted equipment, several degrees of freedom and several natural frequencies become involved. For the general system embodying six degrees of freedom, calculation of the natural frequencies involves the solution of a sixth-order determinant which becomes so complex as to be of little use for practical purposes. Fortunately, the preponderant number of practical problems can be solved without recourse to such complex analysis by decoupling certain modes of vibration and introducing simplifying approximations.

If the principal axes of inertia of the mounted body are respectively parallel to the principal elastic axes of the isolators, the problem becomes simplified to a substantial extent. The extent of the simplification depends on the degree of symmetry involved. If the body and the arrangement of its resilient supports are symmetrical with respect to a principal plane of inertia, or if all motion of the body parallel to such a plane is decoupled from motion normal to the plane, the natural frequencies may be determined from the solution of a cubic equation. If a similar symmetry or decoupling exists with respect to two principal planes of inertia, the natural frequencies may be determined from the solution of quadratic equations. Convenient means are available for handling these equations which makes the results useful for engineering applications. The system having two planes of symmetry would seem at first thought to be hedged with so many limitations that very few applications would be adapted to this method of handling. On the contrary, however, the large majority of vibration problems either fall strictly within the stated limitations or may be approximated in such a manner that generally useful results may be obtained. This problem will be considered first, to be followed by the more general and more complex problem involving only one plane of symmetry.

2·4 Multi-Degree-of-Freedom System Excited by Force—Two Planes of Symmetry

This section includes an analysis of a body supported by isolators located at the four lower corners, as illustrated in Figure 2.7. The system is symmetrical with respect to two planes through the center of gravity of the body, one parallel to the plane of the paper (normal to the Z axis) and the other normal to the X axis. For convenience of nomenclature, these two planes of symmetry are sometimes referred to as vertical planes, in accordance with the illustration of Figure 2.7. It should be understood that this designation is not restrictive, because the analysis that follows is valid for any orientation of the system in space.

In the analysis set forth in this section, vibration of the system results from an oscillating force acting upon the mounted body m.

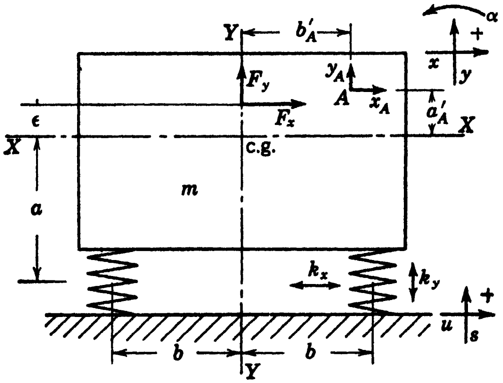

FIGURE 2.7. Elevation view of rigid body mounted upon isolators located at four lower corners, and excited by harmonic forces F_x, F_y applied to mounted body in XY plane. Excitation may also result from motion u, s of support when

$$F_x = F_y = 0.$$

The force is applied at the intersection of the two planes of symmetry, at a distance ϵ above the coordinate center. It is harmonic at the constant frequency ω and has horizontal and vertical components defined by the following expressions:

Horizontal component of force: $F_x \cos \omega t$

Vertical component of force: $F_y \sin \omega t$.

If the force results from an unbalanced member rotating in a plane parallel to the paper, $F_x = F_y$.

It is important to observe the convention of signs indicated in the upper right corner of Figure 2.7. This convention applies to the *directions* of displacements, forces, and couples; and to the *locations* of isolators. Forces and translatory displacements are positive when upward and toward the right; couples and rotational displacements are positive when counterclockwise. Coordinate distances follow the same convention where applicable. A positive horizontal displacement x of the mounted body, for example, causes a negative horizontal restoring force $-4k_xx$. A restoring couple also results. In determining the sign of the couple, it is important to note that the vertical distance from the X axis to the isolators is negative because it is downward. The restoring couple is therefore written $+ak_xx$, and the negative sign of the coordinate distance a gives to the couple the negative sign required by its clockwise direction.

The response of the system to the applied force is determined by writing the differential equations of motion for the mounted body, following the principles derived in Section 1·7 of Chapter 1. Motion in the translatory mode along the Y axis is decoupled because of the two vertical planes of symmetry. Equation 1.72 may then be written as follows:

$$m\ddot{y} = -4k_yy + F_y \sin \omega t. \tag{2.20}$$

Motion in translation along the X axis and in rotation about the Z axis are coupled. Two additional equations of motion, similar to equations 1.73 and 1.76, are now written:

$$m\ddot{x} = -4k_xx + 4k_xa\alpha + F_x \cos \omega t, \tag{2.21}$$

$$I_z\ddot{\alpha} = 4k_xax - 4k_xa^2\alpha - 4k_yb^2\alpha - F_x\epsilon \cos \omega t. \tag{2.22}$$

Equation 2.22 neglects the couple resulting from lateral deflection of the isolators. It can be shown that this couple drops out when the distance a is taken as the vertical distance from the center of gravity of the mounted body to the mid-height of the isolators.

A complete solution of equations 2.20 to 2.22 includes both forced and transient terms. As pointed out in Section 2·1 with reference to the single-degree-of-freedom system, there is always some damping in an actual system, and transient terms may be neglected when considering steady-state vibration. The motion of the mounted body therefore occurs at the forcing frequency, as defined by the following equations:

$$\begin{aligned} y &= y_0 \sin \omega t; \quad \ddot{y} = -y_0\omega^2 \sin \omega t. \\ x &= x_0 \cos \omega t; \quad \ddot{x} = -x_0\omega^2 \cos \omega t. \\ \alpha &= \alpha_0 \cos \omega t; \quad \ddot{\alpha} = -\alpha_0\omega^2 \cos \omega t. \end{aligned} \tag{2.23}$$

It should be noted that equation 2.20 includes only the single variable y, whereas both equations 2.21 and 2.22 include the two variables x and α. An explicit expression for y_0 then can be obtained directly by substituting in equation 2.20 from equations 2.23:

$$y_0 = \frac{(F_y/4k_y)}{1 - \dfrac{\omega^2}{(4k_y/m)}} = \frac{(F_y/4k_y)}{1 - \dfrac{\omega^2}{\Omega_y^2}} = \frac{F_y}{4k_y}(y_0'), \tag{2.24}$$

where $\Omega_y = \sqrt{4k_y/m}$ = vertical natural frequency in radians per second. Equation 2.24 is identical to the previously determined equation 2.7 for the single-degree-of-freedom system, except that the isolator stiffness $4k_y$ is the summation of the stiffnesses in the Y direction of the individual isolators. The term y_0' in the above equation is used below to calculate transmissibility. Because of the assumed symmetry, the displacement amplitude y_0 defined by equation 2.24 is independent of motion in other modes. The freedom to vibrate in other modes has not been restricted, however, and may exist simultaneously with but uninfluenced by the vibration in the direction of the Y axis.

It is evident from an examination of equations 2.21 and 2 22 that vibration in the translatory x and rotational α modes cannot occur independently. These modes are coupled, and expressions for the respective displacement amplitudes can be obtained only by the simultaneous solution of the equations of motion. Substituting in equations 2.21 and 2.22 from equations 2.23 and solving simultaneously for x_0 and α_0:

$$x_0 = \frac{F_x(4a^2k_x + 4b^2k_y - 4\epsilon a k_x - I_z\omega^2)}{mI_z\omega^4 - 4(I_zk_x + ma^2k_x + mb^2k_y)\omega^2 + 16b^2k_xk_y}. \tag{2.25}$$

$$\alpha_0 = \frac{F_x(m\epsilon\omega^2 - 4\epsilon k_x + 4ak_x)}{mI_z\omega^4 - 4(I_zk_x + ma^2k_x + mb^2k_y)\omega^2 + 16b^2k_xk_y}. \tag{2.26}$$

Equations 2.25 and 2.26 are written in terms of convenient dimensionless ratios by making the following substitutions:

$I_z = m\rho_z^2$, where ρ_z is the radius of gyration with respect to the Z axis.
$\eta = k_x/k_y$, a dimensionless stiffness ratio for the isolators.

Dividing the numerator and the denominator of equation 2.25 by $m\rho_z^2\Omega_y^2$; writing $4k_x/m = \Omega_x^2$, $4k_y/m = \Omega_y^2$; and substituting $\Omega_x^2 = \eta\Omega_y^2$; the following expression is obtained:

$$x_0 = -\frac{F_x\left[\dfrac{\eta a^2}{\rho_z^2} + \dfrac{b^2}{\rho_z^2} - \dfrac{\eta\epsilon a}{\rho_z^2} - \dfrac{\omega^2}{\Omega_y^2}\right]}{m\left[\dfrac{\omega^4}{\Omega_y^2} - \left(\eta + \dfrac{\eta a^2}{\rho_z^2} + \dfrac{b^2}{\rho_z^2}\right)\omega^2 + \dfrac{\eta b^2}{\rho_z^2}\Omega_y^2\right.}. \tag{2.27}$$

Multiplying the denominator of equation 2.27 by Ω_y^2/Ω_y^2, the following final expression is obtained for x_0:

$$x_0 = \frac{F_x}{4k_y}\left[\frac{\left(\frac{\eta a^2}{\rho_z^2} + \frac{b^2}{\rho_z^2} - \frac{\eta\epsilon a}{\rho_z^2}\right) - \frac{\omega^2}{\Omega_y^2}}{\frac{\omega^4}{\Omega_y^4} - \left(\eta + \frac{\eta a^2}{\rho_z^2} + \frac{b^2}{\rho_z^2}\right)\frac{\omega^2}{\Omega_y^2} + \frac{\eta b^2}{\rho_z^2}}\right] = \frac{F_x}{4k_y}(x_0'). \quad (2.28)$$

A corresponding expression for α_0 is obtained by performing similar operations upon equation 2.26:

$$\alpha_0 = \frac{F_x}{4\rho_z k_y}\left[\frac{\frac{\epsilon}{\rho_z}\frac{\omega^2}{\Omega_y^2} + \left(\frac{\eta a}{\rho_z} - \frac{\eta\epsilon}{\rho_z}\right)}{\frac{\omega^4}{\Omega_y^4} - \left(\eta + \frac{\eta a^2}{\rho_z^2} + \frac{b^2}{\rho_z^2}\right)\frac{\omega^2}{\Omega_y^2} + \frac{\eta b^2}{\rho_z^2}}\right] = \frac{F_x}{4k_y}\left(\frac{\alpha_0'}{\rho_z}\right). \quad (2.29)$$

The effectiveness of the isolators in reducing the magnitude of the force transmitted to the support is determined as explained in Section 2·1 for the single-degree-of-freedom system. The system illustrated in Figure 2.7 experiences simultaneous displacements in several modes. The displacements are harmonic in nature, but the amplitudes and phase angles vary with frequency. The force exerted upon the support by each isolator is the product of stiffness and deflection of the particular isolator. Inasmuch as the support is considered to remain fixed, the deflection of any particular isolator is numerically equal to the displacement of the point on the mounted body to which the isolator is attached.

The vertical component of deflection for an isolator which is attached to the body at the coordinate distances $-a$, $\pm b$ in Figure 2.7 is given, according to equations 2.23, by

$$\delta_y = y_0 \sin \omega t + b\alpha_0 \cos \omega t. \quad (2.30)$$

The corresponding horizontal component of isolator deflection is

$$\delta_x = (x_0 - a\alpha_0) \cos \omega t. \quad (2.31)$$

Multiplying the deflection δ_y by k_y, and employing the relation given by equation 1.12 of Chapter 1, the following expression is obtained for the vertical component of force transmitted to the support by any isolator:

$$(F_T)_y = k_y \sqrt{y_0^2 + b^2\alpha_0^2} \sin (\omega t + \psi), \quad (2.32)$$

where ψ, according to equation 1.13, is given by

$$\psi = \tan^{-1} \frac{b\alpha_0}{y_0}. \tag{2.33}$$

A corresponding expression for the horizontal component of the transmitted force is obtained by multiplying δ_x by k_x, and substituting the trigonometric relation given by equation 1.7:

$$(F_T)_x = k_x(x - a\alpha_0) \sin\left(\omega t + \frac{\pi}{2}\right). \tag{2.34}$$

The resultant of the force components $(F_T)_y$ and $(F_T)_x$ is obtained by vector addition of equations 2.32 and 2.34. An expression for the sum of two vectors with any phase relation is given by equation 1.15 of Chapter 1. The resultant transmitted force F_T thus becomes:

$$F_T = \sqrt{k_y^2(y_0^2 + b^2\alpha_0^2) + k_x^2(x - a\alpha_0)^2 + 2k_xk_y(x - a\alpha_0)\sqrt{y_0^2 + b^2\alpha_0^2}\cos\left(\frac{\pi}{2} - \psi\right)}. \tag{2.35}$$

Substituting from equation 2.33, the trigonometric term in equation 2.35 reduces to

$$\cos\left(\frac{\pi}{2} - \tan^{-1}\frac{b\alpha_0}{y_0}\right) = \frac{b\alpha_0}{\sqrt{y_0^2 + b^2\alpha_0^2}} \tag{2.36}$$

The relation given by equation 2.36, and the expressions for y_0, x_0, and α_0 given by equations 2.24, 2.28, and 2.29, respectively, are now substituted in equation 2.35. Substituting further, $\eta = k_x/k_y$ and $\sigma = F_y/F_x$, the following expression is obtained for the force transmitted by any isolator:

$$F_T = \frac{F_x}{4}\sqrt{(\sigma y_0')^2 + \left[\alpha_0'\left(\frac{b}{\rho_z} - \frac{a\eta}{\rho_z}\right) + \eta x_0'\right]^2}. \tag{2.37}$$

The significance of transmitted force may perhaps be better understood by comparing its magnitude with that of the force applied to the mounted body. Since the mounted body is supported by four isolators, the designation force transmissibility T_F is used here to indicate the ratio of the maximum force F_T transmitted by a particular isolator to one-fourth of the maximum generated force. When $\sigma = 1$, $F_x = F_y = 0$; and the vertical and the horizontal components of the generated force are equal, as with a rotating, unbalanced member. Then:

$$T_F = \frac{F_T}{F_0/4} = \sqrt{(y_0')^2 + \left[\alpha_0'\left(\frac{b}{\rho_z} - \frac{a\eta}{\rho_z}\right) + \eta x_0'\right]^2}, \quad [\sigma = 1]. \qquad (2.38)$$

Where the generated force is directed along a horizontal line, as in a reciprocating engine, $\sigma = 0$ and the maximum generated force is F_x. The force transmissiblity is:

$$T_F = \frac{F_T}{F_x/4} = \left[\alpha_0'\left(\frac{b}{\rho_z} - \frac{a\eta}{\rho_z}\right) + \eta x_0'\right], \qquad [\sigma = 0]. \qquad (2.39)$$

Different values of force transmissibility T_F are obtained at different isolators, because the deflections of the isolators generally are the sums of rotational and translatory components. The phase of these components differs from one side of the mounted body to the other, and the resultant deflection at any isolator may be either the sum or the difference of the components. The above equations reflect this condition when the appropriate sign is given the coordinate distance b.

The coupled rotational and horizontal translatory motion of the mounted body is expressed as horizontal motion of the center of gravity of the body, and rotation of the body with respect to the Z axis through the center of gravity. This may be envisioned physically as rotational motion of the body, without horizontal translation, about some axis remote from but parallel to the Z axis. This axis experiences no horizontal translation; its location is determined by finding a line on the mounted body where the sum of the horizontal translation and the horizontal component of the rotation is zero:

$$l_c\alpha_0 + x_0 = 0, \quad \text{or} \quad l_c = -\frac{x_0}{\alpha_0}, \qquad (2.40)$$

where l_c is the distance from the Z axis to the axis of rotation. This axis lies in the coordinate plane normal to the X axis, as a result of symmetry of the system. An expression for the distance l_c, comprised of dimensionless ratios, is obtained from equation 2.40 by substituting expressions for x_0 and α_0 from equations 2.28 and 2.29, respectively:

$$\frac{l_c}{\rho_z} = -\left[\frac{\left(\frac{\eta a^2}{\rho_z^2} + \frac{b^2}{\rho_z^2} - \frac{\eta\epsilon a}{\rho_z^2}\right) - \frac{\omega^2}{\Omega_y^2}}{\frac{\epsilon}{\rho_z}\frac{\omega^2}{\Omega_y^2} + \left(\frac{\eta a}{\rho_z} - \frac{\eta\epsilon}{\rho_z}\right)}\right] = -\frac{x_0'}{\alpha_0'}. \qquad (2.41)$$

The location of the center of rotation thus depends not only on the physical characteristics of the mounted body and the isolators but also on the position and frequency of the applied force. The distance l_c has a negative sign when the axis of rotation is above, and a positive sign when below, the center of gravity.

2·5 Multi-Degree-of-Freedom System Excited by Motion—Two Planes of Symmetry

This section analyzes the motion of a body supported by four isolators located at the lower corners, as illustrated in Figure 2.7. Vibration of the system is induced by motion of the support. The same conditions of symmetry and the same limitations on orientation of principal elastic and inertia axes considered in Section 2·4 apply here. The support is assumed to vibrate both vertically and horizontally in translation at a common frequency; rotational vibration of the support is not considered here. The following differential equations of motion are obtained by applying the principles set forth in Section 1·7 of Chapter 1, wherein the external forces and couples acting on the body result entirely from forces applied by the isolators:

$$m\ddot{y} = 4k_y(s - y), \tag{2.42}$$

$$m\ddot{x} = 4k_x(u - x + a\alpha), \tag{2.43}$$

$$I_z\ddot{\alpha} = 4ak_x(u - x + a\alpha) - 4k_yb^2\alpha. \tag{2.44}$$

Equation 2.44 does not include the couple resulting from lateral deflection of the isolator, as explained following equation 2.22.

Taking only the forced terms of the solution of equations 2.42 to 2.44, for reasons discussed in Section 2·2, the expressions for the instantaneous positions of the support and the mounted body are

$$\begin{aligned}
u &= u_0 \sin \omega t. \\
s &= s_0 \sin (\omega t + \psi). \\
x &= x_0 \sin (\omega t + \psi_x); \quad \ddot{x} = -x_0\omega^2 \sin (\omega t + \psi_x). \qquad (2.45)\\
y &= y_0 \sin (\omega t + \psi_y); \quad \ddot{y} = -y_0\omega^2 \sin (\omega t + \psi_y). \\
\alpha &= \alpha_0 \sin (\omega t + \psi_\alpha); \quad \ddot{\alpha} = -\alpha_0\omega^2 \sin (\omega t + \psi_\alpha).
\end{aligned}$$

The motion of the mounted body in the translatory mode along the Y axis is decoupled from motion in other modes, as a result of symmetry. Equation 2.42 therefore may be solved explicitly by substituting the expressions for s, y, and $\ddot{y}$ from equations 2.45:

$$-my_0\omega^2 \sin(\omega t + \psi_y) = 4k_y[s_0 \sin(\omega t + \psi) - y_0 \sin(\omega t + \psi_y)]. \quad (2.46)$$

Equation 2.46 has a solution when and only when $\psi_y = \psi$. The following expression for y_0 is then obtained:

$$y_0 = \frac{s_0}{1 - \dfrac{\omega^2}{4k_y/m}} = \frac{s_0}{1 - \dfrac{\omega^2}{\Omega_y^2}}, \quad (2.47)$$

where Ω_y indicates natural frequency in a translatory mode in the direction of the Y axis. This equation is similar to equation 2.14 previously developed for the single-degree-of-freedom system, except that the isolator stiffness $4k_y$ is the summation of the stiffnesses, in the Y direction, of the individual isolators. Translatory vibration in the direction of the Y axis is thus decoupled and can exist independently of and simultaneously with vibration in other modes.

As in Section 2·4, equations for the displacements x_0 and α_0 in the coupled translatory and rotational modes are obtained from the simultaneous solution of equations 2.43 and 2.44. Substituting u, x, and α, as well as $\ddot{x}$ and $\ddot{\alpha}$, from equations 2.45 in equations 2.43 and 2.44:

$$-mx_0\omega^2 \sin(\omega t + \psi_x) = 4k_x[u_0 \sin \omega t - x_0 \sin(\omega t + \psi_x) + a\alpha_0 \sin(\omega t + \psi_\alpha)]. \quad (2.48)$$

$$-I_z\alpha_0\omega^2 \sin(\omega t + \psi_\alpha) = 4ak_x[u_0 \sin \omega t - x_0 \sin(\omega t + \psi_x) - a\alpha_0 \sin(\omega t + \psi_\alpha)] - 4b^2k_y\alpha_0 \sin(\omega t + \psi_\alpha). \quad (2.49)$$

A solution to the immediately preceding equations exists when and only when $\psi_x = \psi_\alpha = 0$. Equations 2.48 and 2.49 may then be solved simultaneously for x_0 and α_0 as follows:

$$x_0 = \frac{4u_0(4b^2k_xk_y - I_zk_x\omega^2)}{mI_z\omega^4 - 4(ma^2k_x + mb^2k_y + I_zk_x)\omega^2 + 16b^2k_xk_y}. \quad (2.50)$$

$$\alpha_0 = \frac{4mak_x\omega^2u_0}{mI_z\omega^4 - 4(ma^2k_x + mb^2k_y + I_zk_x)\omega^2 + 16b^2k_xk_y}. \quad (2.51)$$

The above expressions for x_0 and α_0 may be written in terms of convenient dimensionless ratios. The necessary conversion is made by dividing the numerator and the denominator of each equation by $m^2 p_z^2 \Omega_y^4$, substituting $k_x = \eta k_y$, and writing $4k_x/m = \Omega_x^2$, $4k_y/m = \Omega_y^2$. Then:

$$x_0 = \frac{\eta\left(\frac{b^2}{p_z^2} - \frac{\omega^2}{\Omega_y^2}\right)u_0}{\frac{\omega^4}{\Omega_y^4} - \left(\frac{\eta a^2}{p_z^2} + \frac{b^2}{p_z^2} + \eta\right)\frac{\omega^2}{\Omega_y^2} + \frac{\eta b^2}{p_z^2}}, \tag{2.52}$$

$$\alpha_0 = \frac{\left(\frac{\eta a}{p_z}\frac{\omega^2}{\Omega_y^2}\right)\frac{u_0}{p_z}}{\frac{\omega^4}{\Omega_y^4} - \left(\frac{\eta a^2}{p_z^2} + \frac{b^2}{p_z^2} + \eta\right)\frac{\omega^2}{\Omega_y^2} + \frac{\eta b^2}{p_z^2}}. \tag{2.53}$$

The direction and amplitude of the vibratory motion at any point on the mounted body may now be determined. Consider, for example, the point A shown in Figure 2.7. The distances from the coordinate axes X and Y are a_A' and b_A', respectively. The vertical and horizontal components of the displacement are given by:

$$y_A = y + b_A'\alpha; \quad x_A = x - a_A'\alpha. \tag{2.54}$$

Substituting for x, y, and α from equations 2.45, the following expressions are obtained:

$$\begin{aligned} y_A &= y_0 \sin(\omega t + \psi_y) + b_A'\alpha_0 \sin(\omega t + \psi_\alpha), \\ x_A &= x_0 \sin(\omega t + \psi_x) - a_A'\alpha_0 \sin(\omega t + \psi_\alpha). \end{aligned} \tag{2.55}$$

It has previously been determined that $\psi_x = \psi_\alpha = 0$, and that $\psi_y = \psi$. The maximum values of the displacement components y_A, x_A are now written from equations 2.55, employing the relation set forth in equation 1.15 of Chapter 1:

$$(y_A)_0 = \sqrt{y_0^2 + (b_A'\alpha_0)^2 + 2b_A'\alpha_0 y_0 \cos\psi}, \tag{2.56}$$

$$(x_A)_0 = x_0 - a_A'\alpha_0. \tag{2.57}$$

It thus becomes evident that the maximum value of the vertical displacement component y_A is a function of the phase angle ψ between the vertical and the horizontal components of the support motion. It is important to note that the values of y_A and x_A are influenced by the signs of the coordinate distances a_A', b_A'. The applicable convention of signs for the coordinate distances is indicated in the upper-right corner of Figure 2.7.

The location of the axis of rotation is determined by applying the relation defined by equation 2.40. Substituting the expressions for x_0 and α_0 from equations 2.52 and 2.53:

$$\frac{l_c}{\rho_z} = \frac{(\omega^2/\Omega_y^2) - (b^2/\rho_z^2)}{(a/\rho_z)(\omega^2/\Omega_y^2)}. \qquad (2.58)$$

2·6 *Natural Frequencies—Two Planes of Symmetry*

It is shown in Figure 2.2 that the transmissibility of a single-degree-of-freedom system decreases as the natural frequency of the system decreases. The same result is generally obtained, although not so readily demonstrated, for a multi-degree-of-freedom system. Expressions have been developed in the preceding sections for the force transmitted by isolators, and for the motion experienced by the mounted body. Means are thus available for computing the transmissibility of a system under any specific conditions. However, it is usually desirable in the preliminary stages of a design problem to determine the natural frequencies of the system being considered. This serves, first, to avoid any resonant condition and, second, to estimate the probable effectiveness of the isolators. Except in special instances which are discussed later, it is advantageous in attaining vibration isolation to maintain all natural frequencies substantially less than the frequency of the principal vibration to be isolated. Convenient means of determining natural frequencies are discussed below.

The natural frequencies in the coupled translatory and rotational modes are the frequencies at which the displacements x_0, α_0 for an undamped system become infinite. Two expressions for x_0, equations 2.28 and 2.52, and two expressions for α_0, equations 2.29 and 2.53, have been derived. Each of these four expressions has the identical denominator. The requirements for a natural frequency, i.e., an infinite displacement, are met by equating the common denominator to zero:

$$\frac{\omega^4}{\Omega_y^4} - \left(\frac{\eta a^2}{\rho_z^2} + \frac{b^2}{\rho_z^2} + \eta\right)\frac{\omega^2}{\Omega_y^2} + \frac{\eta b^2}{\rho_z^2} = 0. \qquad (2.59)$$

This is a quadratic equation whose variable is ω^2/Ω_y^2. The roots of the equation are

$$\left(\frac{\Omega_c}{\Omega_y}\right)^2 = \frac{1}{2}\left[\eta\left(1 + \frac{a^2}{\rho_z^2}\right) + \frac{b^2}{\rho_z^2} \pm \sqrt{\left[\eta\left(1 + \frac{a^2}{\rho_z^2}\right) + \frac{b^2}{\rho_z^2}\right]^2 - \frac{4\eta b^2}{\rho_z^2}}\right], \qquad (2.60)$$

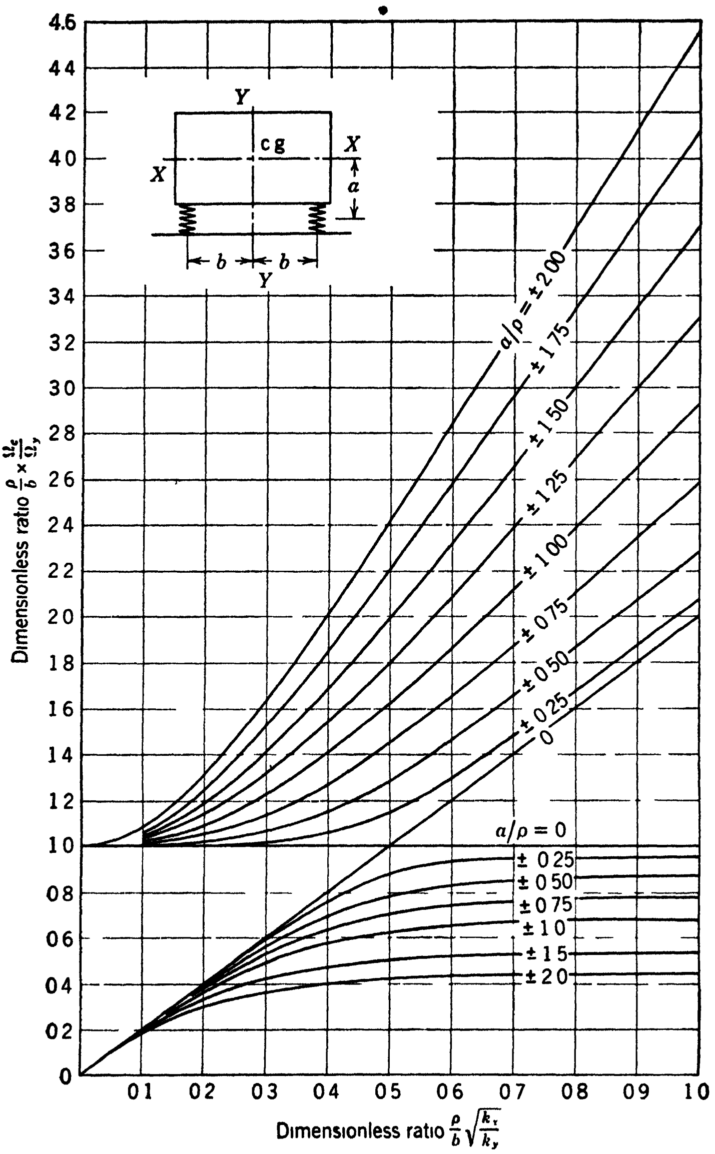

FIGURE 2.8.* Curves showing ratio of two coupled natural frequencies Ω_c in XY plane to decoupled natural frequency Ω_y in translation along Y axis. The isolator stiffnesses in the X and Y directions are indicated by k_x and k_y, respectively, and the radius of gyration with respect to the Z axis through the center of gravity is indicated by ρ (*Journal of Applied Mechanics*, Vol. 14, No. 1, March 1947).

* Figures 2.8, 5.20, 5.21, and 6.1 originally appeared in *Naval Research Laboratory Report* No. V2927, August 1946, entitled "The Design of Vibration-Isolating

where the forcing frequency ω is replaced by Ω_c to indicate natural frequency in a coupled mode. Multiplying both sides of equation 2.60 by ρ_z^2/b^2 and solving for $(\Omega_c/\Omega_y)(\rho_z/b)$:

$$\frac{\Omega_c}{\Omega_y} \times \frac{\rho_z}{b} = \frac{1}{\sqrt{2}}\sqrt{\frac{\eta\rho_z^2}{b^2}\left(1 + \frac{a^2}{\rho_z^2}\right) + 1 \pm \sqrt{\left[\frac{\eta\rho_z^2}{b^2}\left(1 + \frac{a^2}{\rho_z^2}\right) + 1\right]^2 - \frac{4\eta\rho_z^2}{b^2}}}. \tag{2.61}$$

The two coupled natural frequencies Ω_c may now be determined with reference to the decoupled natural frequency Ω_y, as functions of the dimensions a, b, ρ_z, and the dimensionless stiffness ratio $\eta = k_x/k_y$. The various dimensions are grouped into dimensionless parameters in such a manner that the frequency ratio Ω_c/Ω_y is conveniently determined from a graphical representation of equation 2.61. The resultant curves are shown in Figure 2.8. Determination of numerical values for the coupled natural frequencies Ω_c requires that the numerical value of the decoupled natural frequency Ω_y be known. This is given by equation 2.17, and its graphical representation, Figure 2.3.* The decoupled natural frequency is expressed by Figure 2.3 in cycles per second, and the coupled natural frequencies are determined in similar units by multiplying the value determined from Figure 2.3 by the ratio found from Figure 2.8. Only the second power of the dimension a appears in equation 2.61, and the natural frequencies are thus independent of the sign of this dimension.

The preceding analysis has resulted in expressions for the decoupled natural frequency in translation along the Y axis, and for the coupled natural frequencies in the XY plane of symmetry. Since the YZ plane is also a plane of symmetry, coupled natural frequencies corresponding to those in the XY plane may be found using the same methods. Five of the six natural frequencies having thus been determined, there remains the natural frequency in a rotational mode with respect to the Y axis.

Figure 2.9 illustrates a plan view of the body that is shown in elevation in Figure 2.7. The distances from the isolators to the principal planes of inertia are designated by b, c as shown on the diagram, Figure 2.9; and the horizontal stiffnesses of the isolators in the directions of

---

Bases for Machinery," by C. E. Crede and J. P. Walsh. The subject matter of this report was subsequently published in the *Journal of Applied Mechanics*, Vol. 14, No. 1, March 1947.

* The stiffness k_y in equation 2.17 must be taken as the total stiffness in the direction of the Y axis. In the system illustrated by Figure 2.7, the total vertical stiffness is $4k_y$.

the coordinate axes X, Z are indicated by k_x and k_z, respectively. The differential equation of motion which applies to this system is given by equation 1.76 of Chapter 1, wherein the external forces and

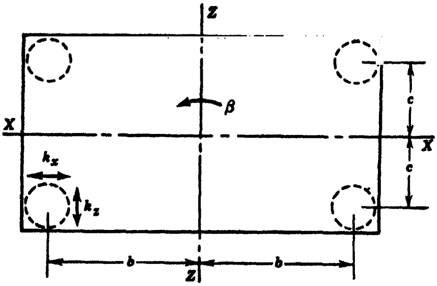

FIGURE 2.9. Plan view of rigid body mounted upon isolators located at four lower corners. The stiffnesses of the isolators in the directions of the X and Z axes are indicated by k_x and k_z, respectively.

couples result from the forces applied by the isolators when the body is rotated through an angle β from its neutral position:

$$I_y\ddot{\beta} = -4\beta b^2k_z - 4\beta c^2k_x. \tag{2.62}$$

The solution of equation 2.62 may be written:

$$\beta = A \sin \sqrt{\frac{4(b^2k_z + c^2k_x)}{I_y}}\, t + B \cos \sqrt{\frac{4(b^2k_z + c^2k_x)}{I_y}}\, t.$$

The coefficients A, B depend on the initial conditions of displacement, and the expression under the radical indicates the natural frequency in accordance with the following expression:

$$\Omega_\beta = 2\sqrt{\frac{b^2k_z + c^2k_x}{I_y}}, \tag{2.63}$$

where Ω_β is the rotational natural frequency in radians per second with respect to the Y axis.

When $k_x = k_z = k$, the expression given by equation 2.63 can be written in terms of the translatory natural frequency in the Y direction by substituting $k = \eta k_y$, $I_y = m\rho_y{}^2$. Then:

$$\frac{\Omega_\beta}{\Omega_y} = \sqrt{\frac{\eta(b^2 + c^2)}{\rho_y{}^2}}, \qquad [k_x = k_z = \eta k_y], \tag{2.64}$$

where $\Omega_y = \sqrt{4k_y/m}$ is the translatory natural frequency in the direction of the Y axis.

The preceding analyses of the system illustrated in Figure 2.7 presume symmetry with respect to coordinate planes normal to the X and Z axes. This symmetry frequently cannot be attained, and the nonsymmetrical arrangement shown in Figure 2.10 must be used. If the respective stiffnesses in the Y direction of the isolators 1 and 2 are made proportional to the dead-weight load supported by each isolator, the system meets the previously defined requirements (see Section 2·3) for decoupling vibration in the translatory mode along the Y axis. This is expressed mathematically by the following relation:

$$\frac{k_{y_1}}{k_{y_2}} = \frac{b_2}{b_1}. \tag{2.65}$$

The results obtained from the non-symmetrical spacing of isolators become evident by referring to the differential equations of motion of

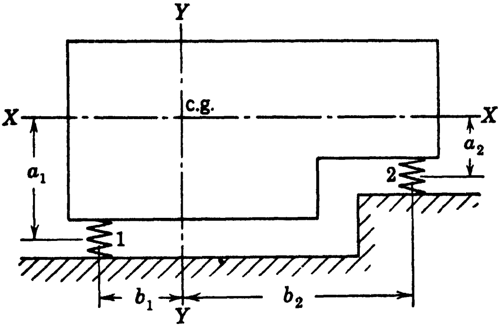

FIGURE 2.10. Elevation view of rigid body mounted upon isolators located at four lower corners. The isolators are unsymmetrically placed with respect to a coordinate plane through the center of gravity and normal to the X axis; they are unequally spaced from a coordinate plane normal to the Y axis.

the system shown in Figure 2.7. The coordinate distance b does not appear in equations 2.20 and 2.21. An equation of motion equivalent to equation 2.22 can be written for the system in Figure 2.10, assuming, for the present, that $a_1 = a_2 = a$:

$$I_z\ddot{\alpha} = 4k_xax - 4k_xa^2\alpha - 2\alpha(b_1^2k_{y_1} + b_2^2k_{y_2}) - F_0\epsilon \cos \omega t. \tag{2.66}$$

Substituting from equation 2.65 in equation 2.66:

$$I_z\ddot{\alpha} = 4k_xax - 4k_xa^2\alpha - 2\alpha b_1b_2(k_{y_1} + k_{y_2}) - F_0\epsilon \cos \omega t. \tag{2.67}$$

Equation 2.67 thus becomes equivalent to equation 2.22, and the curves of Figure 2.8 apply to the system of Figure 2.10, provided that the following relations are satisfied:

$$\sqrt{b_1b_2} = b; \quad 2(k_{y_1} + k_{y_2}) = 4k_y; \quad a_1 = a_2 = a. \tag{2.68}$$

When the isolators are not on the same level, $a_1 \neq a_2$. The coordinate distance a appears in equations 2.21 and 2.22 as both the first and the second power. As a result, it is not possible to find an equivalent value of a whose use with Figure 2.8 would give rigorously correct values of natural frequency. For most practical applications, however, sufficiently accurate results will be obtained by substituting for a in equation 2.61 and Figure 2.8:

$$\sqrt{a_1a_2} = a. \tag{2.69}$$

2·7 Problems in Isolator Application

The problems of applying vibration isolators are often unduly complicated by the fact that the physical characteristics of the machine or structure have been predetermined and are not subject to change. Machines that are designed to incorporate vibration isolators in desirable locations may attain the optimum in efficiency of vibration isolation. Many machines, however, embody a shape or weight distribution that is not conducive to effective vibration isolation; others were designed with the philosophy that vibration isolators represent a detail whose location is of little importance; and in still other machines originally not intended to be mounted the need for vibration isolation has subsequently appeared.

The procedure used in applying isolators to an equipment that is already designed and sometimes in existence is to seek a system whose natural frequencies are substantially lower than the frequency of the vibration to be isolated. The vertical natural frequency in translation may be determined from the weight of the mounted body and the vertical stiffnesses of the isolators, provided that each isolator carries a portion of the weight proportional to its stiffness.* To calculate the other natural frequencies, it is necessary to know, in addition, (1) the radii of gyration ρ with respect to various principal inertia axes, (2) horizontal distances b from the respective isolators to principal planes of inertia, (3) vertical distances a from isolators to center of gravity of mounted equipment, and (4) horizontal stiffnesses of the isolators. The radii of gyration usually will have been established by the equipment designer before consideration is given to application of isolators. The dimensions a and b also are usually fixed. There are exceptions to this, however, and any concession that can be obtained in locating the isolators will facilitate the application and improve the resulting performance. The one characteristic that usually is left to be determined, and freedom in this respect is sometimes restricted by other considerations, is the stiffness of the isolators in the several directions.

---

* Methods for determining the necessary stiffnesses of the isolators for meeting this requirement are discussed in detail in Section 4·10 of Chapter 4.

The natural frequency in vertical translation, expressed in cycles per second, is determined in a straightforward manner from Figure 2.3. It seems desirable, in this respect, to call attention to the expression for the natural frequency in translation, equation 2.17. The form of the equation is such that the natural frequency is not modified by multiplying both the equipment weight and the isolator stiffness by a common factor. This principle can be applied to Figure 2.3, where the parameters are beyond the limits of the coordinate scales, by multiplying or dividing both weight and stiffness by equal powers of 10 to determine the natural frequency.

The coupled natural frequencies in rotation and horizontal translation are obtained from Figure 2.8 as a function of the vertical natural frequency and the dimensionless ratios, a/ρ, ρ/b, and k_x/k_y. For a given combination of these ratios, two separate and distinct numerical values of $(\Omega_c/\Omega_y)(\rho/b)$ generally are obtained from the ordinate scale. These values, divided by the ratio ρ/b and multiplied by the previously determined vertical natural frequency, give the two coupled natural frequencies. Where the designer is probing for optimum isolator characteristics and location, the most expedient method of solution is to assume the required physical parameters and to compute the natural frequencies on a cut-and-try basis. The mode of vibration that occurs at any forcing frequency ω is indicated by the location of the center of rotation as defined by equations 2.41 and 2.58.

Figure 2.8 is generally useful in that the two families of curves included therein cover a wide range of applications. The nature of the various parameters makes it difficult, however, to envision the variations in natural frequency that result from changes in the characteristics of the mounted body and of the isolators. These variations may be envisioned more readily by assuming the mounted body to be a homogeneous cuboid with the isolators attached thereto precisely at the corners. If the height of the cuboid is designated by $2a$ and the width of one of the faces by $2b$, the moment of inertia and radius of gyration with respect to an axis through the center of gravity perpendicular to this face are*

$$I = \frac{m[(2a)^2 + (2b)^2]}{12}; \quad \rho = \sqrt{\frac{a^2 + b^2}{3}}. \tag{2.70}$$

---

* See L. S. Marks, *Mechanical Engineers' Handbook*, McGraw-Hill Book Co., New York, 4th edition, 1941, page 212.

The vertical coordinate distance to the isolators is then expressed approximately by a and the corresponding horizontal coordinate distance approximately by b. Designating the ratio of height to width of the equipment by $\lambda = \frac{2a}{2b}$, the following dimensionless ratios are established by substitution in equation 2.70:

$$\frac{a}{\rho} = \sqrt{\frac{3\lambda^2}{1 + \lambda^2}}; \quad \frac{b}{\rho} = \sqrt{\frac{3}{1 + \lambda^2}}. \tag{2.71}$$

Substitution of these dimensionless ratios in equation 2.61 gives the following:

$$\frac{\Omega_c}{\Omega_y} = \frac{1}{\sqrt{2}}\sqrt{\frac{4\eta\lambda^2 + \eta + 3}{\lambda^2 + 1} \pm \sqrt{\left[\frac{4\eta\lambda^2 + \eta + 3}{\lambda^2 + 1}\right]^2 - \frac{12\eta}{1 + \lambda^2}}}. \tag{2.72}$$

This equation is shown graphically in Figure 2.11. Although data obtained from Figure 2.11 should be used with discretion because of the approximations involved, the curves indicate qualitatively the effect of changes in the various characteristics of the mounted equipment and the isolators. The following important trends are worthy of emphasis:

(*a*) Both of the coupled natural frequencies tend to become a minimum, for any ratio of height to width of the mounted body, when the ratio of horizontal to vertical stiffness k_x/k_y of the isolators is low. Conversely, when the ratio of horizontal to vertical stiffness is high, both coupled natural frequencies also tend to be high. It is thus apparent that, when the vibration isolators are located underneath the mounted body, the favorable condition of low natural frequencies is obtained using isolators whose stiffness in a horizontal direction is less than the stiffness in a vertical direction. A low horizontal stiffness may be a liability under some circumstances, however, and is considered further in sections dealing with specific applications.

(*b*) As the ratio of height to width of the mounted body increases, the lower of the coupled natural frequencies decreases. The trend of the higher of the coupled natural frequencies depends on the stiffness ratio of the isolators. It is evident that one of the coupled natural frequencies tends to become very high when (1) the horizontal stiffness of the isolators is greater than the vertical stiffness and (2) when the height of the mounted body is approximately equal to or greater than the width. For any ratio of height to width of mounted body, the spread between the coupled natural frequencies increases as the ratio k_x/k_y of horizontal to vertical stiffness of the isolators increases.

The above methods of determining natural frequencies, transmissibility, and axis of rotation are illustrated below with respect to two

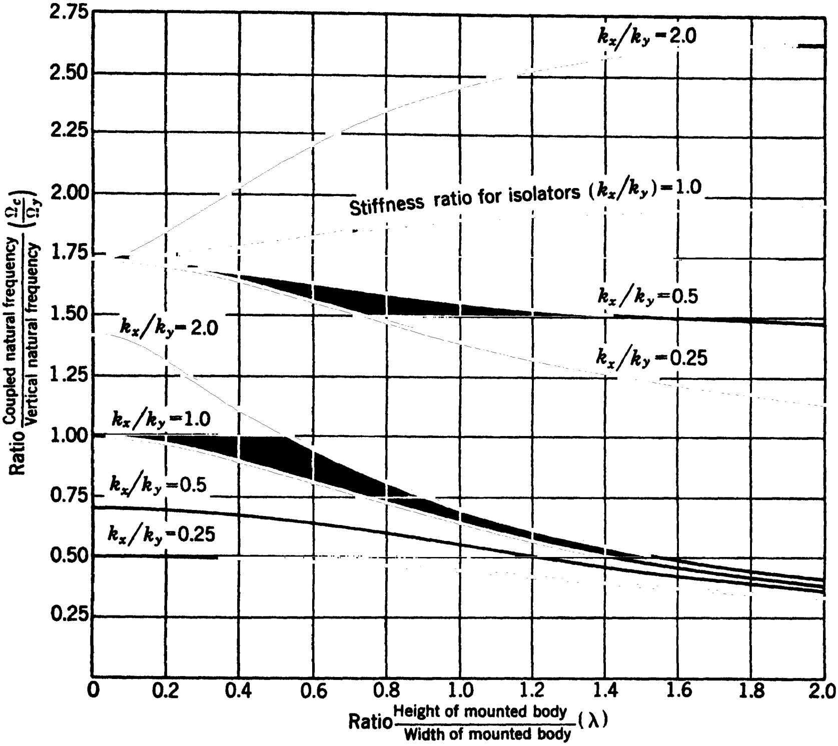

FIGURE 2.11. Curves showing ratio of coupled natural frequencies Ω_c in XY plane to decoupled natural frequency Ω_y in translation along Y axis, for body mounted as shown in Figure 2.7, but having *uniform mass distribution*. The body is assumed to have the shape of a cuboid, and the isolators are attached precisely at the lower corners.

common problems. The first problem involves the isolation of the support from a force created within a machine; the second problem involves the isolation of an equipment from the vibration of its support.

Example 2.1. The machine to be considered, as illustrated schematically in Figure 2.12, is relatively long in the direction of the Z axis and relatively narrow in the direction of the X axis. The force that is to be isolated is harmonic at the constant frequency of 8 cps. It is assumed to result from the rotation of an unbalanced member whose plane of rotation is taken, in the first instance, as a plane perpendicular to the Z axis and, in the second instance, as a plane perpendicular to the X axis. The machine is set upon beams which extend parallel with the X axis and engage the isolators at their opposite ends. The distance between isolators is thus 60 in. measured in the direction of the X axis and 24 in. measured in the direction of the Z axis. The center of coordinates is taken at the center of gravity of the mounted body, i.e., at the center of gravity of the machine-and-beams assembly. The forces are applied on the Y axis 4 in. above the coordinate center ($\epsilon = 4$), and the mid-height of the isolators is 8 in. below the coordinate center ($a = -8$). The total weight of the machine and supporting beam assembly is 100 lb, and its radii of gyration in inches with respect to the three coordinate axes through the center of gravity are $\rho_x = 9$, $\rho_y = 8.5$, $\rho_z = 6$. The isolators are of equal stiffnesses in the directions of the three coordinate axes ($\eta = k_x/k_y = k_z/k_y = 1$).

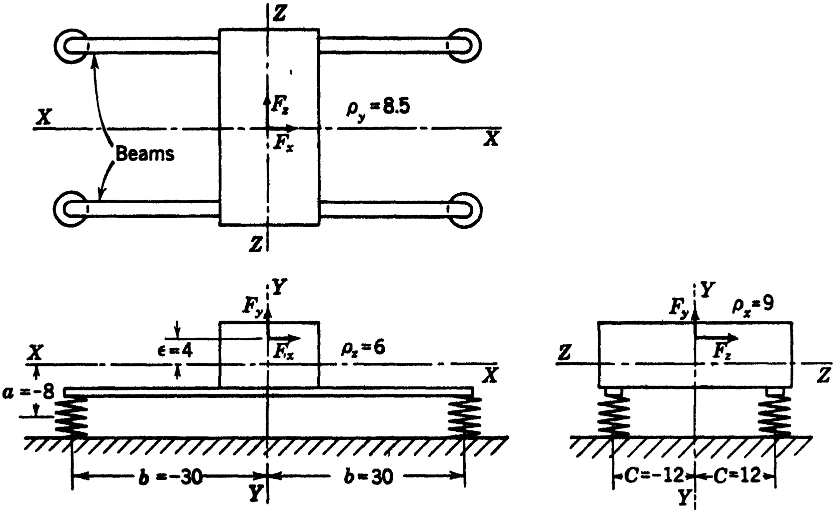

FIGURE 2.12. Mounting method in which isolators are placed at ends of long beams extending in direction of short dimension of mounted body.

The following dimensionless ratios are established as the initial step in the solution:

$$\epsilon/\rho_z = 0.667. \qquad \epsilon/\rho_x = 0.444.$$

$$a/\rho_z = -1.333. \qquad a/\rho_x = -0.889.$$

$$b/\rho_z = \pm 5.0. \qquad c/\rho_x = \pm 1.333.$$

$$a^2/\rho_z^2 = 1.78. \qquad a^2/\rho_x^2 = 0.790.$$

$$b^2/\rho_z^2 = 25.0 \qquad c^2/\rho_x^2 = 1.78.$$

$$\eta\rho_z^2/b^2 = 0.04. \qquad \eta\rho_x^2/c^2 = 0.561.$$

The various natural frequencies are next determined in terms of the vertical natural frequency Ω_y. Referring to Figure 2.8, the coupled natural frequencies for vibration in a plane perpendicular to the Z axis are determined as follows:

$$\frac{\rho_z}{b}\sqrt{\frac{k_x}{k_y}} = 0.2\sqrt{1} = 0.2.$$

For $a/\rho_z = -1.333$, $(\Omega_c/\Omega_y)(\rho_z/b) = 0.19; 1.03$. The signs of the dimensionless ratios a/ρ_z and b/ρ_z require an explanation. According to equation 2.61, the natural frequencies are independent of the sign of a/ρ_z. With regard to the ratio b/ρ_z, the sign chosen should be the same as the sign chosen for the radical on the right side of equation 2.61. The frequency ratio Ω_c/Ω_y then becomes positive. Dividing the above values for $(\Omega_c/\Omega_y)(\rho_z/b)$ by $\rho_z/b = 0.2$: $\Omega_c/\Omega_y = 0.96; 5.15$.

Vibration in a plane perpendicular to the X axis is treated in a similar manner. The expressions for force transmissibility and natural frequency developed in connection with Figure 2.7 consider vibration only in a plane perpendicular to the Z axis. In the present example, exciting forces are not applied concurrently in planes perpendicular to the X and Z axes, and vibration in these two planes is independent. Consequently, the example becomes two independent but similar problems, and similar equations apply:

$$\frac{\rho_x}{c}\sqrt{\frac{k_z}{k_y}} = 0.75\sqrt{1} = 0.75$$

For $a/\rho_x = -0.889$, $(\Omega_c/\Omega_y)(\rho_x/c) = 0.57; 1.29$. Dividing by $\rho_x/c = 0.75$, $\Omega_c/\Omega_y = 0.76; 1.72$.

The natural frequency in rotation with respect to the Y axis is calculated from equation 2.64 as follows:

$$\frac{\Omega_\beta}{\Omega_y} = \sqrt{\frac{1(\overline{30}^2 + \overline{12}^2)}{(8.5)^2}} = 3.80.$$

The six natural frequencies are now tabulated:

(1)	Translatory along Y axis	Ω_y
(2)	Coupled in plane perpendicular to Z axis	$0.96\Omega_y$
(3)	Coupled in plane perpendicular to Z axis	$5.15\Omega_y$
(4)	Coupled in plane perpendicular to X axis	$0.76\Omega_y$
(5)	Coupled in plane perpendicular to X axis	$1.72\Omega_y$
(6)	Rotational with respect to Y axis	$3.80\Omega_y$

An expression for the force transmitted by any isolator is given by equation 2.37. Since the force originates from an unbalanced member rotating in a vertical plane, the term σ in equation 2.37 becomes equal to unity, and the force transmissibility is given by equation 2.38. Expressions for y_0', x_0', and α_0' are given by equations 2.24, 2.28, and 2.29, respectively. Alternate signs are used for the dimensionless ratio b/ρ_z, and numerically different values for transmissibility are obtained at each of two isolators.

In the first instance, the force results from rotation of an unbalanced member in a plane perpendicular to the Z axis, and the force transmissibility as computed from equation 2.38 is shown by the curves in Figure 2.13. The solid line indicates the transmissiblity for each right-hand isolator (ratio b/ρ_z positive); the dotted line indicates the transmissibility for each left-hand isolator (ratio b/ρ_z negative).

When the force results from rotation of the unbalanced member in the plane perpendicular to the X axis, the force transmissibility is shown by the curves in Figure 2.14. The solid curve is applicable to each right isolator (ratio c/ρ_x positive) and the dotted curve is applicable to each left isolator (ratio c/ρ_x negative). Each curve reveals three resonant frequencies. One is in the decoupled vertical mode, which is excited because the force has a component in the direction of the Y axis. The other two are in coupled modes excited by the horizontal component of the force.

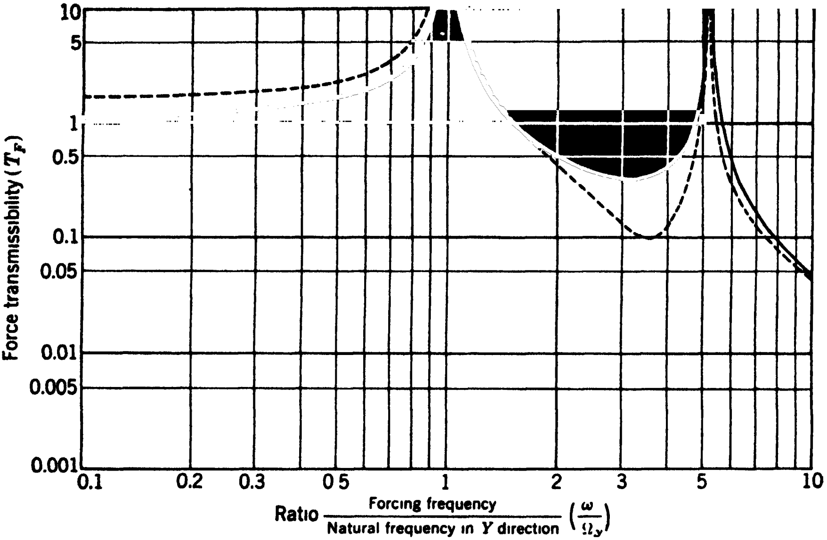

FIGURE 2.13. Force transmissibility attained with arrangement shown in Figure 2.12, when the force arises from rotation of an unbalanced member in a plane normal to the Z axis. The solid curve is applicable to each right-hand isolator (radio b/ρ_z positive), and the dotted curve applies to each left-hand isolator (ratio b/ρ_z negative).

It is desirable to maintain the ratio ω/Ω_y as low as possible, consistent with the required isolation. Effectively, this provides a relatively high value for Ω_y and contributes to good stability. It is evident from Figures 2.13 and 2.14 that a relatively low force transmissibility occurs when $\omega/\Omega_y = 2.5$. This condition is attained at a forcing frequency ω which is greater than any natural frequency shown in Figure 2.14, and between the two coupled natural frequencies indicated in Figure 2.13. Finally, consideration must be given to the natural frequency in rotation with respect to the Y axis. This natural frequency, as indicated above, is $3.8\Omega_y$. A forcing frequency $\omega = 2.5\Omega_y$ thus avoids all natural frequencies.

The stiffness of the isolators is found from the requirement that $\omega/\Omega_y = 2.5$, where $\omega = 8 \times 2\pi$ or 50.3 rad/sec. The vertical natural frequency is then $50.3/2.5 = 20.1$ rad/sec, or 3.2 cps. The necessary stiffness k_y is now computed from equation 2.17, or taken from Figure 2.3, as follows:

$$k_y = \frac{f_n^2 W}{(3.13)^2} = \frac{(3.2)^2 \times 100}{9.80} = 105 \text{ lb/in.}$$

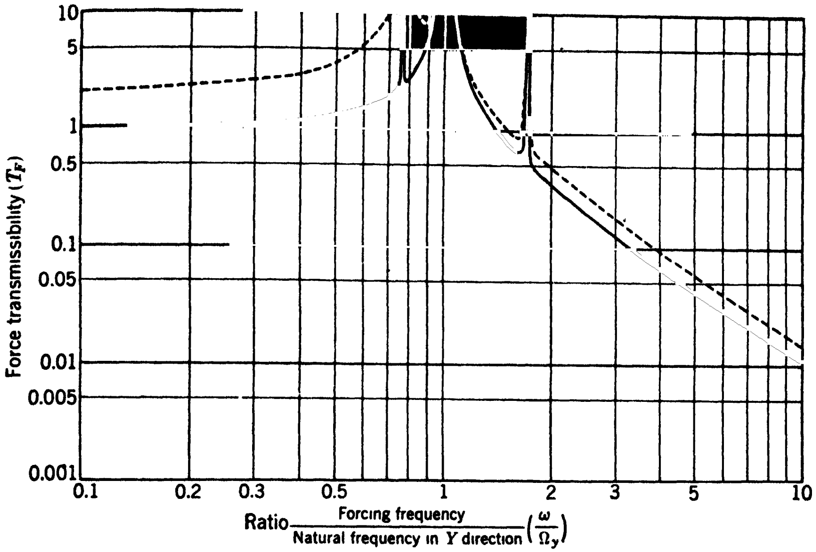

FIGURE 2.14. Force transmissibility attained with arrangement shown in Figure 2.12, when the force arises from rotation of an unbalanced member in a plane normal to the X axis. The solid curve is applicable to each right-hand isolator (ratio c/ρ_x positive), and the dotted curve applies to each left-hand isolator (ratio c/ρ_x negative).

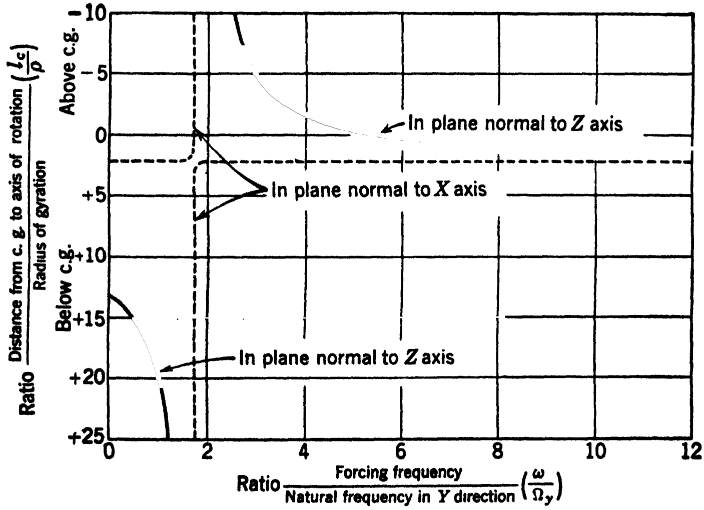

FIGURE 2.15. Location of axes of rotation for system shown in Figure 2.12.

This is the total stiffness of the isolators in the direction of the Y axis. The stiffness of each isolator is $\frac{105}{4} = 26.2$ lb/in. Since the isolators are symmetrical, the stiffnesses in the directions of the X and Z axes are also 26.2 lb/in. for each isolator.

The location of the axis of rotation generally changes as the frequency changes. The distance along the Y axis from the center of coordinates to the axis of rotation, in terms of the radius of gyration, may be determined from equation 2.41. Using the values of x_0' and α_0' calculated above, the ratio l_c/ρ may be plotted as shown in Figure 2.15. The solid line refers to motion in a plane perpendicular to the Z axis; the dotted line refers to motion in a plane perpendicular to the X axis.

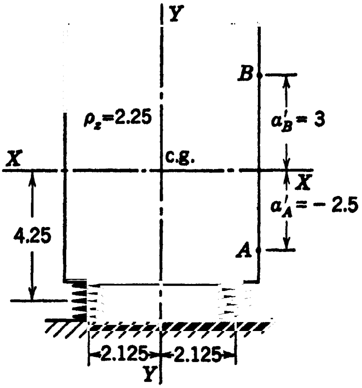

FIGURE 2.16. Rigid body mounted upon isolators located at bottom and excited by horizontal vibration of support. Vibration amplitude at points A and B on mounted body is indicated in Figure 2.17.

Example 2.2. It is desired to determine the horizontal component of vibration at two points on an equipment attached by four isolators to a vibrating support, as illustrated in Figure 2.16. The coordinate center is taken at the center of gravity of the equipment. The isolators are located symmetrically at distances $2\frac{1}{8}$ in. on either side of the coordinate plane normal to the X axis ($b = \pm 2.125$) and $4\frac{1}{4}$ in. below the coordinate plane normal to the Y axis ($a = -4.25$). The stiffness of the isolators in the X direction is 50 percent of their stiffness in the Y direction ($\eta = 0.5$). The radius of gyration with respect to the Z axis is $2\frac{1}{4}$ in. The points A, B whose vibration amplitudes are to be determined are, respectively, $2\frac{1}{2}$ in. below ($a_A' = -2.5$) and 3 in. above ($a_B' = 3$) the X axis. The support vibrates in a horizontal plane in the direction of the X axis in a manner defined by $u = u_0 \sin \omega t$.

The following dimensionless ratios are now established:

$$b/\rho_z = \pm 0.944. \qquad b^2/\rho_z^2 = 0.892.$$

$$a/\rho_z = -1.89. \qquad a^2/\rho_z^2 = 3.57.$$

$$a_A'/\rho_z = -1.11. \qquad a_B'/\rho_z = 1.33.$$

The various natural frequencies that apply to vibration in the XY plane can now be determined as a function of the natural frequency in the direction of the Y axis. Referring to Figure 2.8, the abscissa parameter is determined as follows:

$$\frac{\rho_z}{b}\sqrt{\frac{k_x}{k_y}} = \pm\frac{1}{0.944}\sqrt{0.5} = \pm 0.75.$$

The value of a/ρ_z, as noted above, is -1.89, and the two applicable values of the ordinate are obtained from Figure 2.8 as follows:

$$\frac{\Omega_c}{\Omega_y} \times \frac{\rho_z}{b} = 0.41;\ 1.82.$$

Dividing by $\rho_z/b = \pm 1/0.944$:

$$\frac{\Omega_c}{\Omega_y} = 0.39;\ 1.72,$$

where the sign of ρ_z/b is governed by the considerations set forth on page 63. The three natural frequencies in the XY plane are thus the translatory natural frequency Ω_y in the Y direction, which is decoupled because of symmetry, and the coupled rotational and translatory natural frequencies Ω_c, which are equal to $0.39\Omega_y$ and $1.72\Omega_y$.

The first step in determining the motion at points A, B is to evaluate equations 2.52 and 2.53. This calculation employs the dimensionless ratios noted above and yields x_0/u_0 and $\alpha_0\rho_z/u_0$ as functions of ω/Ω_y. Substitution of these values of x_0/u_0 and $\alpha_0\rho_z/u_0$ in equation 2.57, together with the appropriate values a_A', a_B', gives numerical values for $(x_A)_0/u_0$, $(x_B)_0/u_0$ as functions of ω/Ω_y. These values are plotted in Figure 2.17. Important relevant results indicated by these curves may be summarized as follows:

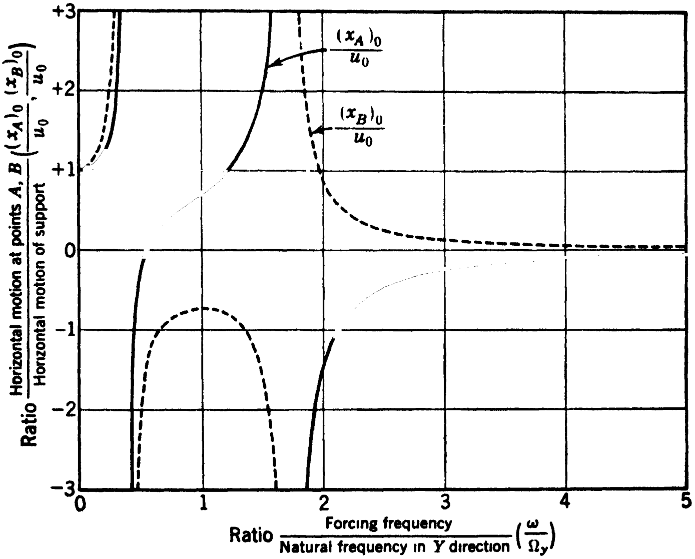

FIGURE 2.17. Horizontal component of motion at points A and B on body shown in Figure 2.16, as a result of horizontal vibration of support. Positive sign indicates that these points move in phase with the support; negative sign indicates out of phase.

(*a*) The horizontal motion $(x_A)_0$ or $(x_B)_0$ is comprised of a translatory component x_0, and a rotational component $a_A'\alpha_0$ or $a_B'\alpha_0$. The coefficients a_A' and a_B' are of opposite sign and cause $(x_A)_0$ and $(x_B)_0$ to take opposite signs when $a'\alpha_0$ is large relative to x_0. In a physical sense, this occurs when the axis of rotation is near the center of gravity, i.e., when $\alpha_0 \gg x_0$, as indicated by equation 2.40.

(*b*) Both the vibration amplitudes x_A, x_B tend to become infinite at the forcing frequencies $\omega = 0.39\Omega_y$, $1.72\Omega_y$. These are the natural frequencies found above. The existence of damping in the isolators would cause the amplitude to remain finite, at a value that depends on the degree of damping.

(*c*) No resonant effect appears at the natural frequency Ω_y. Translatory vibration in the direction of the Y axis is decoupled from vibration in other modes, and is therefore excited only by vibration of the support in the Y direction. The support is assumed here to vibrate only in the X direction.

(*d*) In general, the vibration amplitude at all points on the mounted equipment becomes less than that of the support only at forcing frequencies somewhat higher than the highest natural frequency of the system. Some incidental instances of low transmissibility occasionally are found to occur at certain points on the equipment at forcing frequencies between the natural frequencies.

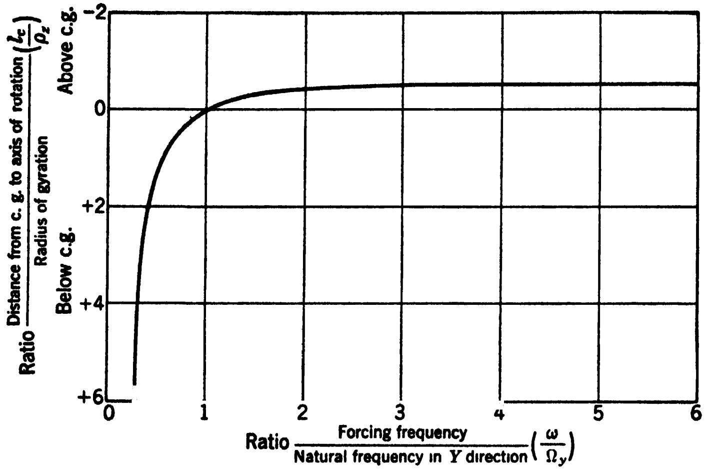

FIGURE 2.18. Location of axis of rotation for mounted body shown in Figure 2.16.

The location of the axis of rotation is given by equation 2.58. Values of l_c/ρ_z are plotted in Figure 2.18 as a function of the frequency ratio ω/Ω_y, using the dimensionless ratios $b/\rho_z = 0.944$, $a/\rho_z = -1.89$ indicated above. At low forcing frequencies, l_c is a large positive number; i.e., the axis of rotation is located far below the equipment. At high forcing frequencies, the axis of rotation is a small distance above the center of gravity of the equipment, as indicated by the small negative value of l_c. It is of interest to note that l_c/ρ_z is a small number when $\omega/\Omega_y > 0.75$. The axis of rotation is then near the center of gravity, and the signs of $(x_A)_0$ and $(x_B)_0$ are different, as indicated in Figure 2.17.

2·8 *Natural Frequencies—One Plane of Symmetry*

The preceding analysis considers systems whose vibration in the vertical translatory mode is decoupled from that in horizontal and rotational modes. This is achieved by symmetry with respect to two vertical principal planes of inertia, or by adjustment of the stiffness of each isolator proportionately to the dead-weight load which it supports. There are occasions when symmetry is not feasible with respect to two principal planes but can be achieved with respect to one vertical principal plane. Motion of the mounted body in a plane parallel with the plane of symmetry is then comprised of three coupled modes of vibration, each having vertical, horizontal, and rotational components. The natural frequencies in these modes are determined in the manner employed heretofore, except that the three coupled modes introduce a third-degree equation. Its solution yields the three natural frequencies.

The analysis is illustrated with respect to the system shown in Figure 2.19, wherein symmetry with respect to the XY plane is assumed. The following equations apply to all systems that embody the assumed symmetry, or in which motion in the XY plane is otherwise decoupled from motion normal to the XY plane. Symbols and notations used are as follows:

X, Y, Z = principal axes of inertia through center of gravity.
$k_{y_1}, k_{y_2}, \cdots, k_{y_n}$ = stiffness of each isolator in Y direction.
$k_{x_1}, k_{x_2}, \cdots, k_{x_n}$ = stiffness of each isolator in X direction.
$a_1, a_2, \cdots, a_n$ = distance to each isolator from XZ plane.
$b_1, b_2, \cdots, b_n$ = distance to each isolator from YZ plane.
m = mass of mounted body.
I_z = moment of inertia of mounted body with respect to Z axis.

The differential equations of motion are derived by writing a summation of forces and couples acting on the mounted body, as explained in Section 1·7 of Chapter 1. The external forces and couples result from the elastic deflection of the isolators, and from the applied couple $M = M_0 \sin \omega t$. These external forces and couples are equated to the inertia forces and couples, care being taken to observe the indicated convention of signs. The proper signs for the distances from the coordinate axes to the isolators must be employed. These distances are taken as positive if upward or toward the right, negative if downward or toward the left.

The differential equations of motion are:

$$\begin{aligned} I_z\ddot{\alpha} = {} & -\alpha[k_{x_1}a_1^2 + k_{x_2}a_2^2 + k_{x_3}a_3^2 + k_{y_1}b_1^2 + k_{y_2}b_2^2 + k_{y_3}b_3^2] \\ & + x[k_{x_1}a_1 + k_{x_2}a_2 + k_{x_3}a_3] - y[k_{y_1}b_1 + k_{y_2}b_2 + k_{y_3}b_3] \\ & + M_0 \sin \omega t, \end{aligned} \tag{2.73}$$

$$m\ddot{x} = -x[k_{x_1} + k_{x_2} + k_{x_3}] + \alpha[k_{x_1}a_1 + k_{x_2}a_2 + k_{x_3}a_3], \tag{2.74}$$

$$m\ddot{y} = -y[k_{y_1} + k_{y_2} + k_{y_3}] - \alpha[k_{y_1}b_1 + k_{y_2}b_2 + k_{y_3}b_3]. \tag{2.75}$$

The terms in the above equations follow regular patterns which may be written as summations to include any number and arrangement of isolators. Equations 2.73 to 2.75 then become:

$$I_z\ddot{\alpha} = -\alpha(\Sigma a_n{}^2 k_{x_n} + \Sigma b_n{}^2 k_{y_n}) + x\Sigma a_n k_{x_n} - y\Sigma b_n k_{y_n} + M_0 \sin \omega t, \qquad (2.76)$$

$$m\ddot{x} = -x\Sigma k_{x_n} + \alpha\Sigma a_n k_{x_n}, \qquad (2.77)$$

$$m\ddot{y} = -y\Sigma k_{y_n} - \alpha\Sigma b_n k_{y_n}. \qquad (2.78)$$

It is necessary now to effect the simultaneous solution of the three equations above. The first step in obtaining such a solution is to write expressions for the translatory and rotational components of displacement of the mounted body at the forcing frequency ω, neglecting transient terms:

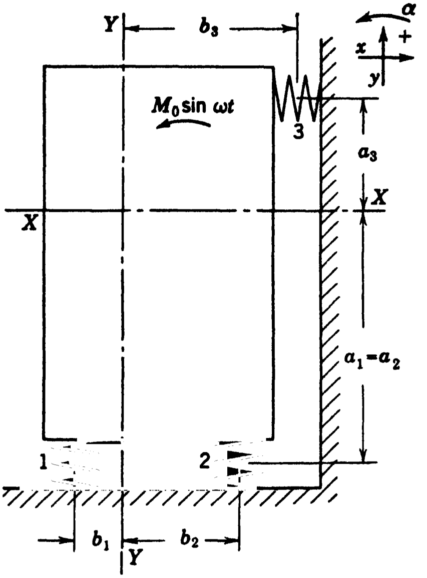

FIGURE 2.19.

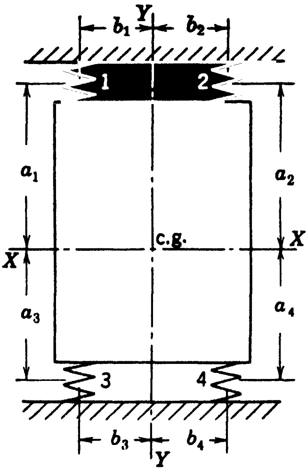

FIGURE 2.20.

FIGURE 2.19. Elevation view of rigid body mounted upon isolators, and having a single plane of symmetry. The mounted body and isolator arrangement are symmetrical with respect to the XY plane passing through the center of gravity of the body.

FIGURE 2.20. Elevation view of rigid body supported by isolators at top and bottom.

$$\begin{aligned} \alpha &= \alpha_0 \sin \omega t; & x &= x_0 \sin(\omega t + \psi_x); \\ & & y &= y_0 \sin(\omega t + \psi_y), \\ \ddot{\alpha} &= -\alpha_0\omega^2 \sin \omega t; & \ddot{x} &= -x_0\omega^2 \sin(\omega t + \psi_x); \\ & & \ddot{y} &= -y_0\omega^2 \sin(\omega t + \psi_y). \end{aligned} \tag{2.79}$$

Upon substitution from equations 2.79 in equations 2.76 to 2.78, it becomes apparent that a solution to the set of equations occurs when and only when $\psi_x = \psi_y = 0$.

The natural frequencies are determined, as in the preceding cases, by obtaining an expression for one of the displacement components and equating its denominator to zero. The following expression is obtained from the simultaneous solution of equations 2.76 to 2.78, after having first substituted from equations 2.79 and set $\psi_x = \psi_y = 0$:

$$\alpha_0 = \frac{M_0(m\omega^2 - \Sigma k_{x_n})(m\omega^2 - \Sigma k_{y_n})}{A\omega^6 + B\omega^4 + C\omega^2 + D}, \tag{2.80}$$

where

$$A = -I_z m^2. \tag{2.81}$$

$$B = m^2(\Sigma b_n{}^2 k_{y_n} + \Sigma a_n{}^2 k_{x_n}) + I_z m(\Sigma k_{x_n} + \Sigma k_{y_n}). \tag{2.82}$$

$$\begin{aligned} C = {} & -m(\Sigma k_{x_n} + \Sigma k_{y_n})(\Sigma b_n{}^2 k_{y_n} + \Sigma a_n{}^2 k_{x_n}) \\ & - I_z \Sigma k_{x_n} \Sigma k_{y_n} + m(\Sigma a_n k_{x_n})^2 + m(\Sigma b_n k_{y_n})^2. \end{aligned} \tag{2.83}$$

$$\begin{aligned} D = {} & \Sigma k_{x_n} \Sigma k_{y_n}(\Sigma b_n{}^2 k_{y_n} + \Sigma a_n{}^2 k_{x_n}) - \Sigma k_{y_n}(\Sigma a_n k_{x_n})^2 \\ & - \Sigma k_{x_n}(\Sigma b_n k_{y_n}).^2 \end{aligned} \tag{2.84}$$

The denominator of equation 2.80, when equated to zero, gives a cubic equation whose variable is ω^2. Three numerically different values of ω are thus obtained, which represent the natural frequencies, expressed in radians per second, of the mounted body in the three coupled modes of vibration. Inasmuch as the modes are coupled, each mode includes components in vertical and horizontal translation and in rotation.

The immediately preceding analysis is useful in determining the characteristics of systems that embody unusual arrangements of isolators, even though three coupled modes of vibration do not exist. The system shown in Figure 2.20, for example, is assumed to be symmetrical with respect to principal inertia planes that are respectively normal to the X and Z axes. The horizontal coordinate distances b to the isolators are then numerically equal; their signs are dependent on the positions of the respective isolators with reference to the YZ plane. As a result of this symmetry, the summation $\Sigma b_n k_{y_n}$ vanishes. Equations 2.76 to 2.78 then become:

$$I_z\ddot{\alpha} = -\alpha[\Sigma a_n{}^2 k_{x_n} + \Sigma b_n{}^2 k_{y_n}] + x\Sigma a_n k_n + M_0 \sin \omega t, \quad (2.85)$$

$$m\ddot{x} = -x\Sigma k_{x_n} + \alpha\Sigma a_n k_{x_n}, \quad (2.86)$$

$$m\ddot{y} = -y\Sigma k_{y_n}. \quad (2.87)$$

Equation 2.87 includes a single variable, the vertical displacement y. The natural frequency in the decoupled vertical translatory mode may then be determined directly from equation 2.87. The horizontal and rotational modes remain coupled, however, as evidenced by the presence of the displacements x, α in both equations 2.85 and 2.86. The natural frequencies in the coupled modes now may be determined from the simultaneous solution of these two equations in the manner discussed in Section 2·6.

Interesting results are obtained from further simplification of the system. The quadratic equation obtained from the simultaneous solution of equations 2.85 and 2.86 includes the expression $(\Sigma b_n{}^2 k_{y_n})/(\Sigma k_{y_n})$. The numerical value of this expression as calculated from the physical constants of the system will be designated b'. Then, if $a_1 = a_2 = \cdots a_n = a'$, the expression obtained from the solution of equations 2.85 and 2.86 will be found identical to equation 2.61, provided that a' is replaced by a and b' is replaced by b. The curves of Figure 2.8 thus apply to the determination of the natural frequencies of the system shown in Figure 2.20 when each isolator is located an equal distance from the horizontal coordinate plane.

Example 2.3. An equipment is mounted in the manner illustrated in Figure 2.19. The data required to calculate the natural frequencies are:

$a_1 = a_2 = -12$ in.; $a_3 = 7$ in.
$b_1 = 4$ in.; $b_2 = 8$ in.; $b_3 = 10$ in.
$k_{y_1} = 250$ lb/in.; $k_{y_2} = 150$ lb/in.; $k_{y_3} = 0$.
$k_{x_1} = 250$ lb/in.; $k_{x_2} = 150$ lb/in.; $k_{x_3} = 200$ lb/in.
Weight of equipment = 100 lb.
Radius of gyration with respect to Z axis, $\rho_z = 10$ in.

The moment of inertia I_z with respect to the Z axis is calculated from the mass and radius of gyration:

$$I_z = m\rho_z{}^2 = \frac{100}{386}(10)^2 = 25.9 \text{ lb-in. sec}^2.$$

The coefficients defined by equations 2.81 to 2.84, inclusive, are now calculated as follows:

$$A = -25.9\left(\frac{100}{386}\right)^2 = -1.74,$$

$$\begin{aligned} B = \left(\frac{100}{386}\right)^2 &[16 \times 250 + 64 \times 150 + 144 \times 250 + 144 \times 150 + 49 \times 200] \\ &+ 25.9\left(\frac{100}{386}\right)[250 + 150 + 250 + 150 + 200] = 12.146 \times 10^3, \end{aligned}$$

$$\begin{aligned} C = -\left(\frac{100}{386}\right) &(250 + 150 + 200 + 250 + 150) \\ &(16 \times 250 + 64 \times 150 + 144 \times 250 + 144 \times 150 + 49 \times 200) \\ &- 25.9(250 + 150 + 200)(250 + 150) \\ &+ \left(\frac{100}{386}\right)(-12 \times 250 - 12 \times 150 + 7 \times 200)^2 \\ &+ \left(\frac{100}{386}\right)(-4 \times 250 + 8 \times 150)^2 = -24.225 \times 10^6, \end{aligned}$$

$$\begin{aligned} D = {} &(250 + 150 + 200)(250 + 150) \\ &(16 \times 250 + 64 \times 150 + 144 \times 250 + 144 \times 150 + 49 \times 200) \\ &- (250 + 150)(-12 \times 250 - 12 \times 150 + 7 \times 200)^2 \\ &- (250 + 150 + 200)(-4 \times 250 + 8 \times 150)^2 = 14.816 \times 10^9 \end{aligned}$$

Substituting these coefficients in the denominator of equation 2.80 and equating the resultant expression to zero:

$$-1.74\Omega^6 + 12.146 \times 10^3\Omega^4 - 24.225 \times 10^6\Omega^2 + 14.816 \times 10^9 = 0.$$

This is a cubic equation whose variable is Ω^2. The three natural frequencies of the system in the three coupled modes of vibration in the XY plane are then the three numerically different roots of the above equation as follows:

$$\Omega = 64.0;\ 40.3;\ 36.5 \text{ rad/sec.}$$

Expressed in cycles per second, the natural frequencies are:

$$f_n = 10.2;\ 6.4;\ 5.8 \text{ cps.}$$

*2·9 Inclined Isolators**

The preceding analyses refer to systems in which the principal elastic axes of the various isolators are respectively parallel with the principal inertia axes of the mounted body. Advantages sometimes derive from inclining the principal elastic axes of the isolators. The properties of a system with inclined isolators are determined below, with reference to Figure 2.21. The coordinate axes X and Y are respectively parallel with the principal inertia axes of the mounted body, but the center of coordinates is taken at the elastic axis, whose significance is explained later. The principal elastic axes of the isolators are indicated by p and q, and the stiffness of each isolator in the direction of the respective principal axis is indicated by k_p and k_q. The principal elastic axis p forms an angle θ with the horizontal. Symmetry with respect to the XY plane is assumed.

---

* Parts of this analysis are suggested by C. D. Pengelley, "Ground Vibration Tests," *Jour. Aero. Sci.*, Vol. 9, No. 13, November 1942, and by private correspondence with Mr. Pengelley.

A displacement of the mounted body in the direction of the coordinate axes X, Y has components in the directions of both principal elastic axes p, q of the isolators. The magnitudes of the elastic forces and couples exerted by the isolators as a result of this displacement can be determined most conveniently by noting the deflections of the isolators in the directions of their principal elastic axes p, q; finding the resultant forces in these directions; and taking the components of these resultant forces in the directions of the coordinate axes. The magnitudes of the various forces in the directions of the principal elastic axes, and their components in the directions of the coordinate axes, are as follows:

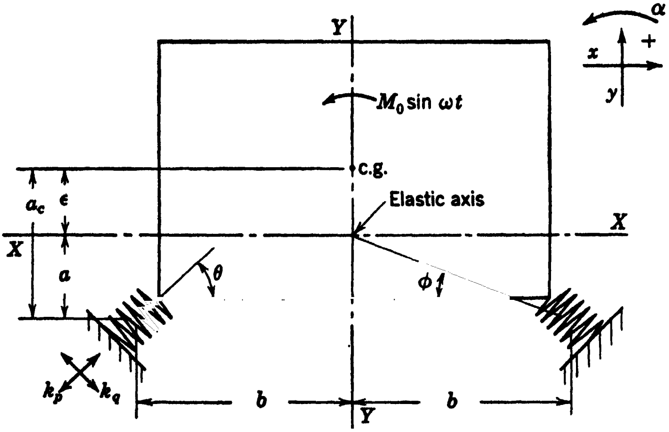

FIGURE 2.21. Elevation view of rigid body mounted upon isolators having principal elastic axes inclined with respect to principal inertia axes of mounted body.

For a positive (upward) displacement δ_y of a corner of the mounted body to which the isolators are attached, the elastic forces resulting from the deflection of one isolator are:

p Direction	q Direction	Vertical Component	Horizontal Component
$k_p\delta_y \sin\theta$		$-k_p\delta_y \sin^2\theta$	$-k_p\delta_y \sin\theta\cos\theta$
	$k_q\delta_y \cos\theta$	$-k_q\delta_y \cos^2\theta$	$+k_q\delta_y \sin\theta\cos\theta$

For a positive (rightward) displacement δ_x of a corner of the mounted body to which the isolators are attached, the elastic forces exerted by a single isolator are:

p Direction	q Direction	Vertical Component	Horizontal Component
$k_p\delta_x \cos\theta$		$-k_p\delta_x \sin\theta\cos\theta$	$-k_p\delta_x \cos^2\theta$
	$k_q\delta_x \sin\theta$	$+k_q\delta_x \sin\theta\cos\theta$	$-k_q\delta_x \sin^2\theta$

Any system comprised of a rigid body and elastic supports has an elastic axis. If a constant force is applied to the body along a line extending through the elastic axis, the body is displaced in translation without rotation; and, if a constant couple is applied with respect to the elastic axis, the body is displaced in rotation without translation. In Figure 2.21, the equipment is supported by isolators at the four lower corners; because of symmetry, the elastic axis extends in a direction normal to the XY plane and intersects the Y axis. The point of intersection with the Y axis is the point through which a static horizontally directed force may be applied to the body and about which the summation of all couples acting on the body then becomes equal to zero. Effecting a small horizontal displacement δ_x of the mounted body, and equating the summation of elastic couples to zero:

$$-4bk_p\delta_x \sin\theta\cos\theta + 4bk_q\delta_x \sin\theta\cos\theta + 4ak_p\delta_x \cos^2\theta + 4ak_q\delta_x \sin^2\theta = 0. \quad (2.88)$$

Dividing both sides of the above equation by $4b\delta_x \sin\theta\cos\theta$:

$$-k_p + k_q + \frac{a}{b}\frac{k_p}{\tan\theta} + \frac{a}{b}k_q \tan\theta = 0.$$

Solving the immediately preceding equation for a/b:

$$\frac{a}{b} = \frac{[1 - (k_q/k_p)]\tan\theta}{(k_q/k_p)\tan^2\theta + 1}. \quad (2.89)$$

Equation 2.89 is shown graphically in Figure 2.22. It defines the location of the elastic axis of the system in terms of the spacing between isolators, the stiffness ratio of the isolators, and the angle of inclination of the principal elastic axes of the isolators. The elastic axis is made to extend through the center of coordinates by taking the Z axis to be coincident with the elastic axis.

Expressions will now be derived for the stiffness of the composite system in several coordinate directions. If a force F_y parallel to the Y axis is applied at the elastic axis and a deflection δ_y results, the following equation of static equilibrium may be written:

$$F_y = 4k_p\delta_y \sin^2\theta + 4k_q\delta_y \cos^2\theta,$$

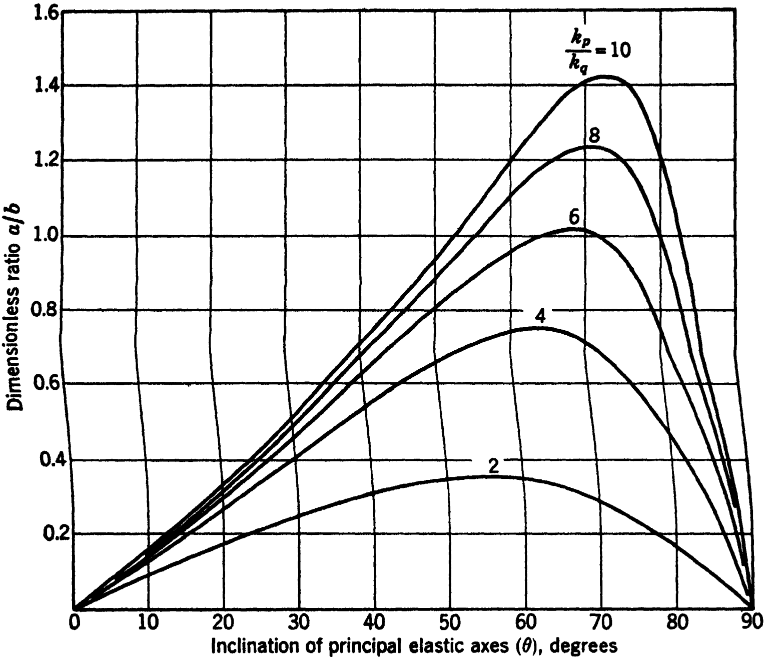

FIGURE 2.22. Relation between position of elastic axis, distance between isolators, angle of inclination of principal elastic axes of isolators, and ratio of principal stiffnesses; for system shown in Figure 2.21.

where the forces exerted by the isolators are taken from the table on page 74. The stiffness in the Y direction is found by dividing both sides of the above equation by the deflection δ_y:

$$k_y = \frac{F_y}{\delta_y} = 4k_q\left(\frac{k_p}{k_q}\sin^2\theta + \cos^2\theta\right). \tag{2.90}$$

Similarly, applying a force F_x at the elastic axis and writing the equation of static equilibrium:

$$F_x = 4k_p\delta_x\cos^2\theta + 4k_q\delta_x\sin^2\theta.$$

The stiffness in the X direction is found by dividing both sides of the immediately preceding equation by the deflection δ_x:

$$k_x = \frac{F_x}{\delta_x} = 4k_q\left(\sin^2\theta + \frac{k_p}{k_q}\cos^2\theta\right). \tag{2.91}$$

The rotational stiffness with respect to the elastic axis is determined by applying a static couple M_α which acts in a positive or counterclockwise direction and causes a positive angular displacement α. The elastic restoring couples resulting from deflection of the isolators are included in the following equation of static equilibrium, using the forces outlined on pages 74 and 75.

$$\begin{aligned}M_\alpha = 4\alpha b^2(k_p \sin^2 \theta + k_q \cos {}^2\theta)& \\ - 4\alpha ba(k_p \sin \theta \cos \theta - k_q \sin \theta \cos \theta)& \\ + 4\alpha a^2(k_q \sin^2 \theta + k_p \cos^2 \theta)& \\ - 4\alpha ba(k_p \sin \theta \cos \theta - k_q \sin \theta \cos \theta).& \quad (2.92)\end{aligned}$$

The rotational stiffness k_α is found from the above equation by dividing both sides by α and writing $a/b = \tan \phi$:

$$k_\alpha = \frac{M_\alpha}{\alpha} = 4b^2k_q\left[\frac{k_p}{k_q}(\sin \theta - \tan \phi \cos \theta)^2 + (\tan \phi \sin \theta + \cos \theta)^2\right]. \quad (2.93)$$

The relation between ϕ and θ is found from equation 2.89 by substituting $a/b = \tan \phi$ and $\tan \theta = \sin \theta/\cos \theta$. Then:

$$\tan \phi = \frac{[1 - (k_q/k_p)] \sin \theta \cos \theta}{\cos^2 \theta + (k_q/k_p) \sin^2 \theta}. \quad (2.94)$$

The angle ϕ is now eliminated as a factor in the expression for rotational stiffness, equation 2.93, by substituting for $\tan \phi$ the expression given by equation 2.94. The following expression for rotational stiffness then results:

$$k_\alpha = \frac{4b^2k_q}{\cos^2 \theta + (k_q/k_p) \sin^2 \theta}. \quad (2.95)$$

Forced vibration at a constant frequency ω is assumed to result only from the couple $M = M_0 \sin \omega t$ applied to the mounted body. The differential equation of motion for the mounted body in the direction of the Y axis is obtained from equation 1.72 of Chapter 1, noting that the only external *force* acting on the body is derived from the deflection of the isolators:

$$-k_y y = m\ddot{y}, \quad (2.96)$$

where k_y is the total stiffness of the system in the direction of the Y axis.

In writing the differential equation of motion for the mounted body in the direction of the X axis, it should be noted that the displacement of the center of gravity in the direction of the X axis is $x - \epsilon\alpha$, and that the corresponding acceleration is $\ddot{x} - \epsilon\ddot{\alpha}$. By definition of the elastic axis, a translatory displacement x produces only an external force $-k_x x$, whereas a rotational displacement α with respect to a coordinate axis produces only an external couple $-k_\alpha \alpha$. Equating the horizontal force applied by the isolators to the horizontal inertia force:

$$m(\ddot{x} - \epsilon\ddot{\alpha}) = -k_x x. \tag{2.97}$$

The differential equation of motion for the mounted body in rotation about the Z axis is obtained from equation 1.75 of Chapter 1. In the system shown in Figure 2.21, the coordinate plane perpendicular to the X axis is a plane of symmetry, and the last term on the right side of equation 1.75 drops out because $b_g = 0$. The external couples are the applied couple M and the couple $-k_\alpha \alpha$ resulting from the rotational displacement α; no *couple* results from the translatory displacement x. Then:

$$m\rho_e^2\ddot{\alpha} - m\epsilon\ddot{x} = -k_\alpha \alpha + M_0 \sin \omega t, \tag{2.98}$$

where ρ_e is the radius of gyration of the mounted body with respect to the elastic axis.

The solution of the above equations of motion is obtained by assuming that the variation of displacement as a function of time is sinusoidal in accordance with the following relations:

$$y = y_0 \sin \omega t; \quad x = x_0 \sin \omega t; \quad \alpha = \alpha_0 \sin \omega t.$$

Substituting these relations in equations 2.96 to 2.98:

$$-my_0\omega^2 = -k_y y_0, \tag{2.99}$$

$$-mx_0\omega^2 + m\epsilon\alpha_0\omega^2 = -k_x x_0, \tag{2.100}$$

$$-m\rho_e^2\alpha_0\omega^2 + m\epsilon x_0\omega^2 = -k_\alpha \alpha_0 + M_0. \tag{2.101}$$

The following substitutions are now made:

$$\frac{k_x}{m} = \Omega_x^2; \quad \frac{k_\alpha}{m\rho_e^2} = \Omega_\alpha^2. \tag{2.102}$$

The frequencies indicated by equations 2.102 do not generally refer to natural modes of vibration. They are designated uncoupled natural frequencies, which are distinct from decoupled natural frequencies in natural modes of vibration. The modes in the x and α directions are coupled, in general, and can exist independently (uncoupled) only if the mounted body is constrained to move in the particular mode being considered.

Substituting from equations 2.102 in equations 2.100 and 2.101:

$$x_0(\omega^2 - \Omega_x^2) - \rho_e\alpha_0\omega^2\left(\frac{\epsilon}{\rho_e}\right) = 0, \qquad (2.103)$$

$$\rho_e\alpha_0(\omega^2 - \Omega_\alpha^2) - \left(\frac{\epsilon}{\rho_e}\right)x_0\omega^2 + \frac{M_0}{m\rho_e} = 0. \qquad (2.104)$$

The two coupled natural frequencies are obtained from the simultaneous solution of equations 2.103 and 2.104. Solving for α_0:

$$\alpha_0 = \frac{-M_0/(m\rho_e)}{\rho_e(\omega^2 - \Omega_\alpha^2) - \dfrac{\rho_e(\epsilon/\rho_e)^2\omega^4}{\omega^2 - \Omega_x^2}}. \qquad (2.105)$$

The maximum displacement α_0 becomes infinite when the denominator of equation 2.105 is equal to zero:

$$[1 - (\epsilon/\rho_e)^2]\omega^4 - (\Omega_\alpha^2 + \Omega_x^2)\omega^2 + \Omega_\alpha^2\Omega_x^2 = 0 \qquad (2.106)$$

The coupled natural frequencies are the numerically different roots of equation 2.106, letting $\omega = \Omega_c$:

$$\Omega_c = \sqrt{\frac{(\Omega_\alpha^2 + \Omega_x^2) \pm \sqrt{(\Omega_\alpha^2 + \Omega_x^2)^2 - 4\Omega_\alpha^2\Omega_x^2[1 - (\epsilon/\rho_e)^2]}}{2[1 - (\epsilon/\rho_e)^2]}} \qquad (2.107)$$

The coupled natural frequencies can be defined with respect to the uncoupled natural frequency Ω_x by writing the relation

$$\lambda_1 = \frac{\Omega_\alpha}{\Omega_x}, \qquad (2.108)$$

and substituting $\Omega_\alpha = \lambda_1\Omega_x$ in equation 2.107. Then

$$\frac{\Omega_c}{\Omega_x} = \sqrt{\frac{1 + \lambda_1^2 \pm \sqrt{(1 + \lambda_1^2)^2 - 4\lambda_1^2[1 - (\epsilon/\rho_e)^2]}}{2[1 - (\epsilon/\rho_e)^2]}} \qquad (2.109)$$

Equation 2.109 is shown graphically in Figure 2.23. To obtain numerical values for the coupled natural frequencies Ω_c, it is necessary to evaluate the uncoupled natural frequency Ω_x and the frequency ratio λ_1. An expression for Ω_x is given by equation 2.102 in terms of k_x. Using the stiffness k_x given by equation 2.91, Ω_x can be written in terms of the fictitious natural frequency $\Omega_p = \sqrt{4k_p/m}$. The latter has no physical significance inasmuch as the p axes of the isolators are not respectively parallel; it is readily calculable, however, and is useful as an aid in analysis. The resulting expression for the frequency ratio Ω_x/Ω_p is:

$$\frac{\Omega_x}{\Omega_p} = \sqrt{\frac{k_q}{k_p}\sin^2\theta + \cos^2\theta}. \tag{2.110}$$

The natural frequency in the direction of the Y axis occurs in a natural mode of vibration and is decoupled because of symmetry of the system. An expression for the frequency ratio Ω_y/Ω_p may be determined in a manner similar to that employed to obtain Ω_x/Ω_p, using the expression for k_y given by equation 2.90:

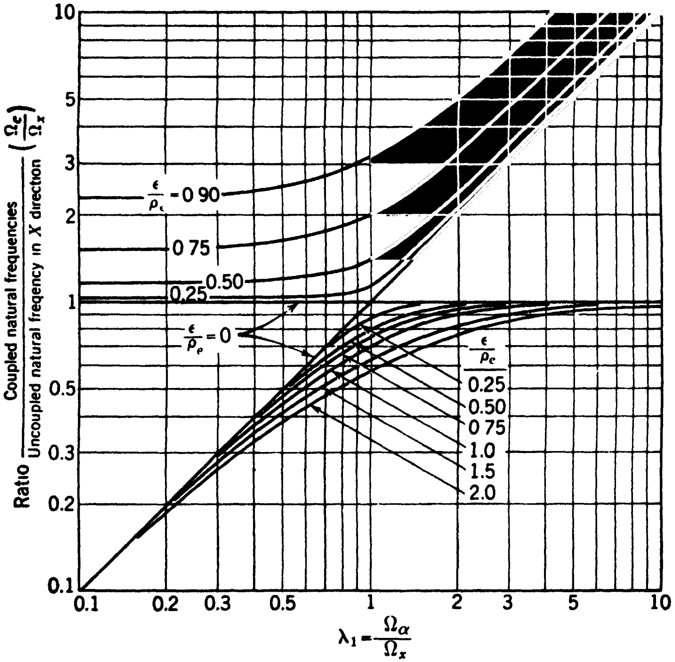

FIGURE 2.23. Ratio of coupled natural frequencies Ω_c to uncoupled natural frequency Ω_x in X direction, for system shown in Figure 2.21. The radius of gyration with respect to the elastic axis is indicated by ρ_e. For definition of Ω_α and Ω_x, see equations 2.102.

$$\frac{\Omega_y}{\Omega_p} = \sqrt{\sin^2\theta + \frac{k_q}{k_p}\cos^2\theta}. \tag{2.111}$$

An expression for the uncoupled natural frequency Ω_α in rotation is given by equation 2.102. Substituting the expression for rotational stiffness k_α given by equation 2.95, and dividing by the fictitious natural frequency $\Omega_p = \sqrt{4k_p/m}$:

$$\frac{\Omega_\alpha}{(b/\rho_e)\Omega_p} = \sqrt{\frac{1}{(k_p/k_q)\cos^2\theta + \sin^2\theta}}. \tag{2.112}$$

An expression for the frequency ratio λ_1 is now obtained as a result of dividing equation 2.112 by equation 2.110, and substituting the relation of equation 2.108:

$$\lambda_1\left(\frac{\rho_e}{b}\right) = \frac{1}{\sqrt{[(k_p/k_q)\cos^2\theta + \sin^2\theta][(k_q/k_p)\sin^2\theta + \cos^2\theta]}}, \tag{2.113}$$

where ρ_e is the radius of gyration with respect to the elastic axis. Equations 2.110, 2.111, and 2.113 are shown graphically in Figures 2.24, 2.25, and 2.26, respectively.

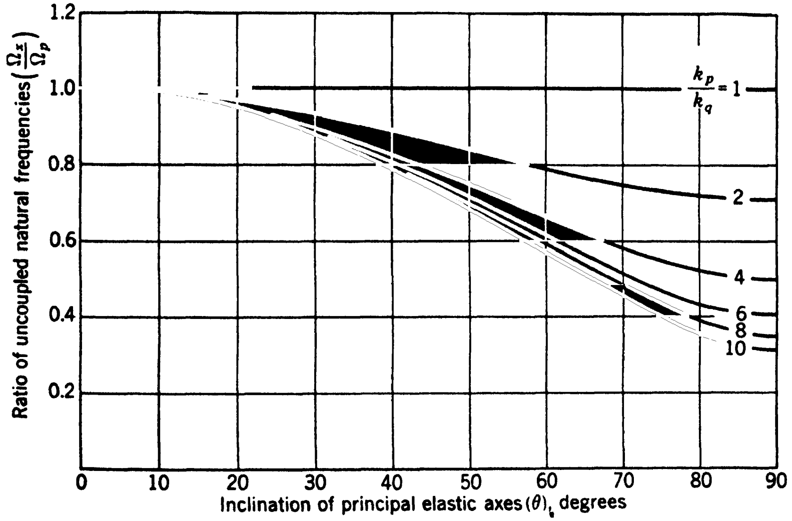

FIGURE 2.24. Ratio of uncoupled natural frequencies Ω_x and $\Omega_p = \sqrt{4k_p/m}$, as a function of angle of inclination θ and ratio k_p/k_q of principal stiffnesses, for system shown in Figure 2.21.

An adequate technique is now available for determining the natural frequencies for all natural modes of vibration in the XY plane. If the principal elastic stiffnesses of the isolators and the directions of their principal elastic axes are known, the location of the elastic axis for the system is determined with the aid of Figure 2.22. This determines the distance ϵ between the elastic axis and the center of gravity. The uncoupled horizontal natural frequency Ω_x is next determined by first obtaining the ratio Ω_x/Ω_p from Figure 2.24 and then multiplying this ratio by Ω_p. The curves of Figure 2.3 may be used to determine Ω_p,* wherein the stiffness on the ordinate scale in Figure 2.3 is the summation of the isolator stiffnesses in the direction of their principal elastic axes p. The quantity λ_1 is evaluated by entering Figure 2.26 at the applicable value of the angle θ, and dividing the resulting value of $\lambda_1(\rho_e/b)$ by the known ratio ρ_e/b. Finally, the coupled natural frequencies Ω_c are determined from Figure 2.23, using the previously determined values for Ω_x and λ_1. The two numerical values represent the natural frequencies in the coupled translatory and rotational modes of vibration in the XY plane of symmetry. The other natural frequency in this plane is associated with the decoupled translatory mode of vibration in the direction of the Y axis. This is readily found from Figure 2.25, using the numerical value of the expression Ω_p determined from Figure 2.3.

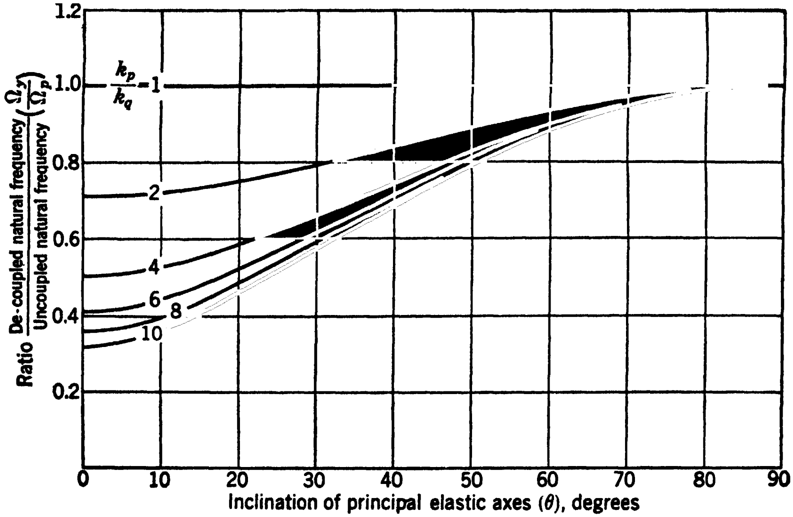

FIGURE 2.25. Ratio of decoupled natural frequency Ω_y to uncoupled natural frequency $\Omega_p = \sqrt{4k_p/m}$, as a function of angle of inclination θ and ratio k_p/k_q of principal stiffnesses, for system shown in Figure 2.21. See page 78 for distinction between "decoupled" and "uncoupled."

---

* This is not rigorously correct, because the units of Ω_p are radians per second and Figure 2.3 gives the natural frequency in units of cycles per second. The coupled natural frequencies are obtained by operating on Ω_p with various dimensionless ratios, and thus they may be expressed in units of cycles per second by expressing Ω_p in units of cycles per second for purposes of this computation.

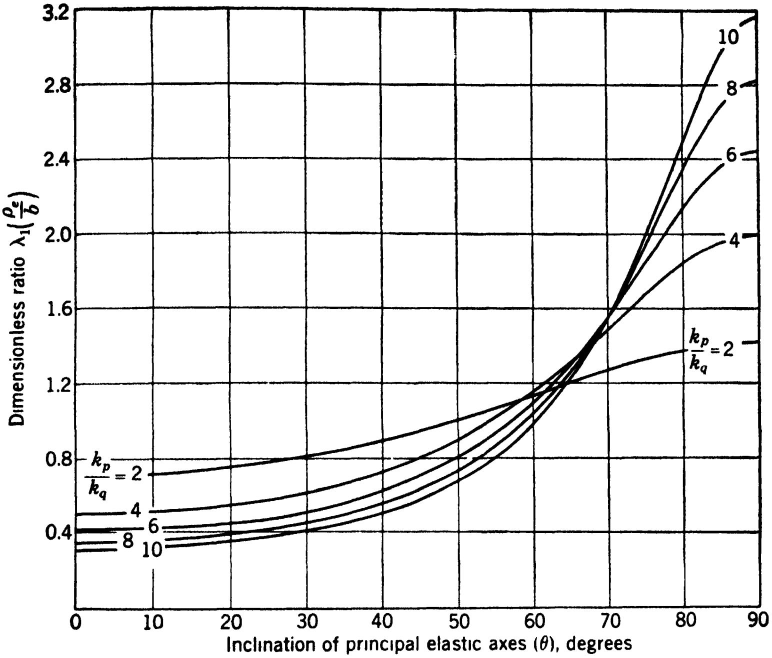

FIGURE 2.26. Curves for evaluating dimensionless ratio $\lambda_1 = \Omega\alpha/\Omega_x$, where $\Omega\alpha$ and Ω_x are uncoupled natural frequencies. This is given in terms of radius of gyration ρ_e of mounted body, distance b from isolators to coordinate plane, inclination θ of principal elastic axes, and ratio k_p/k_q of principal stiffnesses. The radius of gyration ρ_e is taken with reference to the elastic axis.

2·10 Decoupling of Modes

The natural modes of vibration of a body supported by isolators may be decoupled one from another by proper orientation of the isolators. Each mode of vibration then exists independently of the others, and vibration in one mode does not excite vibration in other modes. The necessary conditions for decoupling may be stated as follows: The resultant of the forces applied to the mounted body by the isolators when the mounted body is displaced in translation must be a force directed through the center of gravity; or the resultant of the couples applied to the mounted body by the isolators when the mounted body is displaced in rotation must be a couple about an axis through the center of gravity.

Consider, first, the system shown in Figure 2.7, wherein the principal elastic axes of the isolators are mutually parallel. From an inspection of equations 2.21 and 2.22, it is evident that the reaction of the isolators to a translatory displacement of the mounted body in the X

direction is a force only when $a = 0$. Similarly, the reaction to a rotational displacement α is a couple only when $a = 0$. Equations 2.21 and 2.22 may then be solved explicitly for x and α, the displacements in the decoupled translatory and rotational modes. A similar result is obtained from equations 2.43 and 2.44.

In general, the natural frequencies of a multi-degree-of-freedom system can be made equal only by decoupling the natural modes of vibration. Since decoupling occurs when $a = 0$, the natural frequencies in decoupled modes are indicated by the two straight lines in Figure 2.8 marked $a/\rho = 0$. The natural frequencies in translation along the X axis and in rotation about the Z axis become equal at the intersection of these lines. It can be shown that the requirements for such a condition, in addition to $a/\rho = 0$, are $k_x/k_y = 1$ and $\rho/b = 1$. The physical significance of these mathematical conditions is that the isolators be located in a plane passing through the center of gravity of the mounted body, that the distance between isolators be twice the radius of gyration of the body, and that the stiffness of each isolator in the directions of the X and the Y axes be equal. The lack of a low natural frequency in any natural mode of vibration lends a general firmness to the system, with a consequent tendency toward good stability.

When the isolators cannot be located in a plane that passes through the center of gravity of the mounted body, decoupling can be achieved by inclining the isolators, as illustrated in Figure 2.21. An expression for the position of the elastic axis of this system is given by equation 2.89. The elastic axis is, by definition, a line through which the application of a force causes translation of the mounted body without rotation. If the elastic axis and the center of gravity are made to coincide, the translatory and rotational modes are decoupled because the inertia force of the mounted body is applied through the elastic axis and introduces no tendency for the body to rotate. If this condition is fulfilled, the dimension ϵ in Figure 2.21 becomes equal to zero and the dimension a becomes equal to a_c. The requirements for a decoupled system are now established by setting $a = a_c$ in equation 2.89, and solving for k_p/k_q:

$$\frac{k_p}{k_q} = \frac{(b/a_c) + \tan\theta}{(b/a_c) - \cot\theta}. \tag{2.114}$$

The conditions for decoupling, as indicated by equation 2.114, are shown graphically in Figure 2.27 for ready reference. The decoupled natural frequencies are indicated by the straight lines $\epsilon/\rho_e = 0$ in Figure 2.23. The horizontal line refers to the decoupled natural frequency Ω_x in translation in the direction of the X axis; the inclined line refers to the decoupled natural frequency Ω_α in rotation about the Z axis.

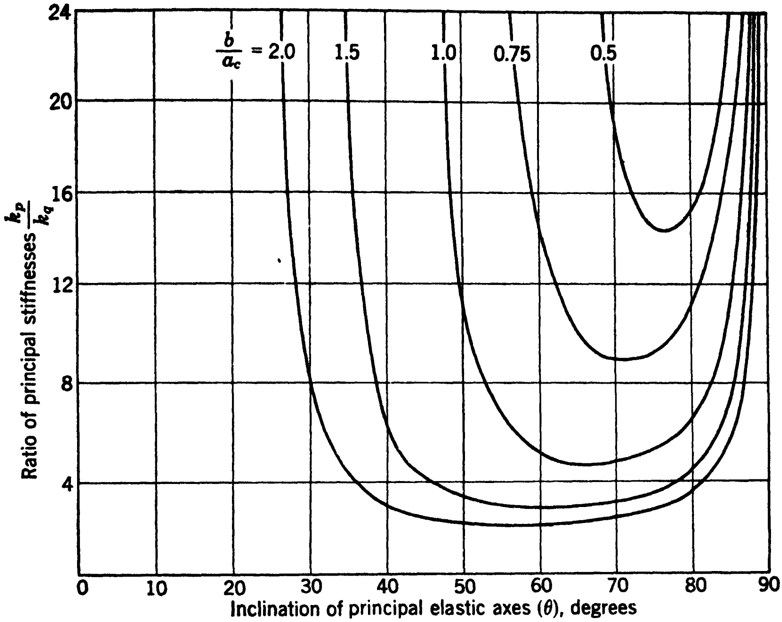

FIGURE 2.27. Required conditions for decoupling natural modes of vibration of system shown in Figure 2.21.

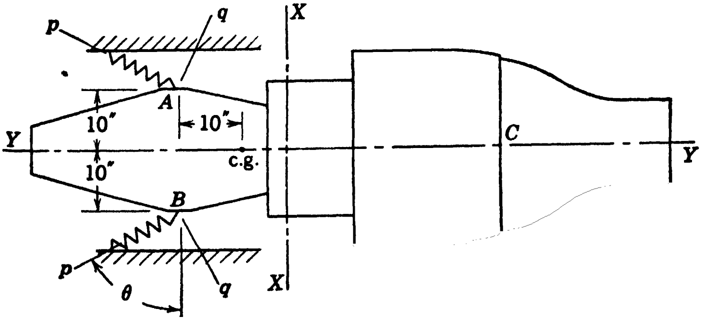

FIGURE 2.28. Plan view of aircraft power plant supported by isolators at points A, B, and C. The isolator at point C offers no resistance to horizontal deflection.

Example 2.4. The plan view of an aircraft power plant is shown schematically in Figure 2.28. It is supported at three points, A, B, C, but the support at point C is arranged to carry only a vertical load. All torque and horizontal reactions are taken at points A and B. The center of gravity is 10 in. aft of points A and B, and the distance from A to B is 20 in. The weight of the power plant is 2,850 lb, and the radius of gyration about a vertical axis through the center of gravity is 29 in. It is desired to determine the principal stiffnesses and inclination of principal elastic axes required to (1) decouple the natural modes of vibration and (2) maintain all natural frequencies in the horizontal plane equal to or less than 10 cps.

Employing the symbols of Figure 2.21, $a_c = 10$ ($\epsilon = 0$ when modes of vibration are decoupled), $b = 10$, and $\rho_g = 29$. The ratio b/a_c is thus established as 1.0. From the requirement that the modes be decoupled, a suitable stiffness ratio for the isolators is determined by entering Figure 2.27 at an assumed inclination of $\theta = 70°$ and finding $k_p/k_q = 5.89$ from the curve for $b/a_c = 1.0$. Since $\epsilon = 0$. $\rho_e = \rho_g = 29$ in.

The dimensionless ratio $\lambda_1(\rho_e/b)$ is now found from Figure 2.26, using the values of θ and k_p/k_q previously established, to be $\lambda_1(\rho_e/b) = 1.54$. Inasmuch as ρ_e and b are known, λ_1 is found from the relation:

$$\lambda_1 = 1.54\left(\frac{b}{\rho_e}\right) = \frac{1.54 \times 10}{29} = 0.531.$$

Now, entering Figure 2.23 at $\lambda_1 = 0.531$ and finding two values of Ω_c/Ω_x corresponding to the two curves for $\epsilon/\rho_e = 0$:

$$\frac{\Omega_c}{\Omega_x} = 0.53;\ 1.00.$$

From Figures 2.24 and 2.25, the following frequency ratios are determined, using values of θ and k_p/k_q already established:

$$\frac{\Omega_x}{\Omega_p} = 0.51;\quad \frac{\Omega_y}{\Omega_p} = 0.95.$$

The ratio Ω_y/Ω_x is now determined as the quotient of the above ratios:

$$\frac{\Omega_y}{\Omega_x} = \frac{0.95}{0.51} = 1.85.$$

The three natural frequencies in the natural modes of vibration in the horizontal plane are thus determined with reference to Ω_x as follows:

$$\Omega_y = 1.85\Omega_x;\quad \Omega_c = 0.53\Omega_x,\ 1.00\Omega_x.$$

It is a condition of the solution that the highest of these natural frequencies, Ω_y, be equal to 10 cps. Employing the above value for the frequency ratio Ω_y/Ω_x:

$$\Omega_x = \frac{\Omega_y}{1.85} = \frac{10 \times 2\pi}{185} = 5.4 \times 2\pi \text{ rad/sec, or } 5.4 \text{ cps.}$$

The fictitious natural frequency Ω_p is now calculated from the above value for the ratio Ω_x/Ω_p:

$$\Omega_p = \frac{\Omega_x}{0.51} = \frac{5.4 \times 2\pi}{0.51} = 10.6 \times 2\pi \text{ rad/sec.}$$

For motion in the horizontal plane, two isolators A and B are effective. Each isolator is therefore assumed to carry one-half the total weight, or 1,425 lb. Entering Figure 2.3 at 1,425 lb, the stiffness k_p of each isolator is read from the ordinate scale opposite the constant natural frequency of 10.6 cps as $k_p = 16{,}320$ lb/in. The principal stiffness k_q is now found from the relation:

$$k_q = \frac{k_p}{5.89} = 2{,}790 \text{ lb/in.}$$

The resulting natural frequencies in the horizontal plane are as follows:

Translatory along Y axis: $\Omega_y = 10.0$ cps.

Translatory along X axis: $\Omega_\iota = 1.00\Omega_x = 5.4$ cps.

Rotational with respect to Z axis: $\Omega_c = 0.53\Omega_x = 2.9$ cps.

BIBLIOGRAPHY

Bastien, C. J., "Vibration Isolation and Shock Mounting," *Prod. Eng.*, Vol. 19, Nos. 9–10, September–October 1948.

Best, J. H., "Vibration and Shock Testing of Mobile Equipment," *Electronics*, Vol. 19, No. 4, April 1946.

Browne, K. A., "Dynamic Suspension, a Method of Aircraft-Engine Mounting," *S.A.E. Jour.* (*Trans.*) Vol. 44, No. 5, May 1939.

Crede, C. E., and J. P. Walsh, "The Design of Vibration-Isolating Bases for Machinery," *Trans. A.S.M.E.* (*Jour. App. Mech.*, Vol. 14, No. 1), March 1947.

Den Hartog, J. P., *Mechanical Vibrations*, McGraw-Hill Book Co., New York, 1947.

Freberg, C. R., and E. N. Kemler, *Elements of Mechanical Vibrations*, John Wiley and Sons, Inc., New York, 1949.

Haringx, J. A., "Vibration-Free Mountings with Auxiliary Mass," *Philips Tech. Rev.*, Vol. 9, No. 1, January 1947.

Hull, E. H., "The Use of Rubber in Vibration Isolation," *Trans. A.S.M.E.* (*Jour. App. Mech.*, Vol. 4, No. 3), September 1937.

Hull, E. H., and W. C. Stewart, "Elastic Supports for Isolating Rotating Machinery," *Trans. A.I.E.E.*, Vol. 50, No. 3, September 1931.

Kennard, D. C., "The Practicability of Vibration Control in Light Aircraft," *Trans. A.S.M.E.*, Vol. 68, No. 2, February 1946.

Lewis, R. C., and K. Unholtz, "A Simplified Method for the Design of Vibration-Isolating Suspensions," *Trans. A.S.M.E.*, Vol. 69, No. 8, November 1947.

Ludeke, C. A., "Resonance," *Jour. App. Phys.*, Vol. 13, No. 7, July 1942.

Macduff, J. N., "Isolation of Vibration In Spring Mounted Apparatus," *Prod. Eng.*, Vol. 17, Nos. 7–8, July–August 1946.

Pengelley, C. D., "Ground Vibration Tests," *Jour. Aero. Sci.*, Vol. 9, No. 13, November 1942.

Product Engineering, "Natural Frequency Calculations," Vol. 19, No. 8, August 1948.

Soroka, W. W., "Energy Method of Calculating Vibration Modes and Frequencies," *Prod. Eng.*, Vol. 20, No. 12, December 1949.

Taylor, E. S., and K. A. Browne, "Vibration Isolation of Aircraft Power Plants," *Jour. Aero. Sci.*, Vol. 6, No. 2, December 1938.

Timoshenko, S., *Vibration Problems in Engineering*, D. Van Nostrand Co., New York, 1937.

CHAPTER THREE

Isolation of Shock

The isolation of shock can be considered adequately only by separating shock conditions into several categories, and considering the mechanics of each one independently. The several categories may be defined briefly as follows:

(*a*) Isolation of a shock motion whose displacement amplitude tends to be greater than the maximum possible deflection of the isolator.
(*b*) Isolation of a shock force of such a nature that it tends to cause a displacement greater than the maximum possible deflection of the isolator.
(*c*) Isolation of a shock force whose nature is such as to cause a displacement less than the maximum possible deflection of the isolator.
(*d*) Isolation of a shock motion whose displacement amplitude is less than the maximum possible deflection of the isolator.

The subject of shock is exceedingly complex because the suddenly applied forces and sudden motions cause mechanical structures to vibrate in a transient manner and in many natural modes simultaneously. The analysis given in this chapter is simplified or idealized, in that the masses are considered to be concentrated and the flexible members to be massless. The effect of this simplification is to discard the harmonics of the fundamental natural frequency. The much less complex analysis of a single-degree-of-freedom system then becomes applicable. Structural components or elements of the equipment are indicated simply by a mass-spring system; and the mounted-equipment-and-isolator assembly is represented by a similar system. There is considerable justification for this simplification, because the cushioning afforded by the isolator reduces the suddenness of forces and motions, and thereby tends to reduce the response of structures in their higher modes of vibration.

A. *ISOLATION OF SHOCK MOTIONS OF LARGE DISPLACEMENT*

3·1 *Velocity Shock*

This section analyzes the conditions of shock that occur in equipment when a sudden change occurs in the linear velocity, or in the direction of motion, of the equipment or its support. This type of shock motion is referred to as velocity shock. For example, a package dropped on the floor experiences a sudden velocity change at the moment its downward fall is arrested by contact with the floor. Equipment mounted in naval vessels or combat vehicles is subjected to a similar experience when the vessel or vehicle is subjected to the action of armament. Railroad rolling stock experiences a sudden change in velocity when the clearance in the coupling mechanism is taken up in starting a train of cars. In general, it is immaterial whether the change is from zero velocity to some finite velocity; from some finite velocity to zero velocity; or from one finite velocity to a numerically different finite velocity. It is evident that an instantaneous velocity change is impossible in a practical sense. It will be shown, however, that the effect is equivalent to an instantaneous change when the velocity change takes place during a time interval that is a small fraction of the natural periods of the systems being considered.*

It is shown in Section 1·1 of Chapter 1 that an equipment, such as a vacuum tube, may be idealized as one or more systems, each comprised of a rigid mass and a massless, linear spring. The likelihood of such an equipment being damaged is indicated by the deflection of the spring. The following analysis is based upon the idealized mass-spring system $m_z k_z$ shown in Figure 3.1. This idealization of the equipment embodies several differences from a real structure which should be recognized:

(*a*) The mass of a real structure is not rigid, nor is the spring massless, as assumed with reference to Figure 3.1. Consequently, a real structure has many natural frequencies which may be excited by the shock. The following analysis considers only the fundamental natural frequency, although brief mention is made later of the influence of higher harmonics.

---

* See footnote to equation 3.47.

(*b*) A real structure always includes some damping, which is neglected in the idealized system, Figure 3.1. The energy dissipated by damping tends to limit the deflection of the elastic elements. The significance of this effect will be included in the discussion that follows.

The function of a shock isolator is best understood by first analyzing the nature of shock damage. Figure 3.1 shows any element $m_z k_z$ of

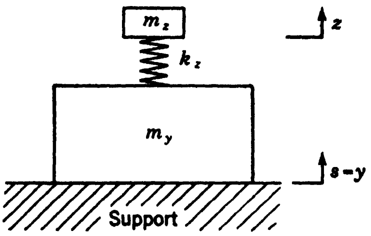

FIGURE 3.1.

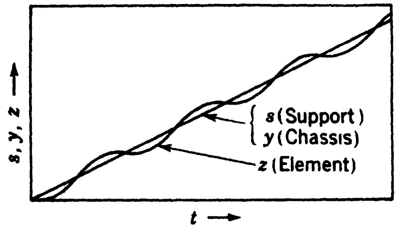

FIGURE 3.2.

FIGURE 3.1. Schematic representation of equipment, comprised of a rigidly mounted chassis m_y and an element $m_z k_z$.

FIGURE 3.2. Displacement of chassis and element shown in Figure 3.1, when support experiences a velocity shock.

the equipment, attached to the equipment chassis m_y. The chassis m_y is secured rigidly to a support. A velocity shock occurs, and the support instantaneously acquires an upward velocity of magnitude $\dot{s} = V_s$, as shown in Figure 3.2. The chassis m_y, being rigidly attached to the support, experiences an equivalent motion. Its position is given at any time t by

$$y = V_s t. \tag{3.1}$$

The motion of the mass m_z is now determined by writing its differential equation of motion:

$$m_z \ddot{z} = k_z(y - z). \tag{3.2}$$

The solution of equation 3.2, where $\Omega_z = \sqrt{k_z/m_z}$ is the natural frequency of the system $m_z k_z$ expressed in radians per second and the initial conditions are $z = \dot{z} = 0$ when $t = 0$, is

$$z = V_s\left(t - \frac{1}{\Omega_z} \sin \Omega_z t\right). \tag{3.3}$$

The displacements y and z of the chassis m_y and mass m_z are shown in Figure 3.2 as functions of time. The deflection of the spring k_z is given by $\delta_{yz} = y - z$. Substituting y and z from equations 3.1 and 3.3, respectively:

$$\delta_{yz} = \left(\frac{V_s}{\Omega_z}\right) \sin \Omega_z t. \tag{3.4}$$

An equivalent result is obtained when equipment having an initial velocity is brought to rest. Referring to Figure 3.3, the element $m_z k_z$ is attached to a relatively heavy chassis m_y. All elements of this assembly, including masses m_z and m_y, are descending at a velocity $\dot{y} = -V_y$. The chassis m_y strikes a rigid support with perfectly inelastic impact and remains in contact therewith continuously. If the time reference is taken as $t = 0$ at the moment of contact, equation 3.2 becomes applicable at time $t \geq 0$ by setting $y = 0$. Taking the initial conditions as $z = 0$, $\dot{z} = -V_y$ when $t = 0$, the solution of the resulting equation is

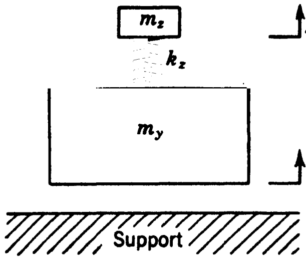

FIGURE 3.3.

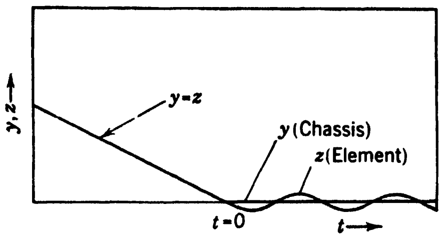

FIGURE 3.4.

FIGURE 3.3. Schematic representation of equipment, comprised of chassis m_y and element $m_z k_z$. The downward velocity of the equipment is arrested when the chassis engages the support.

FIGURE 3.4. Displacement-time curves for chassis and element shown in Figure 3.3 during time interval in which downward velocity of equipment is arrested.

$$z = -\left(\frac{V_y}{\Omega_z}\right) \sin \Omega_z t. \tag{3.5}$$

Displacement-time curves for the chassis m_y and the mass m_z are shown in Figure 3.4. The downward velocity of the chassis m_y suddenly becomes zero at time $t = 0$. The downward velocity of the mass m_z continues and results in transient vibration of the element $m_z k_z$. The deflection of the spring k_z is the difference between the displacement y of the chassis and the displacement z of the mass m_z. Since $y = 0$ when $t \geq 0$:

$$\delta_{yz} = y - z = \left(\frac{V_y}{\Omega_z}\right) \sin \Omega_z t. \tag{3.6}$$

The result given by equation 3.6 is identical to that given by equation 3.4, provided that the velocity V_y of the chassis as it engages the support is numerically equal to the upward velocity V_s experienced by the support illustrated in Figure 3.1. Since the severity of the shock is measured by the maximum value of the spring deflection $(\delta_{yz})_0$, it is evident that initial and final conditions are not significant in determining shock severity. The maximum spring deflection is a function only of the magnitude of the velocity change experienced by the chassis m_y, and of the natural frequency Ω_z of the element $m_z k_z$. This assumes that the change in the velocity of the chassis m_y occurs instantaneously. When an appreciable interval of time is required for the velocity change to take place, an analysis similar to that employed to investigate a shock isolator becomes applicable. This is discussed in Section 3·2.

It is convenient in the following analysis to evaluate the severity of the shock experienced by an element of the equipment in terms of the acceleration of the mass m_z of the element. In the systems shown in Figures 3.1 and 3.3, the acceleration $\ddot{z}$ is directly proportional to the product of spring stiffness k_z and spring deflection δ_{sz}. This becomes apparent by writing the differential equation of motion for the mass m_z:

$$m_z \ddot{z} = k_z \delta_{yz}. \tag{3.7}$$

Substituting for δ_{yz} from equation 3.4, and writing $\Omega_z^2 = k_z/m_z$:

$$\ddot{z} = V_s \Omega_z \sin \Omega_z t. \tag{3.8}$$

The maximum value of equation 3.8 is

$$\ddot{z}_0 = V_s \Omega_z. \tag{3.9}$$

The maximum deflection $(\delta_{yz})_0$ of the spring k_z and the maximum acceleration $\ddot{z}_0$ experienced by the mass m_z are thus both directly proportional to the velocity change V_s. The maximum acceleration $\ddot{z}_0$ may therefore be used interchangeably with the maximum deflection $(\delta_{yz})_0$ of the element $m_z k_z$ as a measure of the severity of the shock experienced by an equipment.

It is possible to obtain results equivalent to those given above by equating the maximum kinetic energy of the mass m_z, Figure 3.3, to the maximum potential energy stored in the elastic element k_z:

$$\tfrac{1}{2} m_z V_y^2 = \tfrac{1}{2} k_z (\delta_{yz})_0^2, \tag{3.10}$$

where the term V_y is the downward velocity of both chassis m_y and element m_z at the moment of contact with the support.

Substituting for m_z from equation 3.7 and for $(\delta_{yz})_0$ from equation 3.4, equation 3.10 becomes, when $V_s = V_y$:

$$\ddot{z}_0 = V_y \Omega_z, \tag{3.11}$$

which is equivalent to equation 3.9 when $V_y = V_s$.

The relation between the approach velocity V_y and the height from which the body falls freely is determined by equating the kinetic energy of the chassis m_y in Figure 3.3 to its potential energy at the height h_f from which it falls:

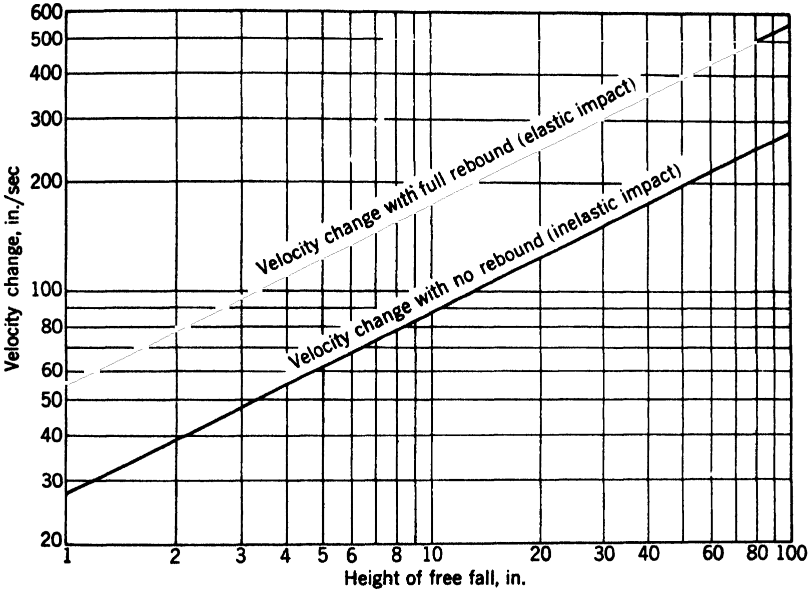

FIGURE 3.5. Velocity change resulting from engagement of a freely falling body with a fixed support. Curves are included for perfectly elastic impact (full rebound) and perfectly inelastic impact (no rebound).

$$\tfrac{1}{2} m_y V_y^2 = m_y g h_f. \tag{3.12}$$

Solving for V_y:

$$V_y = \sqrt{2 g h_f}. \tag{3.13}$$

The velocity given by equation 3.13 is that at which the chassis m_y approaches the support, i.e., the velocity change experienced by the chassis for a condition of inelastic impact, or no rebound. When the impact is elastic, the chassis rebounds upwardly with a velocity that is numerically equal but opposite in direction to the approach velocity. The velocity change is then twice as great as indicated by equation

3.13. The numerical value of the velocity change as a function of height of drop is indicated in Figure 3.5 for the conditions of elastic and inelastic impact. Data from Figure 3.5 may be used with equation 3.11 to determine the maximum acceleration $\ddot{z}_0$ of an element of the equipment.

3·2 *Isolation of Velocity Shock—Inelastic Impact*

The effectiveness of a shock isolator will be evaluated by determining the reduction of $\ddot{z}_0$ afforded to the element discussed above. Consider the combination of systems illustrated schematically in Figure 3.6. The upper system $m_z k_z$ is the element previously considered; the mass m_y represents the chassis of the equipment; and the spring k_y represents the shock isolator. All springs are considered linear for purposes of the immediately following analysis, and the mass m_z is assumed small relative to m_y. The motion of m_y is thus independent of the motion of m_z, and the analysis is considerably simplified.

The differential equation of motion for the chassis m_y is

$$m_y\ddot{y} = k_y(s - y). \tag{3.14}$$

The support is assumed to experience a velocity shock defined by $\dot{s} = V_s$ at time $t \geq 0$, as illustrated by the curve for y in Figure 3.2. The value of s is then given by $s = V_s t$. The designation inelastic impact is used here because the results are identical to those which would be obtained if the system shown in Figure 3.6, with initial downward velocity, should strike the support without rebound. Equation 3.14 is of the form of equation 3.2, and the solution thereof may be written by analogy with equation 3.3:

$$y = V_s\left(t - \frac{1}{\Omega_y}\sin\Omega_y t\right), \tag{3.15}$$

where $\Omega_y = \sqrt{k_y/m_y}$ is the natural frequency, expressed in radians per second, of the elastic system comprised of chassis m_y and isolator k_y.

The differential equation of motion for the mass m_z is

$$m_z\ddot{z} = k_z(y - z). \tag{3.16}$$

Substituting the expression for y from equation 3.15, writing $\Omega_z^2 = k_z/m_z$, and applying the initial conditions, $z = \dot{z} = 0$ when $t = 0$, the following expression is obtained for the displacement z of the mass m_z:

$$z = V_s t - \frac{V_s}{\Omega_z[1 - (\Omega_z^2/\Omega_y^2)]}\sin\Omega_z t - \frac{V_s}{\Omega_y[1 - (\Omega_y^2/\Omega_z^2)]}\sin\Omega_y t. \tag{3.17}$$

The displacement z is thus comprised of two harmonic terms of different frequencies and different amplitudes, superimposed upon the displacement $s = V_s t$ of the support. The two frequencies are the natural frequencies of the element and the isolator,* and the displacement at each frequency is directly proportional to the velocity change V_s. Typical displacement curves for the support and element are shown in Figure 3.7.

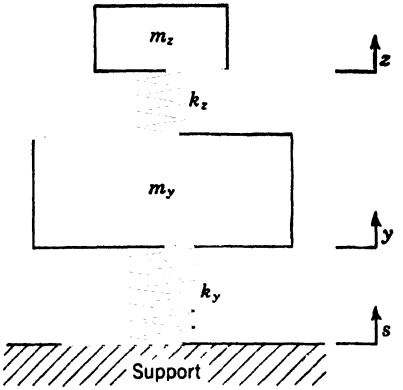

Figure 3.6.

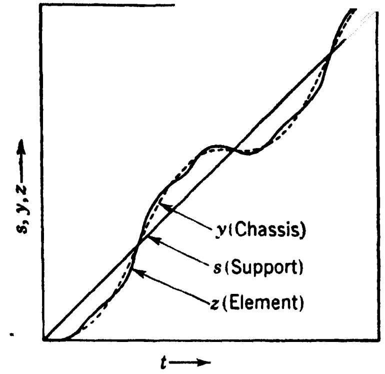

Figure 3.7.

Figure 3.6. Schematic representation of equipment, comprised of chassis m_y and element $m_z k_z$, mounted upon isolator k_y.

Figure 3.7. Displacement-time curves for support, chassis, and element of equipment shown in Figure 3.6. The support experiences velocity shock.

The acceleration experienced by the mass m_z may now be determined by double differentiation of equation 3.17 with respect to time. Carrying out this differentiation and rearranging terms, the following expression is obtained for $\ddot{z}$:

$$\ddot{z} = \frac{V_s \Omega_z}{1 - (\Omega_z^2/\Omega_y^2)} \left[\sin \Omega_z t - \frac{\Omega_z}{\Omega_y} \sin \Omega_y t \right]. \qquad (3.18)$$

The acceleration of the mass m_z is thus the difference of two harmonic components at different frequencies. Since the system is undamped, its motion continues indefinitely and the term within the brackets of equation 3.18 eventually attains the maximum value $[1 + (\Omega_z/\Omega_y)]$. The maximum acceleration of the mass m_z may then be written:

$$\ddot{z}_0 = \frac{V_s \Omega_z}{1 - (\Omega_z^2/\Omega_y^2)} [1 + (\Omega_z/\Omega_y)] = \frac{V_s \Omega_z}{1 - (\Omega_z/\Omega_y)}. \qquad (3.19)$$

---

* The expression *natural frequency of isolator* is used in the interest of simplicity of language and refers to the natural frequency of the system comprised of isolator k_y and chassis m_y.

Expressions have now been derived from which the effectiveness of the isolator may be determined. The maximum acceleration experienced by the mass m_z, in the absence of the isolator k_y, is given by equation 3.9; the maximum acceleration of the same element, when the equipment is supported by the isolator, is given by equation 3.19. Shock transmissibility T_s is defined as the ratio of maximum acceleration $\ddot{z}_0$, *with* the isolator, to the maximum acceleration $\ddot{z}_0$, *without* the isolator. The following expression is now written for T_s:

$$T_s = \frac{\ddot{z}_0 \text{ from equation 3.19}}{\ddot{z}_0 \text{ from equation 3.9}} = \frac{1}{1 - (\Omega_z/\Omega_y)}. \tag{3.20}$$

Shock transmissibility is thus a function of the properties of both the isolator and the mounted equipment.

The expression for T_s given by equation 3.20 becomes infinite when $\Omega_z = \Omega_y$. It will now be shown that this condition prevails only after an infinitely long time. Equation 3.18 may be written as follows, for the region in which $\Omega_z/\Omega_y \approx 1$:

$$\ddot{z} = \frac{V_s\Omega_z}{1 - (\Omega_z^2/\Omega_y^2)}\left[2 \sin\left(\frac{\Omega_z - \Omega_y}{2}\right) t \cos\left(\frac{\Omega_z + \Omega_y}{2}\right) t\right]. \tag{3.21}$$

Since $\Omega_z \approx \Omega_y$,

$$\sin\left(\frac{\Omega_z - \Omega_y}{2}\right) t \approx \left(\frac{\Omega_z - \Omega_y}{2}\right) t \text{ and } \cos\left(\frac{\Omega_z + \Omega_y}{2}\right) t \approx \cos \Omega_y t.$$

Equation 3.21 then becomes

$$\ddot{z} = \frac{-V_s\Omega_z\Omega_y t \cos \Omega_y t}{1 + (\Omega_z/\Omega_y)}. \tag{3.22}$$

The acceleration $\ddot{z}$ of the mass m_z thus increases continuously as time t increases; and the infinite transmissibility indicated by equation 3.20 for $\Omega_z = \Omega_y$ occurs only after an infinitely long time.

It is apparent from the physical concept of this condition that the vibration of the chassis m_y must continue indefinitely in order that the infinite acceleration $\ddot{z}_0$ be reached. This cannot occur, because no energy is added after the initial sudden velocity change, and the chassis amplitude y must inevitably decrease as energy is dissipated from the isolator k_y. The maximum acceleration $\ddot{z}_0$ which is ultimately reached represents a balance between the tendency to increase with time, equation 3.22, and the constantly decreasing amplitude of the chassis m_y due to energy dissipation. The mathematics required to determine such results in general form is tremendously laborious.

R. D. Mindlin investigated this problem and presented numerical results* obtained by electrical analogy from the Westinghouse Analog Computer. Mindlin's results are given in terms of an amplification factor H_I, which is defined for the system of Figure 3.6 by

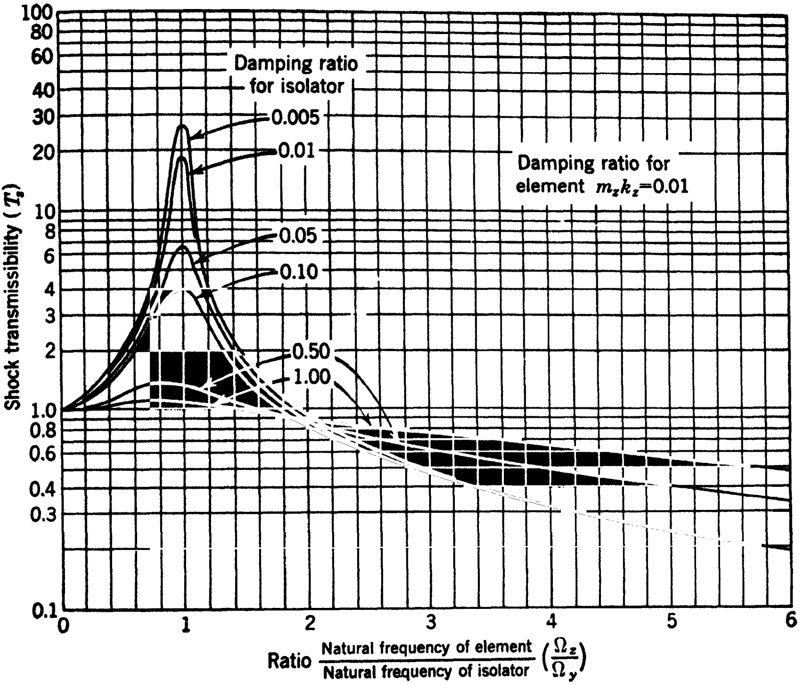

FIGURE 3.8. Shock transmissibility for system shown in Figure 3.6, when subjected to velocity shock as illustrated in Figure 3.7. Shock transmissibility T_s is the ratio of the maximum acceleration of the massive element m_z to the maximum acceleration of the same element which would occur if the isolator k_y were infinitely rigid.

$$H_I = \frac{\ddot{z}_0}{\ddot{y}_0}. \tag{3.23}$$

The amplification factor H_I is thus the ratio of the maximum acceleration of the element to the maximum acceleration of the chassis; or, in other words, a factor by which the maximum chassis acceleration is multiplied to obtain the maximum element acceleration. The subscript I is used here to denote inelastic impact, as distinguished from elastic impact considered in a later section.

---

* See R. D. Mindlin, "Dynamics of Package Cushioning," *Bell System Technical Journal*, Vol. XXIV, Nos. 3–4, July–October 1945, page 431.

An expression for H_I in the undamped system analyzed above is derived by substituting $\ddot{z}_0$ from equation 3.19, and taking the maximum value of $\ddot{y}$ obtained by double differentiation of equation 3.15:

$$H_I = \frac{\ddot{z}_0}{\ddot{y}_0} = \frac{V_s\Omega_z}{1 - (\Omega_z/\Omega_y)} \div V_s\Omega_y = \frac{\Omega_z}{\Omega_y}\left[\frac{1}{1 - (\Omega_z/\Omega_y)}\right]. \qquad (3.24)$$

Combining equations 3.20 and 3.24, an expression is obtained that relates shock transmissibility T_s and amplification factor H_I:

$$T_s = H_I\left(\frac{\Omega_y}{\Omega_z}\right). \qquad (3.25)$$

The expression for shock transmissibility, equation 3.25, may be made to include the effect of damping and thereby remain finite when values for the amplification factor H_I are taken from the work of Mindlin. Shock transmissibility as determined in this manner is plotted in Figure 3.8 for a range of values of damping ratio* for the isolator. The damping in the element m_zk_z is assumed constant at the typical value of one percent of critical damping, although the results are influenced but little by rather wide variations in the degree of damping in the element.

3·3 Effectiveness of Isolators—Inelastic Impact

The requisite conditions for effective shock isolation become readily evident from a study of the shock transmissibility curves included in Figure 3.8. Two aspects of these curves are worthy of note:

(*a*) The maximum acceleration experienced by an element of the equipment is reduced by the provision of a shock isolator only if the natural frequency of the element is at least two times as great as the natural frequency of the isolator. This maximum acceleration continues to decrease as the element becomes more rigid and is influenced but little by the degree of damping in the isolator, provided that the damping is small.

(*b*) The maximum acceleration experienced by an element of the equipment is increased by the provision of a shock isolator if the *natural frequency of the element is less than two times the natural frequency of the isolator. The magnitude of the increase depends largely on the damping in the isolator, being higher for a small degree of damping.*

---

* The damping ratio is the ratio of the coefficient of viscous damping for the system to the coefficient for a critically damped system. This subject is discussed in detail in Section 4·5 of Chapter 4.

The effectiveness of a shock isolator in affording protection for a particular element of known natural frequency is thus readily determined. Equipment is comprised, in general, of numerous elements having a range of natural frequencies. Some discernment is required to determine the overall effectiveness of isolators. Equipment comprised solely of relatively rigid elements benefits most from isolators. If the equipment includes no rigid elements, it is likely that little benefit will derive from the provision of isolators, and it is possible that isolators will decrease the ability of the equipment to withstand shock. The ultimate test is whether the increase in shock resistance of rigid elements is sufficient to compensate for the decrease in shock resistance of flexible elements.

In the design of mechanical structures, it is generally considered good practice to employ relatively flexible elements in order to keep the weight and cost as low as possible. Such elements tend to experience large deflections when subjected to velocity shock, as becomes evident from the substitution of a small value for Ω_z in equation 3.6. It is necessary in such instances to employ a type of construction and a material that permit large deflection without danger of failure. Some structures are not well adapted, for structural or functional reasons, to withstand large deflections. The following examples illustrate this condition:

(*a*) The use of a brittle material, i.e., a material with a small elongation prior to failure, is often required for functional reasons. For example, porcelain is regularly employed because of its electrical properties, glass because of its transparency, and cast iron because of ease of casting and machining. It appears to be characteristic of most brittle materials that their tensile strengths are low; large cross sections are thus required for normal operation and handling. When such materials are utilized, the large cross sections contribute to relatively high natural frequencies Ω_z.

(*b*) The deflection of an element is sometimes functionally undesirable, aside from the strength and elongation requirements set forth in the above paragraph. The proper operation of certain types of vacuum tubes, for example, requires that a predetermined spacing between filaments be maintained. Similarly, in a surface grinder, it is important to maintain minimum variations in the position of the grinding wheel relative to the work. Such structures are normally made as rigid as possible, consistent with other requirements of the equipment.

It is evident that several of the rigid elements mentioned in the immediately preceding paragraphs are critical components of equipment, and that it is essential to afford protection to such components. A low shock transmissibility for these components may be attained because their natural frequencies are high. Other components of the same equipment may be less rigid, and not well adapted to the use of isolators. It becomes necessary at this point to determine whether the protection afforded the rigid components is justified in view of the detriments suffered by the less rigid components. These detriments will often be found to be of little consequence; in other instances, it will be found feasible to stiffen the less rigid components in order to take advantage of the protection offered by the isolators.

The analysis in the preceding sections has been carried out on the assumption that the elements of the equipment are single-degree-of-freedom systems comprised of rigid masses and massless, linear springs. It is desirable to examine this assumption now, since it is well known that a suddenly acquired motion tends to excite natural frequencies of high order. This problem has been analyzed by Symonds and Vigness,* who replace the simple system of Figure 3.1 by a cantilever beam of constant cross section and uniformly distributed mass. Theoretical equations for the undamped beam have been derived and indicate that the stress in the beam continues to increase with a decrease in the time interval during which the velocity change occurs. When the velocity change is instantaneous, the stress theoretically is infinite.

Later work† takes the internal damping of the beam into consideration and shows that this damping limits the stress to a finite value, even when the velocity change is instantaneous. The applicable numerical values here are not well established, but there is an indication that the actual stress does not exceed 1.75 times the stress calculated in accordance with the theory for the single-degree-of-freedom system. This occurs when the velocity change is instantaneous. When the velocity change occurs during a time interval that is equal to or greater than the natural period of the element being considered, the simple theory is sufficiently accurate for practical purposes.

The function of an isolator is to increase the time interval during which the velocity change occurs. The value of $\ddot{z}_0$ in the numerator of equation 3.20 is therefore likely to be accurate, even though calculated from the idealized single-degree-of-freedom concept. The value of $\ddot{z}_0$ in the denominator, on the other hand, tends to be low because the idealized concept discards the effect of higher modes of vibration which are more likely to occur in the absence of an isolator. The transmissibility T_s, as given by equation 3.20 and Figure 3.8, thus tends to be a conservative indication of the effectiveness of isolators.

---

* P. Symonds and I. Vigness, "Influence of Duration of Impact on Damage to Some Elastic Systems," *Naval Research Laboratory, Washington, D. C. Report* No. 0-2293, May 15, 1944.

† R. D. Mindlin, F. W. Stubner, and H. L. Cooper, "Response of Damped Elastic Systems to Transient Disturbances," *Proc. Soc. Exp. Stress Anal.*, Vol. V, No. II, page 69.

3·4 *Magnitude of Shock Transmitted by Isolators—Inelastic Impact*

It frequently is necessary to know, not only the relative effectiveness of a shock isolator, but the magnitude of the acceleration experienced by elements of the mounted equipment. An expression for the displacement of equipment supported by isolators and subjected to a velocity shock is given by equation 3.15. The acceleration experienced by the equipment chassis, designated the transmitted acceleration, is obtained by double differentiation of equation 3.15. The maximum value of this transmitted acceleration is

$$\ddot{y}_0 = V_s \Omega_y. \tag{3.26}$$

The natural frequency Ω_y in equation 3.26 is in units of radians per second, and the acceleration $\ddot{y}_0$ is in units of linear distance (inches or feet) per second per second. These units are not convenient for engineering purposes. It is more convenient to express frequency in units of cycles per second, and acceleration in multiples of the acceleration resulting from the gravitational force. Then:

$$\frac{\ddot{y}_0}{g} = \frac{V_s(2\pi f_y)}{386} = \frac{V_s f_y}{61.4}, \tag{3.27}$$

where V_s = shock velocity change, in./sec.
f_y = natural frequency of isolator, cps.
$\ddot{y}_0/g$ = maximum acceleration experienced by chassis, expressed as a dimensionless multiple of the acceleration due to gravity.

The maximum acceleration experienced by the chassis of the equipment is thus directly proportional to the magnitude of the velocity change and to the natural frequency of the isolator. The maximum acceleration as computed from equation 3.27 is shown graphically by the solid lines in Figure 3.9.

The maximum acceleration experienced by the chassis of the mounted equipment, as indicated in Figure 3.9, should not be confused with the maximum acceleration experienced by various elements of the equipment. The latter is equal to the product of the maximum chassis acceleration $\ddot{y}_0$ and the amplification factor H_I. Rearranging equation 3.23:

$$\ddot{z}_0 = H_I \ddot{y}_0. \tag{3.28}$$

The amplification factor H_I, in the absence of damping, is a function only of the element natural frequency Ω_z and the isolator natural

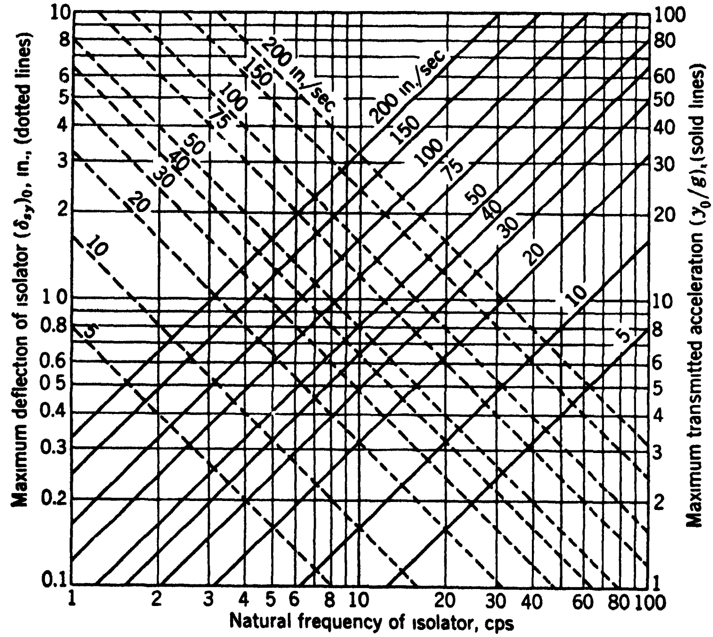

FIGURE 3.9. Maximum acceleration of chassis m_y and maximum deflection of linear isolator k_y shown in Figure 3.6, when support experiences velocity shock as illustrated in Figure 3.7.

frequency Ω_y. This is shown by equation 3.24. When the isolator or element is damped, the problem becomes much more complex. An amplification factor H_I for damped systems has been calculated by R. D. Mindlin, as explained on page 97, and is shown by the family of curves reproduced in Figure 3.10.* The damping in the element is the typical value of one percent of critical. Curves are included for various damping ratios of the isolator ranging from 0.005 to 1.0, the latter being critical damping. Several pertinent conclusions may be drawn from Figure 3.10 as follows:

---

* This figure includes one curve from each of Figures 3.5.2 to 3.5.7 of R. D. Mindlin's paper, "Dynamics of Package Cushioning," *Bell System Technical Journal*, Vol. XXIV, Nos. 3–4, July–October 1945.

(*a*) When the natural frequencies of the element and the isolator are approximately equal, $\Omega_z/\Omega_y = 1$, and the amplification factor

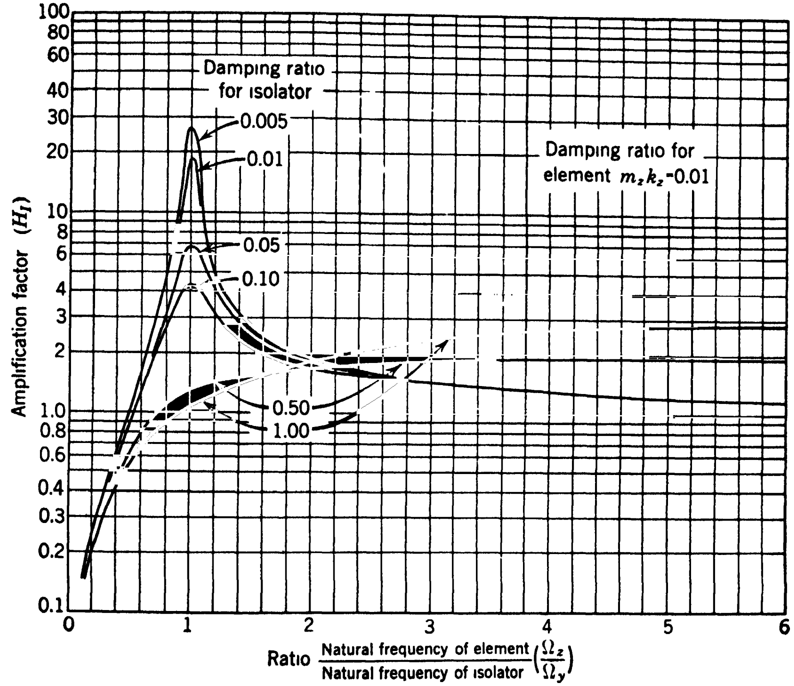

FIGURE 3.10. Amplification factor H_I for system shown in Figure 3.6, when support experiences velocity shock as illustrated in Figure 3.7. The factor H_I is the ratio of the maximum acceleration of m_z to the maximum acceleration of m_y. (*The Bell System Technical Journal.*)

H_I increases as the damping of the isolator decreases. The high amplification factor is the result of resonant vibration of the element, which is excited by the continuing transient vibration of the equipment upon the lightly damped isolators. When the equipment is comprised of relatively flexible members, it is thus advantageous to employ isolators with a large damping ratio.

(*b*) When the natural frequency of the element is substantially greater than the natural frequency of the isolator, the presence of damping in the isolator to a moderate degree has a negligible effect upon the amplification factor H_I. When the damping of the isolator becomes as great as 50 percent of critical and greater, the effect is detrimental; i.e., the value of H_I increases with damping at large values of Ω_z/Ω_y. This is ascribed to (1) the fact that the amplification factor H_I compares the acceleration of the element with the relatively low maximum acceleration of a chassis supported by undamped isolators, as given by equation 3.26, and (2) the fact that a highly damped isolator transmits a large force immediately upon inception of the velocity shock, with consequent impact effects upon the chassis and the element. This latter effect is shown graphically in Figure 4.25 of Chapter 4.

The significant reduction in the severity of shock experienced by equipment mounted upon isolators results from the storage of energy within the isolators, and its subsequent release in a form that is less capable of causing a large deflection of elements of the equipment. The energy storage can occur only by deflection of the isolator. The deflection of the isolator is easily calculated by subtracting the displacement y of the equipment, equation 3.15, from the displacement of the support, $s = V_s t$:

$$\delta_{sy} = s - y = \frac{V_s}{\Omega_y} \sin \Omega_y t. \tag{3.29}$$

The maximum deflection of the isolator is the maximum value of equation 3.29 as follows:

$$(\delta_{sy})_0 = \frac{V_s}{\Omega_y}. \tag{3.30}$$

This equation can be expressed in units more suitable for engineering analysis by writing the natural frequency in cycles per second as follows:

$$(\delta_{sy})_0 = \frac{V_s}{2\pi f_y}. \tag{3.31}$$

The maximum deflection of the isolator as defined by equation 3.31 is shown graphically by the dotted lines in Figure 3.9. For a given velocity change, the maximum deflection is inversely proportional to the natural frequency. This may be envisioned physically by the fact that isolators of low natural frequency embody low spring stiffness, and a large deflection consequently is necessary in order to store the necessary energy.

The above expression for the maximum deflection of the isolator may also be derived by equating the potential energy stored in the isolator, at moment of maximum deflection, to the kinetic energy of the chassis m_y at the moment of contact of the isolator with the support. Assuming that the change in the potential energy of the chassis m_y as a result of deflection of the isolator is negligible compared with its kinetic energy as it approaches the support:

$$\int_0^{(\delta_{sy})_0} F\,d\delta_{sy} = \tfrac{1}{2}m_yV_s^2, \tag{3.32}$$

where F is the force exerted upon the chassis m_y at any deflection δ_{sy} of the isolator. If the force-deflection curve for the isolator is linear, k_y is a constant and the force F is equal to $k_y\delta_{sy}$. Making this substitution in equation 3.32, carrying out the indicated integration, and solving the resulting equation for $(\delta_{sy})_0$:

$$(\delta_{sy})_0 = \frac{V_s}{\Omega_y}, \tag{3.33}$$

which is identical to equation 3.30.

The inertia forces which cause the deflection of elastic elements during conditions of shock are similar to gravitational forces, except with respect to their magnitudes. A convenient design rule thus becomes available. If the magnitude of the maximum acceleration experienced by any element is expressed as a multiple of the acceleration due to gravity, the element must have a static strength sufficient to support its own weight multiplied by this dimensionless multiple. The required strength, assuming a linear isolator, may then be determined from Figures 3.9 and 3.10. For example, it may be determined from Figure 3.9 that the maximum acceleration transmitted to the chassis by the isolator is twenty-five times the acceleration due to gravity. This is commonly written $25g$. If the frequency ratio Ω_z/Ω_y plotted as the abscissa of Figure 3.10 is 3, the amplification factor H_l is 1.5. Elements of the equipment, therefore, must have static strength sufficient to support 25 × 1.5, or 37.5 times their normal static loads.

Example 3.1. It is desired to isolate radio equipment installed in the caboose of a railroad train from the shock that occurs when the train is started. Customary practice in starting freight trains calls for first moving the locomotive in reverse a short distance so that the coupling mechanisms between the cars acquire lost motion. The locomotive then moves forward, and each car impulsively acquires a velocity as all lost motion to the locomotive is taken up. The caboose, at the rear of the train, experiences a velocity change which is approximately equal numerically to the velocity of the locomotive at the moment the caboose acquires its velocity. Assuming that the caboose suddenly attains a velocity of three miles per hour, the properties of a linear shock isolator are to be determined so that the maximum acceleration experienced by rigid elements of the radio equipment does not exceed 25*g*.

The first step in the solution is to convert the velocity change of the caboose, three miles per hour, to inch-second units:

$$V_s = \frac{5280 \times 12 \times 3}{60 \times 60} = 52.8 \text{ in./sec.}$$

Referring to Figure 3.10, it is noted that the amplification factor H_I for lightly damped isolators is approximately 1.15 for large values of the frequency ratio Ω_z/Ω_y. Since $\ddot{z}_0$ must not exceed 25*g*, a maximum permissible value for $\ddot{y}_0$ is obtained from equation 3.23:

$$\ddot{y}_0 = \frac{\ddot{z}_0}{H_I} = \frac{25g}{1.15} = 21.7g.$$

The maximum permissible natural frequency f_y for the isolator is calculated from equation 3.27, or Figure 3.9, using the value 52.8 in./sec for V_s and 21.7*g* for $\ddot{y}_0$:

$$f_y = \frac{61.4(\ddot{y}_0/g)}{V_s} = \frac{61.4 \times 21.7}{52.8} = 25.3 \text{ cps.}$$

The required unobstructed deflection of the isolator is obtained from equation 3.31, or Figure 3.9, using the above values for V_s and f_y:

$$(\delta_{sy})_0 = \frac{V_s}{2\pi f_y} = \frac{52.8}{6.28 \times 25.3} = 0.33 \text{ in.}$$

The maximum acceleration of 21.7*g* as calculated above applies only to very rigid elements of the equipment. For less rigid elements, the acceleration is greater because of a condition of near resonance with the isolator. Assuming damping ratios for the element and isolator of 0.01 and 0.05, respectively, the maximum value of the amplification factor H_I is determined from Figure 3.10 to be approximately 6.7. The corresponding value of $\ddot{z}_0$ is then determined from equation 3.28:

$$\ddot{z}_0 = H_I\ddot{y}_0 = 6.7 \times 21.7g = 145.4g.$$

This relatively high value of acceleration may be materially reduced by slightly changing the natural frequency of the element so as to avoid complete resonance with the isolator. For an element with a natural frequency of 50.6 cps ($\Omega_z/\Omega_y = 2$), $H_I = 1.8$ and $\ddot{z}_0 = 1.8 \times 21.7g = 39g$.

3·5 *Isolation of Velocity Shock—Elastic Impact*

It is necessary now to distinguish between velocity shocks with elastic and inelastic impact. In the system illustrated in Figure 3.6, the isolator k_y is attached to the support, and the chassis m_y experiences a continuing vibration at the characteristic natural frequency of the isolator. This is equivalent to inelastic impact, and not only the initial half cycle but ensuing cycles of vibration are significant. In the system shown in Figure 3.11, the equipment is housed within a container; the entire assembly is considered to be moving downward with a velocity V_y at moment of contact with the support. If the container is massive, it is not moved upward as a result of the force applied by the isolator k_y during upward displacement of the chassis m_y. Further, if the impact with the support is inelastic, there is no rebound. The analysis set forth in Section 3·2 is then applicable.

If the container is not massive, however, the entire assembly tends to rebound from the support. This tendency persists, independently of the nature of the impact, because the relatively massive chassis m_y has acquired an upward velocity at the end of a time interval equal to one-half the natural period of the isolator. This is designated elastic impact. It is fundamentally different from the condition of inelastic impact in that vibration of the chassis at the natural frequency of the isolator is limited to one half cycle.

Referring to Figure 3.11, and assuming the container to be massless, the differential equation of motion for the chassis m_y is written as follows, taking the coordinate distance y to be zero at moment of contact of the container with the support:

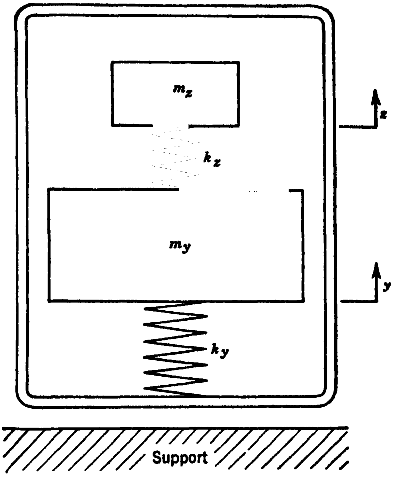

FIGURE 3.11. Diagram representing equipment comprised of a relatively massless case housing a heavy chassis m_y and a light element m_zk_z. The equipment is assumed to have a downward velocity immediately before striking the support, and to attain an equal upward velocity as a result of perfect rebound.

$$m_y\ddot{y} = -k_y y. \tag{3.34}$$

The above equation is solved first for the time interval $0 \leq t \leq \pi/\Omega_y$. Taking the time reference as zero at the moment of contact of the container with the support, and substituting the initial conditions, $y = 0$ and $\dot{y} = -V_y$ when $t = 0$:

$$y = \frac{-V_y}{\Omega_y}\sin \Omega_y t, \qquad \left(0 \leq t \leq \frac{\pi}{\Omega_y}\right). \tag{3.35}$$

The acceleration of the chassis m_y is obtained from double differentiation of equation 3.35 with respect to time:

$$\ddot{y} = V_y \Omega_y \sin \Omega_y t, \qquad \left(0 \le t \le \frac{\pi}{\Omega_y}\right). \tag{3.36}$$

The displacement y of the chassis m_y, measured from its position at moment of contact of the container with the support, is numerically equal to the deflection δ_{sy} of the isolator. The deflection of the isolator is related to the acceleration of the chassis by equations 3.35 and 3.36. Taking the maximum values $y_0 = -(\delta_{sy})_0$ and $\ddot{y}_0 = V_y \Omega_y$ from these equations, the following relation is readily obtained:

$$\ddot{y}_0 = V_y \left[\frac{V_y}{(\delta_{sy})_0}\right] = \frac{V_y^2}{(\delta_{sy})_0}. \tag{3.37}$$

An expression for the maximum acceleration $\ddot{y}_0$ in terms of isolator natural frequency and maximum deflection of the isolator is obtained by first solving equation 3.35 for V_y in terms of y_0 and Ω_y. Substituting this expression for V_y in equation 3.37, and letting $y_0 = (\delta_{sy})_0$ for reasons explained above:

$$\ddot{y}_0 = (\delta_{sy})_0 \Omega_y^2. \tag{3.38}$$

Expressions that define the motion z of the mass m_z will now be derived, assuming m_z to be small compared with m_y. The differential equation of motion for m_z is

$$m_z \ddot{z} = k_z (y - z). \tag{3.39}$$

Since $\delta_{yz} = y - z$, $z = y - \delta_{yz}$ and $\ddot{z} = \ddot{y} - \ddot{\delta}_{yz}$. Making these substitutions in equation 3.39, substituting for $\ddot{y}$ the derivative of the expression given by equation 3.35, and writing $k_z/m_z = \Omega_z^2$, equation 3.39 becomes:

$$\ddot{\delta}_{yz} + \Omega_z^2 \delta_{yz} = V_y \Omega_y \sin \Omega_y t. \tag{3.40}$$

The solution of equation 3.40, applying the initial conditions, $\delta_{yz} = \dot{\delta}_{yz} = 0$ when $t = 0$, is

$$\delta_{yz} = \frac{V_y \Omega_y}{\Omega_y^2 - \Omega_z^2} \left[\frac{\Omega_y}{\Omega_z} \sin \Omega_z t - \sin \Omega_y t\right], \qquad \left(0 \le t \le \frac{\pi}{\Omega_y}\right). \tag{3.41}$$

The relative displacement δ_{yz} between the chassis m_y and the mass m_z includes a component at the natural frequency Ω_y of the isolator, and a superimposed component at the natural frequency Ω_z of the element $m_z k_z$. The maximum value of the relative displacement δ_{yz} from equation 3.41 is

$$(\delta_{yz})_0 = \frac{V_y}{\Omega_z[(\Omega_z/\Omega_y) - 1]} \sin \frac{2n\pi}{(\Omega_z/\Omega_y) + 1}, \qquad \left(0 \leq t \leq \frac{\pi}{\Omega_y}\right), \tag{3.42}$$

where n is a positive integer chosen so as to make the sine term as large as possible while the argument remains less than π.*

The maximum acceleration $\ddot{z}_0$ of the element is determined directly from the maximum deflection $(\delta_{yz})_0$ of the element by using the following relation: $m_z\ddot{z}_0 = k_z(\delta_{yz})_0$. Substituting $\Omega_z^2 = k_z/m_z$, the following expression is obtained for $\ddot{z}_0$:

$$\ddot{z}_0 = \Omega_z^2(\delta_{yz})_0. \tag{3.43}$$

It is convenient to express the maximum acceleration $\ddot{z}_0$ of the element in terms of the maximum acceleration $\ddot{y}_0$ of the chassis m_y. An amplification factor H_E for elastic impact is now established to denote the ratio of $\ddot{z}_0$ to $\ddot{y}_0$. The maximum acceleration $\ddot{z}_0$ of the element in the time interval $0 \leq t \leq \pi/\Omega_y$ is found by substituting the expression for $(\delta_{yz})_0$ from equation 3.42 in equation 3.43; the maximum acceleration $\ddot{y}_0$ of the chassis is the maximum value of equation 3.36. The amplification factor H_E is then

$$H_E = \frac{\ddot{z}_0}{\ddot{y}_0} = \frac{\Omega_z/\Omega_y}{(\Omega_z/\Omega_y) - 1} \sin \frac{2n\pi}{(\Omega_z/\Omega_y) + 1}, \qquad \left(0 \leq t \leq \frac{\pi}{\Omega_y}\right). \tag{3.44}$$

After the assembly rebounds from the support, its motion is characterized initially by a substantially constant upward velocity. Neglecting the gravitational force, the acceleration $\ddot{y}$ of the chassis m_y may be considered zero. The differential equation of motion for the time interval $t \geq \pi/\Omega_y$ is thus obtained from equation 3.40 by setting $\ddot{y} = 0$ ($\ddot{y} = V_y\ \Omega_y \sin \Omega_y t$ from equation 3.36):

$$\ddot{\delta}_{yz} + \Omega_z^2\delta_{yz} = 0, \qquad \left(t \geq \frac{\pi}{\Omega_y}\right). \tag{3.45}$$

Establishing a new time reference $t' = 0$ when $t = \pi/\Omega_y$, the above equation is evaluated from the boundary conditions at time $t = \pi/\Omega_y$. Equating the relative displacements δ_{yz} as given by equations 3.41

---

* This result is given by R. D. Mindlin: "Dynamics of Package Cushioning," *Bell System Technical Journal*, Vol. XXIV, Nos. 3–4, July–October 1945, page 424. The details of the solution are set forth in *Bureau of Ships, Navy Department publication* Navships 250-660-30, September 1949: "A Guide for Design of Shock Resistant Naval Equipment," by C. E. Crede and M. C. Junger, Appendix B.

and the solution of equation 3.45, and the relative velocities $\dot{\delta}_{yz}$ as given by the derivatives of these equations:

$$\dot{\delta}_{yz} = \frac{2V_y \cos(\pi\Omega_z/2\Omega_y)}{\Omega_z[1 - (\Omega_z^2/\Omega_y^2)]} \sin\left(\Omega_z t' + \frac{\pi\Omega_z}{2\Omega_y}\right), \quad \left(t \geq \frac{\pi}{\Omega_y}\right), \tag{3.46}$$

The maximum value of δ_{yz} for the time interval $t \geq \pi/\Omega_y$ is obtained from equation 3.46 by setting the sine term equal to unity. Then:

$$(\delta_{yz})_0 = \frac{2V_y \cos(\pi\Omega_z/2\Omega_y)}{\Omega_z[1 - (\Omega_z^2/\Omega_y^2)]}, \quad \left(t \geq \frac{\pi}{\Omega_y}\right). \tag{3.47}^*$$

The amplification factor H_E for the time interval $t \geq \pi/\Omega_y$, as in the previous case, is the ratio of $\ddot{z}_0$ to $\ddot{y}_0$. The expression for $\ddot{z}_0$ is $(\delta_{yz})_0\Omega_z^2$, where $(\delta_{yz})_0$ is given by equation 3.47, and the expression for $\ddot{y}_0$ is obtained from the maximum value of equation 3.36. The maximum value of $\ddot{y}_0$ always occurs in the time interval $0 \leq t \leq \pi/\Omega_y$ since $\ddot{y} = 0$ when $t \geq \pi/\Omega_y$. Equation 3.36 is therefore used as a reference in determining H_E, whether the maximum value of $\ddot{z}_0$ occurs in the time interval $0 \leq t \leq \pi/\Omega_y$ or $t \geq \pi/\Omega_y$.

$$H_E = \frac{\ddot{z}_0}{\ddot{y}_0} = \frac{2(\Omega_z/\Omega_y)\cos(\pi\Omega_z/2\Omega_y)}{1 - (\Omega_z^2/\Omega_y^2)}, \quad \left(t \geq \frac{\pi}{\Omega_y}\right). \tag{3.48}$$

Two expressions are thus available for the amplification factor H_E. When $\Omega_z \geq \Omega_y$, the maximum value of H_E occurs during contact of the container with the support; i.e., when $0 \leq t \leq \pi/\Omega_y$. The value of H_E calculated from equation 3.44 is then the larger. When $\Omega_z \leq \Omega_y$, the maximum value of H_E occurs after the assembly has rebounded from the support; i.e., when $t \geq \pi/\Omega_y$. The value of H_E computed from equation 3.48 is then the larger. In other words, when the element has a natural frequency that is greater than that of the

---

* If the change in velocity of the chassis m_y takes place in a time interval that is small compared with the natural period of the element $m_z k_z$, the frequency ratio Ω_z/Ω_y is numerically small. Equation 3.47 then becomes:

$$(\delta_{yz})_0 \approx \frac{2V_y}{\Omega_z}.$$

Since the velocity of approach of the equipment is $-V_y$, the velocity change upon rebound is numerically equal to $2V_y$. This result should be compared with equation 3.4 for inelastic impact, wherein the velocity change V_s occurs instantaneously and the maximum relative displacement $(\delta_{yz})_0$ is equal to V_s/Ω_z. Thus, when the natural period of the element is large relative to the interval during which the velocity change occurs, the effect approximates that of an instantaneous velocity change.

isolator, the maximum deflection of the element occurs during contact of the assembly with the support. If the natural frequency of the element is less than that of the isolator, however, the maximum deflection of the element occurs after contact has ended. The amplification factor H_E, as determined from equations 3.44 and 3.48, is shown

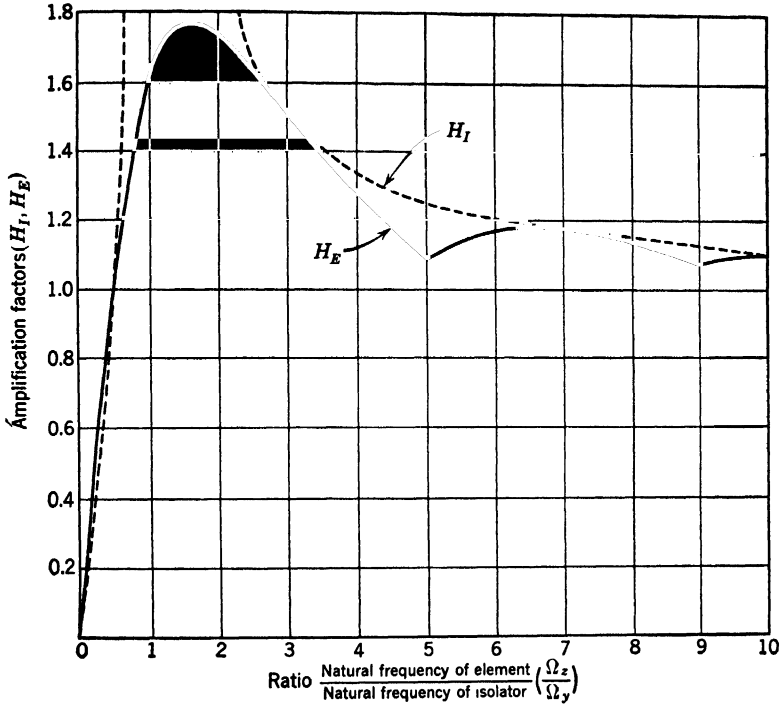

FIGURE 3.12. Comparison of amplification factors H_I and H_E. The dotted curve H_I is identical to a curve from Figure 3.10 and refers to inelastic impact of a system in which the isolator has a small damping ratio. The factor H_E is the ratio of the maximum acceleration of m_z to the maximum acceleration of m_y in Figure 3.11, for the condition of elastic impact and no damping. (*The Bell System Technical Journal.*)

by the full line in Figure 3.12 as a function of the frequency ratio Ω_z/Ω_y.

A comparison of the amplification factor H_I for velocity shock with inelastic impact and the amplification factor H_E for elastic impact reveals interesting information. In order to facilitate the comparison, the amplification factor H_I for inelastic impact, as calculated from equation 3.24 for the undamped case, is included as a dotted line in Figure 3.12. The following characteristics are important to note:

(*a*) With very rigid elements, for which the frequency ratio Ω_z/Ω_y is large, the maximum acceleration experienced by the element is approximately equal to the maximum acceleration transmitted by the isolator to the chassis of the equipment. This is true for both elastic and inelastic impact: $H_I \approx H_E \approx 1.0$. *It is therefore reasonable to evaluate an isolator on the basis of the maximum acceleration experienced by the chassis of the mounted equipment, provided that it is understood that the evaluation applies rigorously only to relatively rigid elements.* This concept is of particular value in analyzing non-linear isolators, because the response of elements of the equipment is difficult to calculate.

(*b*) When the frequency ratio Ω_z/Ω_y becomes less than approximately 2.5, the maximum acceleration of the element as indicated by H_I becomes substantially greater than the maximum acceleration as indicated by H_E. This increase is due to resonance of the element with the isolator. The effect does not appear in elastic impact because the system rebounds from the support, and transient vibration at the natural frequency of the isolator is limited to one half cycle.

3·6 *Effect of Snubbing*

It is shown in Figure 3.9 that the maximum deflection of a linear isolator increases in direct proportion to the magnitude of the velocity change. For applications where the velocity change may have any magnitude within a wide range, provision must be made either for adequate deflection of the isolator or for means to limit the deflection to a permissible value. It is shown in the following paragraphs that such a limiting means should be in the form of a resilient snubber, and that the use of a rigid snubber may result in the amplification rather than the reduction of the shock.

The necessary clearance required to permit unrestricted deflection of a linear isolator under conditions of velocity shock is indicated by equations 3.30 and 3.31. If the clearance δ_c between the chassis m_y and a snubber is less than the required free clearance V_s/Ω_y, snubber engagement occurs at a time that is determined by equating δ_{sy} from equation 3.29 to δ_c and solving for t:

$$\frac{V_s}{\Omega_y} \sin \Omega_y t = \delta_c; \quad t = \frac{1}{\Omega_y} \sin^{-1} \frac{\delta_c}{V_s/\Omega_y}. \tag{3.49}$$

Assuming the coefficient of restitution of the chassis in engagement with the snubber to be unity, the chassis rebounds from the snubber in the manner illustrated in Figure 3.13. The total velocity change experienced by the chassis at the instant of engagement with the snubber is thus twice the difference $\dot{s} - \dot{y}$, at time t given by equation

3.49. Differentiating equation 3.29 and multiplying by 2 to obtain the difference in velocities:

$$2\dot{\delta}_{sy} = 2(\dot{s} - \dot{y}) = 2V_s \cos \Omega_y t.$$

Substituting the time t at moment of engagement as given by equation 3.49, the velocity change ΔV resulting from engagement of chassis with snubber is obtained from the above equation:

$$\Delta V = 2V_s \cos \Omega_y \left(\frac{1}{\Omega_y} \sin^{-1} \frac{\delta_c}{V_s/\Omega_y} \right) = 2V_s \sqrt{1 - \frac{{\delta_c}^2}{(V_s/\Omega_y)^2}}. \quad (3.50)$$

The expression for velocity change given by equation 3.50 is plotted in Figure 3.14. It is evident that the chassis m_y may experience a

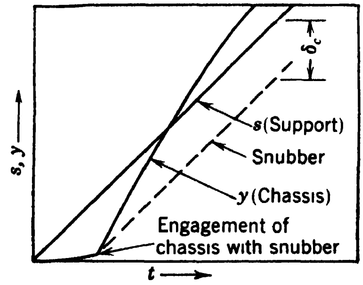

FIGURE 3.13.

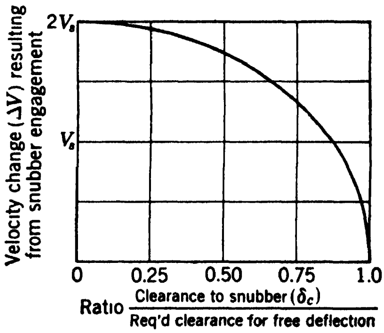

FIGURE 3.14.

FIGURE 3.13. Displacement-time diagrams for system similar to that shown in Figure. 3.6, but wherein deflection of isolator k_y is limited by engagement of chassis with a snubber. The system undergoes velocity shock, as illustrated in Figure 3.7.
FIGURE 3.14. Velocity change experienced by chassis m_y as a result of engagement with snubber, for condition of velocity shock illustrated by Figure 3.13.

velocity change twice as great as the shock velocity change V_s if adequate clearance to the snubber is not provided. When the snubber clearance is zero, the isolator is not operative and the chassis experiences the shock velocity change V_s. For a small clearance, the total velocity change approaches $2V_s$. A detrimental condition exists; i.e., $\Delta V > V_s$, for almost all conditions under which snubber engagement occurs.

Snubber engagement exhibits the characteristics of velocity shock with elastic impact, as discussed in the preceding section. The maximum acceleration experienced by the chassis of the equipment, upon engagement with the snubber, is obtained from equation 3.36 by substituting $V_y = \Delta V$ from equation 3.50 and $\Omega_y = \Omega_c$. The latter is designated snubber natural frequency Ω_c and is obtained from the snubber stiffness and the mass of the chassis in accordance with the relation $\Omega_c^2 = k_c/m_y$, where k_c is the stiffness of the snubber. Appropriate values for the amplification factor H_E then are obtained from equations 3.44 and 3.48 by substituting $\Omega_y = \Omega_c$.

Example 3.2. A snubber with a clearance $\delta_c = 0.5$ inch is now added to the system analyzed in Example 3.1. The stiffness of the snubber is 10 times as great as the stiffness of the isolator. If the starting velocity of the caboose is increased from three to five miles per hour, what is the maximum acceleration experienced by the equipment?

The starting velocity is first converted to units of inches per second as follows:

$$V_s = \frac{5280 \times 12 \times 5}{60 \times 60} = 88 \text{ in./sec.}$$

The velocity change that occurs at the moment of snubber engagement is calculated from equation 3.50:

$$\Delta V = 2 \times 88 \sqrt{1 - \frac{(0.5)^2}{\left(\dfrac{88}{2\pi \times 25.3}\right)^2}} = 75.7 \text{ in./sec.}$$

The natural frequency of a simple system varies directly as the square root of the stiffness. Consequently, the snubber natural frequency is given by the relation $\Omega_c = \Omega_y \sqrt{10}$:

$$\Omega_c = 25.3 \sqrt{10} = 80 \text{ cps.}$$

The maximum acceleration of the chassis m_y during snubber engagement is calculated from equation 3.27 by substituting $V_s = \Delta V$ and $\Omega_y = \Omega_c$:

$$\ddot{y}_0 = \frac{75.7 \times 80 \times 2\pi}{386} = 98.3g.$$

By comparing this value of acceleration with the corresponding value of 21.7g previously computed for a starting velocity of three miles per hour, it is evident that an increase in starting velocity of 67 percent causes more than a fourfold increase in maximum acceleration. This greater maximum acceleration can be materially reduced by increasing the isolator stiffness sufficiently to prevent snubber engagement. The minimum natural frequency required to accomplish this is calculated by substituting $(\delta_{sy})_0 = \delta_c = 0.5$ and solving equation 3.31 for f_y:

$$f_y = \frac{V_s}{2\pi(\delta_{sy})_0} = \frac{88}{2\pi \times 0.5} = 28 \text{ cps.}$$

The maximum acceleration experienced by the chassis with this increased isolator natural frequency is now calculated from equation 3.27:

$$\ddot{y}_0 = \frac{88 \times 2\pi \times 28}{386} = 40g.$$

The increase in the starting velocity of the caboose from 52.8 inches per second to 88 inches per second causes an increase in maximum deflection of the isolator from 0.36 to 0.50 inch when the natural frequency of the isolator is increased from 21.7 to 28 cps. The maximum acceleration experienced by the chassis is thereby increased from 21.7*g* to 40*g*. If snubber engagement is permitted to occur, however, the maximum acceleration may become as great as 98.3*g*.

3·7 Preloaded Isolators

An advantage is sometimes obtained by subjecting the isolator to an initial deflection, thereby attaining relatively great energy storage for subsequent deflection. Such an isolator is referred to as preloaded. In Figure 3.11, for example, the isolator may be considered to have an initial deflection δ_p and a maximum possible additional deflection δ_c. Designating the isolator stiffness by k_p, the preload is given by $F_p = k_p\delta_p$. The force-deflection curve for this isolator is shown in Figure 3.15, where the chassis displacement y is taken as zero when the isolator has the initial deflection δ_p.

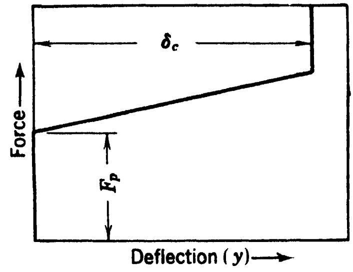

FIGURE 3.15.

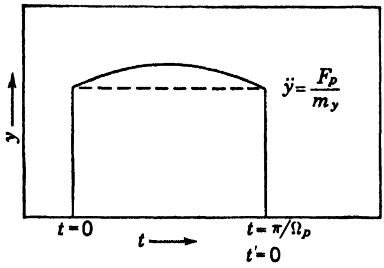

FIGURE 3.16.

FIGURE 3.15. Force-deflection curve for preloaded isolator.

FIGURE 3.16. Acceleration-time diagram for chassis m_y supported by preloaded isolator and subjected to velocity shock.

The acceleration $\ddot{y}$ experienced by the chassis m_y for the condition of elastic impact (see Section 3.5) is indicated by the solid line in Figure 3.16. At the moment of engagement of the isolator with the support, the acceleration $\ddot{y}$ increases instantaneously from zero to F_p/m_y, where F_p is the initial compressive force in the spring k_p. The acceleration increases to a maximum as compression of the spring continues. The latter half of the acceleration-time diagram is a mirror image of the first half, as the spring extends to its initial length and the assembly bounces clear of the support.

As the total length of the spring k_p is increased, the inclined line in Figure 3.15 approaches the horizontal and the acceleration-time diagram tends to become rectangular, as indicated by the dotted line in Figure 3.16. Such a condition is assumed, in the interests of simplification, for the following analysis. The acceleration $\ddot{y}$ experienced by m_y is then defined as follows:

$$\begin{aligned} \ddot{y} &= \frac{F_p}{m_y}, \quad \left(0 \leq t \leq \frac{\pi}{\Omega_p}\right), \\ \ddot{y} &= 0, \quad \left(t \geq \frac{\pi}{\Omega_p}\right), \end{aligned} \tag{3.51}$$

where Ω_p is a circular frequency such that the half natural period π/Ω_p is the time of contact with the support.

It is desired now to determine the relative deflection δ_{yz} of the element $m_z k_z$. The equation of motion for the mass m_z is similar to equation 3.39. It is written in terms of the relative displacement δ_{yz} by analogy with equation 3.40 as follows:

$$\ddot{\delta}_{yz} + \Omega_z^2 \delta_{yz} = \frac{F_p}{m_y}, \quad \left(0 \leq t \leq \frac{\pi}{\Omega_p}\right). \tag{3.52}$$

Solving equation 3.52 for δ_{yz} and applying the initial conditions, $\delta_{yz} = \dot{\delta}_{yz} = 0$ when $t = 0$, the following expression is obtained for δ_{yz} in the time interval $0 \leq t \leq \pi/\Omega_p$:

$$\delta_{yz} = \frac{F_p}{m_y \Omega_z^2}(1 - \cos \Omega_z t), \quad \left(0 \leq t \leq \frac{\pi}{\Omega_p}\right). \tag{3.53}$$

When $t \geq \pi/\Omega_p$, the chassis m_y has bounced clear of the support and its acceleration is zero. The differential equation of motion for the mass m_z in this time interval, by analogy with equation 3.45, is

$$\ddot{\delta}_{yz} + \Omega_z^2 \delta_{yz} = 0, \quad \left(t \geq \frac{\pi}{\Omega_p}\right). \tag{3.54}$$

In obtaining a solution to this equation, it is convenient to establish a new time reference defined by $t' = 0$ when $t = \pi/\Omega_p$. The solution of equation 3.54 may then be obtained, the undetermined coefficients being evaluated from boundary conditions at time $t' = 0$, as explained with reference to equation 3.46:

$$\delta_{yz} = \frac{F_p}{m_y \Omega_z^2}\left[\sin \frac{\Omega_z}{\Omega_p}\pi \sin \Omega_z t' + \left(1 - \cos \frac{\Omega_z}{\Omega_p}\pi\right) \cos \Omega_z t'\right],$$

which may be written

$$\delta_{yz} = \frac{F_p}{m_y \Omega_z^2}\left[\cos \Omega_z t' - \cos\left(\frac{\Omega_z}{\Omega_p}\pi + \Omega_z t'\right)\right], \quad (t' \geq 0). \tag{3.55}$$

The maximum value of the relative displacement δ_{yz} is obtained from equation 3.53 when $\Omega_z/\Omega_p \geq 1$, and from equation 3.55 when $\Omega_z/\Omega_p \leq 1$. The former is determined simply from the condition that a time t can always be found such that $\cos \Omega_z t = -1$. Then, from equation 3.53:

$$(\delta_{yz})_0 = \frac{2F_p}{m_y \Omega_z^2}, \qquad \frac{\Omega_z}{\Omega_p} \geq 1. \tag{3.56}$$

Writing equation 3.55 in terms of the sum and difference of two angles:

$$\delta_{yz} = \frac{F_p}{m_y \Omega_z^2}\left[-2 \sin\left(\frac{2\Omega_z t' + (\Omega_z \pi/\Omega_p)}{2}\right) \sin\left(\frac{-\Omega_z \pi}{2\Omega_p}\right)\right], \qquad (t' \geq 0).$$

A time t' can always be found such that the first sine term is equal to unity. The maximum relative displacement then is

$$(\delta_{yz})_0 = \frac{2F_p}{m_y \Omega_z^2} \sin \frac{\Omega_z \pi}{2\Omega_p}, \qquad \frac{\Omega_z}{\Omega_p} \leq 1. \tag{3.57}$$

Substituting $F = F_p$, a constant, in equation 3.32 and carrying out the indicated integration:

$$F_p(\delta_{sy})_0 = \tfrac{1}{2} m_y V_y^2, \tag{3.58}$$

where $(\delta_{sy})_0$ = maximum deflection of the preloaded isolator.
V_y = downward velocity of assembly at moment of engagement with support.*

The acceleration of the chassis m_y during engagement of the isolator with the support is equal to the quotient of the constant force F_p divided by the chassis mass m_y. Referring to equation 3.58:

$$\ddot{y}_0 = \frac{F_p}{m_y} = \frac{V_y^2}{2(\delta_{sy})_0}. \tag{3.59}$$

The maximum acceleration of the element $m_z k_z$ is obtained from the relation given by equation 3.43, using the expressions for $(\delta_{yz})_0$ from equations 3.56 and 3.57. Employing the relation given by equation 3.59, the following expressions are obtained for $\ddot{z}_0$:

---

* The substitution of V_y for V_s in equation 3.32 is justified because the maximum deflection of the isolator has the same numerical value for both elastic and inelastic impact and because the deflection is a function of the velocity change. The latter is discussed on page 92, where it is pointed out that the same value is obtained for isolator deflection when the support acquires a velocity and when a moving equipment is brought to rest, provided that $V_y = V_s$.

$$\ddot{z}_0 = \frac{2F_p}{m_y} = \frac{V_y^2}{(\delta_{sy})_0}, \qquad \frac{\Omega_z}{\Omega_p} \geq 1; \tag{3.60}$$

$$\ddot{z}_0 = \frac{2F_p}{m_y} \sin\frac{\Omega_z \pi}{2\Omega_p} = \frac{V_y^2}{(\delta_{sy})_0} \sin\frac{\Omega_z \pi}{2\Omega_p}, \qquad \frac{\Omega_z}{\Omega_p} \leq 1. \tag{3.61}$$

The merits of the preloaded isolator may be illustrated by comparing its protective properties with those of a linear isolator. The usual basis for comparison, as employed previously, is the magnitude of the maximum acceleration experienced by elements of the mounted equipment. For the linear isolator which experiences elastic impact, this is expressed in Figure 3.12 as the ratio H_E of the maximum element acceleration to the maximum chassis acceleration. A similar ratio H_p is now designated and defined as the ratio of the maximum acceleration of the element when supported by a *preloaded* isolator to the maximum acceleration of the chassis when supported by a *linear* isolator. The distinction between H_E and H_p should be noted. The ratio H_E refers to the relative accelerations of element and chassis, both in the same system. The ratio H_p, on the other hand, refers to the acceleration of the element in the system with the preloaded isolator and the acceleration of the chassis in the system with the linear isolator. By comparing equations 3.37 and 3.59, it is evident that the maximum chassis acceleration with the preloaded isolator is one-half that with the linear isolator if $(\delta_{sy})_0$ is equivalent for the two cases. The following expressions for H_p are now written, assuming the maximum deflection $(\delta_{sy})_0$ to be equivalent for the linear and preloaded isolators:

$$\begin{aligned} H_p &= \frac{\ddot{z}_0(\text{equation 3.60})}{\ddot{y}_0(\text{equation 3.37})} = 1, \qquad \frac{\Omega_z}{\Omega_p} \geq 1; \\ H_p &= \frac{\ddot{z}_0(\text{equation 3.61})}{\ddot{y}_0(\text{equation 3.37})} = \sin\frac{\Omega_z \pi}{2\Omega_p}, \qquad \frac{\Omega_z}{\Omega_p} \leq 1. \end{aligned} \tag{3.62}$$

Equations 3.62 are shown graphically in Figure 3.17. The curve for H_E (see Figure 3.12) is reproduced in Figure 3.17 in order to facilitate the comparison between the linear and the preloaded isolator.

The advantages afforded by the preloaded isolator in comparison with the linear isolator are evident from Figure 3.17, as indicated by the lower position of the curve H_p. The advantage is particularly marked in the region where the natural frequency of the element is approximately equal to the natural frequency of the linear isolator. Under the conditions assumed, the preloaded isolator has no natural frequency which is significant with respect to the problem being investigated. The advantage associated with the preloaded isolator decreases as the natural frequency of the elements increases; i.e., as the frequency ratios Ω_z/Ω_p, Ω_z/Ω_y increase.

It is instructive to investigate the reasons for the conditions indicated in Figure 3.17. For equal values of maximum isolator deflection $(\delta_{sy})_0$ and approach velocity V_y, the maximum acceleration experienced by the chassis supported on preloaded isolators is 50 percent as great as that of the chassis supported on linear isolators. This relation exists because a preloaded isolator stores twice as much energy per unit of deflection. It is evident from Figure 3.17, however, that $H_p \approx H_E$ when the frequency ratio Ω_z/Ω_y (or Ω_z/Ω_p) is large. The important consideration here is the time at which the maximum

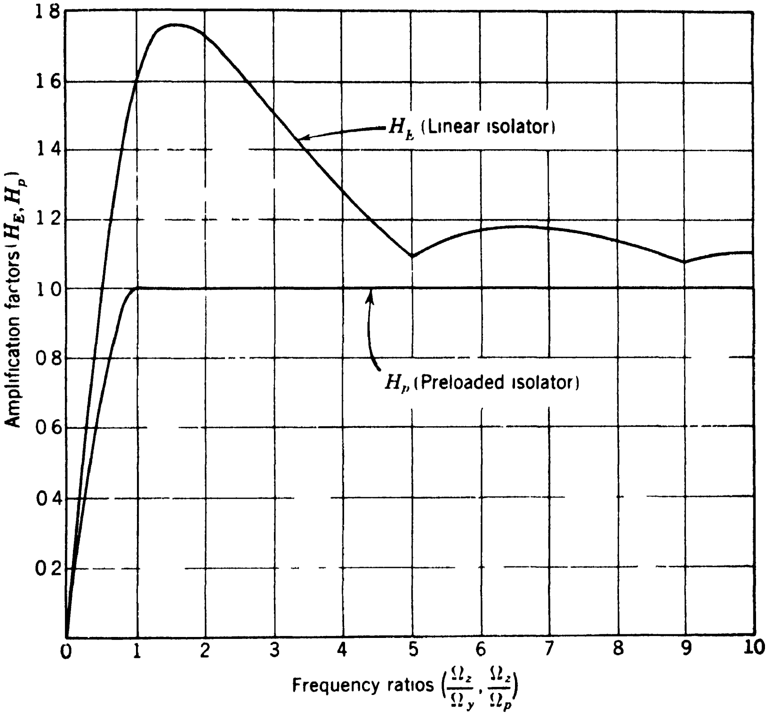

FIGURE 3.17. Amplification factor H_p obtained with preloaded isolator. The factor H_p is the ratio of the maximum accelerations of m_z and m_y in Figure 3.11, when the equipment strikes the support and rebounds perfectly therefrom. The isolator k_y is initially deflected a distance δ_p. The corresponding curve H_E for a linear isolator is reproduced from Figure 3.12 to permit ready comparison with H_p. (*The Bell System Technical Journal.*)

acceleration occurs. For the linear isolator, the acceleration increases gradually; for the preloaded isolator, it increases suddenly. The response of the element to the latter is greater and practically cancels the advantage associated with a lower chassis acceleration. This conclusion is predicated on theoretical considerations and probably is not actually realized to the extent indicated in isolators whose inherent flexibility prevents an instantaneous build-up of acceleration.

A shock isolator in the form of a buckling rubber column embodies the principle of preloading. Such an isolator is constructed in the form of either a long strip or a ring; Figure 3.18 is a cross section through either the strip or the periphery of the ring. The rubber is usually bonded between flat metal members by which the force is applied, and its thickness becomes a minimum midway between the metal members to control the buckling action. A typical force-deflection curve is shown in Figure 3.19. When the applied force is less than the buckling force, the isolator exhibits the characteristics of rubber in compression for small deflections, as shown by the initial substantially linear portion of the force-deflection curve. As the force continues to increase, the rubber column ultimately buckles and the applied force remains substantially constant while the deflection increases. The buckled column then becomes folded between the metal members, and additional application of force produces a force-deflection curve having the characteristics of rubber in compression for large deflections.

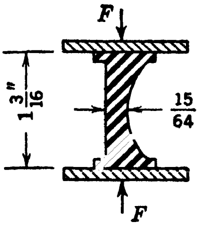

FIGURE 3.18.

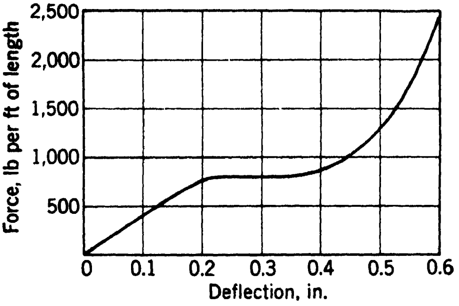

FIGURE 3.19.

FIGURE 3.18. Cross section through buckling isolator. (Signal Corps Engineering Laboratories.)

FIGURE 3.19. Force-deflection curve for buckling isolator shown in Figure 3.18.

It may be recognized that the force-deflection curve for this isolator shows some resemblance to the curve of Figure 3.15. The relatively large energy storage capacity is a characteristic favorable to effective shock isolation. Furthermore, the rubber is loaded in compression when the isolator is subjected to large forces, and thereby eliminates the undesirable effect obtained with a rigid snubber.

The buckling-type shock isolator has been investigated extensively.* The maximum acceleration experienced by the equipment as a result of shock is a function of the velocity change, the thickness of the isolator, the supported load, and the buckling force for the isolator. A typical relation is shown in Figure 3.20 for a particular isolator thickness. Each curve represents a discrete velocity change, and each reaches a minimum acceleration at a different ratio of buckling force to supported load. Tests show that the isolator deflection corresponding to this minimum transmitted acceleration is slightly greater than that represented by the flat part of the force-deflection curve illustrated in Figure 3.19. If the supported load is reduced, the acceleration is greater than the minimum because a smaller mass is being acted upon by substantially the same force. If the load is increased, the deflection becomes greater and the transmitted force increases rapidly, owing to the rapidly increasing slope of the force-deflection curve. The force increases faster than the load, and the acceleration consequently increases. As the velocity change increases, the maximum transmitted acceleration also increases; the ratio of buckling force to supported load that is necessary to maintain a low

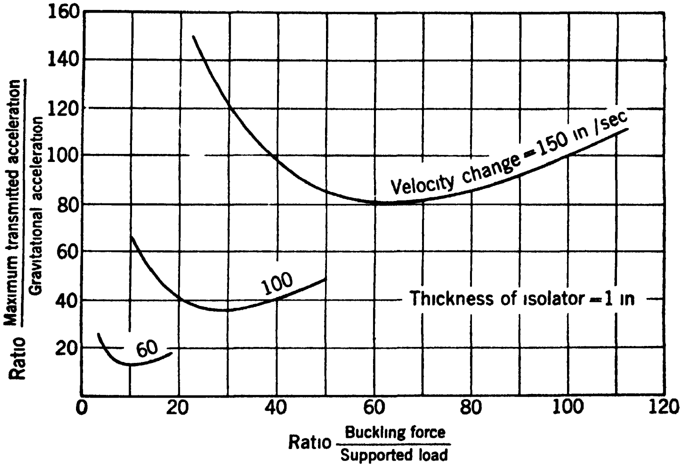

FIGURE 3.20 Maximum acceleration transmitted by buckling isolator, as a function of the buckling force and the load that the isolator supports.

---

* C. E. Crede and S. E. Young, "Theoretical and Experimental Investigation of Buckling Shock Mount," *Proc. Soc. Exp. Stress Anal.*, Vol. V,No. II.

maximum acceleration then decreases. When used under optimum conditions, the maximum acceleration transmitted by the buckling isolator is substantially less than that transmitted by the most commonly used types of isolators. The advantages are not so clearly defined when conditions deviate from the optimum.

B. ISOLATION OF SHOCK FORCES THAT CAUSE DISPLACEMENTS OF LARGE MAGNITUDE

3·8 Shock Severity with Rigidly Supported Machines

The next problem to be considered involves the isolation of a shock force resulting from the impulsive addition of energy to a machine or equipment. The external energy that is added in this manner imparts a velocity to the machine whose motion can be arrested only through the action of externally applied forces. A drop forging machine acquires a downward velocity as a result of the force applied to the anvil by the freely falling hammer. This downward motion of the machine must be resisted by its support, and the support is deflected downward in response to the force applied by the machine. Another instance that illustrates the same principle arises in connection with a scale employed for weighing heavy bulk material. This material is permitted to fall upon the scale platform, whose impulsively acquired downward velocity endangers the delicate mechanism of the weighing system.

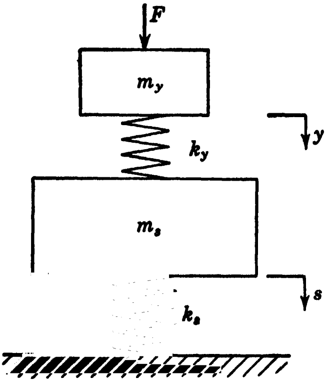

FIGURE 3.21. Schematic representation of machine m_y supported by means of isolator k_y on relatively massive supporting structure m_sk_s. Operation of the machine creates the force F.

The nature of this problem and the relief that is afforded by isolation are best understood by first analyzing the conditions that exist when such a machine is secured rigidly to its support. In Figure 3.21, the support is represented schematically by the simple system m_sk_s, the machine by the mass m_y, and the isolator by k_y. The support may be idealized in this manner if m_s is defined as the mass of a single-degree-of-freedom system whose natural frequency is equal to the lowest natural frequency of the support. When the machine is secured rigidly to its support, $k_y \rightarrow \infty$ and $y = s$ at all times.

The impulsively applied force is indicated by F. The result of the force is a displacement of the machine and a deflection of its support. Troublesome conditions introduced by operation of the machine are generally due either to excessive stress in the support or to excessive motion of the support. Whichever the cause, the magnitude of the trouble tends to be proportional to the maximum deflection of the support. The deflection experienced by the support when the machine is rigidly attached thereto is considered in this section; an analysis directed to determining the effect of isolators is set forth in the next section.

If the transfer of momentum to the machine is completed in a relatively short period of time, the analysis may be based on the proposition that the change in momentum of the machine and its support is numerically equal to the impulse of the force acting upon the machine. This relation is expressed mathematically, referring to Figure 3.21, and assuming $k_y \rightarrow \infty$:

$$Q = \int F\,dt = (m_s + m_y)\,\Delta\dot{s}, \tag{3.63}$$

where F = force applied to the machine.
Q = impulse of the force.
$\Delta\dot{s}$ = velocity change of machine-and-support assembly. (Assuming the machine and support to be at rest initially, the velocity change $\Delta\dot{s}$ is numerically equal to the velocity $\dot{s}$ at the completion of the impulse.)

The velocity of the machine-and-support assembly at the completion of the impulse having been determined from equation 3.63, its ensuing motion is investigated by writing the differential equation of motion for $(m_s + m_y)$ considered as a mass supported by the spring k_s and vibrating freely without application of external force:

$$(m_s + m_y)\ddot{s} + k_s s = 0. \tag{3.64}$$

The above equation is solved for s, and the undetermined coefficients are evaluated from the initial conditions: when $t = 0$, $s = 0$, and $\dot{s} = Q/(m_s + m_y)$. The transfer of momentum is assumed to take place instantaneously, so that the mass assembly $(m_s + m_y)$ acquires the velocity $\dot{s}$ at time $t = 0$. The expression for $\dot{s}$ is obtained from equation 3.63. The solution of equation 3.64 is then:

$$s = \frac{Q}{\Omega_s m_s \sqrt{1 + (m_y/m_s)}} \sin \frac{\Omega_s t}{\sqrt{1 + (m_y/m_s)}}. \tag{3.65}$$

The term $\Omega_s = \sqrt{k_s/m_s}$ in the above equation is the natural frequency, in radians per second, of the support alone. The expression in the argument of the sine term, $\Omega_s/\sqrt{1 + (m_y/m_s)}$, is the natural frequency of the support-and-machine assembly. The maximum displacement s_0 of the support is thus readily determined from equation 3.65, employing the known impulse Q and the properties of the machine and the support.

The support for a machine usually is in the form of a structure with distributed mass, instead of the simple system m_sk_s illustrated in Figure 3.21. This introduces the need for calculating the characteristics of such a system, and for determining which properties are significant. The procedure for obtaining approximate results is illustrated below by reference to two representative examples.

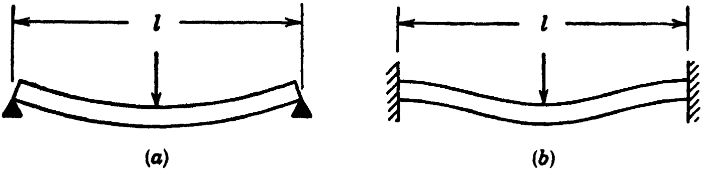

Figure 3.22. Representative types of beams which may be used as the supporting structure for the purpose indicated in Figure 3.21.

Many types of support or floor can be idealized as a simply supported beam, or a beam with built-in ends, supporting a load at the center. Such beams are shown in Figure 3.22 (*a*) and (*b*), respectively. The important physical parameters of the beams are:

l = length of beam, in.
μ = mass of beam per unit length, lb sec^2/in.^{2}
I = moment of inertia of cross section, in.^{4}
E = Young's modulus, psi.

The stiffness of each beam when loaded at the center, and the lowest natural frequency, are:*

Simply Supported Beam	Built-in Beam	
$k_s = \frac{48EI}{l^3}$	$k_s = \frac{192EI}{l^3}$	(3.66)
$\Omega_s = 9.87\sqrt{\frac{EI}{\mu l^4}}$	$\Omega_s = 22.4\sqrt{\frac{EI}{\mu l^4}}$	(3.67)

Substituting for k_s and Ω_s in the relation $\Omega_s = \sqrt{k_s/m_s}$, and solving for m_s for the respective beams:

$$m_s = 0.493\mu l \qquad m_s = 0.383\mu l \tag{3.68}$$

The above calculation considers only the deflection in the fundamental mode of vibration. The vibration amplitude associated with the higher modes of vibration

---

* See J. P. Den Hartog, *Mechanical Vibrations*, McGraw-Hill Book Co., New York, 1947, Appendix II.

decreases rapidly as the natural frequencies increase and usually is a negligible portion of the overall deflection of the support. The stress resulting from vibration in higher modes may be considerable, however. The contribution of the higher modes depends on the suddenness with which the force is applied, and on the internal damping of the beam. An investigation of the stress in a cantilever beam subjected to a sudden motion shows that damping tends to decrease the stress and that the stress usually can be calculated with reasonable accuracy by considering only the fundamental mode of vibration.[*]

When the transfer of momentum to the machine takes place in a time interval that is of the same order as or of greater duration than the natural period of the support, the simple relation given by equation 3.63 becomes more difficult to apply. It then becomes convenient to solve the differential equation of motion for the system. In the interests of expediency in the following analysis, it is assumed that the force F applied to the machine is harmonic, and endures for one-half period in accordance with the following relations:

$$\begin{aligned} F &= F_0 \sin \omega t, \qquad \left(0 \le t \le \frac{\pi}{\omega}\right); \\ F &= 0, \qquad \left(t \ge \frac{\pi}{\omega}\right). \end{aligned} \tag{3.69}$$

The equation of motion for the mass combination $(m_s + m_y)$ in Figure 3.21, employing the above expression for F, is

$$(m_s + m_y)s + k_s s = F_0 \sin \omega t, \quad \left(0 \le t \le \frac{\pi}{\omega}\right). \tag{3.70}$$

It is convenient to express the applied force F in terms of its impulse, in accordance with the relation indicated by the left and center terms of equation 3.63. Substituting from equation 3.69 in equation 3.63, and carrying out the indicated integration:

$$F_0 = \frac{Q\omega}{2}. \tag{3.71}$$

An expression for the displacement s of the support is obtained from equation 3.70 by substituting for F_0 from equation 3.71, and solving the differential equation. The coefficients are evaluated from the initial conditions: $s = \dot{s} = 0$ when $t = 0$. Then:

---

[*] R. D. Mindlin, F. W. Stubner, and H. L. Cooper, "Response of Damped Elastic Systems to Transient Disturbances," *Proc. Soc. Exper. Stress Anal.*, Vol. V, No. II.

$$s = \frac{\dfrac{Q\omega}{2m_s}\left(\dfrac{1}{1 + (m_y/m_s)}\right)}{\omega^2 - \dfrac{\Omega_s^2}{1 + (m_y/m_s)}}\left[\frac{\omega\sqrt{1 + (m_y/m_s)}}{\Omega_s}\sin\frac{\Omega_s t}{\sqrt{1 + (m_y/m_s)}} - \sin\omega t\right], \quad \left(0 \leq t \leq \frac{\pi}{\omega}\right). \tag{3.72}$$

The maximum value of s from equation 3.72 is

$$s_0 = \frac{\left(\dfrac{Q}{2m_s\Omega_s\sqrt{1 + (m_y/m_s)}}\right)}{\left(\dfrac{\Omega_s}{\omega\sqrt{1 + (m_y/m_s)}} - 1\right)}\sin\frac{2n\pi}{\dfrac{\Omega_s}{\omega\sqrt{1 + (m_y/m_s)}} + 1}, \quad \left(0 \leq t \leq \frac{\pi}{\omega}\right), \tag{3.73}$$

where n is a positive integer chosen so that the sine term is as great as possible while its argument remains less than π.*

The equation of motion of the mass combination $(m_y + m_s)$ in the time interval $t \geq \pi/\omega$ is similar to equation 3.70, except that the applied force has become zero:

$$(m_s + m_y)\ddot{s} + k_s s = 0, \quad \left(t \geq \frac{\pi}{\omega}\right). \tag{3.74}$$

Establishing a new time reference $t' = 0$ when $t = \pi/\omega$, the solution to equation 3.74 is obtained, using the displacement s and velocity $\dot{s}$ at time $t = \pi/\omega$ to evaluate the coefficients:

$$s = \frac{\left(\dfrac{Q}{2m_s\Omega_s\sqrt{1 + (m_y/m_s)}}\right)}{\left(1 - \dfrac{\Omega_s^2}{\omega^2[1 + (m_y/m_s)]}\right)}\left[2\sin\frac{\Omega_s(2\omega t - \pi)}{2\omega\sqrt{1 + (m_y/m_s)}}\cos\frac{\pi\Omega_s}{2\omega\sqrt{1 + (m_y/m_s)}}\right], \quad \left(t \geq \frac{\pi}{\omega}\right). \tag{3.75}$$

The maximum value of the displacement s occurs when the sine term in equation 3.75 becomes equal to unity and is given by the following expression:

---

* See footnote on page 109 in connection with equation 3.42.

$$s_0 = \frac{\left(\dfrac{Q}{m_s\Omega_s\sqrt{1+(m_y/m_s)}}\right)}{\left(1-\dfrac{\Omega_s^2}{\omega^2[1+(m_y/m_s)]}\right)}\cos\frac{\pi\Omega_s}{2\omega\sqrt{1+(m_y/m_s)}}, \qquad \left(t \geq \frac{\pi}{\omega}\right). \tag{3.76}$$

In calculating values for the maximum displacement s_0, equation 3.73 applies when $\Omega_s/\omega \geq 1$, and equation 3.76 applies when $\Omega_s/\omega \leq 1$.

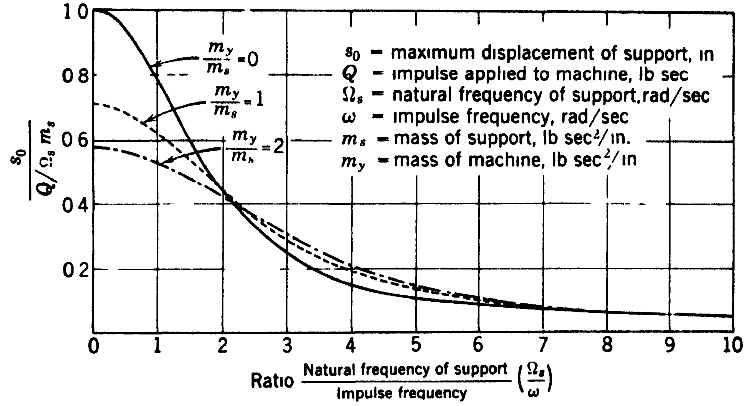

FIGURE 3.23. Relation among the several parameters which determine the maximum deflection s_0 of the supporting structure $m_s k_s$ illustrated in Figure 3.21, when k_y is infinitely stiff.

The value of s_0 for the special case $\Omega_s/\omega = 0$ obtained from equation 3.76 is identical to that obtained from equation 3.65. These values for the maximum displacement s_0 of the support resulting from the impulsively applied force F are shown graphically in Figure 3.23 for several discrete values of the mass ratio m_y/m_s. The ordinate scale is expressed in terms of $Q/m_s\Omega_s$. The maximum displacement of the support thus varies directly as the impulse of the force F, and inversely as both the mass m_s and the natural frequency Ω_s of the support.

It is worth noting that the maximum displacement s_0 of the support may be decreased substantially for small values of Ω_s/ω, i.e., for very suddenly applied forces, by increasing the mass m_y of the machine. This explains the success of the common practice of mounting forging hammers and similar machines upon heavy concrete blocks as means to reduce the motion of the support. When Ω_s is greater than ω, however, the force cannot be classed as suddenly applied. It is applied over a relatively long period of time, and the resulting condition tends to approach that of static equilibrium. The addition of mass to the machine then becomes of decreasing importance; at large values of Ω_s/ω, the displacement of the support becomes independent of the mass ratio m_y/m_s.

3·9 *Isolation of Shock*

The benefits to be gained by interposing a shock isolator between the machine and its support are indicated below by further reference to Figure 3.21, wherein the isolator stiffness k_y is small relative to the stiffness k_s of the support. The force acting on the machine is given by equations 3.69.

Assuming the mass m_s to be large compared with m_y, the differential equation of motion for m_y is written as follows, employing the relation given by equation 3.71:

$$m_y\ddot{y} + k_y y = \frac{Q\omega}{2}\sin\omega t, \qquad \left(0 \le t \le \frac{\pi}{\omega}\right). \tag{3.77}$$

This equation is solved for y, and the coefficients are evaluated by taking as the initial conditions: $y = \dot{y} = 0$ when $t = 0$. The resulting expression for y is

$$y = \frac{Q\omega/2m_y}{\Omega_y^2 - \omega^2}\left[\sin\omega t - \frac{\omega}{\Omega_y}\sin\Omega_y t\right], \qquad \left(0 \le t \le \frac{\pi}{\omega}\right). \tag{3.78}$$

Similarly, the differential equation of motion for the mass m_y in the time interval $t \ge \pi/\omega$ is

$$m_y\ddot{y} + k_y y = 0, \qquad \left(t \ge \frac{\pi}{\omega}\right), \tag{3.79}$$

and the resulting expression for y, employing the method used to obtain equation 3.75, is:

$$y = \frac{-(Q\omega/m_y)(\omega/\Omega_y)}{\Omega_y^2 - \omega^2}\left[\cos\frac{\pi\Omega_y}{2\omega}\sin\left(\Omega_y t' + \frac{\pi\Omega_y}{2\omega}\right)\right], \qquad \left(t \ge \frac{\pi}{\omega}\right). \tag{3.80}$$

The maximum displacement y_0 of the machine is the maximum value of y from equations 3.78 and 3.80. The maximum value of equation 3.78 is*

$$y_0 = \frac{Q/m_y\Omega_y}{(\Omega_y/\omega) - 1} \sin \frac{2n\pi}{(\Omega_y/\omega) + 1}, \qquad \left(0 \le t \le \frac{\pi}{\omega}\right), \qquad (3.81)$$

where n is a positive integer chosen so as to make the sine term as large as possible while its argument remains less than π. The maximum value of equation 3.80 is

$$y_0 = \frac{Q/m_y\Omega_y}{1 - (\Omega_y^2/\omega^2)} \cos \frac{\pi\Omega_y}{2\omega}, \qquad \left(t \ge \frac{\pi}{\omega}\right). \qquad (3.82)$$

The maximum displacement of the machine resulting from the impulse Q is shown graphically in Figure 3.24, as calculated from equations 3.81 and 3.82. When $\Omega_y/\omega \le 1$, the maximum displacement occurs when $t \ge \pi/\omega$; i.e., after the impulse is completed, and y_0 is calculated from equation 3.82. When $\Omega_y/\omega \ge 1$, the maximum displacement occurs during the impulse and y_0 is calculated from equation 3.81. The ordinate of Figure 3.24 is the dimensionless ratio of the maximum displacement y_0 to the parameter $Q/\Omega_y m_y$. The displacement of the machine thus varies directly as the magnitude of the impulse Q, and inversely as both the mass m_y of the machine and the natural frequency Ω_y of the isolator.

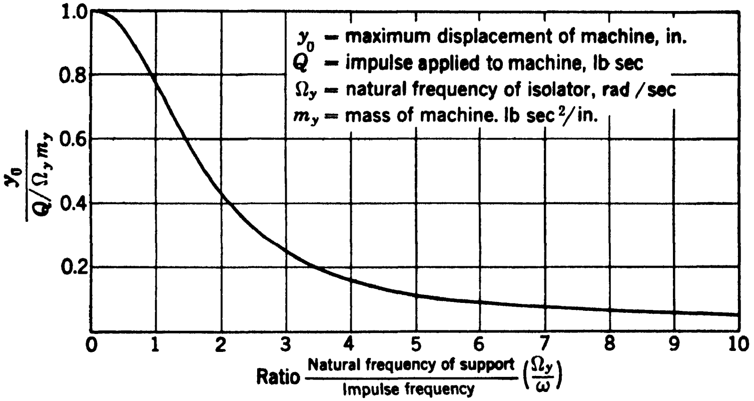

FIGURE 3.24. Relation among the several parameters which determine the maximum displacement y_0 of the machine in Figure 3.21, when k_y is small compared to k_s.

The displacement of the support for the machine is determined by writing the differential equation of motion for the mass m_s of the system shown in Figure 3.21. The following equation is predicated on the assumption, set forth with reference to equation 3.77, that m_s is large relative to m_y:

---

* See footnote on page 109 in connection with equation 3.42.

$$m_s\ddot{s} = k_y(y - s) - k_s s. \tag{3.83}$$

The following analysis has reference to a system in which the stiffness of the support k_s is great relative to the stiffness of the isolator k_y. It follows, therefore, that $k_y + k_s \approx k_s$ and equation 3.83 may be written:

$$\ddot{s} + \Omega_s^2 s = \frac{k_y}{m_s} y, \tag{3.84}$$

where $\Omega_s^2 = k_s/m_s$ and y is given by equations 3.78 and 3.80 for the applicable time intervals.

The solution of equation 3.84 for the time interval $0 \leq t \leq \pi/\omega$, using the expression for y from equation 3.78 and employing as initial conditions, $s = \dot{s} = 0$ when $t = 0$, is

$$s = \frac{(Q\omega/2m_y)(k_y/m_s)}{\Omega_y^2 - \omega^2}\left[\left(\frac{\omega/\Omega_s}{\Omega_s^2 - \Omega_y^2} - \frac{\omega/\Omega_s}{\Omega_s^2 - \omega^2}\right)\sin \Omega_s t + \frac{1}{\Omega_s^2 - \omega^2}\sin \omega t - \frac{\omega/\Omega_y}{\Omega_s^2 - \Omega_y^2}\sin \Omega_y t\right], \quad \left(0 \leq t \leq \frac{\pi}{\omega}\right). \tag{3.85}$$

The solution of equation 3.84 for the time interval $t \geq \pi/\omega$ is obtained by substituting the expression for y from equation 3.80. Coefficients in the solution are evaluated by equating corresponding expressions for s at time $t = \pi/\omega$ ($t' = 0$) and, similarly, corresponding expressions for $\dot{s}$. Then:

$$s = \frac{(Q\omega/m_y)(k_y/m_s)(\omega/\Omega_s)}{(\Omega_s^2 - \Omega_y^2)(\Omega_s^2 - \omega^2)}\cos\frac{\Omega_s\pi}{2\omega}\sin\left(\Omega_s t' + \frac{\pi\Omega_s}{2\omega}\right) + \frac{(Q\omega/m_y)(k_y/m_s)(\omega/\Omega_y)}{(\omega^2 - \Omega_y^2)(\Omega_s^2 - \Omega_y^2)}\cos\frac{\Omega_s\pi}{2\omega}\sin\left(\Omega_y t' + \frac{\pi\Omega_y}{2\omega}\right), \quad \left(t \geq \frac{\pi}{\omega}\right). \tag{3.86}$$

Expressions have now been derived, equations 3.85 and 3.86, for the displacement of the support during the time intervals $0 \leq t \leq \pi/\omega$ and $t \geq \pi/\omega$. The present analysis has reference to the effectiveness of a relatively flexible isolator in alleviating the disturbance caused in a rigid support by an impulsively applied force. The displacement y of the machine therefore reaches a maximum after the applied force is reduced to zero; i.e., during the time interval $t \geq \pi/\omega$. The displacement s of the support results from the force applied by the isolator k_y and likewise reaches a maximum in the time interval $t \geq \pi/\omega$. An expression for maximum displacement s_0 of the support is thus obtained from equation 3.86 by noting that the expression for the instantaneous value of s is comprised of two sine terms of different frequency. In the undamped case being considered, there inevitably will be a time when the sine terms are simultaneously equal to unity. The maximum displacement s_0 occurs at this time and is given by the following expression:

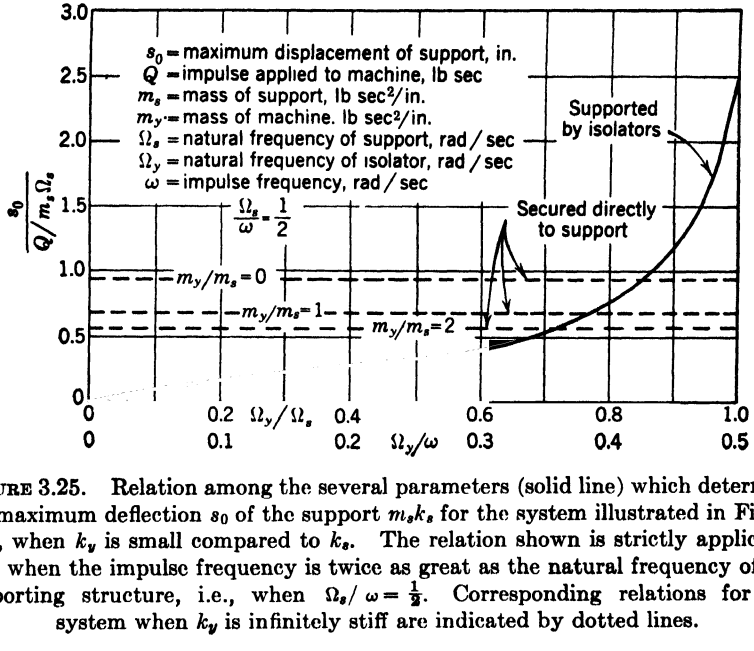

FIGURE 3.25. Relation among the several parameters (solid line) which determine the maximum deflection s_0 of the support m_sk_s for the system illustrated in Figure 3.21, when k_y is small compared to k_s. The relation shown is strictly applicable only when the impulse frequency is twice as great as the natural frequency of the supporting structure, i.e., when $\Omega_s/\omega = \frac{1}{2}$. Corresponding relations for the system when k_y is infinitely stiff are indicated by dotted lines.

$$s_0 = \frac{(Q/m_s\Omega_s)(\Omega_s/\omega)}{(\Omega_s^2/\Omega_y^2) - 1}\left[\frac{(\Omega_y/\Omega_s)\cos(\pi\Omega_s/2\omega)}{(\Omega_s^2/\omega^2) - 1} + \frac{(\omega/\Omega_y)\cos(\pi\Omega_y/2\omega)}{1 - (\Omega_y^2/\omega^2)}\right], \quad \left(t \geq \frac{\pi}{\omega}\right). \tag{3.87}$$

The maximum displacement s_0 of the support is thus a function of various ratios of the support and isolator natural frequencies Ω_s, Ω_y, and the forcing frequency ω. The latter is inversely proportional to the duration of the impulse and may be designated impulse frequency.

Only two of the three ratios are independent. The frequency ratio Ω_s/ω may be assumed constant for any given installation, Ω_s being characteristic of the support and ω being characteristic of the machine. Assuming the impulse Q and the mass m_s of the support to be predetermined, and letting $\Omega_y/\omega = (\Omega_y/\Omega_s)(\Omega_s/\omega)$, the maximum displacement s_0 is a function only of the ratio Ω_y/Ω_s.

Characteristic results are shown in Figure 3.25, as computed from equation 3.87, for the typical frequency ratio $\Omega_s/\omega = \frac{1}{2}$. In order to indicate the relation between isolator natural frequency Ω_y and impulse frequency ω, a second abscissa scale in terms of the ratio Ω_y/ω is included. The displacement is indicated in terms of the dimensionless ratio $s_0/(Q/m_s\Omega_s)$, which is identical to the ordinate of Figure 3.23. In order to provide a basis to evaluate the effectiveness of the isolator, curves for the displacement of the support when the machine is rigidly attached are also included in Figure 3.25. These curves are in the form of dotted horizontal lines, being independent of the isolator natural frequency Ω_y. The ordinates of the dotted lines are determined from Figure 3.23 for the applicable value of the frequency ratio Ω_s/ω and mass ratio m_y/m_s.

3·10 *Effectiveness of Isolators*

The preceding analysis indicates available methods for alleviating the disturbance experienced by a support as a result of the impulsive addition of energy to a machine that is secured to the support. A summary of these methods, together with an indication of the results expected from each, is included in the following paragraphs.

When the impulse frequency ω is high relative to the natural frequency Ω_s of the support, the maximum displacement s_0 experienced by the support may be reduced by adding to the mass m_y of the machine; i.e., by increasing the ratio m_y/m_s. The magnitude of the reduction is indicated by Figure 3.23. This usually is accomplished by mounting the machine securely to a concrete block, which in turn rests directly upon the support. The additional mass of the concrete block may be considered alternatively as an increase in the mass m_s of the support. When considered in this manner, the maximum displacement s_0 is determined from Figure 3.23 by referring to a lower value of the ratio m_y/m_s, but entering the graph at a lower value on the ordinate scale as required by the increased magnitude of m_s.

When the frequency of the impulse is low relative to the natural frequency of the support, $\Omega_s/\omega \gg 1$, and the curves in Figure 3.23 for various values of the mass ratio m_y/m_s converge. Little is gained under these conditions from the addition of mass to the machine, because of the resemblance to a static application of force to the support.

The maximum displacement s_0 of the support usually may be reduced by interposing a relatively flexible isolator between the machine and its support. The extent of the reduction is ascertained from curves of the type shown in Figure 3.25. The solid lines refer to a machine supported by shock isolators; the dotted lines refer to the same machine secured directly to the support. It is evident that the maximum displacement s_0 of the support decreases as the isolator natural frequency Ω_y decreases; this results, however, in an increase in maximum displacement y_0 of the machine, as indicated by Figure 3.24. In any particular application, the isolator natural frequency must be chosen so that the displacements of both the machine and the support are maintained within tolerable limits.

It may be surprising to observe that the maximum displacement s_0 of the support, when the machine is supported by isolators, is independent of the mass m_y of the machine. This apparent paradox is resolved by noting that any increase in the mass of the machine necessitates a corresponding increase in the stiffness of the isolators to maintain the status quo with respect to frequencies. The displacement experienced by the machine decreases as the mass of the machine increases, but the force transmitted by the isolators to the support remains unchanged because of the increase in the stiffness of the isolators. The support responds to this transmitted force, and its displacement consequently remains unchanged.

Example 3.3. A drop forging machine weighs 10,000 lb, exclusive of the hammer. The hammer weighs 1,000 lb, and falls freely a distance of five feet before striking the anvil. The forging being worked is of such a nature that the hammer travels $\frac{1}{4}$ inch after striking the material and before being brought to rest. The machine is supported by six 18-inch × 80-lb/ft steel I beams (moment of inertia $= 1{,}176.8$ in.^{4} each) 25 feet long. The ends of the beams are embedded in concrete abutments. The maximum deflection of the beams is to be calculated, with and without shock isolators.

The natural frequency Ω_s and the effective mass m_s of the support are calculated from equations 3.67 and 3.68 for the built-in beam. Substituting $E = 30 \times 10^6$ psi; $I = 6 \times 1{,}176.8 = 7{,}060.8$ in.^{4} (the machine is supported by six beams) $l = 25 \times 12 = 300$ in.; and $\mu = \frac{6 \times 80}{12 \times 386} = 0.1037$ lb sec^2/in.^{2}, the following values are calculated:

$$\Omega_s = 355 \text{ rad/sec}; \qquad m_s = 11.9 \text{ lb sec}^2\text{/in.}$$

In order to determine the impulse frequency ω, it is necessary to calculate the downward velocity of the hammer at the moment it strikes the work, and to assume the manner in which this velocity is reduced to zero. The hammer velocity as it strikes the work is calculated from equation 3.13:

$$V = \sqrt{2 \times 386 \times 5 \times 12} = 215 \text{ in./sec.}$$

It is assumed now that the velocity of the hammer decreases at a constant rate during contact with the work. The average velocity during this interval is thus $\frac{1}{2} \times 215 = 107.5$ in./sec. The period of contact is the displacement divided by the average velocity and is defined in terms of impulse frequency by π/ω on page 131. Then:

$$\frac{\pi}{\omega} = \frac{0.25}{107.5}; \qquad \omega = 1{,}355 \text{ rad/sec.*}$$

The impulse Q is calculated from the change in momentum of the hammer, as indicated by equation 3.63. Assuming no rebound of the hammer, the velocity change is 215 in./sec and the impulse is

$$Q = \frac{1{,}000}{386} \times 215 = 557 \text{ lb sec.}$$

The mass m_y of the machine is $m_y = 10{,}000/386 = 25.9$ lb sec^2/in., and the mass ratio m_y/m_s is

$$\frac{m_y}{m_s} = \frac{25.9}{11.9} = 2.17$$

The maximum deflection s_0 of the beams resulting from the impulse Q is now calculated from equation 3.76, substituting $Q = 557$ lb sec, $m_s = 11.9$ lb sec^2/in., $\Omega_s = 355$ rad/sec, $\omega = 1{,}355$ rad/sec, and $m_y/m_s = 2.17$. Then:

$$s_0 = 0.074 \text{ in.}$$

The expression based upon an instantaneous transfer of momentum, equation 3.65, yields approximately the same numerical result for s_0 because ω in this instance is much greater than Ω_s.

It is evident from reference to Figure 3.25 that an isolator is useful for reducing the beam deflection only if the isolator natural frequency Ω_y is somewhat less than the natural frequency Ω_s of the beam. The stiffness k_y of an available isolator is 50,000 lb/in. The isolator natural frequency Ω_y is then calculated from equation 2.16:

$$\Omega_y = \sqrt{\frac{k_y}{m_y}} \quad \sqrt{\frac{50{,}000}{25.9}} \quad 44 \text{ rad/sec.}$$

The maximum deflection of the beams when the impulse Q is cushioned by the isolators is calculated from equation 3.87. Substituting $Q = 557$ lb sec, $m_s = 11.9$ lb sec^2/in., $\Omega_s = 355$ rad/sec, $\omega = 1{,}355$ rad/sec, and $\Omega_y = 44$ rad/sec, the maximum beam deflection is

$$s_0 = 0.0166 \text{ in.}$$

---

* The assumption of constant rate of velocity decrease perhaps is not justified by the nature of the forging work being done. It can be shown, however, that the results are largely independent of the exact function selected if ω is large compared with Ω_s and Ω_y.

This compares with the value of $s_0 = 0.074$ in. when the machine is attached directly to the beams.

The reduction in the beam deflection resulting from the use of isolators is accompanied by an increase in the displacement of the machine. The maximum displacement of the machine mounted upon isolators is readily calculated from equation 3.82. Substituting $Q = 355$ lb sec, $m_y = 25.9$ lb sec^2/in., $\Omega_y = 44$ rad/sec, and $\omega = 1{,}355$ rad/sec, the calculated value of y_0 is

$$y_0 = 0.494 \text{ in.}$$

This compares with the previously calculated value $s_0 = 0.074$ in., which applies to the displacements of both the beams and the machine when the machine is secured directly to the beams. The reduction of more than 75 percent in beam deflection is thus attained at the expense of more than a sevenfold increase in the displacement of the machine.

C. ISOLATION OF SHOCK FORCES THAT CAUSE DISPLACEMENTS OF SMALL MAGNITUDE

3·11 Machines of Conservative Momentum

In the analyses of shock isolation heretofore considered, one of the principal functions of the isolator has been to effect a change in velocity of a massive body. In the velocity shock considered initially, the support experiences a change in velocity; an equivalent change in the velocity of the mounted equipment is brought about as a result of the force applied to the equipment by the isolator. Next, a moving body striking a fixed support is considered; its motion is arrested by the force applied to the body by the isolator. Finally, the problem of shock created by the impulsive addition of energy to a machine is considered. The machine thus acquires a velocity and is brought to rest by the force applied by the isolator. The following paragraphs consider the isolation of shock created by the operation of a machine that receives no momentum from external sources. By the law of conservation of momentum, such a machine cannot attain a continuing velocity. It can temporarily acquire a velocity, however, which may be the cause of shock forces applied to the support for the machine. Since this phenomenon is difficult to visualize abstractly, the principles are illustrated in this section by two common examples. These two examples are then referred to frequently in succeeding sections in pointing out the significance of certain conditions involved in the isolation of shock.

The first example refers to the punch press shown in outline in Figure 3.26. Metal-working operations are performed between the moving platen *a* and the stationary platen *b*. The moving platen *a* is commonly actuated by a crank and connecting rod driven from a crankshaft. The latter carries a heavy flywheel, usually driven by a belt- or gear-coupled electric motor. The kinetic energy of the rotating flywheel provides the energy required for the metal-working operation. The time required for such operation is usually but a fraction of the time required for one revolution of the flywheel; the motor thus has an opportunity to restore the flywheel velocity before the inception of the next working stroke.

The forces and couples involved in operation of the press are indicated in Figure 3.27. The upward force acting on the moving platen is designated by F. The reaction along the line of the connecting rod is $F/\cos\theta$, and the horizontal component is $F\tan\theta$. A similar force diagram can be drawn to indicate forces applied at the crankshaft bearing. An upward-directed force F is applied to the crankshaft bearing, which balances the downward force applied by the moving platen through the work to the stationary platen. The left-directed force $F\tan\theta$ applied by the moving platen to the platen guide combines, however, with a right-directed force $F\tan\theta$ applied to the crankshaft bearing to form a couple $M_1 = FL\tan\theta$ which tends to rotate the entire press in a clockwise direction. It can be shown that this couple is equal in magnitude and duration to the counterclock-

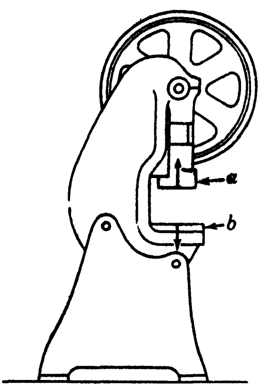

FIGURE 3.26.

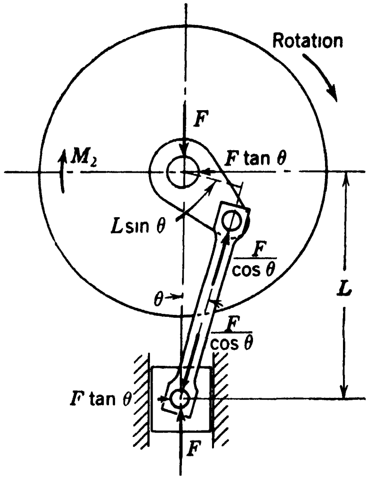

FIGURE 3.27.

FIGURE 3.26. Typical punch press with vertically moving platen.

FIGURE 3.27. Diagram of significant forces and couples acting on crankshaft and moving platen of punch press shown in Figure 3.26. Forces and couples acting on the body of the press are equal in magnitude but opposite in direction.

wise couple applied to the crankshaft as a result of the metal-working operation being performed by the press.

The function of the electric motor is to attempt to maintain the velocity of the flywheel constant at all times. When no work is being done by the press, the torque output of the motor is required only to compensate for friction losses in the machine. When the flywheel velocity is decreased as a result of the counterclockwise couple $FL \tan \theta$ applied to the crankshaft, a clockwise couple M_2 is applied by the motor in an attempt to restore the initial flywheel velocity. The nature of the couple M_2 depends on the characteristics of the force F and of the motor. If the motor is mounted upon the press, a reactive couple of magnitude M_2 acts on the body of the press in a counterclockwise direction. The motion resulting from this couple tends to counteract the motion of the press resulting from the couple $FL \tan \theta$, in a manner that will become evident from the following paragraphs.

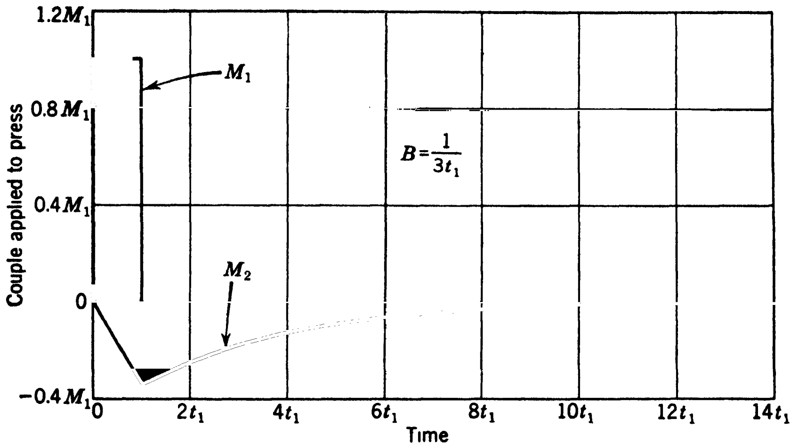

FIGURE 3.28. Couples acting on body of punch press shown in Figure 3.26, as a result of working stroke and restoration of flywheel velocity. This is for a particular condition of motor torque defined by $B = 1/(3t_1)$.

The mechanics of this problem may be illustrated by assuming certain hypothetical conditions. The couple $M_1 = FL \tan \theta$ which results from the metal-working force is considered to be constant throughout the time interval $0 \leq t \leq t_1$. The couple M_2 applied by the motor is assumed to increase at a constant rate as the flywheel velocity decreases in response to couple M_1, and to decrease exponentially with time as the flywheel velocity is restored to its initial value. The time history of the couples applied to the body of the press is illustrated in Figure 3.28, taking the time reference as zero at the inception of the metal-working operation. The clockwise direction is taken as positive. If the press is considered to be freely supported in space, i.e., having supporting means of negligible stiffness, its motion as a result of the couples illustrated in Figure 3.28 is determined by the proposition that its total change in angular momentum at any instant is equal to the summation of the impulses of the couples acting on the press. This is expressed mathematically by:

$$\int_0^t M_1\,dt + \int_0^t M_2\,dt = I(\dot{\alpha} - \dot{\alpha}_{t=0}), \tag{3.88}$$

where I = moment of inertia of entire press.
$\dot{\alpha}$ = angular velocity of press at any time t.
$\dot{\alpha}_{t=0}$ = angular velocity of press at time $t = 0$. (This is taken as zero by assuming the press to be motionless at the inception of the metal-working operation; i.e., when $t = 0$.)
M_1, M_2 = couples as defined above.

The relation between the couples M_1 and M_2 is determined from the fact that the velocity of the flywheel at time $t = 0$ is the same at each cycle. The summation of the impulses of M_1 and M_2 over a complete cycle therefore must be zero:

$$\int_0^{t_1} M_1\,dt + \int_0^{t_1} M_2\,dt + \int_{t_1}^{\infty} M_2\,dt = 0. \tag{3.89}$$

The metal-working operation characteristically takes place in a relatively short time interval; i.e., $t_1 \rightarrow 0$. Consequently, the second term on the left side of equation 3.89 may be neglected, and the lower limit of integration in the third term may be set equal to zero. The upper limit of integration in the third term is taken as infinity, because the couple M_2 becomes substantially equal to zero before the completion of the cycle. The value of the integral over one cycle is then approximately equal to its value to infinity. An expression that meets the requirements for the couple M_2 in the time interval $t \geq t_1$ is $M_2 = -Ae^{-B(t-t_1)}$, in which the coefficients A, B are evaluated approximately by setting $t_1 = 0$. Making these substitutions in equation 3.89 and carrying out the integration:

$$\frac{A}{B} = M_1 t_1. \tag{3.90}$$

The angular velocity $\dot{\alpha}$ and angular displacement α of the press in the time interval $0 \leq t \leq t_1$ are obtained by solving equation 3.88 for $\dot{\alpha}$, neglecting the effect of the couple M_2 and assuming the velocity

$\dot{\alpha}$ and displacement α of the press to be zero at time $t = 0$. Performing the indicated integration:

$$\dot{\alpha} = \frac{M_1 t}{I}; \qquad \alpha = \frac{M_1 t^2}{2I}; \qquad (0 \leq t \leq t_1). \tag{3.91}$$

The angular velocity $\dot{\alpha}$ of the press in the time interval $t \geq t_1$ is determined from equation 3.88 by neglecting the effect of the couple M_2 in the time interval $0 \leq t \leq t_1$ and substituting $M_2 = -Ae^{-B(t-t_1)}$. Equation 3.88 then becomes:

$$\int_0^{t_1} M_1\,dt - \int_{t_1}^{t} Ae^{-B(t-t_1)}\,dt = I\dot{\alpha}. \tag{3.92}$$

Carrying out the indicated integration, and substituting for A/B from equation 3.90:

$$\dot{\alpha} = \frac{M_1 t_1}{I} e^{-B(t-t_1)}, \qquad (t \geq t_1). \tag{3.93}$$

The displacement α in the time interval $t \geq t_1$ is obtained by integrating equation 3.93 as follows:

$$\alpha = \frac{M_1 t_1}{I}\left[-\frac{1}{B}e^{-B(t-t_1)} + c\right], \qquad (t \geq t_1). \tag{3.94}$$

The constant of integration c is evaluated by substituting $t = t_1$ in equations 3.91 and 3.94, and equating the two values for α obtained in this manner. Substituting the resulting expression for c in equation 3.94 gives the following expression for the displacement α in the time interval $t \geq t_1$:

$$\alpha = \frac{M_1 t_1}{I}\left[\frac{t_1}{2} + \frac{1}{B}\left(1 - e^{-B(t-t_1)}\right)\right], \qquad (t \geq t_1). \tag{3.95}$$

The value of $\alpha/(M_1 t_1^2/I)$ as calculated from equations 3.91 and 3.95, is shown graphically in Figure 3.29 for a particular value, $B = 1/(3t_1)$. It should be noted that the press, as the couple M_2 approaches zero after a long interval of time, has a resultant angular displacement but not a resultant angular velocity. The final displacement depends on the integral of the couples M_1, M_2 with respect to time. A generally similar, though not numerically equal, result is obtained independently of the particular nature of the couples assumed.

Before considering means to isolate the force generated by the punch press, it will be interesting to consider the cloth-weaving loom used in the textile industry. The essential parts of a loom,* for purposes of the present discussion, are a chassis of mass m_l, a shuttle of mass m_s which travels at high velocity V_s from side to side, and a rather complex cam mechanism which propels the shuttle. The left cam may be considered to propel the shuttle toward the right, imposing a left-directed impulse $\int F\,dt = m_sV_s$ upon the loom frame. Upon reaching the right side, the shuttle has its motion arrested momentarily by a trap-like device, and a right-directed impulse $\int F\,dt = m_sV_s$ is applied to the loom frame as the shuttle is brought to rest. The shuttle is

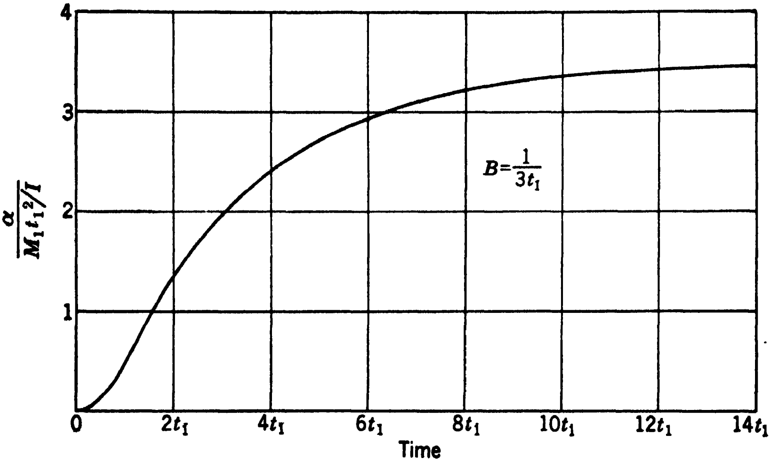

FIGURE 3.29. Diagram showing angular displacement α of punch press as a function of time, in response to couples shown in Figure 3.28, for a particular value $B = 1/(3t_1)$.

then propelled toward the left, and the second half of the cycle is carried out in the reverse direction. Assuming the impulses associated with the propelling and arresting of the shuttle to embody force-time curves of half-sinusoidal shape, the forces applied to the loom frame may be illustrated as in Figure 3.30. The left pulse 1 represents the force applied to the loom frame in propelling the shuttle toward the right. The time interval between oppositely directed pulses represents the time during which the shuttle is in motion; the time interval between pulses of the same direction represents the time during which the shuttle is at rest, pending reversal of its velocity.

In visualizing the effect of the forces illustrated in Figure 3.30, the loom is considered to be freely supported in space; i.e., supported in such a manner that the support offers no restraint to the movement of the loom. The forces that propel the shuttle therefore are opposed only by the inertia of the loom frame. The resulting displacement of the loom is illustrated in Figure 3.31, in which the time coordinate is drawn to the same scale as in Figure 3.30. The first pulse 1, involving a left-directed force, causes the loom to move toward the left with a velocity indicated by the slope at A of the displacement-time diagram in Figure 3.31. The next pulse 2 is equal in magnitude but opposite in direction. It acts to arrest the motion of the loom frame, and the loom velocity is reduced to zero as indicated by the horizontal portion B of the curve in Figure 3.31. The cycle then continues upon the inception of the next pulse, with directions reversed.

---

* A more complete description of a loom is given in Section 6·5 and illustrated in Figure 6.10 of Chapter 6.

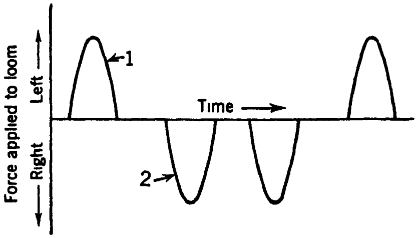

FIGURE 3.30.

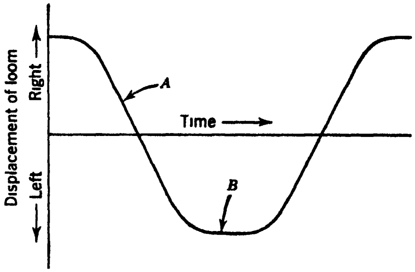

FIGURE 3.31.

FIGURE 3.30. Force-time diagram of forces acting on the chassis of a loom.

FIGURE 3.31. Diagram of loom displacement as a function of time, in response to forces shown in Figure 3.30.

The above examples are fairly typical of a large class of machines to which no momentum is supplied from external sources. The variation in position of the machine during one working cycle depends on the nature of the forces. In the cloth-weaving loom, the oppositely directed impulsive forces are identical except for sign, and the loom returns to the same position as each cycle is completed. In the punch press, the oppositely directed impulses are equal in magnitude but different in nature. If unconstrained by its supports, the press tends to rotate progressively with each cycle of operation. A rigid support for the press prevents such rotation but is subjected to the couple that tends to cause the rotation. An isolator relieves the support by permitting limited movement of the press and provides a couple that tends to restore the press to its initial position after each cycle of operation. These effects are analyzed in detail in subsequent sections.

3·12 Isolation of Shock

When the machine rests upon or is secured directly to a relatively rigid support, it is unable to experience the motion of a freely supported body as described in the preceding section. The machine and its support must experience the same motion. The type of machine considered in Section 3·8 receives an impulsive addition of momentum and as a result acquires a velocity that ultimately must be opposed by its support. In machines of conservative momentum being considered here, the initial impulse is followed by a counteracting impulse. This latter impulse in some instances occurs after the lapse of an appreciable time interval; in other instances it is distributed over such a long period of time that its counteracting influence does not appear until after the full effect of the initial impulse upon the relatively rigid support has become evident. With rigidly mounted machines of conservative momentum, the disturbance experienced by the support therefore is governed largely by the nature of the initial impulse.

The effectiveness that may be obtained from isolators in alleviating movement of the support depends to a considerable extent on the displacement of the machine that is permissible from an operating viewpoint. The loom, for example, tends to move with a reciprocating motion whose total excursion is indicated by the limits of the displacement-time diagram shown in Figure 3.31. If this excursion is not objectionable in the operation of the machine, the most effective isolator is one with a relatively low stiffness, which permits substantially unrestrained movement of the machine. The maximum force transmitted to the support is then the product of isolator stiffness and maximum travel of the machine from its neutral position. Since the machine restores itself to its neutral position, the isolators are not required to perform this function but only to support the machine in a sufficiently stable position to permit normal operation.

A somewhat different condition exists with the punch press illustrated in Figure 3.26. The combination of impulses operates to cause a resultant angular displacement, but substantially no resultant angular velocity, after a complete cycle of operation. The freely supported machine would thus tend to move progressively in discrete steps unless restrained by its support. Important considerations in isolator design for a machine of this type may be summarized as follows:

(*a*) For maximum effectiveness, the isolator should be designed to accomodate the maximum displacement of the machine which results from the initial impulse. If this displacement cannot be tolerated for operational reasons, the isolator should be sufficiently stiff to maintain the necessary constraints upon the motion of the machine. The problem then becomes similar to one in which momentum (the momentum of the initial impulse in this instance) is added from an external source, and the effectiveness of the isolators can be evaluated from the analysis set forth in Sections 3·9 and 3·10.

(*b*) The isolator should embody sufficient stiffness to restore the machine to substantially its initial position, before the completion of the cycle of operation. This result usually is attained incidently where the isolator is required to constrain the displacement resulting from the initial impulse. Where the isolators are designed to permit unrestricted motion as a result of the initial impulse, however, adequate stiffness should be provided to restore the machine to its initial position before the next cycle begins.

The effectiveness of a shock isolator used with a machine of conservative momentum is determined from the effectiveness of isolators in general. When the impulse frequency associated with the operation of a machine is high, large forces generally are involved if the impulse is of appreciable magnitude. As indicated in Figure 3.25, the effectiveness of the isolator increases as the frequency ratio Ω_y/ω decreases. The same considerations apply to machines of conservative momentum, where ω usually can be considered as applying to the initial impulse. For maximum effectiveness, then, the natural frequency of the isolator should be made as low as practical requirements permit.

3·13 *Positioning Means*

Difficulties often are encountered in maintaining a machine secured to the floor when operation of the machine involves shock forces of large magnitude. Punch presses of the type shown in Figure 3.26 are often secured to the floor by lag screws, and it is common experience to have such lag screws pulled loose from the floor. Shock isolators not only reduce the magnitude of the force applied to these securing screws but also sometimes make it possible to position the machine entirely by friction forces. The reasons for this will become apparent from the following analysis.

The force between the machine and its support, when the machine is mounted directly on the support, will first be determined. The analysis makes reference to the system illustrated in Figure 3.21, wherein the stiffness k_y is infinitely great. An expression for the displacement of the support m_s (and also of the machine m_y), when the momentum transfer to the machine takes place suddenly, is given by equation 3.65. At the conclusion of the impulse Q, the machine has acquired a velocity that is ultimately opposed only by the support. The magnitude of the force exerted by the support, designated F_T, is $m_y\ddot{s}$ where $\ddot{s}$ is obtained from double differentiation of equation 3.65 as follows:

$$\ddot{s} = \frac{-Q\Omega_s}{m_s[1 + (m_y/m_s)]^{3/2}} \sin \frac{\Omega_s t}{\sqrt{1 + (m_y/m_s)}}. \tag{3.96}$$

The maximum value of the force F_T is found from the maximum value of acceleration $\ddot{s}_0$ obtained from equation 3.96:

$$(F_T)_0 = m_y\ddot{s}_0 = \frac{Q\Omega_s(m_y/m_s)}{[1 + (m_y/m_s)]^{3/2}}. \tag{3.97}$$

This force will now be compared with the force exerted by the isolator k_y upon the support m_s when k_y is small relative to k_s. The displacement y of the equipment m_y is assumed large relative to the displacement s of the support m_s. The deflection of the isolator is thus approximately equal to the displacement y. Since the momentum transfer is assumed to take place in a relatively short interval of time, the maximum displacement y_0 occurs in the time interval $t \geq \pi/\omega$ and is given by equation 3.82. The maximum force at the isolator, designated $(F_T')_0$, is the product of the isolator stiffness and the maximum displacement of the equipment:

$$(F_T')_0 = k_y y_0 = \frac{Q\Omega_y}{1 - (\Omega_y^2/\omega^2)} \cos \frac{\pi\Omega_y}{2\omega}. \tag{3.98}$$

An expression for the ratio of the force at the isolator to that at the base of the directly supported machine is now obtained by dividing equation 3.98 by equation 3.97:

$$\frac{(F_T')_0}{(F_T)_0} = \frac{[\Omega_y/\Omega_s][1 + (m_y/m_s)]^{3/2}}{[m_y/m_s][1 - (\Omega_y^2/\omega^2)]} \cos \frac{\pi\Omega_y}{2\omega}. \tag{3.99}$$

Numerical evaluation of equation 3.99 reveals that the force ratio $(F_T')_0/(F_T)_0$ is substantially independent of the mass ratio m_y/m_s. Equation 3.99 is shown graphically in Figure 3.32 as a function of the frequency ratio Ω_y/ω, for several discrete values of the ratio Ω_y/Ω_s. It is evident that a substantial reduction in transmitted force is achieved when Ω_y/Ω_s is small; i.e., when the isolator is substantially less stiff than the support.

Assume, now, that the force F in Figure 3.21 acts in a horizontal direction and that no bolts are used to secure the machine to its support. The machine is positioned only by its weight. It is evident that, if $(F_T)_0$ or $(F_T')_0$ exceeds the product of this weight and the coefficient of friction of the engaging surfaces, the machine will move horizontally upon the support. By means of isolators, $(F_T')_0$ can often be made less than this product, and the machine tends to remain positioned upon its support without the use of securing bolts. As indicated in Figure 3.32, this condition is attained by making Ω_y small. The consequent elimination of mounting bolts, including the cost of installation and maintenance, often is economic justification for the use of isolators even though the reduction of shock is of minor importance. The punch presses shown in Figure 6.7 are positioned only by isolators, whereas these same presses formerly were rigidly secured to the floor by lag screws in order to maintain them in position.

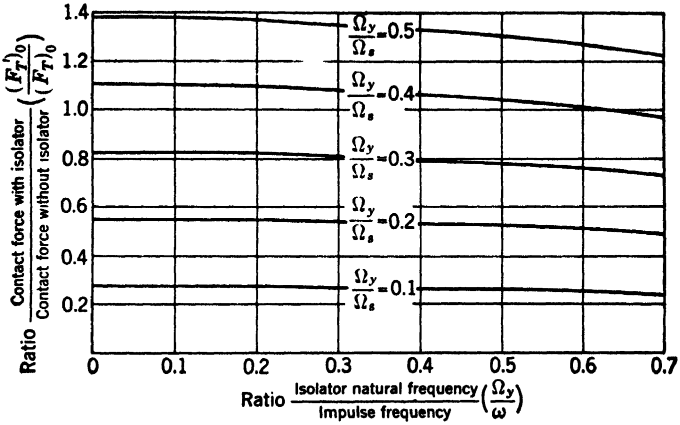

FIGURE 3.32. Ratio of contact forces with and without isolator. This refers to Figure 3.21, wherein the machine m_y is considered to be rigidly secured to the floor when the isolator stiffness k_y becomes infinitely great, and is significant in understanding ability of an isolator to position a machine without use of securing

D. ISOLATION OF SHOCK MOTIONS OF SMALL DISPLACEMENT

3·14 Shock Severity

Problems involved in the isolation of shock motions having large displacements are considered in Part *A* of this chapter. The velocity shock discussed there involves a large displacement of the support, and it becomes a function of the isolator to bring about a change in the velocity of the mounted equipment so that it experiences sensibly the same displacement as the support. When the maximum displacement of the support during shock is less than the permissible deflection of the isolator, however, there is no necessity of effecting a change in the velocity of the equipment. The problem then becomes the less exacting one of permitting motion between the equipment and its support so that the equipment receives a minimum disturbance.

The nature of the shock in a typical instance is illustrated by referring to Figure 3.33. The support is represented by the simple system m_sk_s, which simulates the floor of a building, or the chassis of a road or rail vehicle. The equipment, represented by m_y, is secured directly to the support. The equipment generally includes many elements, one of which is represented by the system m_zk_z. The shock excitation is an impulse Q of short duration applied to the mass m_s. This impulse may result, for example, from the operation of adjacent machinery in the building, or from the bottoming of the springs in the vehicle. As a result of the impulse, the massive members m_s, m_y acquire an initial velocity whose magnitude is determined from the proposition that the change in their momentum is equal to the applied impulse, provided that the transfer of momentum takes place in a relatively small time interval. Assuming an initial value of zero, the velocity of the support resulting from the impulse is

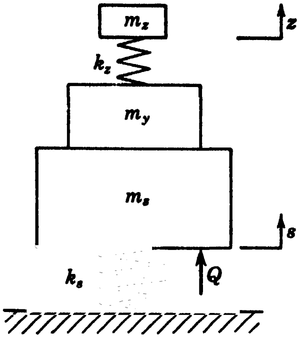

FIGURE 3.33. Schematic diagram illustrating machine, comprised of chassis m_y and typical element m_zk_z, and supporting structure m_sk_s. The supporting structure is acted upon by an impulse Q.

$$\dot{s} = \frac{Q}{m_s + m_y} = \frac{Q}{m_s[1 + (m_y/m_s)]}. \tag{3.100}$$

The differential equation of motion for the mass combination $(m_s + m_y)$ in Figure 3.33 is identical to equation 3.64, and the motion of the support therefore is defined by equation 3.65. The effect of this shock motion upon the equipment is evaluated by investigating the response of the system m_zk_z. Writing the differential equation of motion for the mass m_z in Figure 3.33:

$$m_z\ddot{z} = k_z(s - z). \tag{3.101}$$

Employing the relations $\delta_{sz} = s - z$, $\ddot{\delta}_{sz} = \ddot{s} - \ddot{z}$, and substituting s from equation 3.65, equation 3.101 becomes:

$$\ddot{\delta}_{sz} + \Omega_z^2\delta_{sz} = \frac{-Q\Omega_s}{m_s[1 + (m_y/m_s)]^{3/2}} \cos \frac{\Omega_s t}{\sqrt{1 + (m_y/m_s)}}. \qquad (3.102)$$

This equation is now solved for δ_{sz}, and the coefficients are evaluated from the conditions at time $t = 0$: $\delta_{sz} = 0$ and $\dot{\delta}_{sz} = \dfrac{Q}{m_s[1 + (m_y/m_s)]}$ (see equation 3.100). The resulting expression for the relative displacement δ_{sz} is

$$\delta_{sz} = \frac{Q}{\Omega_s m_s(\Omega_z^2/\Omega_s^2)[1 + (m_y/m_s)] - 1} \left[\frac{\Omega_z}{\Omega_s}\sin \Omega_z t - \frac{1}{\sqrt{1 + (m_y/m_s)}} \sin \frac{\Omega_s t}{\sqrt{1 + (m_y/m_s)}}\right]. \qquad (3.103)$$

The maximum value of δ_{sz} occurs when the sine terms in the above equation are numerically equal to unity but of opposite sign. The expression for $(\delta_{sz})_0$ then may be written:

$$(\delta_{sz})_0 = \left(\frac{Q}{\Omega_s m_s}\right)\left(\frac{1}{\sqrt{1 + (m_y/m_s)}[(\Omega_z/\Omega_s)\sqrt{1 + (m_y/m_s)} - 1]}\right). \qquad (3.104)$$

Equation 3.104 is shown graphically in Figure 3.34. The maximum deflection $(\delta_{sz})_0$ of the element, i.e., the maximum relative displacement between masses m_s and m_z, is given with reference to the dimensionless ratio $Q/m_s\Omega_s$. In many types of machinery and equipment, it is of critical importance to maintain the alignment of structural members. The maximum relative displacement $(\delta_{sz})_0$ is therefore a measure of the disrupting effects of the shock. Practical aspects of this condition are discussed in subsequent chapters.

It is interesting to note that large values of element deflection $(\delta_{sz})_0$ occur when the natural frequency of the element coincides with the natural frequency of the support. This is at a frequency ratio $\Omega_z/\Omega_s = 1$, when the equipment is considered massless, and at lower values of Ω_z/Ω_s, when the effective natural frequency of the support is reduced by the addition of mass to the equipment. Considered from a physical viewpoint, the support is caused to vibrate at its natural frequency by the applied impulse. An element whose natural frequency coincides with that of the support will experience an amplitude that increases continuously with time. A similar condition is expressed by equation 3.22, and discussed on page 96. The amplitude of the element does not reach infinity in practical instances, because the inevitable dissipation of energy causes the vibration of the support to decrease gradually. The support often is a structure with small internal damping, however, and the elements of equipment mounted on the support may therefore experience an induced vibration of appreciable magnitude. This phenomeon, referred to here as structural resonance, represents a common source of trouble in equipment mounted upon a support that is subjected to relatively moderate shock forces.

3·15 Isolation of Shock

It becomes evident from the data presented in Figure 3.34 that two methods may be used to reduce the maximum deflection $(\delta_{sz})_0$ experienced by elements of the equipment:

(*a*) An increase in the mass m_y of the equipment tends to reduce the maximum deflection $(\delta_{sz})_0$, because a greater mass is available to oppose the change in velocity resulting from the impulse Q.

(*b*) A decrease in the natural frequency Ω_s of the support is highly beneficial in reducing $(\delta_{sz})_0$, provided that the decrease attains a frequency ratio Ω_z/Ω_s greater than approximately two. The frequency ratio necessary to achieve a reduction in $(\delta_{sz})_0$ varies somewhat as the mass ratio varies, as indicated in Figure 3.34.

Of the two methods outlined above, the latter is the more generally practicable for attaining the desired reduction in the deflection $(\delta_{sz})_0$. It usually is impracticable to increase the mass of the equipment sufficiently to achieve a significant reduction in $(\delta_{sz})_0$. An effect equivalent to decreasing Ω_s is attained by inserting a relatively flexible isolator between the equipment m_y and its support m_s. A complete analysis of such a system becomes more laborious than the results justify. For practical purposes, Figure 3.34 may be used to estimate the effectiveness of an isolator by assuming Ω_s to be the natural frequency of the isolator. A very significant reduction in maximum deflection $(\delta_{sz})_0$ is thus attained from an isolator whose natural frequency Ω_s is 0.1 to 0.2 times the natural frequency Ω_z of a critical element of the equipment. In a vacuum tube or surface grinder, the natural frequencies of critical elements often are as high as 100 cycles per second, and higher. An isolator with a natural frequency of 10 to 20 cycles per second then is very effective.

It may happen that two types of shock motion occur simultaneously. The support, for example, may experience a velocity shock as discussed in Part *A* of this chapter, and simultaneously be subjected to shock motions of small displacement as discussed in Part *D*. An example of this condition is found in a vehicle. The overall motion of the chassis upon the springs and the vibration of the chassis structure occur simultaneously. A single isolator often affords protection against both types of shock. It usually will be found a more exacting

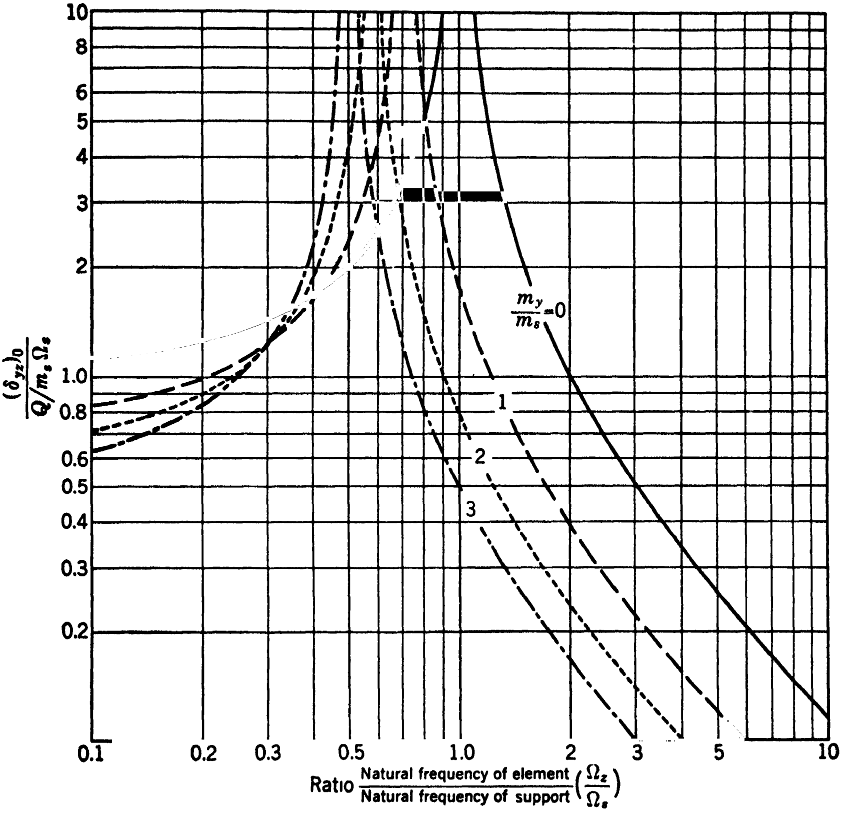

FIGURE 3.34. Maximum deflection $(\delta_{yz})_0$ of element m_zk_z in Figure 3.33, as a result of shock motion of the supporting structure caused by the impulse Q.

task to design the isolator to afford protection against the velocity shock. This accomplished, protection for the shock motions of small displacement is attained more or less incidently, and the effectiveness of the isolators may be estimated by referring to Figure 3.34. To achieve this effectiveness, the maximum possible deflection of the isolator must be at least as great as the maximum amplitude s_0 of the support.

BIBLIOGRAPHY

BIOT, M. A., "A Mechanical Analyzer for the Prediction of Earthquake Stresses," *Bulletin, Seismological Soc. of Amer.*, Vol. 31, No. 2, April 1941.

BIOT, M. A., "Analytical and Experimental Methods in Engineering Seismology," *Proc. A.S.C.E.*, Vol. 68, No. 1, January 1942.

CREDE, C. E., and S. E. YOUNG, "Theoretical and Experimental Investigation of Buckling Shock Mount," *Proc. Soc. Exp. Stress Anal.*, Vol. V, No. II.

FRANKLAND, J. M., "Effect of Impact on Simple Elastic Structures," *Proc. Soc. Exp. Stress Anal.*, Vol. VI, No. II.

HUDSON, G. E., "A Method of Estimating Equivalent Static Loads in Simple Elastic Structures," *Proc. Soc. Exp. Stress Anal.*, Vol. VI, No. II.

MINDLIN, R. D., "Dynamics of Package Cushioning," *Bell System Tech. Jour.*, Vol. XXIV, Nos. 3–4, July–October 1945.

MINDLIN, R. D., F. W. STUBNER, and H. L. COOPER, "Response of Damped Elastic Systems to Transient Disturbances," *Proc. Soc. Exp. Stress Anal.*, Vol. V, No. II.

SCHILLING, R., and H. O. FUCHS, "Modern Passenger-Car Ride Characteristics," *Trans. A.S.M.E.* (*Jour. App. Mech.*, Vol. 8, No. 2), June 1941.

SPOTTS, M. R., "Impact Stress in Elastic Bodies Calculated by the Energy Method," *Prod. Eng.*, Vol. 18, No. 3, March 1947.

ST. DENIS, M., "Dynamic Strength," *Jour. Am. Soc. Naval Eng.*, Vol. 50, No. 2, November 1948.

SYMONDS, P., and I. VIGNESS, "Influence of Duration of Impact on Damage to Some Elastic Systems," *Naval Research Laboratory, Washington, D. C., Report* No. 0-2293, May 15, 1944.

WALSH, J. P., and R. E. BLAKE, "The Equivalent Static Accelerations of Shock Motions," *Proc. Soc. Exp. Stress Anal.*, Vol. VI, No. II.

CHAPTER FOUR

Further Considerations in Vibration and Shock Isolation

The two preceding chapters treat vibration and shock isolation by means of linear, undamped isolators. The foregoing relatively simple analysis leads to results that are significant because applicable principles are demonstrated, and the quantitative results are accurate in most cases to at least a first approximation. The analysis is extended in this chapter to include isolators whose force-deflection curves are non-linear. Damped systems are discussed in both a theoretical and a practical sense. Several miscellaneous considerations that arise in the application of isolators are discussed, and, finally, sound isolation by means of resilient supports is treated briefly.

4·1 Vibration Characteristics of System with Non-Linear Isolators

The differential equation of motion for a single-degree-of-freedom system, equation 2.1 of Chapter 2, is readily solved when the force-deflection characteristic of the isolator is linear. The restoring force on the mounted body is then proportional to the deflection of the isolator, and the system exhibits a natural frequency which is independent of the amplitude of vibration. A different result is obtained when the force-deflection characteristic is non-linear. Two typical non-linear force-deflection curves are shown in Figure 4.1. The initial portions of these curves, indicated by the solid line, are linear. If the maximum displacement of the mounted body during the vibration cycle does not exceed y_1, the result indicated by equation 2.3 applies. The motion of the mounted body is then harmonic; the

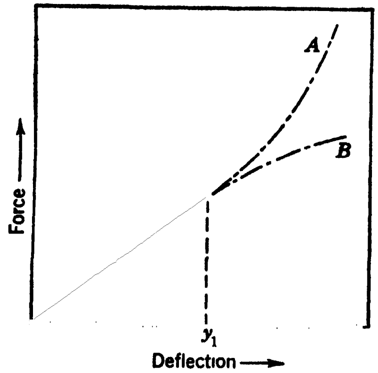

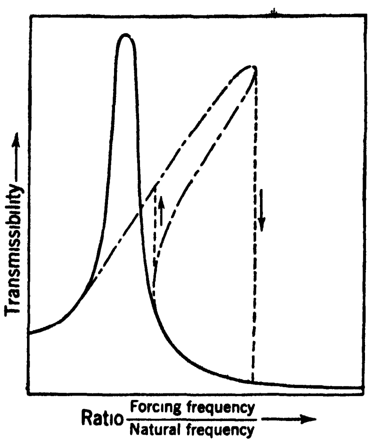

FIGURE 4.1. FIGURE 4.2.

FIGURE 4.1. Force-deflection curves for typical non-linear isolators.

FIGURE 4.2. Transmissibility curves for linear system (solid line) and for system whose stiffness increases as deflection increases, curve A in Figure 4.1 (broken line).

transmissibility curve is shown by Figure 2.2, and by the solid lines in Figures 4.2 and 4.3.

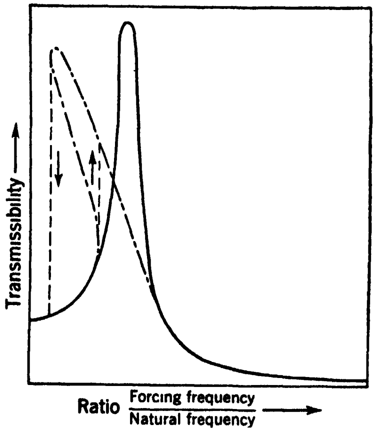

FIGURE 4.3. Transmissibility curves for linear system (solid line) and for system whose stiffness decreases as deflection increases, curve B in Figure 4.1 (broken line).

When the displacement amplitude of the mounted body exceeds the deflection y_1 in Figure 4.1, an unusual result is obtained. Reference is made, for the moment, to the force-deflection curve with increasing stiffness shown at A in Figure 4.1. The force exerted upon the mounted body by the isolator becomes greater than would be obtained from a continuation of the solid line, and the natural frequency is effectively increased for a fraction of the vibration cycle. The vertically extending peak shown by the solid line in Figure 4.2 is thus deflected to the right, as indicated by the broken line. If the forcing frequency is continuously increasing toward resonance, each added increment of frequency tends to move closer to the peak. The amplitude increase resulting therefrom causes a corresponding stiffness increase, and the peak moves farther to the right. In an undamped system, the peak is never reached. As will be shown in a later section, the energy dissipated in a viscously damped system ultimately equals the energy added to the system, and a limit is established for the displacement amplitude. The right-deflected peak shown by the broken line in Figure 4.2 thus acquires its closed top.

If a damped system represented by curve *A* of Figure 4.1 is subjected to vibration whose frequency increases, an abrupt change in vibration amplitude occurs as the peak of the broken curve in Figure 4.2 is reached. To continue to follow the curve would require that the frequency suddenly decrease. A continuing increase in the frequency causes the system to seek the only applicable curve in this region, and the vibration amplitude suddenly decreases along the dotted vertical line identified by the downward-directed arrow in Figure 4.2. Upon reaching the solid line, which involves relatively small displacement amplitudes, the relations of the linear system again apply.

The forcing frequency will now be considered to decrease from a high to a low value. The transmissibility curve with the right-deflected peak in Figure 4.2 determines the vibration amplitude until the vertical portion of the curve is reached. To continue toward the peak would require an increasing frequency. A continuing decrease in frequency causes an amplitude increase along the dotted line identified by the upward-directed arrow in Figure 4.2. The amplitude thereafter decreases gradually along the broken line as the frequency continues to decrease. The transmissibility curve illustrated by the broken line in Figure 4.2 thus becomes applicable to both increasing and decreasing frequency, except for the portion between the dotted vertical lines designated by vertically directed arrows.

When the force-deflection characteristic for the isolator exhibits a stiffness that decreases when the deflection increases, as shown by curve *B* of Figure 4.1, the transmissibility curve shows similar though inverted characteristics. This is illustrated in Figure 4.3. An increasing displacement amplitude associated with the vibration results in less stiffness and, consequently, in a lower natural frequency for a fraction of the vibration cycle. As the amplitude continues to increase, the natural frequency continues to decrease and the resonance peak becomes deflected to the left, as illustrated by the broken curve in Figure 4.3. By the type of reasoning employed above, it may be seen that the system follows the dotted line designated by the upward-directed arrow when the forcing frequency increases, and the dotted line designated by the downward-directed arrow when the forcing frequency decreases.

The term resonant frequency tends to lose its significance when the force-deflection curve is not linear. In a linear system, resonance may be considered to occur when the transmissibility becomes a maximum. If the damping is small, the transmissibility reaches a maximum approximately at the undamped natural frequency. In a non-linear system, however, the frequency at which maximum transmissibility occurs is determined by the following considerations:

(*a*) The vibration amplitude determines the extent to which the non-linearity becomes effective and, therefore, the extent to which the peak of the transmissibility curve is deflected from the vertical.

(*b*) The damping in any system determines the value of maximum transmissibility; in a non-linear system, the damping also determines the frequency at which maximum transmissibility occurs.

(*c*) The maximum transmissibility and the frequency at which this maximum occurs depend on whether the frequency of the forcing vibration is increasing or decreasing.

(*d*) Finally, the regions between the vertical dotted lines designated by arrows in Figures 4.2 and 4.3 are regions of instability in that two values of transmissibility are possible for each forcing frequency. A system vibrating in accordance with the upper curve may suddenly drop to the lower curve if disturbed, or may rise from the lower to the upper curve in a similar manner.

4·2 Natural Frequency of System with Non-Linear Isolators

In a system comprised of mounted body and isolator with the axis of the isolator extending vertically, as shown in Figure 2.1, the isolator experiences a certain static deflection as a result of the dead-weight load that it supports. This position of static equilibrium becomes the neutral position above and below which the mounted body vibrates. The natural frequency is determined by the force exerted upon the body by the isolator as the body vibrates in the region of its neutral position. The proper value of the stiffness k_y in equation 2.17 is the slope of the force-deflection curve of the isolator, measured at the value of force that corresponds to the weight of the body supported by the isolator.

If the force-deflection curve for the isolator is a straight line, the stiffness k_y is a constant and the natural frequency f_n becomes inversely proportional to the square root of the weight of the mounted body. A linear force-deflection curve is illustrated at A in Figure 4.4; and the resulting natural frequency is illustrated as a function of the weight of the mounted body by curve A in Figure 4.5. Where a non-linear force-deflection curve can be defined analytically, an expression that relates the natural frequency of the system and the weight of the supported body may be derived by substituting $dF/d\delta$ for k_y in equation 2.17.

It is common in practical applications to express the stiffness of a non-linear isolator graphically rather than analytically. Equation 2.17 is then evaluated numerically or graphically to obtain the natural frequency. A typical force-deflection curve for a resilient material loaded in compression is shown at B in Figure 4.4. The stiffness k_y is the slope $dF/d\delta$ of the curve, and equation 2.17 may then be written:

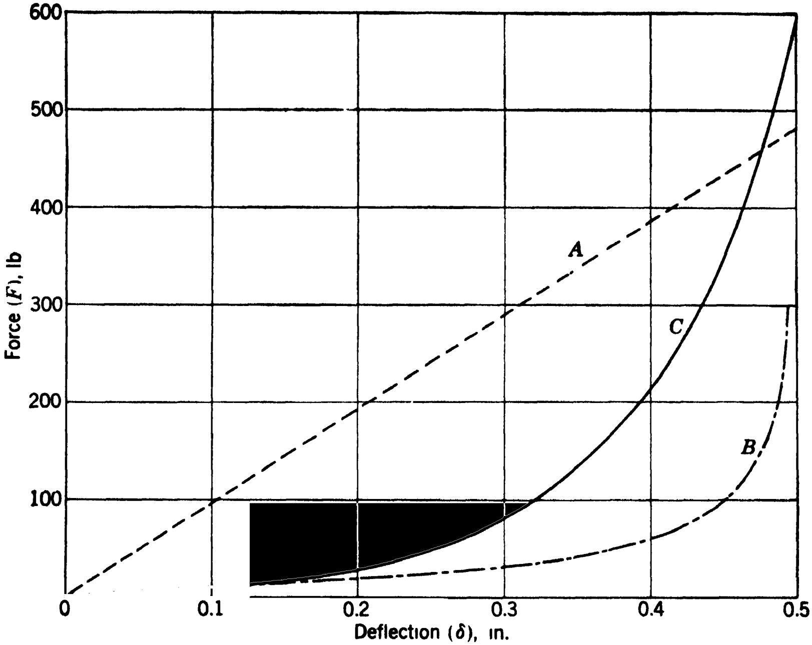

FIGURE 4.4. Force-deflection curves for typical linear and non-linear isolators.

$$f_n = 3.13\sqrt{\frac{dF/d\delta}{W}}. \tag{4.1}$$

Equation 4.1 is evaluated by assuming various values for the weight W of the mounted body (the force F on the isolator is equal to the weight W), measuring the slope $dF/d\delta$, and calculating the natural frequency f_n. Numerical values of $dF/d\delta$ and f_n at several values of W are given in Table 4.1 for curve B in Figure 4.4.

The calculated values of natural frequency f_n are shown by curve *B* in Figure 4.5 as a function of the weight supported by the isolator. Where the weight of the mounted body is small and the force-deflection curve approaches a straight line, the natural frequency curve shows the same type of inverse relation exhibited by curve *A* for the linear isolator. For a mounted body of greater weight, the stiffness increases faster than the weight, and the natural frequency increases.

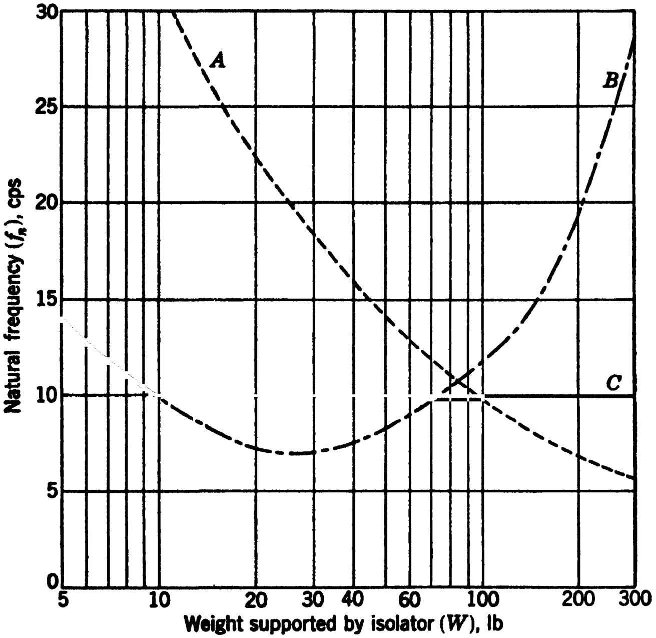

FIGURE 4.5. Natural frequency as a function of supported weight for isolators whose force-deflection curves are shown in Figure 4.4. Lines of similar pattern refer to the same isolator.

It should be recognized that the natural frequency as determined in this manner is exactly correct only for vibration whose displacement amplitude is infinitesimally small. When the vibration amplitude becomes large, the stiffness k_y varies throughout the vibration cycle and the natural frequency becomes a function of the vibration amplitude. This effect sometimes appears in laboratory tests of isolators, but the amplitudes encountered under service conditions usually are so small that the natural frequency may be considered constant for all practical purposes.

An interesting condition arises when the isolator has a non-linear force-deflection curve whose stiffness k_y remains proportional to the weight of the mounted body W at all points on the force-deflection curve. The right side of equation 2.17 then reduces to a constant, and the natural frequency f_n becomes independent of the weight supported by the isolator. Substituting $k_y = dW/d\delta$ in équation 2.17 (the force F is equal to the supported weight W) and rearranging terms:

$$\frac{4\pi^2 f_n^2}{g}\, d\delta = \frac{dW}{W}. \tag{4.2}$$

An expression for the force-deflection curve is obtained from the integration of equation 4.2. A family of curves results from this process, depending on the constant of integration. A particular curve is specified by selecting a point with the coordinates W_0, δ_0 such that all points of the curve whose coordinates are numerically greater than W_0, δ_0 will represent conditions of constant natural frequency. Integrating equation 4.2:

TABLE 4.1

Data for Calculating Natural Frequency from Curve B in Figure 4.4

Weight W (or Force F), lb	Slope $dF/d\delta$, lb/in.	Natural Frequency f_n, cps
10	100	10.0
25	125	7.0
50	350	8.3
75	780	10.1
100	1,400	11.6
125	2,200	13.1
150	3,500	15.0
175	5,200	17.1
200	7,500	19.3
250	15,000	24.3
300	25,000	28.7

$$\frac{4\pi^2 f_n^2}{g}\, \delta \Bigg|_{\delta_0}^{\delta} = \log W \Bigg|_{W_0}^{W}. \tag{4.3}$$

Equation 4.3 may be written exponentially as follows:

$$W = W_0 e^{A(\delta-\delta_0)}, \tag{4.4}$$

where $A = 4\pi^2 f_n^2/g$.

An isolator whose force-deflection curve conforms to equation 4.4 thus exhibits a constant natural frequency f_n when supporting any load greater than W_0. For example, curve C in Figure 4.4 passes through the point $W_0 = 10$ lb, $\delta_0 = 0.1$ in. The curve is linear for values of W less than 10 lb and is in accordance with equation 4.4 for values of W greater than 10 lb. The natural frequency, as indicated by curve C of Figure 4.5, remains constant at 10 cps when the weight of the mounted body is greater than 10 lb. When the weight of the mounted body is less than 10 lb, the natural frequency shows the inverse tendency which is characteristic of linear isolators.

The discussion of vibration isolation in Chapter 2 makes extensive use of isolator stiffnesses in the directions of the principal elastic axes. These analyses are generally applicable to non-linear isolators provided that appropriate values are used for stiffness, as pointed out in the above discussion. The presence of a dead-weight load introduces the consideration that the vertical stiffness of the isolator must be taken as the slope of the force-deflection curve at the position of static equilibrium. The applicable value for the horizontal stiffness is the slope of the force-deflection curve in a horizontal direction, taken with the isolator deflected vertically by the dead-weight load.

The discussion in the preceding paragraphs presumes that the static and the dynamic stiffnesses are equal, and that dynamic results therefore can be calculated from static properties. This is generally true for a metal spring. For many other materials, discrepancies arise as a result of a difference between the static and the dynamic moduli. This condition is discussed in detail in Chapter 5, as a part of the discussion of properties of various resilient materials used in isolators. Although calculations based on the static force-deflection curve may yield approximate results, it is necessary to perform dynamic tests in order to determine the exact value of natural frequency. Any discrepancies that would arise as a result of differences in moduli and unsuspected non-linearity of the force-deflection curve are thus eliminated.

4·3 Shock Isolation with Non-linear Isolators—Analytical Treatment

A force-deflection curve whose stiffness increases as the deflection increases may be defined by the following tangent expression:*

$$F = \frac{2k_t h_i}{\pi} \tan \frac{\pi \delta}{2h_i}, \qquad (4.5)$$

where F = force applied to isolator, lb.
δ = deflection of isolator resulting from force F, in.
h_i = thickness of isolator, in.
k_t = stiffness of isolator for very small deflection, lb/in.

---

* This expression and the following analysis is presented by R. D. Mindlin, "Dynamics of Package Cushioning," *Bell System Technical Journal*, Vol. XXIV, Nos. 3–4, July–October 1945.

The characteristics of equation 4.5 are typical of resilient materials loaded in compression in that the deflection δ must always be less than the thickness h_i, and the force F becomes very great as δ approaches h_i. Its application to isolation problems is convenient inasmuch as the parameter k_t is the stiffness for small deflections, which is significant for vibration and shock of low amplitude. A wide range of force-deflection curves is obtainable by varying the parameter k_t, as illustrated in Figure 4.6.

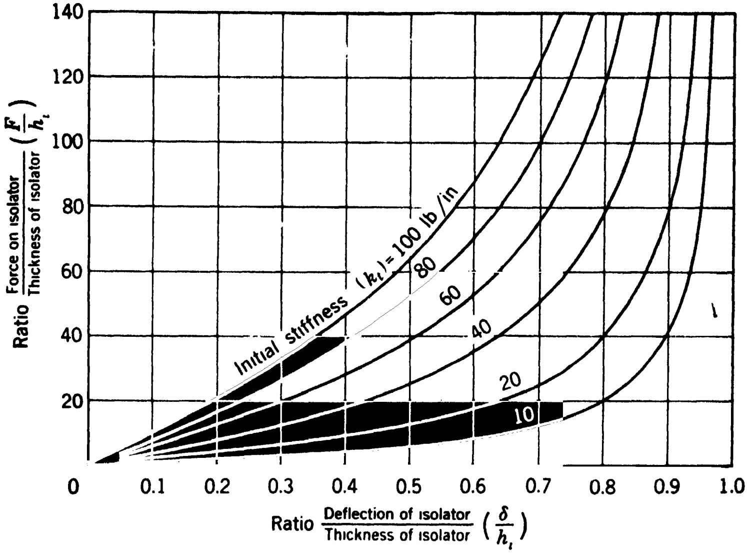

FIGURE 4.6. Typical force-deflection curves defined by tangent function, equation 4.5. An isolator having a force-deflection curve of this type is referred to here as a tangent isolator. (*The Bell System Technical Journal.*)

The system shown in Figure 3.6 of Chapter 3 may experience shock as a result of a suddenly acquired velocity V_s of the support, or the system shown in Figure 3.11 may have its downward velocity V_y arrested by striking the support. If $V_y = V_s$, the response of the two systems is identical for the initial half-natural period of isolator deflection. The results may be evaluated by equating kinetic and potential energy, from which equation 3.32 is derived. This equation is used in the following paragraphs to analyze the response of isolators whose force-deflection curves are shown in Figure 4.6.

The applicable expression for F in equation 3.32 is given by equation 4.5. Making this substitution, equation 3.32 becomes:

$$\int_0^{\delta_0} \frac{2k_t h_i}{\pi} \tan \frac{\pi\delta}{2h_i}\, d\delta = \frac{1}{2} m_y V_y^2. \tag{4.6}$$

Performing the indicated integration:

$$\frac{4k_t h_i^2}{\pi^2} \log_e \cos \frac{\pi\delta_0}{2h_i} = -\frac{1}{2} m_y V_y^2.$$

Combining the coefficient of the left side with the right side and writing the equation in exponential form:

$$\cos^2 \frac{\pi\delta_0}{2h_i} = \exp\left[-\left(\frac{\pi^2 m_y V_y^2}{4k_t h_i^2}\right)\right]. \tag{4.7*}$$

The above equation may be simplified by introducing the maximum deflection $(\delta_t)_0$ of a linear isolator whose stiffness is equal to the stiffness k_t for small deflections. Referring to equation 3.33, $(\delta_{sy})_0 = (\delta_t)_0$, $V_s = V_y$, and $\Omega_y = \sqrt{k_t/m_y}$. Making these substitutions in equation 4.7:

$$\cos^2 \frac{\pi\delta_0}{2h_i} = \exp\left[-\left(\frac{\pi(\delta_t)_0}{2h_i}\right)^2\right]. \tag{4.8}$$

This equation may be written in terms of the tangent function as follows:

$$\tan \frac{\pi\delta_0}{2h_i} = \sqrt{\exp\left(\frac{\pi(\delta_t)_0}{2h_i}\right)^2 - 1}. \tag{4.9}$$

The force F_0 exerted by the isolator at its maximum deflection is obtained from equation 4.5 by substituting $\delta = \delta_0$. Combining the resulting expression with equation 4.9 produces the following expression for F_0:

$$F_0 = \frac{2k_t h_i}{\pi} \sqrt{\exp\left(\frac{\pi(\delta_t)_0}{2h_i}\right)^2 - 1}. \tag{4.10}$$

The maximum acceleration experienced by the chassis of the equipment is obtained by dividing F_0 from equation 4.10 by m_y. This may be expressed as the ratio ζ of F_0/m_y to the maximum acceleration $\ddot{y}_0$ of a linear system whose stiffness is equal to the initial stiffness k_t of the tangent isolator. Substituting $\ddot{y}_0$ from equation 3.38 and noting that $k_t/m_y = \Omega_t^2$, the following expression for ζ is obtained:

---

* The designation exp (A) is used here for e^A.

$$\zeta = \frac{F_0/m_y}{\Omega_t^2(\delta_t)_0} = \frac{2h_i}{\pi(\delta_t)_0}\sqrt{\exp\left(\frac{\pi(\delta_t)_0}{2h_i}\right)^2 - 1}. \tag{4.11}$$

Equation 4.11 is illustrated by Figure 4.7, which reveals the expected result that the maximum acceleration transmitted by a tangent isolator is never less than the maximum acceleration transmitted by a linear isolator whose stiffness is equivalent to the initial stiffness of the tangent isolator. When the deflection of the equivalent linear isolator would exceed the thickness of the tangent isolator, i.e., when $h_i/(\delta_t)_0 < 1$, the maximum acceleration transmitted by the tangent isolator tends to become relatively great. The effect upon the mounted equipment is generally less severe when the stiffness increases gradually, as with the tangent isolator, than when a relatively rigid snubber is employed, as discussed in Section 3·6 of Chapter 3.

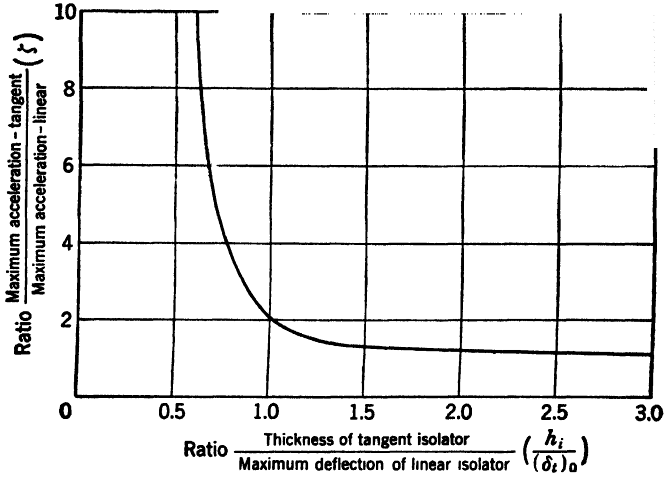

FIGURE 4.7. Maximum acceleration transmitted by tangent isolator, expressed in terms of maximum acceleration transmitted by linear isolator having equivalent stiffness at small deflections. (*The Bell System Technical Journal.*)

The maximum deflection δ_0 of the tangent isolator in terms of its thickness h_i may be determined by solving equation 4.8 for the ratio δ_0/h_i as follows:

$$\frac{\delta_0}{h_i} = \frac{2}{\pi}\cos^{-1}\exp\left[-\frac{\pi^2}{8}\left(\frac{(\delta_t)_0}{h_i}\right)^2\right]. \tag{4.12}$$

This equation is plotted in Figure 4.8. When the thickness of the tangent isolator is small relative to the deflection experienced by a linear isolator of equivalent initial stiffness, i.e., when $h_i/(\delta_t)_0 \ll 1$, the deflection of the tangent isolator is almost equal to its thickness. The isolator is very stiff under these conditions, and the transmitted acceleration is high, as indicated by Figure 4.7. From a comparison of Figures 4.7 and 4.8, it is evident that a reasonably low chassis acceleration is attained only by selecting the stiffness and thickness so as to avoid excessively large values of the ratio δ_0/h_i.

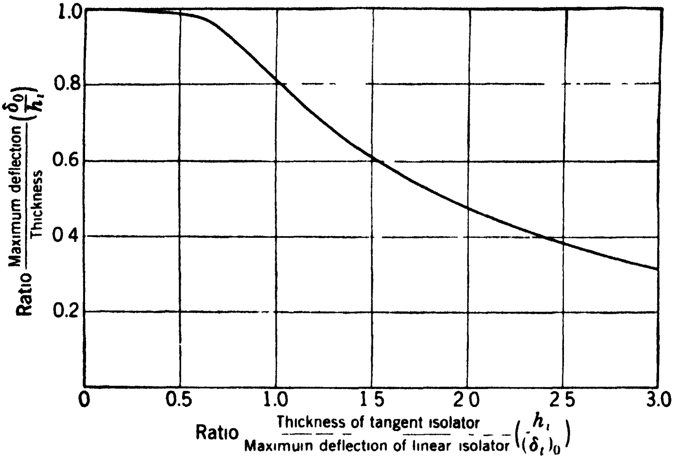

FIGURE 4.8. Maximum deflection of tangent isolator, expressed in terms of its thickness and the maximum deflection of a linear isolator having the same stiffness at small deflections. (*The Bell System Technical Journal.*)

4·4 Shock Isolation with Non-linear Isolators—Numerical Treatment

Analytical expressions for the force-deflection characteristics of many common isolators are difficult to obtain. This is due largely to the fact that the theory of large strains in elastic members has not been successfully applied to members of complex shape. As a result, expressions for the force-deflection characteristics of isolators usually are empirical in nature. Such equations are determined by assuming a form for the equation, and evaluating the constants by fitting the equation to an experimentally determined force-deflection curve. This is unnecessary because the maximum acceleration and the maximum deflection of a non-linear isolator are readily obtainable by the graphical and numerical method explained in this section. The method is general, but it will be illustrated by means of the force-deflection curve for a typical rubber isolator loaded in compression.*

---

* See C. E. Crede and S. E. Young, "Theoretical and Experimental Investigation of Buckling Shock Mount," *Proc. Soc. Exp. Stress Anal.*, Vol. V, No. II, p. 144.

It is characteristic of most isolators that the force-deflection curve can be expressed by dimensionless parameters. The dimensionless force parameter, $\gamma = F/(k_t h_i)$, is the ratio of the force exerted by the isolator to a hypothetical force required to completely deflect a linear isolator of equivalent initial stiffness. The dimensionless deflection parameter, $\xi = \delta/h_i$, is the ratio of the deflection of the isolator to its thickness. The dimensionless force-deflection curve, when once drawn for a particular type of isolator, applies to the majority of isolators having geometric similarity and employing the same type of resilient material. A typical curve for an isolator that utilizes rubber in compression is illustrated in Figure 4.9.

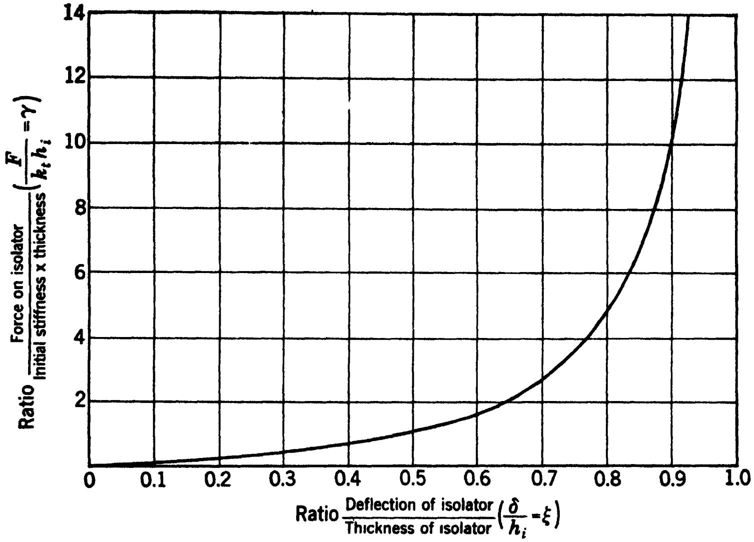

FIGURE 4.9. Typical force-deflection curve for isolator employing rubber in compression, expressed in dimensionless parameters.

An expression for the equivalence of kinetic and potential energy can be obtained in terms of the above dimensionless parameters by dividing both sides of equation 3.32 by $k_t h_i^2$. The following expression then results:

$$2\int_0^{\xi_0} \gamma\, d\xi = \frac{m_y V_y^2}{k_t h_i^2}. \tag{4.13}$$

The stiffness and mass terms in the above equations are eliminated by substituting $k_t/m_y = (2\pi f_t)^2$, where f_t is the natural frequency of the isolator for small deflections, expressed in cycles per second. Then:

$$\int_0^{\xi_0} \gamma \, d\xi = \frac{1}{8\pi^2}\left(\frac{V_y}{f_t h_i}\right)^2. \tag{4.14}$$

The integral on the left side of equation 4.14 is the area under the force-deflection curve, Figure 4.9. This area is plotted in Figure 4.10.

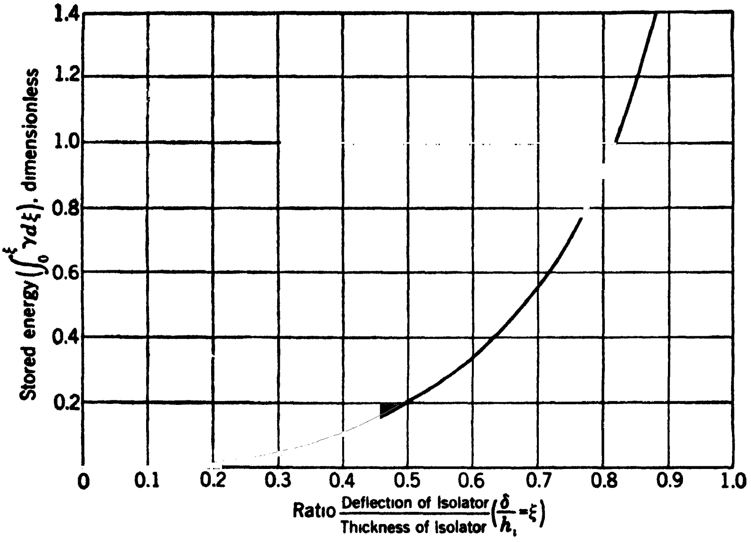

FIGURE 4.10. Energy stored in isolator whose force-deflection curve is shown in Figure 4.9, expressed in dimensionless parameters. The stored energy is proportional to the area under the force-deflection curve shown in Figure 4.9.

The maximum acceleration $\ddot{y}_0$ experienced by the mounted chassis m_y is defined by the following expression, using the relation given above to introduce the dimensionless force γ:

$$\ddot{y}_0 = \frac{F_0}{m_y} = \frac{k_t h_i \gamma_0}{m_y}, \tag{4.15}$$

where γ_0 is the maximum value of the dimensionless force ratio γ. Substituting $k_t/m_y = (2\pi f_t)^2$, as indicated above, and multiplying both sides by h_i/gV_y^2, equation 4.15 becomes:

$$\left(\frac{\ddot{y}_0}{g}\right)\left(\frac{h_i}{V_y^2}\right) = \frac{4\pi^2}{g}\left(\frac{f_t h_i}{V_y}\right)^2 \gamma_0, \tag{4.16}$$

where the maximum acceleration $\ddot{y}_0/g$ is expressed in multiples of the acceleration due to gravity.

The relation among the various parameters of the system may now be determined by the following numerical procedure:

(*a*) Numerical values covering a wide range are arbitrarily assumed for the parameter $V_y/(f_t h_i)$. The corresponding values for $\int_0^{\xi_0} \gamma\, d\xi$ are then calculated from equation 4.14.

(*b*) Entering the energy curve of Figure 4.10 with the values for $\int_0^{\xi_0} \gamma\, d\xi$ determined in step (*a*), corresponding values of the maximum dimensionless deflection ξ_0 are obtained. The dotted curve in Figure 4.11 is plotted from the values of ξ_0 determined in this manner.

(*c*) Using the values of maximum deflection ξ_0 determined in step (*b*), corresponding values of maximum dimensionless force γ_0 are determined from Figure 4.9.

(*d*) All the factors comprising the right-hand term of equation 4.16 are now determined, and values of $(\ddot{y}_0/g)(h_i/V_y^2)$ are then calculated.

(*e*) The solid curve shown in Figure 4.11 is plotted, using as coordinates the parameter $V_y/(f_t h_i)$ initially assumed in step (*a*), and the expression calculated in step (*d*).

The curve shown by the solid line of Figure 4.11 thus completely expresses the relation between the maximum transmitted acceleration $\ddot{y}_0/g$ and the shock velocity V_y, in terms of the isolator thickness h_i and the natural frequency f_t based on the stiffness for small deflections. The single qualification is that the dimensionless force-deflection curve, Figure 4.9, remain constant. This usually can be assured by maintaining geometrical similarity of the isolator. Variations in stiffness can be attained by modifying the dimensions and the modulus of the resilient material used in the isolator. Figure 4.11 is best utilized in a cut-and-try manner to obtain the desired conditions. Although the force-deflection characteristics of rubber in compression vary considerably with the shape factor of the member, as pointed out in Chapter 5, the curve in Figure 4.9 is quite typical, and the performance curves of Figure 4.11 may be used to approximate the performance of any rubber isolator loaded in compression. Similar curves are readily drawn for any type of force-deflection curve, using the procedure outlined above.

The expressions $V_y/f_t h_i$ and $(\ddot{y}_0/g)(h_i/V_y^2)$ which define the coordinate scales of Figure 4.11 have little physical significance. Their usefulness resides in the fact that they are comprised of terms that determine the physical properties of the system being investigated. It may be known, for example, that isolation is to be provided for a given velocity change V_y. The characteristics of an isolator, assuming that it conforms to the dimensionless force-deflection curve of Figure 4.9, are completely determined by the thickness h_i of the rubber and the natural frequency f_t for small deflections. A suitable isolator is found as a result of cut-and-try methods by assuming values of h_i, f_t, and calculating the parameter $V_y/(f_t h_i)$. The solid curve in Figure 4.11 then indicates the value of $(\ddot{y}_0/g)(h_i/V_y^2)$, from which $\ddot{y}_0/g$ is readily obtained because h_i, V_y are known. By a similar procedure, a value for the maximum dimensionless deflection ξ_0 is obtained from the right-hand scale of Figure 4.11, using the dotted curve. The maximum isolator deflection, in linear units, is the product of ξ_0 and the isolator thickness h_i. This procedure can be repeated, using different assumed values for h_i, f_t, until suitable values of $\ddot{y}_0/g$ and ξ_0 are obtained.

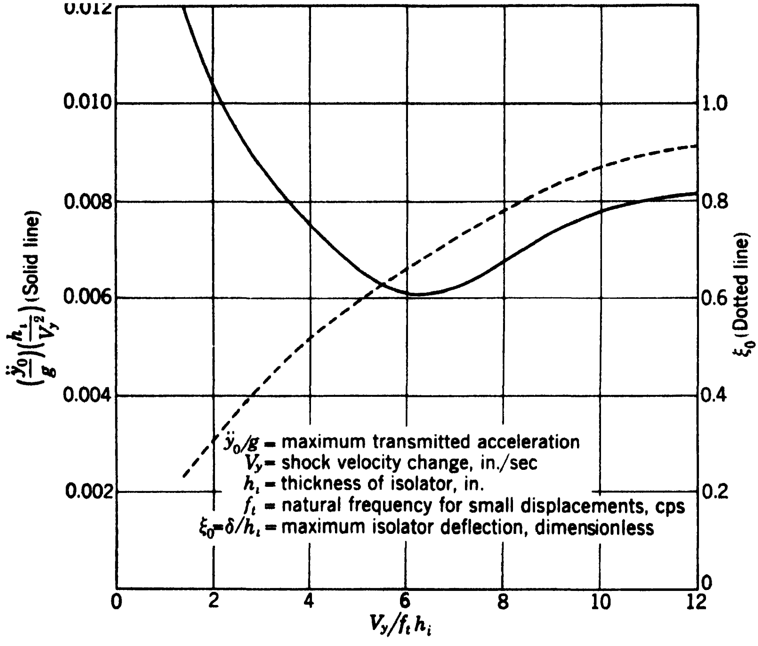

FIGURE 4.11. Curves indicating performance of isolator employing rubber in compression and subjected to velocity shock. The maximum deflection of the isolator, in dimensionless terms, is indicated by the dotted curve. The maximum acceleration, expressed as a multiple of the acceleration due to gravity, is obtained from the solid curve.

Example 4.1. Equipment weighing 50 lb is supported within a relatively heavy shipping container by rubber shock isolators. See Figures 6.19 and 6.20 of Chapter 6 for typical designs. The thickness of the rubber in the isolators is one inch, and the natural frequency for small displacements is 10 cps. The configuration of the rubber is such that its force-deflection curve is defined by equation 4.5. The container and its equipment are dropped from a height of six inches upon a rigid wooden floor and come to rest without bouncing. The maximum acceleration experienced by the equipment, and the maximum deflection of the isolators, will be computed by both the analytical and the numerical methods outlined in the preceding sections.

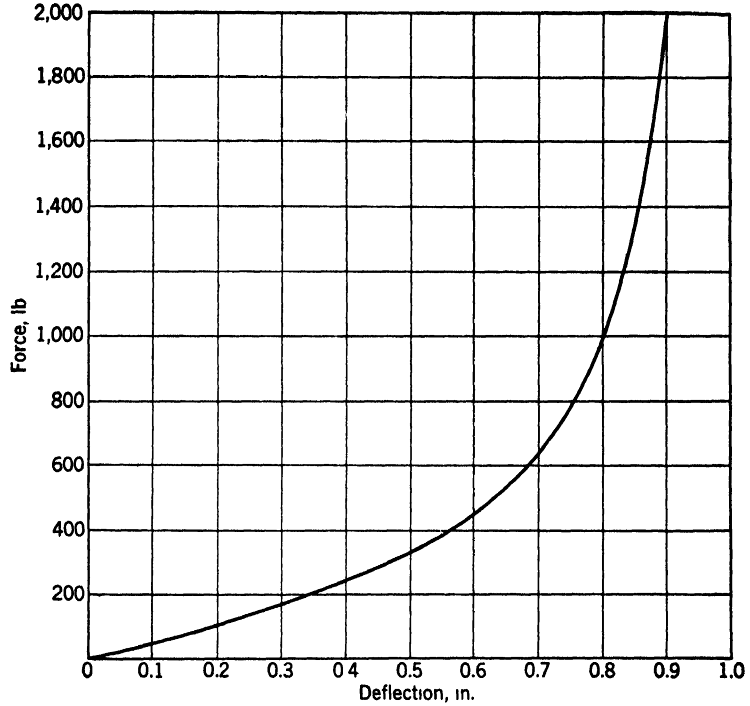

FIGURE 4.12. Force-deflection curve for isolator which embodies rubber in compression, as calculated from equation 4.5, using h_t = one inch and k_t = 511 lb/in.

The force-deflection curve is substantially linear for small deflections, and the initial stiffness k_t may be calculated from equation 2.17 as follows:

$$k_t = 4\pi^2 f_t^2 m = 4\pi^2(10)^2 \times \frac{50}{386} = 511 \text{ lb/in.}$$

This is the total initial stiffness of the group of isolators that function in a particular direction, and it is taken as numerically equal to the stiffness of the hypothetical linear isolator. The force-deflection curve for the actual isolator is shown in Figure 4.12, as calculated from equation 4.5 using h_t = one inch and k_t = 511 lb/in.

The downward velocity of the container at moment of striking the wooden floor is readily calculated from equation 3.13 as follows:

$$V_y = \sqrt{2gh_f} = \sqrt{2 \times 386 \times 6} = 68 \text{ in./sec.}$$

The maximum deflection $(\delta_t)_0$ of the hypothetical linear isolator is now calculated from equation 3.33:

$$(\delta_t)_0 = \frac{V_y}{\Omega_t} = \frac{68}{10 \times 2\pi} = 1.09 \text{ in.}$$

The maximum force F_0 transmitted by the actual isolator is calculated from equation 4.10, using the value for $(\delta_t)_0$ obtained above:

$$F_0 = \frac{2 \times 511 \times 1}{\pi} \sqrt{\exp\left(\frac{1.09\pi}{2 \times 1}\right)^2 - 1} = 1{,}365 \text{ lb.}$$

The maximum acceleration experienced by the equipment, expressed as a multiple of the acceleration due to gravity, is the quotient obtained by dividing F_0 by the total weight supported by the isolators:

$$\text{Maximum acceleration} = \frac{1{,}365}{50} = 27.3\ g.$$

This result may also be obtained from the curve, Figure 4.7. It is necessary to calculate, first, the maximum acceleration experienced with the hypothetical linear isolator. This is obtained from equation 3.36 as follows:

TABLE 4.2

CALCULATION OF ENERGY STORAGE FOR CURVE OF FIGURE 4.12

Deflection in.	Area under curve of Figure 4.12, from origin to deflection given in first column, in.^{2}	Energy stored in isolator at deflection given in first column, lb in.
0	0	0
0.1	0.01	1.8
0.2	0.04	7.2
0.3	0.11	19.8
0.4	0.23	41.4
0.5	0.38	68.4
0.6	0.59	106.2
0.7	0.87	156.6
0.8	1.32	237.6
0.9	2.10	378.0

$$\ddot{y}_0 = V_y\Omega_y = 68 \times 10 \times 2\pi = 4260 \text{ in./sec}^2.$$

Expressed as a multiple of the acceleration due to gravity, $\ddot{y}_0/g = 4260/386 = 11\ g$. Entering Figure 4.7 at the ratio $h_i/(\delta_t)_0 = 1/1.09 = 0.92$, a value $\zeta = 2.45$ is read from the ordinate scale. The maximum acceleration experienced by the equipment on the actual isolators is thus the product of $\ddot{y}_0/g$ and ζ:

$$\text{Maximum acceleration} = 11 \times 2.45 = 27.1g.$$

This corresponds to the value 27.3g obtained by the alternate method above.

The maximum deflection of the isolator is obtained by entering Figure 4.8 at the value $h_i/(\delta_t)_0 = 0.92$, and reading $\delta_0/h_i = 0.85$ from the ordinate scale. Since the isolator thickness h_i is one inch, the maximum deflection δ_0 is 0.85 in.

The above method of calculating maximum acceleration and maximum deflection is generally applicable only when an analytical expression is available for the force-deflection curve, and specifically only when this expression is the tangent function given by equation 4.5. The numerical method outlined in Section 4.4 is applicable, on the other hand, to any force-deflection curve. The method will be illustrated below, using conditions employed in the first part of this example.

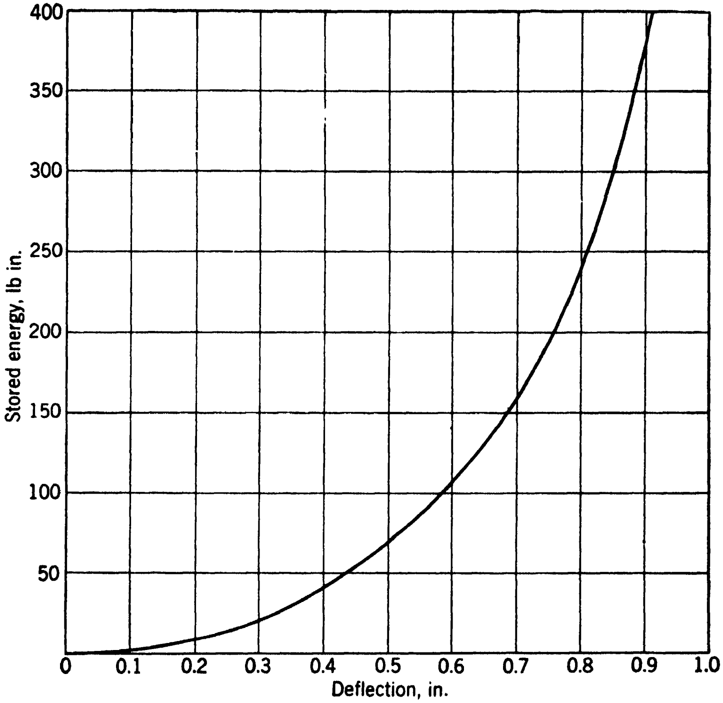

FIGURE 4.13. Energy storage in isolator which embodies rubber in compression. This is determined by measuring the area under the curve of Figure 4.12.

The first step in applying the numerical method is to construct a curve of energy storage as a function of deflection of the isolator. The energy storage is the area under the force-deflection curve, Figure 4.12, and may be obtained by counting squares or by the use of a planimeter. The area under the curve, integrated by discrete increments, is tabulated in Table 4.2 in square inches. In the scale used in Figure 4.12, one inch on the ordinate equals 600 lb, and one inch on the abscissa equals 0.3 in. One square inch therefore is equal to 600 × 0.3 = 180 lb in. The area in square inches, given in the second column, is thus multiplied by 180 to obtain the energy, expressed in pound inches, given in the third column. This energy is plotted in Figure 4.13 as a function of deflection.

The expression for energy equivalence, equation 3.32, is employed to obtain maximum deflection of the isolator. Substituting in equation 3.32:

$$\int_0^{\delta_0} F\,d\delta = \frac{1}{2} \times \frac{50}{386} \times (68)^2 = 300 \text{ lb in.}$$

Entering Figure 4.13 at an energy storage of 300 lb in., the maximum deflection, $\delta_0 = 0.85$ in., is read directly from the abscissa scale. Referring then to Figure 4.12, the maximum force exerted by the isolator, at a deflection of 0.85 in., is $F_0 =$ 1,350 lb. The maximum acceleration experienced by the equipment is:

$$\text{Maximum acceleration} = \frac{1{,}350}{50} = 27g.$$

The values of $27g$ and 0.85 in. for maximum acceleration and maximum deflection, respectively, as computed numerically, correspond to the values $27.3g$ and 0.85 in. determined analytically.

4·5 Free Vibration with Viscous Damping

The introduction of damping into a system often creates unsuspected difficulty in the analysis. The principal source of difficulty is that viscous damping, which is susceptible to mathematical analysis, is seldom encountered in pure form in practice; whereas the common types of damping actually encountered are not well adapted to mathematical analysis. Certain important properties of a damped system, however, become evident from the analysis of viscous damping. Such an analysis is carried out in this and the several following sections, and the results are then interpreted with regard to the types of damping commonly encountered.

A viscously damped, single-degree-of-freedom system capable of experiencing free vibration is illustrated schematically in Figure 4.14. The force exerted by the spring k upon the mass m is proportional to the displacement y, and the force exerted by the damper c upon the mass m is proportional to the velocity $\dot{y}$. The differential equation of motion of the mass is

$$m\ddot{y} = -ky - c\dot{y}. \tag{4.17}$$

The solution of the above equation evidently is a function that retains its form upon being differentiated repeatedly with respect to time. The exponential expression Ae^{Bt} meets this test, and therefore it is a solution of equation 4.17. Substituting $y = Ae^{Bt}$ in equation 4.17:

$$AmB^2e^{Bt} + AcBe^{Bt} + Ake^{Bt} = 0. \tag{4.18}$$

Dividing both sides of the equation by Ae^{Bt} and solving for B:

$$B = -\frac{c}{2m} \pm \sqrt{\left(\frac{c}{2m}\right)^2 - \frac{k}{m}}. \tag{4.19}$$

Two values of B result from the alternate sign in equation 4.19. Designating these two values by B_1, B_2, the most general solution of equation 4.17 is

$$y = A_1e^{B_1t} + A_2e^{B_2t}. \qquad (4.20)$$

The physical significance of the solution, equation 4.20, depends on whether the values of B given by equation 4.19 are real or complex. When $(c/2m)^2 > k/m$, all terms are real. The value of the radical then is numerically smaller than $c/2m$, and both values of B are negative. The expression for y given by equation 4.20 is thus the sum of two decreasing exponentials whose sum becomes asymptotic to zero as time increases indefinitely. This is a condition of greater than critical damping, in which there is no vibration in the sense of an oscillating motion. This condition is of little practical significance in vibration and shock isolation, and it will not be considered further here.

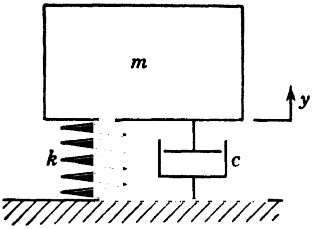

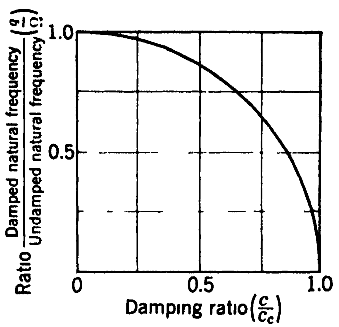

FIGURE. 4.14. FIGURE 4.15.

FIGURE 4.14. Schematic diagram of single-degree-of-freedom system with viscous damping.

FIGURE 4.15. Ratio of damped to undamped natural frequencies, as a function of viscous damping ratio c/c_c.

It will be shown that a condition of less than critical damping exists when the expressions for B given by equation 4.19 are complex. The radical in equation 4.19 is imaginary when $(c/2m)^2 < k/m$. The expression for B thus changes from real to imaginary when

$$\left(\frac{c}{2m}\right)^2 = \frac{k}{m}. \qquad (4.21)$$

The value of damping at which this transition occurs is designated critical damping. The symbol for critical damping is c_c, for which the following expression is obtained from equation 4.21:

$$c_c = 2\sqrt{km}. \qquad (4.22)$$

The expression for the natural frequency of an undamped, single-degree-of-freedom system, from equation 2.16, is

$$\Omega = \sqrt{\frac{k}{m}}. \tag{4.23}$$

Combining equations 4.22 and 4.23,

$$c_c = 2m\Omega. \tag{4.24}$$

When the damping is less than critical, i.e., when $(c/2m)^2 < k/m$, the expressions for B given by equation 4.19 may be written as complex numbers by introducing the imaginary symbol $j = \sqrt{-1}$:

$$B = -\frac{c}{2m} \pm jq, \tag{4.25}$$

where

$$q = \sqrt{\frac{k}{m} - \left(\frac{c}{2m}\right)^2}. \tag{4.26}$$

The expression for y given by equation 4.20 may now be written as follows, using the relation given by equation 4.25 and employing the procedure of equation 1.23:

$$y = A_1 e^{\frac{-c}{2m}t} e^{jqt} + A_2 e^{\frac{-c}{2m}t} e^{-jqt}.$$

The terms in the above equation that embody the imaginary exponent are evaluated by substituting from equation 1.21:

$$\begin{aligned} y &= e^{\frac{-c}{2m}t}[A_1(\cos qt + j \sin qt) + A_2(\cos qt - j \sin qt)], \\ &= e^{\frac{-c}{2m}t}[(A_1 + A_2) \cos qt + j(A_1 - A_2) \sin qt]. \end{aligned} \tag{4.27}$$

The coefficients A_1 and A_2 are arbitrary constants, and new constants D_1 and D_2 may therefore be substituted in place of the original coefficients as follows:

$$y = e^{\frac{-c}{2m}t}(D_1 \cos qt + D_2 \sin qt). \tag{4.28}$$

The values of the coefficients D_1, D_2 depend on particular conditions, and they may be evaluated from known values of the initial displacement and velocity of the mass m.

The expression given by equation 4.26 appears in the argument of the trigonometric terms in equation 4.28. It therefore defines the frequency of free vibration of the damped system and is designated the damped natural frequency. The relation between the damped and the undamped natural frequencies is determined by dividing equation 4.26 by $\Omega = \sqrt{k/m}$, and employing the expression for critical damping given by equation 4.22:

$$q = \Omega\sqrt{1 - \left(\frac{c}{c_c}\right)^2}. \tag{4.29}$$

The term c/c_c in the above equation appears often in the discussion of damped vibrations. It is the ratio of the actual damping coefficient for the system to the damping coefficient for a critically damped system. The designation, viscous damping ratio or, simply, damping ratio is applied; it is sometimes expressed as a percentage of critical damping. The ratio of the damped natural frequency q to the undamped natural frequency Ω, as indicated by equation 4.29, is thus a function only of the damping ratio. Figure 4.15 depicts the relation given by equation 4.29.

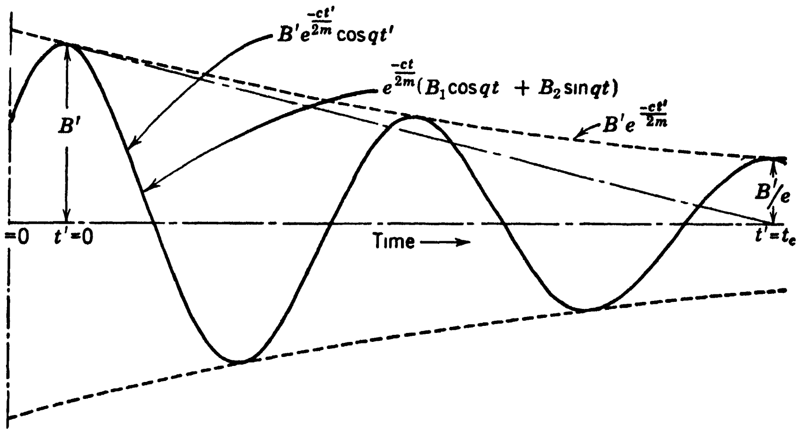

FIGURE 4.16. Free vibration of single-degree-of-freedom system with viscous damping.

The free vibration of the mass m in the viscously damped system is defined by the product of exponential and trigonometric terms, equation 4.28. This vibration is illustrated by the typical displacement-time curve shown in Figure 4.16, in which each successive peak has a lower amplitude as determined by the envelope representing the exponential term. Equation 4.27 may be written as follows, employing a new time reference $t' = 0$ when the envelope amplitude is B'

and the envelope becomes tangent to the displacement-time curve for the mass m:

$$y = B'e^{\frac{-c}{2m}t'} \cos qt'. \tag{4.30}$$

Designating the vibration at $t' = 0$ as the nth cycle, a displacement $(y_n)_0$ is obtained directly from equation 4.30:

$$(y_n)_0 = B'e^{\frac{-c}{2m}t'}. \tag{4.31}$$

The displacement after n_1 additional cycles of vibration is

$$(y_{n+n_1})_0 = B'e^{\frac{-c}{2m}\left(t'+\frac{2\pi n_1}{q}\right)}. \tag{4.32}$$

These values of $(y_n)_0$ and $(y_{n+n_1})_0$ occur when $\cos qt' = 1$, and they do not represent maximum values of y. The maxima occur slightly earlier, owing to the inverted exponential function. For practical purposes, however, $(y_n)_0$ and $(y_{n+n_1})_0$ may be considered maximum values at the respective cycles of vibration. The ratio of any two displacement peaks separated by n_1 complete cycles of free vibration is now found by dividing equation 4.32 by equation 4.31:

$$\frac{(y_{n+n_1})_0}{(y_n)_0} = \frac{B'e^{\frac{-c}{2m}t' - \frac{c}{2m}\times\frac{2\pi n_1}{q}}}{B'e^{\frac{-c}{2m}t'}} = e^{\frac{-n_1\pi c}{mq}}. \tag{4.33}$$

Substituting the expression for damped natural frequency, equation 4.29, and the expression for critical damping, equation 4.24, equation 4.33 becomes:

$$\frac{(y_{n+n_1})_0}{(y_n)_0} = \exp\left[\frac{-2\pi n_1(c/c_c)}{\sqrt{1-(c/c_c)^2}}\right]. \tag{4.34}^*$$

The relation given by equation 4.34 is shown graphically in Figure 4.17, which affords convenient means to determine the damping ratio c/c_c from the measured peaks of a free vibration record.

The ratio of the maximum amplitude at two successive cycles of free vibration is commonly used to indicate the degree of damping in a system. This is expressed by the following relation:

$$\frac{(y_{n+1})_0}{(y_n)_0} = e^{-\Delta}, \tag{4.35}$$

---

* The designation exp (A) is used here for e^A.

where Δ is designated the logarithmic decrement. It is evident that equations 4.34 and 4.35 can be made identical by setting $n_1 = 1$ in equation 4.34, and writing the following expression for Δ:

$$\Delta = \frac{2\pi(c/c_c)}{\sqrt{1 - (c/c_c)^2}}. \tag{4.36}$$

When the damping in the system is small, the denominator of equation 4.36 approaches unity, and an approximate expression for logarithmic decrement is

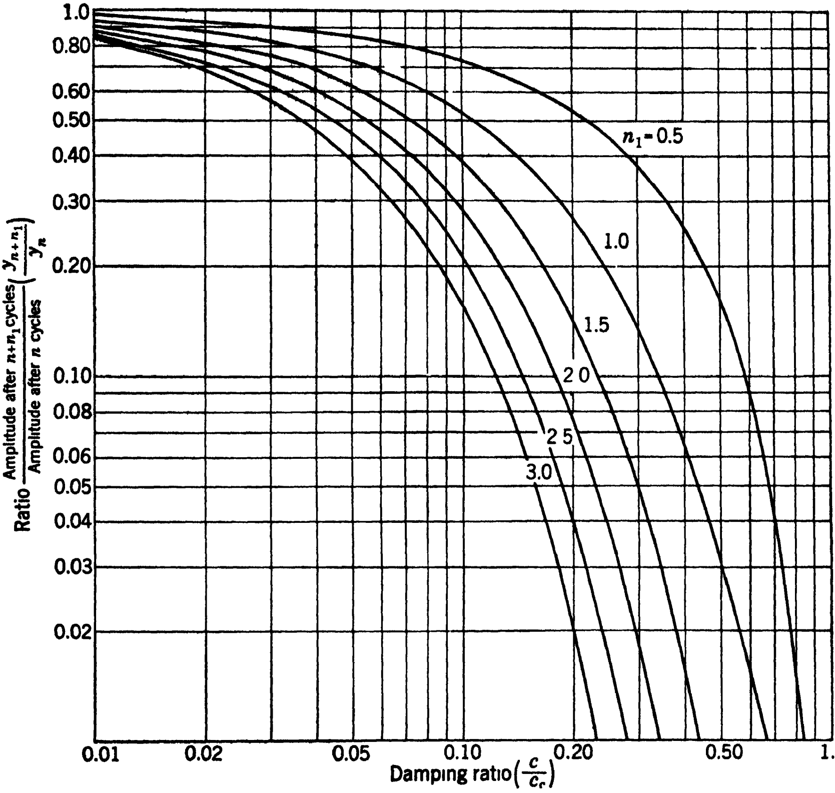

FIGURE 4.17. Relation between any two peak amplitudes in a viscously damped system executing free vibration.

$$\Delta \approx 2\pi\left(\frac{c}{c_c}\right). \tag{4.37}$$

The decrement is sometimes expressed in terms of the ratio of the difference of maximum amplitudes at two successive cycles to the maximum amplitude at the initial cycle as follows:

$$\frac{(y_n)_0 - (y_{n+1})_0}{(y_n)_0} = 1 - \frac{(y_{n+1})_0}{(y_n)_0} = 1 - e^{-\Delta}. \tag{4.38}$$

Another method sometimes used to designate the damping in a freely vibrating system is to specify the time for the vibration amplitude to decay to a specified value. A line drawn tangent with the envelope defined by the inverse exponential function, equation 4.30, intersects the base line at a time designated the time constant t_c, measured from the point of tangency. See Figure 4.16. The amplitude of the envelope then has decreased to $1/e$ times its initial value. It may be considered that n_1 cycles* of free vibration are required to effect this reduction in amplitude. Setting the amplitude ratio of equation 4.33 equal to $1/e$:

$$e^{-\frac{n_1\pi c}{mq}} = \frac{1}{e}, \tag{4.39}$$

from which it is evident that

$$\frac{n_1\pi c}{mq} = 1. \tag{4.40}$$

The time constant t_c is the product of the damped natural period $2\pi/q$ and the total number of cycles n_1 of free vibration, during which time the amplitude decays from $(y_n)_0$ to $(y_{n+n_1})_0$:

$$t_c = \frac{2\pi n_1}{q}. \tag{4.41}$$

Combining equations 4.40 and 4.41, and substituting the expression for critical damping, equation 4.24:

$$t_c = \frac{1}{\Omega(c/c_c)}. \tag{4.42}$$

The time constant t_c is thus inversely proportional to both the undamped natural frequency Ω and the damping ratio c/c_c.

4·6 Forced Vibration with Viscous Damping

The vibration of a viscously damped single-degree-of-freedom system may be forced as a result of (1) an oscillating force applied to the mounted body or (2) oscillating motion of the support. The system is shown schematically in Figure 4.18. The mass m simulates the mounted body, and the isolator is represented by the combination of elastic element k and damper c.

---

* This relation is derived from the equation for the envelope of the peaks of the vibration, and it is not necessary that n_1 be an integer.

Assume, first, that the support is fixed ($s = 0$) and that the mounted body m is acted upon by the force $F = F_0 \cos \omega t$. The differential equation of motion for the mounted body m is

$$m\ddot{y} = F_0 \cos \omega t - c\dot{y} - ky. \qquad (4.43)$$

Equation 4.43 is conveniently solved by the use of complex notation, as explained in Section 1·2. This assumes that the transient vibration disappears as a result of the damping, and that the mass m vibrates with harmonic motion at the forcing frequency ω. Single differentiation is then equivalent to multiplication by $j\omega$, and double differentiation to multiplication by $-\omega^2$. Carrying out these operations, and substituting from equations 1.25 and 1.26 for F and y, equation 4.43 becomes:

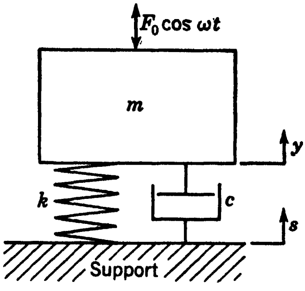

FIGURE 4.18. Schematic diagram of viscously damped single-degree-of-freedom system excited by force $F_0 \cos \omega t$. Excitation may also result from motion s of support when $F_0 = 0$.

$$(-m\omega^2 + j\omega c + k)y_0 e^{j(\omega t + \psi_1)} = F_0 e^{j\omega t}. \qquad (4.44)$$

Dividing equation 4.44 by $e^{j\omega t}$:

$$[(k - m\omega^2) + j\omega c]y_0 e^{j\psi_1} = F_0. \qquad (4.45)$$

The maximum displacement y_0 of the mounted body and the phase angle ψ_1 between the force F_0 and the displacement y_0 are now readily determined from equation 4.45. The former is evaluated by noting, from equation 1.21, that the absolute value of $e^{j\psi_1}$ is unity. The absolute value of the complex quantity in brackets in equation 4.45 is found, in a similar manner, to be the square root of the sum of the squares of the real and imaginary parts. Equation 4.45 then becomes, in terms of the maximum values y_0 and F_0:

$$y_0 = \frac{F_0}{\sqrt{(k - m\omega^2)^2 + \omega^2 c^2}}, \qquad (4.46)$$

where y_0 indicates the maximum vibration amplitude of the mounted body as defined by the expression:

$$y = y_0 \cos (\omega t + \psi_1). \qquad (4.47)$$

Dividing both numerator and denominator of equation 4.46 by k, and substituting $k/m = \Omega^2$ from equation 2.16 and $k = c_c^2/(4m)$ from equation 4.22:

$$y_0 = \frac{F_0/k}{\sqrt{[1 - (\omega^2/\Omega^2)]^2 + [2(\omega/\Omega)(c/c_c)]^2}}. \tag{4.48}$$

The numerator of equation 4.48 is the static deflection that would

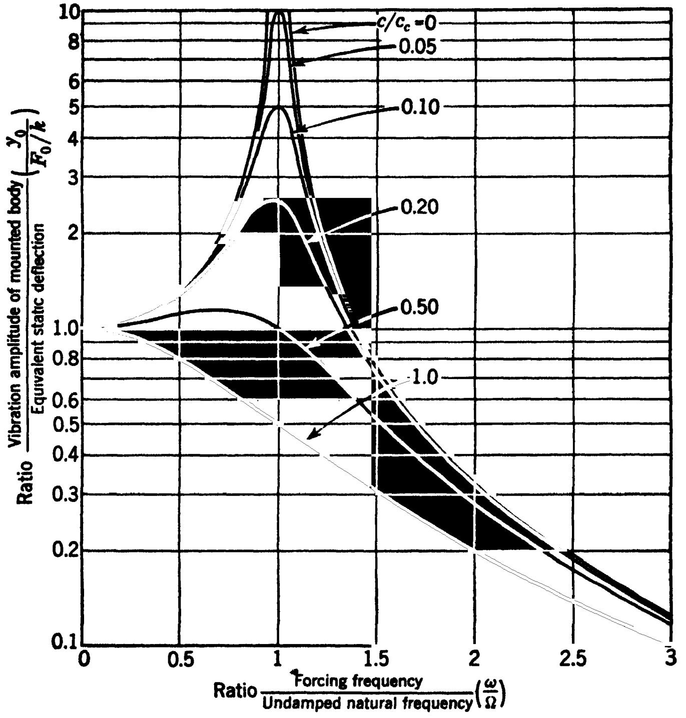

FIGURE. 4.19. Curves showing ratio of vibration amplitude to equivalent static deflection, as a function of the ratio of forcing to undamped natural frequencies. These curves apply to the viscously damped, single-degree-of-freedom system excited by the force $F_0 \cos \omega t$, as shown in Figure 4.18.

be experienced by the mounted body m subjected to a constant force of magnitude F_0. The concept is thus similar to that indicated by equation 2.3 for an undamped system. The amplitude in an undamped system becomes infinite at the resonant frequency, $\omega = \Omega$. When the system embodies viscous damping, energy is absorbed by the damper and an equilibrium amplitude is reached at which the energy absorbed by the damper is equal to that supplied by the force

F. A maximum vibration amplitude of the mounted body is thus reached, depending on the degree of damping, as shown analytically by equation 4.48 and graphically by Figure 4.19. A high degree of damping limits the vibration amplitude of the mounted body m, not only at the resonant frequency but also at all frequencies. *Figure 4.19 does not show transmissibility curves.* The relatively low vibration amplitude for the highly damped system does not indicate low transmissibility, inasmuch as the damper may transmit a large force even at small amplitude. This is emphasized later in deriving an expression for force transmissibility.

The force that is applied to the mounted body m is $F = F_0 \cos \omega t$ (see equation 4.43), and the displacement of the mounted body is $y = y_0 \cos(\omega t + \psi_1)$ (see equation 4.47). The angle ψ_1 is thus the phase angle between the force F_0 and the displacement y_0. It is evaluated by solving equation 4.45 for $y_0 e^{j\psi_1}$, and equating the resultant to the expression given by equation 1.21:

$$y_0 e^{j\psi_1} = \frac{F_0}{(k - m\omega^2) + j\omega c} = y_0(\cos \psi_1 + j \sin \psi_1). \qquad (4.49)$$

Multiplying the numerator and the denominator of equation 4.49 by $(k - m\omega^2) - j\omega c$ to obtain a real denominator:

$$\frac{F_0[(k - m\omega^2) - j\omega c]}{(k - m\omega^2)^2 + \omega^2 c^2} = y_0(\cos \psi_1 + j \sin \psi_1). \qquad (4.50)$$

The angle ψ_1 is defined by

$$\tan \psi_1 = \frac{\sin \psi_1}{\cos \psi_1},$$

where $\sin \psi_1$ and $\cos \psi_1$ are obtained by equating the real and imaginary parts of equation 4.50. Then:

$$\tan \psi_1 = \frac{-\omega c}{k - m\omega^2}. \qquad (4.51)$$

Dividing numerator and denominator of the above equation by k, and noting that $k/m = \Omega^2$ (see equation 2.16) and $k = \Omega c_c/2$ (see equation 4.22):

$$\tan \psi_1 = \frac{-2(\omega/\Omega)(c/c_c)}{1 - (\omega^2/\Omega^2)}. \qquad (4.52)$$

The angle ψ_1 given by the above equation is shown graphically in Figure 4.20. The significance of the negative sign may be interpreted by noting that the tangent of a negative angle less than 90° is negative. For small values of ω/Ω, ψ_1 is a small negative angle; i.e., the displacement y_0 lags the force F_0 by a small angle. For values of ω/Ω greater than unity, ψ_1 approaches a negative value of 180°. The displacement is thus almost fully out of phase with the force.

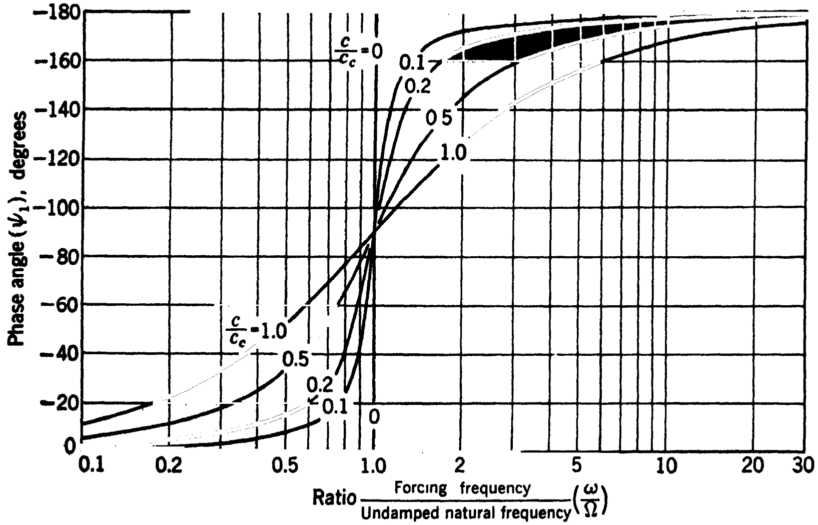

FIGURE 4.20. Phase angle between the displacement y and the force F in the viscously damped, single-degree-of-freedom system excited by applied force $F = F_0 \cos \omega t$, as shown in Figure 4.18. The negative sign indicates that the displacement lags the force.

The force experienced by the support of the system shown in Figure 4.18 is the sum of the forces transmitted by the elastic element k and damper c. These two forces are not generally in phase, i.e., they do not reach their maxima simultaneously, and must therefore be added vectorially as follows:

$$F_t = ky + c\dot{y} = (k + j\omega c)y. \tag{4.53}$$

Substituting $y = y_0 e^{j(\omega t + \psi_1)}$ in equation 4.53, and combining the resultant with equation 4.49:

$$\frac{F_t}{F_0} = \frac{(k + j\omega c)e^{j\omega t}}{(k - m\omega^2) + j\omega c}. \tag{4.54}$$

The force transmissibility $T_F = F_t/F_0$ is determined by noting, from equation 1.21, that the absolute value of $e^{j\omega t}$ is unity. The absolute values of the numerator and the denominator of equation 4.54 are the square roots of the sums of the squares of the real and imaginary parts. Then:

$$T_F = \left|\frac{F_t}{F_0}\right| = \sqrt{\frac{k^2 + \omega^2 c^2}{(k - m\omega^2)^2 + \omega^2 c^2}}. \tag{4.55}$$

Dividing both numerator and denominator under the radical by k^2;

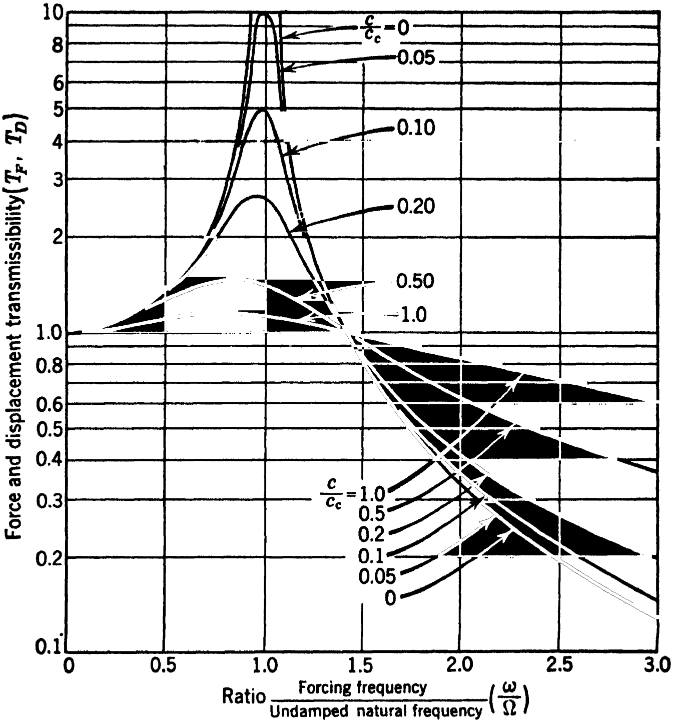

FIGURE 4.21. Force and displacement transmissibility for a viscously damped, single-degree-of-freedom system. Referring to the system shown in Figure 4.18, force transmissibility is the ratio of maximum transmitted force to maximum applied force F_0. Displacement transmissibility is the ratio of maximum displacement y_0 of the mounted body to maximum displacement s_0 of the support.

and noting that $k/m = \Omega^2$ and $k = c_c^2/(4m)$:

$$T_F = \sqrt{\frac{1 + [2(\omega/\Omega)(c/c_c)]^2}{[1 - (\omega^2/\Omega^2)]^2 + [2(\omega/\Omega)(c/c_c)]^2}}. \tag{4.56}$$

The force transmissibility T_F, equation 4.56, is shown graphically in Figure 4.21. It is evident that the presence of damping in the isolator reduces the magnitude of the transmitted force in the region of the resonant frequency, but increases the transmitted force at frequencies greater than $\sqrt{2}$ times the undamped natural frequency. The greater transmissibility at the higher frequencies results from the force transmitted by the viscous damper.

The effectiveness of a damped isolator in reducing the vibration experienced by a body mounted upon a vibrating support will now be investigated by a similar procedure. Referring to Figure 4.18, $F_0 = 0$ and $s = s_0 \cos \omega t$. The differential equation of motion for the mounted body m is

$$m\ddot{y} = k(s - y) + c(\dot{s} - \dot{y}). \tag{4.57}$$

The transient vibration is again assumed to disappear as a result of the damping, and the mounted body m to vibrate with harmonic motion at the forcing frequency ω. A phase angle ψ_2 exists between the displacements of the support and the mounted body. Assuming the displacements to be real components of complex quantities, the following expressions are written, using the relations of equation 1.22:

$$\begin{aligned} s &= s_0 \cos \omega t = s_0 e^{j\omega t}, \\ y &= y_0 \cos (\omega t + \psi_2) = y_0 e^{j(\omega t + \psi_2)}. \end{aligned} \tag{4.58}$$

Equation 4.57 can now be expressed in complex notation. As pointed out above, double differentiation is equivalent to multiplication by $-\omega^2$, and single differentiation is equivalent to multiplication by $j\omega$. Then, substituting from equation 4.58, equation 4.57 becomes:

$$(-m\omega^2 + j\omega c + k)y_0 e^{j(\omega t + \psi_2)} = (k + j\omega c)s_0 e^{j\omega t}.$$

Employing the relation of equation 1.23:

$$[(k - m\omega^2) + j\omega c]y_0 e^{j\psi_2} = (k + j\omega c)s_0, \tag{4.59}$$

and solving for the amplitude ratio:

$$\left(\frac{y_0}{s_0}\right)e^{j\psi_2} = \frac{k + j\omega c}{-m\omega^2 + j\omega c + k}. \tag{4.60}$$

The displacement transmissibility T_D is the absolute value of the amplitude ratio y_0/s_0. Following the procedure used to obtain equation 4.55:

$$T_D = \left|\frac{y_0}{s_0}\right| = \sqrt{\frac{k^2 + \omega^2 c^2}{(k - m\omega^2)^2 + \omega^2 c^2}}. \tag{4.61}$$

Dividing both numerator and denominator under the radical by k^2; and noting that $k/m = \Omega^2$ and $k = c_c^2/(4m)$:

$$T_D = \left|\frac{y_0}{s_0}\right| = \sqrt{\frac{1 + [2(\omega/\Omega)(c/c_c)]^2}{[1 - (\omega^2/\Omega^2)]^2 + [2(\omega/\Omega)(c/c_c)]^2}}. \tag{4.62}$$

This expression for T_D is identical to equation 4.56 for T_F, and it is thus also illustrated by the curves shown in Figure 4.21.

An expression for the displacement of the mounted body m is given by equation 4.58 as follows:

$$y = y_0 \cos(\omega t + \psi_2), \tag{4.63}$$

where ψ_2 indicates the phase angle between the displacements of the support and the mounted body. This phase angle is evaluated by substituting in equation 4.60 the expression for $e^{j\psi_2}$ given by equation 1.21, and multiplying both numerator and denominator of the right side by $(k - m\omega^2) - j\omega c$ to obtain a real denominator:

$$\frac{y_0}{s_0}(\cos\psi_2 + j\sin\psi_2) = \frac{k^2[1 - (m\omega^2/k)] + \omega^2c^2 - jm\omega^3c}{(k - m\omega^2) + \omega^2c^2}. \tag{4.64}$$

The phase angle ψ_2 is indicated by

$$\tan\psi_2 = \frac{\sin\psi_2}{\cos\psi_2},$$

where $\sin\psi_2$ and $\cos\psi_2$ are found by equating the real and the imaginary parts of equation 4.64. Then:

$$\tan\psi_2 = \frac{-m\omega^3c}{k^2[1 - (m\omega^2/k)] + c^2\omega^2}. \tag{4.65}$$

Dividing both numerator and denominator of this expression by k^2, and substituting $k/m = \Omega^2$ and $k = c_c^2/(4m)$:

$$\tan\psi_2 = \frac{-2(c/c_c)(\omega/\Omega)^3}{[1 - (\omega^2/\Omega^2)] + [2(\omega/\Omega)(c/c_c)]^2}. \tag{4.66}$$

The phase angle ψ_2, as indicated by equation 4.66, is shown graphically in Figure 4.22. For small values of the frequency ratio ω/Ω, ψ_2 is a small negative angle. The displacement of the mounted body thus lags the displacement of the support. For very large values of the frequency ratio, ψ_2 approaches −90°; i.e., the displacement of the mounted body lags the displacement of the support by 90°. The value of ψ_2 for intermediate values of the frequency ratio depends to a great extent on the degree of damping, as indicated in Figure 4.22.

The transmissibility, equations 4.56 and 4.62, is a function only of the frequency ratio ω/Ω and the damping ratio c/c_c. The transmissibility reaches a maximum, as shown by Figure 4.21, at a frequency ratio $\omega/\Omega = 1$ when $c/c_c = 0$ and at a frequency ratio always less than unity when the damping ratio c/c_c is greater than zero. The numerical value of the maximum transmissibility, and the frequency ratio at which maximum transmissibility occurs, depend only on the damping ratio c/c_c. The frequency ratio at which maximum transmissibility occurs is determined by differentiating equation 4.62 with respect to ω/Ω, equating the derivative to zero, and solving for ω/Ω. The resultant is

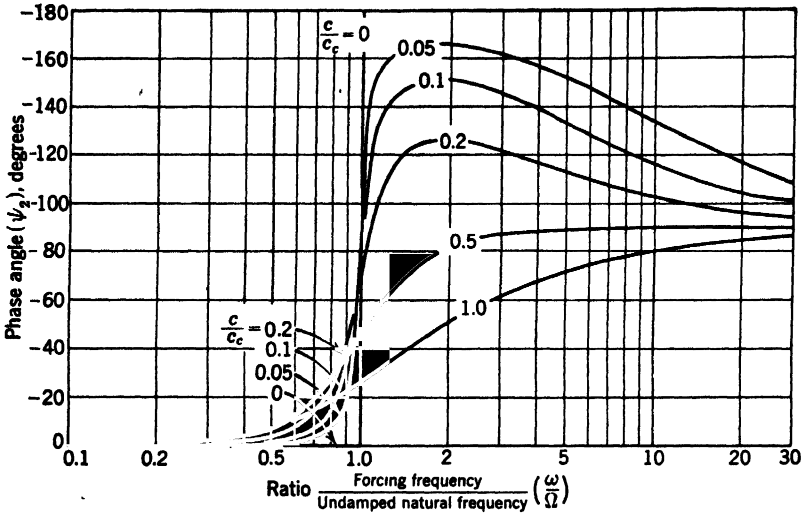

FIGURE 4.22. Phase angle between the displacement y of the mounted body and the displacement s of the support in the viscously damped, single-degree-of-freedom system excited by harmonic motion of the support, as shown in Figure 4.18. The negative sign indicates that the displacement of the mounted body lags that of the support.

$$\frac{\omega}{\Omega} = \sqrt{\frac{-1 + \sqrt{1 + 8(c/c_c)^2}}{4(c/c_c)^2}}. \tag{4.67}$$

The sign preceding the radical within the radical is rigorously an alternate sign, but only the positive sign gives a real value to the frequency ratio ω/Ω.

The maximum value of the transmissibility is found by substituting in equation 4.62 the expression for ω/Ω given by equation 4.67. This gives the following expression for the maximum value of T_D (also T_F):

$$(T_D)_0 = (T_F)_0 = \frac{4(c/c_c)^2}{\sqrt{16(c/c_c)^4 - 8(c/c_c)^2 - 2 + 2\sqrt{1 + 8(c/c_c)^2}}}, \quad (4.68)$$

where the sign preceding the radical within the radical is an alternate sign, but is written positive to obtain a real value for transmissibility.

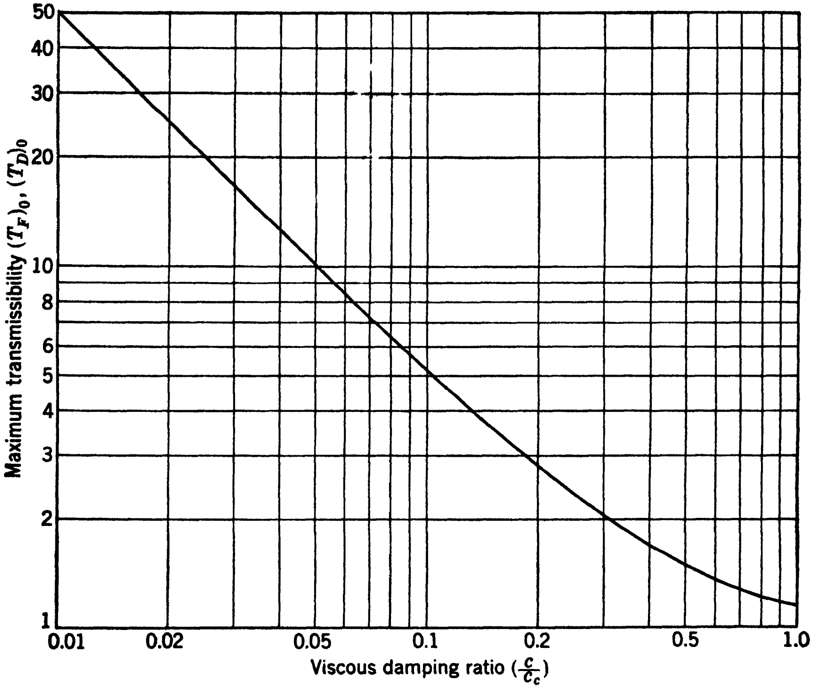

FIGURE 4.23. Maximum transmissibility as a function of viscous damping ratio, for a viscously damped, single-degree-of-freedom system.

The maximum transmissibility is thus a function only of the damping ratio c/c_c and occurs at the frequency ratio indicated by equation 4.67. The relation given by equation 4.68 is shown graphically in Figure 4.23. When the damping ratio c/c_c is equal to 0.1 or less, the maximum transmissibility is defined approximately by

$$(T_D)_0 = (T_F)_0 \approx \frac{1}{2(c/c_c)}. \quad (4.69)$$

The relation given by equation 4.69 is a very useful one in evaluating the performance of isolators that embody damping to only a small degree.

The effect of changes in the mass, stiffness, and damping coefficient of a system may be visualized by writing a relation for the damping ratio, using the expression for critical damping given by equation 4.22:

$$\frac{c}{c_c} = \frac{c}{2\sqrt{km}}. \tag{4.70}$$

The above expression, together with the relation given by equation 4.69, indicates the influence of changes in various parameters of a system with small damping:

(*a*) If the mass of the system is changed while leaving other parameters unchanged, the undamped natural frequency Ω and the damping ratio c/c_c vary inversely as the square root of the change in mass. The maximum transmissibility varies directly as the square root of the change in mass. For example: If the mass of the system is doubled, the natural frequency and the damping ratio are divided by $\sqrt{2}$, and the maximum transmissibility is multiplied by $\sqrt{2}$.

(*b*) If the stiffness of the system is changed while leaving other parameters unchanged, the natural frequency and the maximum transmissibility are increased directly as the square root of the change in stiffness. The damping ratio varies inversely as the square root of the change in stiffness.

(*c*) If the damping coefficient is changed while leaving other parameters of the system unchanged, the undamped natural frequency remains unchanged whereas the damped natural frequency varies somewhat. The change in the latter is negligible, however, for the degree of damping usually encountered in vibration isolators. The damping ratio c/c_c varies directly as the change in the damping coefficient, and the maximum transmissibility varies inversely as the change in the damping coefficient.

4·7 Velocity Shock with Viscous Damping

The response of the system shown in Figure 4.24, when the support s experiences a sudden velocity change V_s, is considered in some detail in Section 3·4 of Chapter 3. It is shown that the maximum acceleration experienced by the element m_zk_z becomes great, for small values of isolator damping coefficient c_y, when the natural frequency of the element m_zk_z is approximately equal to the natural frequency of the isolator system m_yk_y. This is caused by resonance of the element with the continuing transient vibration of the isolator. When the element

$m_z k_z$ is relatively rigid, i.e., when its natural frequency is substantially greater than the isolator natural frequency, the maximum acceleration experienced by the element increases as the isolator damping increases. The reason for this increase of maximum acceleration will become apparent from the following analysis.

The differential equation of motion for the chassis m_y in Figure 4.24, assuming m_z to be small compared with m_y, is

$$m_y \ddot{y} = k_y(s - y) + c_y(\dot{s} - \dot{y}). \quad (4.71)$$

Rearranging terms,

$$m_y \ddot{y} + c_y \dot{y} + k_y y = k_y s + c_y \dot{s}. \quad (4.72)$$

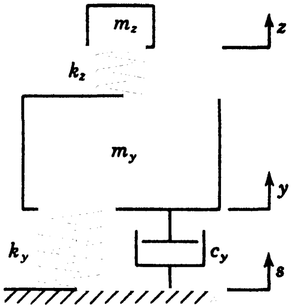

FIGURE 4.24. Schematic diagram of equipment m_y supported by viscously damped isolator and including an element $m_z k_z$ of the equipment.

The complete solution of equation 4.72 is the sum of the general and the particular solutions. The general solution is obtained by setting the right side of the equation equal to zero, and writing the solution of the remainder by analogy with equation 4.28. The particular solution is obtained by substituting $s = V_s t$, $\dot{s} = V_s$ in equation 4.72. The complete solution may then be written:

$$y = e^{\frac{-c_y}{2m_y}t}(B_1 \cos q_y t + B_2 \sin q_y t) + V_s t, \quad (4.73)$$

where q_y is the damped natural frequency of the isolator system. The coefficients B_1, B_2 are evaluated from the initial conditions: $y = \dot{y} = 0$ when $t = 0$. The resulting expression for y is

$$y = V_s\left(t - \frac{1}{q} e^{\frac{-c_y}{2m_y}t} \sin qt\right) \cdot \quad (4.74)$$

The acceleration $\ddot{y}$ of the chassis m_y is found from double differentiation of equation 4.74:

$$\ddot{y} = \frac{V_s}{q_y} e^{\frac{-c_y}{2m_y}t} \left\{\left[q_y^2 - \left(\frac{c_y}{2m_y}\right)^2\right] \sin q_y t + 2q_y \left(\frac{c_y}{2m_y}\right) \cos q_y t\right\} \cdot \quad (4.75)$$

The ratio $c_y/(2m_y)$ in the above equation may be expressed in more useful terms by substituting, from equation 4.24, $2m_y = c_{cy}/\Omega_y$. Then:

$$\frac{c_y}{2m_y} = \left(\frac{c_y}{c_{cy}}\right) \Omega_y. \quad (4.76)$$

Substituting $c_y/(2m_y)$ from equation 4.76 and q_y from equation 4.29, equation 4.75 is written:

$$\ddot{y} = \frac{V_s\Omega_y}{\sqrt{1 - (c_y/c_{cy})^2}} e^{-\Omega_y (c_y/c_{cy})t} \sin\left(\Omega_y \sqrt{1 - (c_y/c_{cy})^2}t + \psi\right), \quad (4.77)$$

where $\Omega_y = \sqrt{k_y/m_y}$ = undamped natural frequency of isolator, and

$$\psi = \tan^{-1} \frac{2(c_y/c_{cy}) \sqrt{1 - (c_y/c_{cy})^2}}{1 - 2(c_y/c_{cy})^2}. \quad (4.78)$$

For purposes of comparison, the maximum acceleration experienced by the chassis m_y when supported by undamped isolators is given by equation 3.26 of Chapter 3 as follows:

$$(\ddot{y}_0)_{\frac{c}{c_c}=0} = V_s\Omega_y. \quad (4.79)$$

The acceleration experienced by the chassis m_y of the system illustrated in Figure 4.24 may now be expressed with reference to the corresponding maximum acceleration with undamped isolators:

$$\frac{\ddot{y}}{(\ddot{y}_0)_{\frac{c}{c_c}=0}} = \frac{1}{\sqrt{1 - (c_y/c_{cy})^2}} e^{-\Omega_y (c_y/c_{cy})t} \sin\left(\Omega_y \sqrt{1 - (c_y/c_{cy})^2}\, t + \psi\right). \quad (4.80)$$

Equation 4.80 is shown graphically in Figure 4.25. The curve for $c_y/c_{cy} = 0$ is sinusoidal at the circular frequency Ω_y; it starts at zero at time $t = 0$ and reaches a maximum when $\Omega_y t = \pi/2$; i.e., after one quarter cycle of the chassis motion. The curves for the damped isolators exhibit a marked difference. Since the support acquires a constant velocity V_s in an instantaneous manner, the absolute displacement of the chassis m_y remains substantially zero for a brief time interval immediately following the inception of the shock motion. The velocity across the damper c_y is then approximately equal to V_s, and a large force is transmitted by the damper. This accounts for the relatively high acceleration experienced by the chassis m_y when $c/c_c \gg 0$ and $\Omega_y t \approx 0$. As time increases, the relative velocity between the chassis m_y and the support decreases; the acceleration of the chassis m_y then results increasingly from the force transmitted by the elastic element k_y rather than by the damper c_y.

It is pointed out in the preceding paragraph that the chassis m_y acquires an acceleration immediately upon inception of the shock motion, when damping in the isolator is great. The response of the

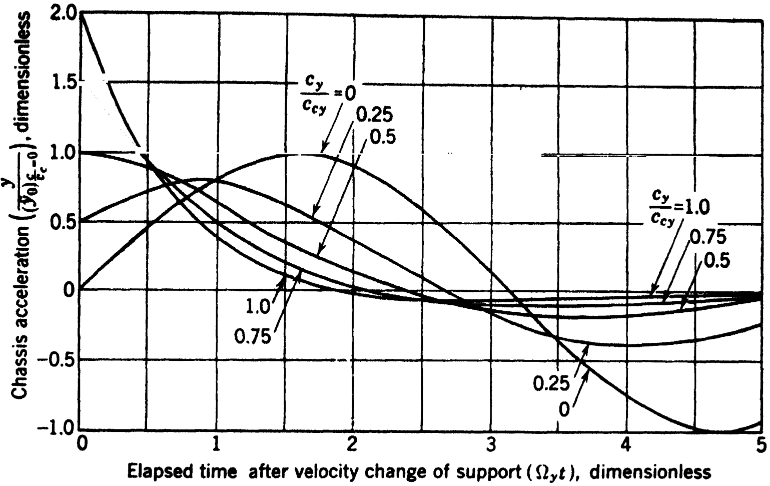

FIGURE 4.25. Time history of the acceleration experienced by chassis m_y of equipment supported by viscously damped isolator, as shown in Figure 4.24. The acceleration is expressed with reference to the maximum acceleration that would be experienced by a chassis supported by an undamped isolator. (*The Bell System Technical Journal.*)

element $m_z k_z$ in Figure 4.24 will be estimated by assuming the chassis to instantaneously acquire a constant acceleration defined by

$$\ddot{y} = \Lambda, \qquad (t > 0). \tag{4.81}$$

The differential equation of motion of the mass m_z is

$$m_z \ddot{z} = k_z(y - z). \tag{4.82}$$

Writing $y - z = \delta_{yz}$ and substituting the relation of equation 4.81, equation 4.82 becomes:

$$\ddot{\delta}_{yz} + \Omega_z^2 \delta_{yz} = \Lambda, \tag{4.83}$$

where $\Omega_z = \sqrt{k_z/m_z}$. In obtaining the solution of equation 4.83, the undetermined coefficients are evaluated from the initial conditions: $\delta_{yz} = \dot{\delta}_{yz} = 0$ when $t = 0$. Then:

$$\delta_{yz} = \frac{\Lambda}{\Omega_z^2}(1 - \cos \Omega_z t). \tag{4.84}$$

The acceleration $\ddot{z}$ of the mass m_z is calculated from the relation given by equation 3.43:

$$\ddot{z} = \Lambda(1 - \cos \Omega_z t). \tag{4.85}$$

When $\Omega_z \to \infty$ and $t \to 0$, $\ddot{z} = \ddot{z}_0 = 2\Lambda$. The maximum acceleration of a very rigid element is thus twice as great as the maximum chassis acceleration when the latter arises instantaneously. Taking the maximum acceleration $\ddot{z}_0$ of the element when $c_y/c_{cy} = 0$ as a reference, $\ddot{z}_0$ becomes twice as great as the reference when $c_y/c_{cy} = 0.5$ because the chassis acceleration arises instantaneously. When $c_y/c_{cy} = 1.0$, $\ddot{z}_0$ becomes four times as great as the reference because $\ddot{y}_0$ is twice as great and arises instantaneously. This tendency is indicated in Figure 3.10, wherein the maximum acceleration experienced by rigid elements on damped isolators becomes several times as great as on undamped isolators.

4·8 Damper Design

A damped isolator is represented schematically in the preceding analyses by the combination of an elastic element and a damper. For certain applications, the internal hysteresis of the elastic element dissipates sufficient energy to function as the damper. Internal hysteresis is discussed in Section 4·9. The present section discusses the design of separate dampers adapted for use with relatively undamped elastic elements in applications requiring damped isolators.

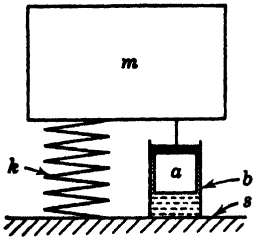

FIGURE 4.26.

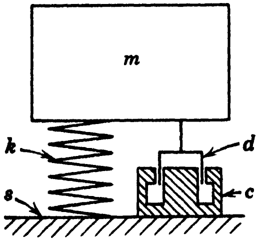

FIGURE 4.27.

FIGURE 4.26. Schematic illustration of dashpot used as viscous damping means.
FIGURE 4.27. Schematic illustration of magnetic damping means.

One of the most commonly used damping devices is a dashpot, as shown schematically in Figure 4.26. A piston *a* is attached to the mounted body *m* and is arranged to move vertically through the liquid in a cylinder *b* secured to the support *s*. If the piston is relatively long, the force required to cause the liquid to flow through the annular space between the piston and the cylinder is approximately proportional to the velocity of the piston in the cylinder. This is viscous or velocity damping. The magnitude of the damping force is controlled by the viscosity of the liquid and by the radial clearance between the piston and cylinder walls.

Damping is also attainable as a result of a current induced in a conductor moving through a magnetic field. Such a damper may have any of several different physical embodiments, of which one is shown schematically in Figure 4.27. A magnet *c* similar to that used in a dynamic loud speaker is secured to the support *s*, and a conductor *d* attached to the mounted body *m* moves vertically through the field of the annular air gap. A flow of current is induced in the conductor, and the energy absorbed thereby is withdrawn from the vibrating system. The resultant damping force can be made proportional to the velocity of the conductor moving through the field, although some difficulty may be experienced in maintaining a constant damping coefficient throughout a substantial displacement.

Although dashpots and magnetic dampers are very effective in certain special applications, their usefulness in vibration and shock isolators is limited by several undesirable features. Both types, as commonly constructed, are operative only for motion along a single straight line. Furthermore, their construction is such as to restrict motion in other directions, unless a mechanically complex mechanism is added. The dashpot commonly operates only in the vertical position shown in Figure 4.26, but it can be made to operate horizontally by adding a packing gland to retain the liquid. The magnetic damper requires either a power source to energize an electromagnet or an excessively large permanent magnet, except for applications wherein the mounted body is light in weight. Both types of damper are subject to variations in properties as a result of temperature fluctuations. The properties of the dashpot vary because of changes in viscosity of the liquid, and those of the magnetic damper because of changes in the resistance of the conductor. Finally, the cost of constructing such dampers may be excessive except for special applications. These many limitations greatly restrict the usefulness of dashpots and magnetic dampers for isolation applications in general.

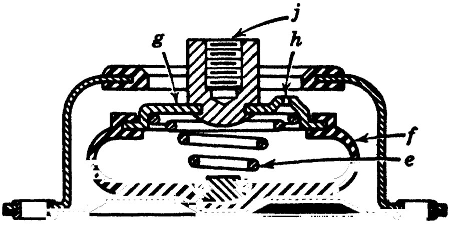

Figure 4.28. Damped isolator with flexible bellows. Flow of air through orifice to and from bellows provides damping. (*Courtesy The Barry Corporation.*)

The need for an inexpensive damper which is operative for motion in all directions has led to the development of the air-damped isolator illustrated in Figure 4.28. It embodies a load-supporting metal spring *e* located within a rubber bellows *f*. The rubber bellows and metal cap *g* combine to form an enclosure which is substantially air tight, except for a small orifice *h* through the cap. The mounted equipment is attached to the central member *j*, and its motion in the vertical direction causes the volume within the bellows to change. Air thus flows through the orifice either into or out of the bellows. The volume within the bellows also changes somewhat as a result of horizontal motion of the mounted body. The work expended in forcing air through the orifice withdraws energy from the vibrating system, thereby providing the desired damping. The viscosity of air varies but little with temperature, and the characteristics of the damper are thus relatively independent of temperature changes. The ability of the rubber bellows to change volume slightly without expelling air through the orifice provides a relatively undamped isolator for vibration of small amplitude. The orifice establishes a restriction on the rate at which air may escape and thereby provides an air cushion against severe shock. Because of its simplicity and low cost, this damper is adapted to isolators manufactured in mass production.

Damping may be obtained by causing one substantially dry member to slide upon another. A typical damper of this type is illustrated schematically in Figure 4.29. A tongue *n* is attached to the mounted body *m* and is arranged to slide between two blocks *o* which are forced against the tongue by the tension spring *p*. The force exerted by the damper in opposition to the vertical motion of the mounted body is the product of the normal force and the coefficient of friction between the tongue and blocks. The damping force is nominally a constant, which is independent of the position or velocity of the mounted body. This type of damping is termed dry friction or Coulomb damping. Actually, the coefficient of friction varies somewhat with changes in velocity and is generally considered to be relatively high at the inception of motion at the damper.

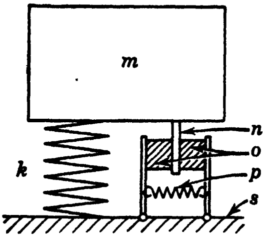

FIGURE 4.29. Schematic illustration of friction damper.

The characteristics of Coulomb damping are not well adapted to mathematical analysis. Some analyses have been carried out* and indicate certain basic differences between viscous and Coulomb damping. In viscous damping, the energy dissipated is proportional to the square of the vibration amplitude, and the energy added to the system is proportional to the first power of the amplitude. These two energies come into balance at some finite amplitude, and a limit is thus imposed upon the maximum amplitude at resonance. In Coulomb damping, both dissipated and added energy are proportional to the first power of the vibration amplitude, and an infinite amplitude becomes theoretically possible. Experience with actual systems having dampers of the type illustrated in Figure 4.29 indicates that the amplitude at resonance remains finite and can be made to have a relatively small value.

---

* See L. S. Jacobsen, "Steady Forced Vibration as Influenced by Damping," *Trans. A.S.M.E.*, Vol. 52 (APM-52-15), 1930; and J. P. Den Hartog, "Forced Vibrations with Combined Coulomb and Viscous Friction," *Trans. A.S.M.E.*, Vol. 53 (APM-53-9), 1931.

The nominally constant force transmitted by the Coulomb damper may introduce characteristic advantages or disadvantages. When the amplitude and the frequency of the vibration are low, the acceleration of the mounted body is low and the resultant inertia force may be less than the friction force of the damper. The damper then functions as a rigid connection, and the isolator has no resilience. At higher frequencies, greater than the natural frequency, the relative motion between the support and the mounted body tends to become small. The force transmitted by the elastic element thus becomes correspondingly small. The damper, however, transmits a force whose magnitude is independent of the vibration amplitude. This may be relatively great when the vibration amplitude is small and may thus increase the transmissibility at higher frequencies.

The friction damper, like many other damping devices, adds mechanical complexity to the isolator. In order to be operative for motion in all directions, the damper must embody at least two sets of friction surfaces that respond to motion in different directions. It must generally embody means to permit adequate freedom of motion in all directions. The characteristics of the isolator may change after operation over a period of time, owing to changes in the properties of the materials as a result of wear and exposure to water or oil.

4·9 Damping from Internal Hysteresis

In many applications, economic considerations preclude the use of discrete dampers. It becomes necessary then to rely upon the internal hysteresis of the elastic elements. This often leaves much to be desired, because the damping available from hysteresis falls far short of the requirements for many applications. Materials with high hysteresis frequently embody other undesirable characteristics, among which one of the most prominent is a tendency to creep or drift excessively under a constant application of load. Engineering data on internal hysteresis are neither sufficiently plentiful nor sufficiently orderly to permit a completely rational evaluation of this type of damping.

In the field of vibration and shock isolation, the principal interest in damping concerns its effect upon transmissibility in forced vibration and shock, and upon the decrement of free vibration. An artifice is sometimes employed to evaluate various kinds of damping in a practical sense. The maximum transmissibility of a viscously damped system, as a function of the damping ratio, is given exactly by equation 4.68 and approximately by equation 4.69 for small values of the damping ratio. If a system with any arbitrary type of damping is caused to vibrate throughout a frequency range and the maximum amplitude of vibration is noted, the numerical value of maximum transmissibility $(T_D)_0$ becomes established. A value for the viscous damping ratio c/c_c can then be found from equation 4.68, or Figure 4.23. The value of c/c_c found in this manner is known as the equivalent viscous damping ratio. This equivalent damping ratio may then be used in all the foregoing equations where the ratio c/c_c appears. Where the damping is small, as in the case of internal hysteresis, results calculated with the equivalent viscous damping ratio are sufficiently accurate for most practical applications. The accuracy decreases, however, as the degree of damping increases.

A few representative values of equivalent viscous damping ratio for typical materials are given in Table 4.3, so that the designer may be aware of the order of magnitude of this property. It is important to recognize that the values given in Table 4.3 are only approximate. They represent the averages of several somewhat diverse values obtained under various conditions of forced and free vibration. It is probable that the equivalent damping ratio depends on the magnitude of the strain, and possibly on other parameters. The values indicated tend to be low rather than high, particularly for structures that include unbonded rubber members and bolted steel members. The increase in damping in these instances is ascribed to additional energy loss as a result of friction between sliding surfaces.

TABLE 4.3

EQUIVALENT VISCOUS DAMPING RATIO FOR TYPICAL MATERIALS

Material	$\frac{c}{c_c}$
Rubber, 30-durometer	0.02
Rubber, 60-durometer	0.08
Steel	0.005

Damping is of tremendous importance in a system required to operate even momentarily at resonance. It is common for the frequency of operation of a machine to coincide for an instant with a natural frequency of the isolator, as the machine is being started or stopped. If the isolator consists of a metal spring, whose equivalent damping ratio is relatively low, vibration of considerable amplitude may develop unless acceleration and deceleration of the machine occur rapidly. A rubber isolator is considerably more suitable than a steel spring on machines that must operate momentarily at resonance, because a higher equivalent damping ratio results from the internal hysteresis.

4·10 Applications Involving Superimposed Loads and Non-Uniform Weight Distribution

There is occasional need to support an equipment on an isolator of low natural frequency, wherein the equipment is subjected to a substantially constant force of relatively large magnitude. This force may result from a belt or chain drive, or it may be the gravitational force. In order to prevent excessive deformation of the isolators, this constant force may be compensated by an oppositely directed spring force. Certain precautions should be observed in providing a compensating spring, in order not to cause deterioration of the isolation. The necessary precautions are indicated by the following analysis.

The system that forms the basis for the analysis is illustrated schematically in Figure 4.30. It is functionally equivalent to that shown in Figure 2.1, except for the addition of the downward-directed constant force F'. A spring k' is added to neutralize the force F' and maintain the mounted body m in its initial position. The equation of static equilibrium for the system, neglecting the harmonic force $F_0 \cos \omega t$, is

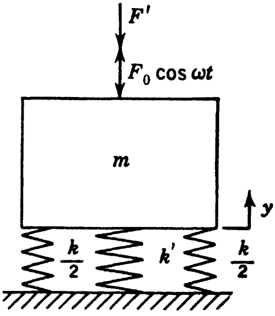

FIGURE 4.30. Schematic diagram of mounted equipment subjected to oscillating force F_0 cos ωt and superimposed steady force F'. The compensating spring k' opposes the force F'.

$$-mg + ky_{st} - F' + k'\delta' = 0, \tag{4.86}$$

where y_{st} = static displacement of mounted body m, taken negatively downward.

δ' = deflection of added spring k'.

From the requirement that the static displacement y_{st} not be influenced by the action of the force F' and spring k', the following relation may be written:

$$F' = k'\delta' \tag{4.87}$$

The stiffness that has been added to the system by the compensating spring k' is evaluated by applying a downward-directed increment of force F, and noting the additional displacement y resulting therefrom. A new equation of equilibrium similar to equation 4.86 is now written:

$$-mg - F + k(y_{st} + y) + k'(\delta' + y) - F' = 0 \tag{4.88}$$

Subtracting equation 4.86 from equation 4.88, and solving the remainder for F/y:

$$\frac{F}{y} = k + k', \tag{4.89}$$

where F/y is the stiffness of the composite system. An expression for the natural frequency of the system shown in Figure 4.30 is now obtained by substituting F/y from equation 4.89 for k_y in equation 2.16 of Chapter 2:

$$\Omega = \sqrt{\frac{k + k'}{m}}. \tag{4.90}$$

It is evident from equation 2.15 and Figure 2.2 that the transmissibility increases as the natural frequency Ω increases. It is thus desirable to maintain Ω low, which requires that k' be maintained as small as possible. This can be achieved, at the same time satisfying the requirements of equation 4.87, by maintaining δ' numerically large and k' numerically small. One means of accomplishing this is by the use of a long tension spring with a large extension. The total force acting on the mounted equipment then is not materially altered by small displacements of the equipment, and the vibration characteristics of the system are not affected. A method of applying this principle to an electric motor with belt drive is shown schematically in Figure 4.31. It is necessary to maintain the spring in the same plane as the belt, by a bracket or other suitable means attached to the motor, to avoid introducing a couple about an axis normal to the base of the motor.

The following analyses are directed to determining the static deflection experienced by each of several isolators supporting a rigid equipment, and to proportioning the stiffnesses in such a manner that the isolators experience equal static deflections. A system in which the isolators experience equal static deflections meets the requirements for decoupling vibration in the vertical translatory mode from vibration in other modes, as set forth in Section 2·10 of Chapter 2.

An equipment supported by three isolators, as discussed on page 17 of Chapter 1, may be readily analyzed to determine the load supported by each isolator. This analysis cannot be extended to a system with more than three supports without making certain assumptions. Such a system is statically indeterminant if the mounted body is flexible. If the body is assumed to be infinitely rigid, a solution can be obtained statically. A common problem is presented by an equipment with the isolators arranged at the four corners of a rectangle, as illustrated by the schematic plan view of Figure 4.32. The center of gravity is in a non-symmetrical location. The following analysis develops equations for the static position of the mounted body, and for the isolator stiffness required to maintain uniform static deflection at all isolators.

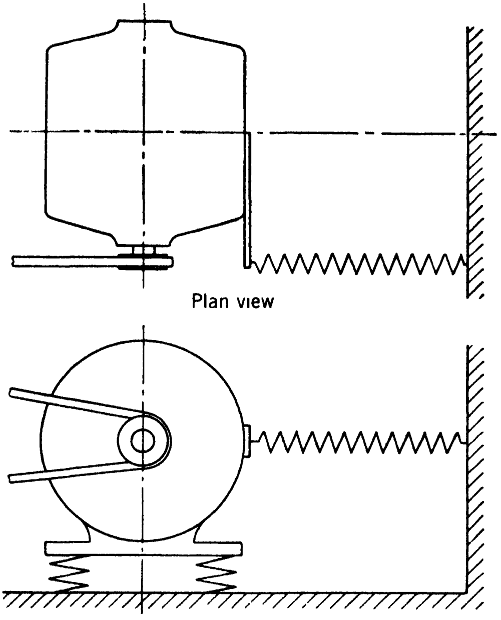

FIGURE 4.31. Electric motor supported by isolators and provided with compensating spring to oppose belt tension.

Equations of static equilibrium for the body shown in Figure 4.32 are obtained by taking moments with respect to horizontal axes X and Z through the center of gravity of the body. With respect to the Z axis:

$$k_A\delta_A d - k_B\delta_B c - k_C\delta_C c + k_D\delta_D d = 0, \tag{4.91}$$

where the isolator stiffness is indicated by k and the isolator deflection δ. The subscript indicates the location of the isolator, as shown in Figure 4.32. This analysis assumes that all the isolators are of the same free height; that they rest upon a rigid, plane support; and that the supported body has a rigid, plane bottom face for engagement with the isolators. A similar equation is written with respect to the X axis:

$$k_A\delta_A a + k_B\delta_B a - k_D\delta_D b - k_C\delta_C b = 0. \tag{4.92}$$

It is a condition of the problem that the mounted body be rigid. This is expressed mathematically by stating that the deflection of point E, the intersection of the diagonals between isolators, must equal the average deflection of diagonal pairs of isolators A, C and B, D:

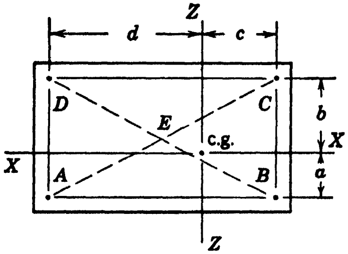

FIGURE 4.32.

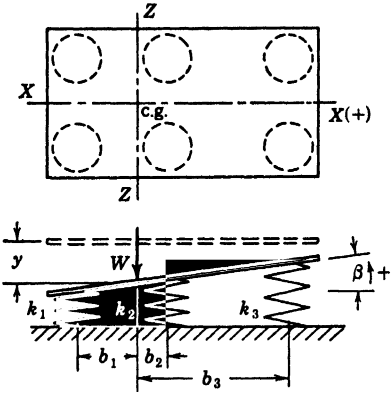

FIGURE 4.33.

FIGURE 4.32. Plan view of rigid body supported at the corners of a rectangle.

FIGURE 4.33. Plan and elevation views of a rigid body supported by several isolators arranged in two parallel lines.

$$\frac{\delta_A + \delta_C}{2} = \frac{\delta_B + \delta_D}{2},$$

which is written in the following form:

$$\delta_A - \delta_B + \delta_C - \delta_D = 0. \tag{4.93}$$

The expressions given by the above equations may be reduced to a group of three simultaneous equations by assigning an arbitrary value to the deflection δ_A. The other three deflections are now determined from the simultaneous solution of equations 4.91, 4.92, and 4.93:

$$\delta_B = \delta_A\,(B/A)(k_A/k_B); \quad \delta_C = \delta_A(C/A)(k_A/k_C); \quad \delta_D = \delta_A(D/A)(k_A/k_D), \tag{4.94}$$

where

$$\begin{aligned} A &= ac + 3bc + bd - ad. \\ B &= ad + 3bd + bc - ac. \\ C &= ac + 3ad + bd - bc. \\ D &= ad + 3ac + bc - bd. \end{aligned} \tag{4.95}$$

A summation of vertical forces acting on the mounted body gives the following expression:

$$k_A\delta_A + k_B\delta_B + k_C\delta_C + k_D\delta_D = W. \tag{4.96}$$

If the stiffnesses of all isolators are equal, $k_A = k_B = k_C = k_D = k$. Substituting this relation, and combining equations 4.94 and 4.96:

$$\delta_A = \frac{W}{k[1 + (B/A) + (C/A) + (D/A)]}, \quad \delta_B = \delta_A(B/A); \quad \delta_C = \delta_A(C/A); \quad \delta_D = \delta_A(D/A). \tag{4.97}$$

The stiffnesses necessary to attain uniform static deflection of all isolators is determined from the relation: $\delta_A = \delta_B = \delta_C = \delta_D = \delta$. Substituting this relation, and combining equations 4.94 and 4.96:

$$k_A = \frac{W}{\delta[1 + (B/A) + (C/A) + (D/A)]}; \quad k_B = k_A(B/A); \quad k_C = k_A(C/A); \quad k_D = k_A(D/A). \tag{4.98}$$

It is thus evident that the static deflection at each isolator may be determined from equation 4.97 when the isolator stiffnesses are equal; and that the isolator stiffnesses required to maintain uniform static deflections at all isolators is given by equation 4.98. Where neither the stiffness nor deflection of the isolators is uniform, the unknown quantities may be calculated by combining equations 4.94 and 4.96.

A body supported by more than four isolators may be analyzed in a somewhat similar manner. Figure 4.33 shows a body, symmetrical with respect to a plane perpendicular to the Z axis, supported by six isolators. The isolators are of equal free height; the position that the mounted body would assume if it were made massless is thus illustrated by the dotted lines. If the body is rigid, the deflection of any isolator is given by

$$\delta_n = y - b_n\beta, \tag{4.99}$$

where b and β are positive in the directions indicated in Figure 4.33.

The equations of static equilibrium for the body are obtained from a summation of vertical forces and a summation of moments with respect to the Z axis:

$$\Sigma k_n \delta_n = W; \quad \Sigma b_n k_n \delta_n = 0 \tag{4.100}$$

Substituting for δ_n from equation 4.99, equations 4.100 become:

$$y \Sigma k_n - \beta \Sigma b_n k_n = W, \tag{4.101}$$

$$y \Sigma b_n k_n - \beta \Sigma b_n^2 k_n = 0. \tag{4.102}$$

Solving equations 4.101 and 4.102 simultaneously for y and β:

$$y = \frac{W \Sigma b_n^2 k_n}{\Sigma k_n \Sigma b_n^2 k_n - (\Sigma b_n k_n)^2}, \tag{4.103}$$

$$\beta = \frac{W \Sigma b_n k_n}{\Sigma k_n \Sigma b_n^2 k_n - (\Sigma b_n k_n)^2}. \tag{4.104}$$

The necessary condition for equal deflection of all isolators, $\beta = 0$, is that $\Sigma b_n k_n = 0$ in equation 4.104. Making this substitution in equation 4.103, $y = W/\Sigma k_n$. It is evident from reference to Figure 4.33 that the isolators k_2, for example, may be deleted and the position of the mounted body maintained unchanged by proper modification of the stiffnesses of the other isolators. For a body supported by several isolators, then, certain of the stiffnesses are first selected arbitrarily; and the remainder are calculated to meet the prescribed conditions. This is illustrated by the following example.

Example 4.2. An equipment arranged as illustrated in Figure 4.33 weighs 1,000 lb and is to be supported so that the static deflection at each isolator is 0.10 in. The coordinate distances in inches of the isolators, measured from the center of gravity, are $b_1 = -7$, $b_2 = 3$ and $b_3 = 13$. Each coordinate distance refers to two isolators. The stiffnesses of the isolators are to be determined.

The requirement that the static deflection of each isolator be 0.1 in. is expressed mathematically: $y = 0.1$, $\beta = 0$. From equation 4.104, $\Sigma b_n k_n = 0$; and from equation 4.103, $W/\Sigma k_n = 0.1$. Therefore:

$$2(-7)k_1 + 2(3)k_2 + 2(13)k_3 = 0,$$

and

$$\frac{1{,}000}{2k_1 + 2k_2 + 2k_3} = 0.1.$$

Since there are three unknown stiffnesses to determine and only two conditions to be fulfilled simultaneously, one stiffness may be selected arbitrarily. Letting $k_2 = k_1$, the following stiffnesses are found from the simultaneous solution of the above equations:

$$k_1 = k_2 = 2{,}167 \text{ lb/in.}$$

$$k_3 = 667 \text{ lb/in.}$$

4·11 Lack of Stiffness in Equipment

In the design and application of isolators, care should be taken to consider the isolators in conjunction with the equipment to be supported. The structural members of equipment are not infinitely rigid and, therefore, are not entirely analogous to the idealized systems employed in foregoing chapters to illustrate the principles of vibration and shock isolation. In general, the structural members are appreciably more rigid than the isolators. If the rigidities are of the same order of magnitude, however, it is important to recognize the influence of this condition in regard to vibration and shock.

The effects of lack of stiffness in the equipment may be appraised by reference to Figure 4.34 which shows, schematically, an equipment comprised of two rigid masses $m/2$ with a flexible chassis interposed between the rigid masses and the isolator. The stiffnesses of the chassis and isolator are indicated by k_c and k_i, respectively. The dynamic properties of this system are determined by the mass and the resultant stiffness of the structure that supports the mass. The resultant stiffness is evaluated by simultaneously applying vertical forces $F/2$ to each of the masses. The displacement of each mass is then the sum of the deflections of the two elastic members k_i, k_c:

$$\delta = \frac{(F/2) + (F/2)}{k_c} + \frac{(F/2) + (F/2)}{k_i} = F\left(\frac{1 + (k_i/k_c)}{k_i}\right). \tag{4.105}$$

The resultant stiffness k_r is

$$k_r = \frac{F}{\delta} = \frac{k_i}{1 + (k_i/k_c)}. \tag{4.106}$$

The results that are obtained when the system shown in Figure 4.34 is subjected to shock may be perceived from a graphical interpretation of equation 4.105. This is shown in Figure 4.35. The stiffness k_i of the isolator is assumed to increase as the deflection increases; the stiffness k_c of the chassis is shown as a constant which is independent of deflection. The force-deflection curves for the isolator and chassis are shown as dotted lines, and the corresponding curve for the combination as a solid line. The latter is obtained by adding the deflections of isolator and chassis at corresponding forces.

The analysis set forth in the discussion that begins on page 105 shows that the maximum deflection of a non-linear isolator and the maximum acceleration experienced by the mounted body may be determined by equating the change in kinetic energy of the mounted body to the potential energy stored in the isolator. Considering the chassis in Figure 4.34 to be infinitely rigid, assume that the change in kinetic energy is such that the isolator is deflected to point A in Figure 4.35 when storing equivalent potential energy. If the chassis is now considered to exhibit some flexibility, maximum deflection is at B in accordance with the requirement that the area OBB' must be equal to area OAA'. The resultant influence upon maximum deflection and acceleration is as follows:

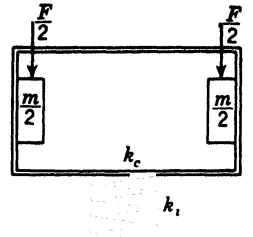

Figure 4.34.

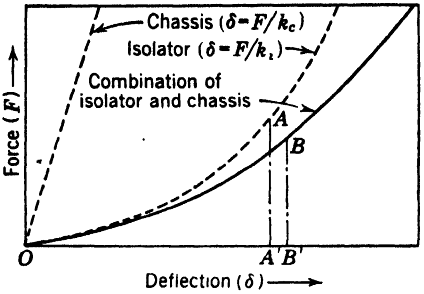

Figure 4.35.

Figure 4.34. Schematic diagram of equipment supported by isolator, wherein flexible chassis is interposed between the isolator and the principal masses of the equipment.

Figure 4.35. Force-deflection curves for isolator, and for isolator in series with flexible chassis.

(*a*) The maximum force transmitted by the isolator, and therefore the maximum acceleration experienced by the mounted body, are lower when the chassis embodies flexibility.

(*b*) The maximum total deflection of the system is greater when the chassis is flexible, the deflection being the sum of isolator and chassis deflections. The isolator deflection is thus reduced by adding flexibility to the chassis.

The expression for the natural frequency of a single-degree-of-freedom system, equation 2.16, includes a stiffness term k_y which is considered to be the resultant stiffness of the system. Substituting the resultant stiffness k_r from equation 4.106, the resultant natural frequency becomes:

$$\Omega_r = \Omega \sqrt{\frac{1}{1 + (k_i/k_c)}}, \qquad (4.107)$$

where Ω_r natural frequency of system shown in Figure 4.34.
Ω natural frequency of same system with k_c infinitely great.

The relation given by equation 4.107 is shown graphically in Figure 4.36. The magnitude of the discrepancy in calculated natural frequency which may be introduced by lack of stiffness in the equipment thus becomes evident. This effect is not great in many applications where the stiffness of the isolators is low. Where relatively stiff isolators are used, however, the degree of rigidity of the equipment should receive careful attention. This is particularly true for equipment to be used on Naval vessels where the isolators are relatively stiff, the equipment is necessarily light in weight, and the natural frequencies are of critical importance. Naval applications are considered in detail in Section 6·12 of Chapter 6.

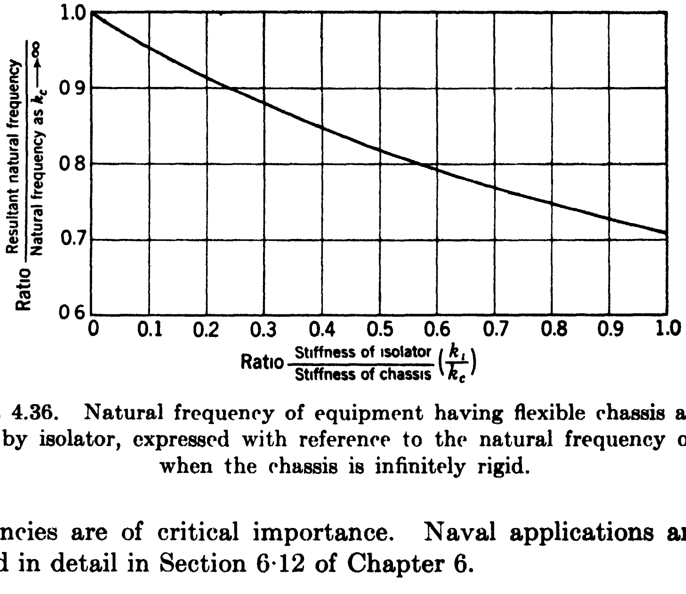

FIGURE 4.36. Natural frequency of equipment having flexible chassis and supported by isolator, expressed with reference to the natural frequency obtained when the chassis is infinitely rigid.

4·12 Sound Isolation

This section is comprised of a brief discussion of certain principles involved in the isolation of sound or noise. Sound, for purposes of the present discussion, may be considered as vibration of audible frequency. The frequency limits of the audible range vary from one person to another, but representative values for general purposes are 20 and 20,000 cps. Frequencies in the lower part of this range, though audible, generally are treated as vibration in the manner heretofore explained. When higher frequencies are present, additional factors must be considered to assure effective sound isolation. These factors are discussed in the following paragraphs.

Sound becomes evident to the senses when a vibrating structure causes waves of compression and rarefaction to propagate through the air. Such a structure generally is driven by an oscillating force. Methods of lowering the sound level include modification and refinement of the offending machine to reduce the magnitude of the driving force. Vibration of the structure frequently is great because of a condition of resonance; this condition can be alleviated by stiffening the structure to change its natural frequency, or by adding damping to reduce the amplitude of the resonant vibration. If the machine is not adapted to these modifications, the sound level in the room housing the machine may be decreased by constructing an enclosure around the machine, and lining the enclosure with sound-absorbing material.

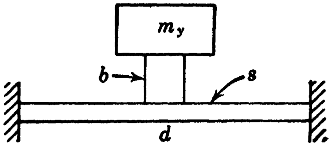

FIGURE 4.37.

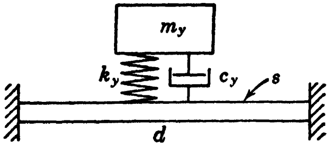

FIGURE 4.38.

FIGURE 4.37. Schematic diagram of machine m_y mounted upon rigid support *b*. High sound intensity in space *d* may result from transmission of force by support *b* to panel *s*.

FIGURE 4.38. Schematic diagram of machine m_y mounted upon isolator $k_y c_y$. Sound intensity in space *d* may be reduced by employing isolator to reduce magnitude of force transmitted to panel *s*.

Sound originating from operation of a machine often becomes evident in adjacent regions of a building, because the forces generated by the machine are transmitted by the building structure and cause vibration of wall and ceiling panels. The nature of this condition is illustrated schematically by Figure 4.37. The noisy machine is indicated at m_y, mounted upon a rigid support *b* which rests directly upon a floor panel *s*. The vibratory force generated within the machine is transmitted through the support to the panel, whose vibration transmits sound energy to the air in the space *d*. This is a common occurrence, in which the panel *s* functions as the ceiling of room *d*. The sound intensity in room *d* increases with the vibration velocity of the panel *s*. For any given sound source, the frequency spectrum remains constant, and the sound intensity is reduced by decreasing the vibration amplitude of the panel.

The method of isolating sound calls for the replacement of the rigid support *b* in Figure 4.37 with the isolator shown schematically by k_y, c_y in Figure 4.38. The effectiveness of the isolator depends on the relation existing among several variables, including the nature of the vibratory force, the dimensions and properties of the isolator, and the characteristics of the panel. Certain important relations in this respect are as follows:

(*a*) When the half wavelength of the forcing vibration is great relative to the thickness of the resilient material in the isolator, the results appear to be in accordance with the theory for a single-degree-of-freedom system subjected to a force that varies in a harmonic manner. The application of this theory to problems in sound isolation is considered in detail below.

(*b*) When the half wavelength of the forcing vibration is small relative to the thickness of the resilient material in the isolator, the theory of the single-degree-of-freedom system becomes generally inapplicable. Each element along the path of sound flow becomes alternately elongated and compressed as the sound energy passes through the isolator. The effectiveness of an isolator then depends on its ability to reduce the transmission of sound energy.

It becomes convenient now to establish the wavelength of the sound, with reference to the dimensions of the isolator and the velocity of sound in the resilient material. The wavelength is given by the following relation:

$$\lambda = \frac{v}{f}, \tag{4.108}$$

where λ = wavelength of sound in isolator, cm.
v = velocity of sound in isolator, cm/sec.
f = sound frequency, cps.

Equation 4.108 is shown graphically in Figure 4.39, using the data given in Table 4.4 for velocity of sound in rubber of different durometers. In 30-durometer rubber, for example, the wavelength of vibration having the typical medium frequency of 1,000 cps is approximately 3.5 cm. The half wavelength is 1.75 cm, a common dimension for the thickness of resilient material in isolators. Inasmuch as the audible frequency range extends both above and below 1,000 cps, an investigation of sound isolation should explore both the single-degree-of-freedom concept and the wave-transmission concept.

The single-degree-of-freedom concept will be considered first, employing the analysis of a damped, single-degree-of-freedom system set forth in Section 4·6 of this chapter. Assuming the mass of the panel s in Figure 4.38 to be large compared with the mass of the machine m_y, an expression for the force transmitted through the isola-

TABLE 4.4

ACOUSTICAL PROPERTIES OF VARIOUS MATERIALS*

Material	Density μ, gm/cm^3	Velocity of sound v, cm/sec	Specific Acoustical Impedance R, gm/cm^2 sec
Steel	7.8	501×10^3	391×10^4
Brass	8.4	275×10^3	232×10^4
Lead	11.4	71.8×10^3	82×10^4
Wood (Fir)	0.45	443×10^3	20×10^4
Water	1.0	140×10^3	14×10^4
Rubber, 30-durometer	1.01	3.5×10^3	0.35×10^4
40-durometer	1.06	5.0×10^3	0.53×10^4
50-durometer	1.11	6.4×10^3	0.71×10^4
60-durometer	1.18	10.0×10^3	1.18×10^4
70-durometer	1.25	23.0×10^3	2.87×10^4
Air (0° C)	0.00129	33×10^3	0.0042×10^4
Cork	0.25	50×10^3	1.2×10^4
Concrete	2.6	310×10^3	81×10^4

* The properties included in Table 4.4 are selected from among those published in P. E. Sabine, *Acoustics and Architecture*, McGraw-Hill Book Co., New York, 1932, and in *Some Physical Properties of Rubber*, United States Rubber Co., New York, 1941.

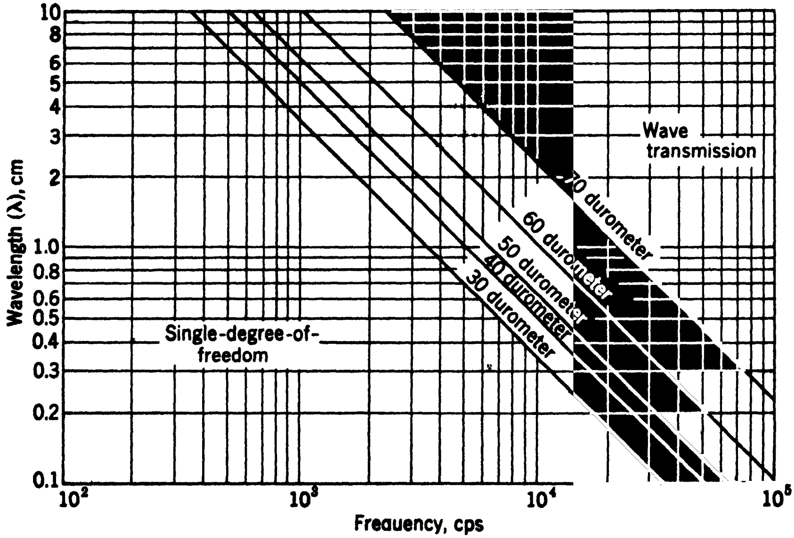

FIGURE 4.39. Wavelength of sound in rubber of various durometers, as a function of sound frequency. The regions are indicated in which the single-degree-of-freedom and wave transmission concepts are applicable.

tor may be written after equation 4.56 as follows:

$$F_T = F_0\sqrt{\frac{1 + [2(\omega/\Omega_y)(c_y/c_{cy})]^2}{[1 - (\omega^2/\Omega_y^2)]^2 + [2(\omega/\Omega_y)(c_y/c_{cy})]^2}}, \tag{4.109}$$

where F_T = maximum force transmitted to panel s, lb.
F_0 = maximum value of oscillating force generated by operation of machine a, lb.
ω = circular frequency of oscillating force, rad/sec.
Ω_y = natural frequency of machine-and-isolator assembly, rad/sec.
c_y/c_{cy} = damping ratio for machine-and-isolator assembly, dimensionless.

The displacement amplitude of the vibrating panel s is a function of the force F_T transmitted by the isolator, and of various frequency and damping relations. An expression for the maximum vibratory displacement of the panel, resulting from the maximum transmitted force F_T, may be written after equation 4.48 as follows:

$$s_0 = \frac{F_T/k_s}{\sqrt{[1 - (\omega^2/\Omega_s^2)]^2 + [2(\omega/\Omega_s)(c_s/c_{cs})]^2}} \tag{4.110}$$

where s_0 = maximum vibratory displacement of panel c, in.
k_s = stiffness of panel s, lb/in.
F_T = maximum force transmitted to panel s by isolator, lb.
ω = circular frequency of oscillating force, rad/sec.
Ω_s = circular natural frequency of panel s, rad/sec.
c_s/c_{cs} = damping ratio for panel s, dimensionless.

Combining equations 4.109 and 4.110, the following expression is obtained:

$$\frac{S_0}{F_0/k_s} = \sqrt{\frac{1 + \left(2\frac{\omega}{\Omega_y}\frac{c_y}{c_{cy}}\right)^2}{\left[\left(1 - \frac{\omega^2}{\Omega_y^2}\right)^2 + \left(2\frac{\omega}{\Omega_y}\frac{c_y}{c_{cy}}\right)^2\right]\left[\left(1 - \frac{\omega^2}{\Omega_s^2}\right)^2 + \left(2\frac{\omega}{\Omega_s}\frac{c_s}{c_{cs}}\right)^2\right]}}, \tag{4.111}$$

Equation 4.111 gives the maximum panel displacement s_0 with reference to the term F_0/k_s, which is the deflection of the panel that would result from a constant force of magnitude F_0 applied directly to the panel. In a system of the type being discussed, the results for a small degree of damping in the isolator are substantially equivalent to the results for zero damping, except in the vicinity of the resonant condition defined by $\omega/\Omega_y = 1$. This is a condition to be avoided and is therefore of little interest in analyzing the performance of isolators. Consequently, the term c_y/c_{cy} in the above equation is set equal to zero. Then, substituting $\omega/\Omega_s = (\omega/\Omega_y)\,(\Omega_y/\Omega_s)$, equation 4.111 is written as follows:

$$\frac{s_0}{F_0/k_s} = \frac{1}{\sqrt{\left(1-\frac{\omega^2}{\Omega_y^2}\right)^2\left[\left(1-\frac{\omega^2}{\Omega_y^2}\frac{\Omega_y^2}{\Omega_s^2}\right)^2+\left(2\frac{c_s}{c_{cs}}\frac{\omega}{\Omega_y}\frac{\Omega_y}{\Omega_s}\right)^2\right]}}. \qquad (4.112)$$

Numerical values of $s_0/(F_0/k_s)$ are plotted in Figure 4.40 as a function of ω/Ω_y, for several discrete values of the frequency ratio Ω_y/Ω_s, and for the typical value of damping in structural members, $c_s/c_{cs} = 0.01$.

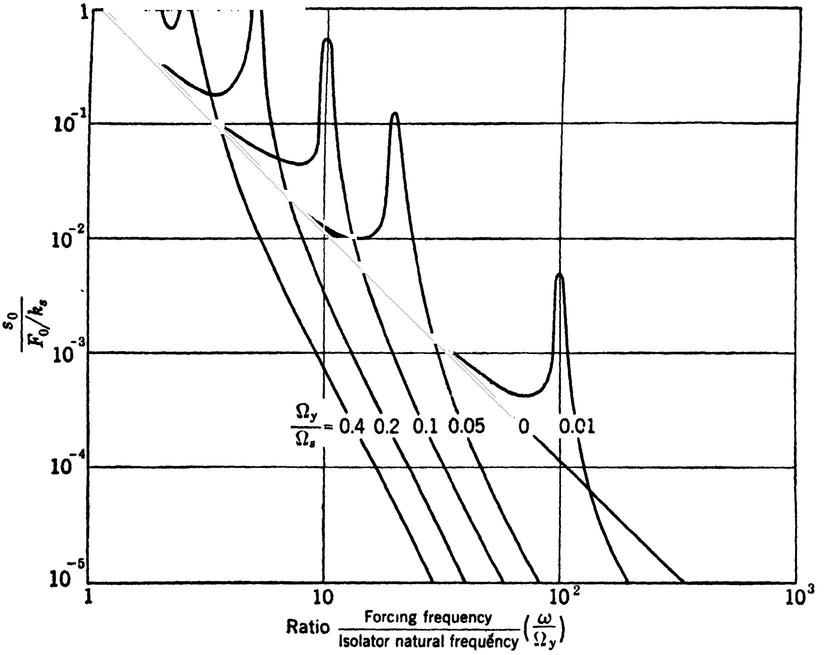

FIGURE 4.40. Curves showing relation between maximum panel displacement s_0 and frequency ratios ω/Ω_y, Ω_y/Ω_s for system illustrated in Figure 4.38.

If the natural frequencies of the panel s could be made high relative to the sound frequencies, the maximum panel displacement would become directly proportional to the magnitude of the force F_T transmitted by the isolator. This displacement is shown in Figure 4.40 by the curve marked $\Omega_y/\Omega_s = 0$; i.e., $\Omega_s \rightarrow \infty$. The panel displacement evidently decreases as the isolator natural frequency Ω_y decreases. In a practical sense, however, certain natural frequencies of the panel always fall within the range of sound frequencies. As indicated in Figure 4.40, a peak in the maximum panel displacement s_0 occurs when ω and Ω_s coincide; i.e., when the vibration generated by the machine becomes resonant with a natural frequency of the panel. This is probably an important reason for high sound levels, and the effectiveness of an isolator depends to a considerable extent on its success in eliminating or lowering the peaks of the curves shown in Figure 4.40. The addition of damping to the panel introduces the same trend in that the amplitude of resonant vibration is decreased.

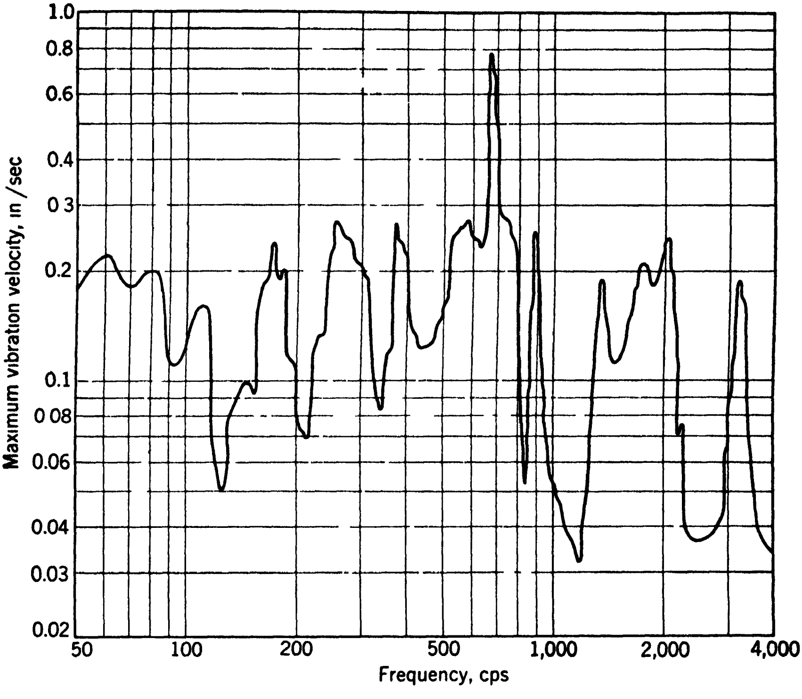

FIGURE 4.41. Vibration spectrum measured at support for a typical machine.

The vibratory forces emitted by a machine commonly include components at many frequencies and with different magnitudes. The vibration velocity throughout the frequency spectrum, as measured at the foundation of a typical machine, is illustrated in Figure 4.41. The forcing frequency ω thus has multiple values. The panel natural frequency Ω_s also has multiple values, because the panel s usually is a structure with distributed mass. The probability thus exists that several resonant peaks of the type shown in Figure 4.40 will occur, and that high sound levels will occur at certain frequencies. The existence of such peaks is something of a coincidence, which accounts at least partially for the difficulty in predicting the success of an application of sound isolators. Certain conditions indicated by Figure 4.40, which contribute to the likelihood of a successful installation, may be summarized as follows:

(*a*) By decreasing Ω_y, i.e., by making the isolator less stiff, the ratio ω/Ω_y is increased and the ratio Ω_y/Ω_s is decreased for all values of ω. The operating condition thus moves toward the right in Figure 4.40. The heights of the peaks in the right-hand region are lower, and the value of $s_0/(F_0/k_s)$ becomes lower. The sound intensity decreases as $s_0/(F_0/k_s)$ decreases.

(*b*) By increasing Ω_s, i.e., by making the panel s more rigid, the ratio Ω_y/Ω_s is decreased. The result of this change is to move all resonant peaks toward the right. The resonances thus occur in the region where the isolator is more effective, and the resultant values of $s_0/(F_0/k_s)$ are lower.

When the half wavelength of the sound in the resilient medium is small relative to the thickness of the medium, the theory of the single-degree-of-freedom system becomes inapplicable. Consideration must then be given to the phenomenon of wave transmission through the medium. This is a complex subject which involves both absorption of energy within the medium and reflection at interfaces with dissimilar media. With the relatively short paths for wave transmission which commonly prevail in isolators, the reflection at interfaces with dissimilar media is probably the more important. An analysis of this aspect of the problem introduces the concept of acoustical impedance, which is defined as the quotient of the sound pressure impressed upon the resilient medium divided by the deformation rate at the plane of sound impression. The specific acoustical impedance for a material is the acoustical impedance per unit of cross-sectional area. Specific acoustical impedance is expressed in terms of density and sound velocity by

$$R = \mu v, \tag{4.113}$$

where μ = density of the medium, gm/cm^3.
v = velocity of sound in the medium, cm/sec.
R = specific acoustical impedance, gm/cm^{2}sec.

The acoustical properties of some commonly used materials are given in Table 4.4.

The significance of the acoustical impedance may be perceived from the transfer of acoustical energy across an interface between two media of infinite extent. An expression for the ratio of the energy transmitted in medium 2 to that incident in medium 1 may be derived from an expression given by Olson* as follows:

$$P_{12} = \frac{4R_1R_2}{[(R_1/S_2) + (R_2/S_1)]^2 S_1 S_2}, \tag{4.114}$$

where P_{12} = ratio of energy transmitted in medium 2 to energy incident in medium 1, dimensionless.
R_1 = specific acoustical impedance of medium 1, gm/cm²sec.
R_2 = specific acoustical impedance of medium 2, gm/cm²sec.
S_1 = cross-sectional area of medium 1, cm².
S_2 = cross-sectional area of medium 2, cm².

If $S_1 = S_2$, equation 4.114 reduces to:

$$P_{12} = \frac{4(R_1/R_2)}{[1 + (R_1/R_2)]^2}. \tag{4.115}$$

Equation 4.115 is shown graphically in Figure 4.42. It is evident that, when the specific acoustical impedances of the two media are equal, all the energy incident in medium 1 is transmitted to medium 2. When there is a mismatch of impedances, however, the transmitted energy decreases. The decrease becomes very large when the respective media are, for example, steel and rubber; this becomes evident by substituting the values for specific acoustical impedance from Table 4.4 in equation 4.115 or Figure 4.42. The relation shown by Figure 4.42 applies strictly only when the media are of almost infinite extent. In an isolator, the media are relatively small, and the percentage of the energy transmitted tends to be greater than that indicated by Figure 4.42. The difference is one only of degree, however, and this general principle accounts for the ability of an isolator to isolate the higher-frequency components of the sound.

The many uncertainties involved in applying the principles of sound isolation make it difficult to predict the degree of success that may be expected from a given installation. The above analyses point toward the objectives, however, and promise a successful installation if the following considerations are placed in effect:

---

* See H. F. Olson, *Elements of Acoustical Engineering*, McGraw-Hill Book Co., New York, Second Edition, 1947, page 119. Olson's equation 5.101 employs the acoustical resistance r_A, for example, which is taken equal to the product of acoustical impedance R_1 and cross-sectional area S_1 in the terminology used here.

(*a*) The natural frequency of the machine-and-isolator system should be as low as possible, consistent with other requirements of the installation. The natural frequency should be substantially lower, in any event, than the frequency of any sound component having appreciable magnitude. The effectiveness of the isolator generally increases as its natural frequency decreases.

(*b*) The fundamental natural frequency of the floor or support for the machine should be as great as possible and, under any circumstances, substantially greater than the natural frequency of the isolator. The advantage of attaining low values of Ω_y/Ω_s is illustrated in Figure 4.40. In installations where the isolator natural frequency Ω_y is required to be relatively high for stability or other reasons, the possibility of satisfactory sound isolation may be enhanced by increasing Ω_s; i.e., by stiffening the support.

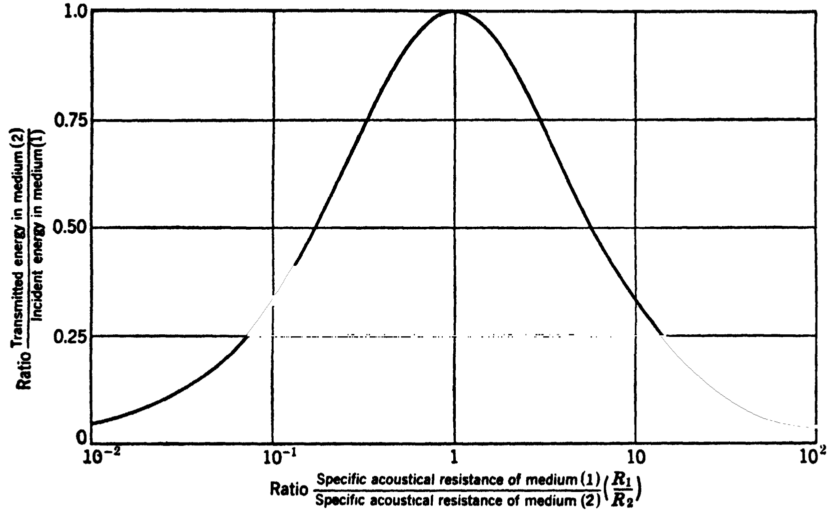

FIGURE 4.42. Ratio of sound energy transmitted in medium 2 to energy incident in medium 1.

(*c*) The isolator should be constructed so that the sound is required to flow across at least one interface between acoustically dissimilar materials. Even though the predominant sound frequencies are sufficiently low to fall within the single-degree-of-freedom concept, harmonics usually exist at higher frequencies, and the wave-transmission concept must be considered. In general, acoustically dissimilar materials should always be used for sound isolation, even though the isolator natural frequency is maintained very low by means of a metal spring.

(*d*) The effectiveness of a sound isolator may be increased by adding mass to the machine. The force transmitted through an isolator, as defined by equation 4.109, is directly proportional to the relative motion between the machine and its support.* The motion of the machine is reduced by increasing its mass, and the transmitted force F_T consequently is reduced. An effective procedure is to mount the machine upon a concrete base, which in turn is supported by isolators. This adds not only mass but also rigidity at an important location and assists in achieving an acoustic dissimilarity of materials. Concrete bases that are suitable for this type of application are illustrated in Figures 6.13 and 6.14 of Chapter 6.

The type of sound isolator that is required for any particular application depends on various circumstances. In many applications, substantially all the vibration energy emitted by a machine is of audible frequencies. This is likely to be true where the machine operates at relatively high speed, with no unbalanced low-speed mechanism; or where the vibration is caused by magnetic forces operated from an alternating-current power source. A sound isolator designed to have a moderately high natural frequency then gives satisfactory results, provided that the support for the machine is rigid. If the support lacks rigidity, there is no alternative but to maintain a low value for isolator natural frequency. An isolator designed in accordance with the principles of vibration and shock isolation expounded in preceding chapters usually provides effective sound isolation, provided that the principles of sound isolation set forth above are also followed.

Where the noisy machine includes an unbalanced low-speed mechanism, a somewhat different solution is sometimes called for. If transmission of the low-frequency vibration is not objectionable, or if the natural frequency required to attain isolation is so low as to result in an objectionably unsteady condition, the solution resides in a relatively stiff isolator. The objective in this type of application is to transmit the low-frequency vibration, but to isolate the sound.

If the low-frequency vibration must be isolated, an isolator capable of sustaining a large static deflection must be provided. Where the required static deflection is greater than can be safely sustained by rubber and other effective sound-isolating materials, it becomes necessary to resort to metal springs in order to attain the required vibration isolation. Metal springs, however, usually are not acoustically dissimilar to the material of the machine and its support, and it becomes necessary to form a combination of a vibration isolator and a sound isolator. This is accomplished most effectively by arranging a metal spring and a pad of acoustically dissimilar material in series. An example of such a combination isolator is shown in Figure 4.43. The helical spring isolates vibration of low frequency, while the rubber cup which encases the lower spring seat intercepts the flow of sound energy at the higher frequencies.

---

* F_T is actually the product of isolator stiffness and maximum relative displacement between machine and support, added vectorially to the product of damping coefficient and maximum relative velocity between the machine and its support.

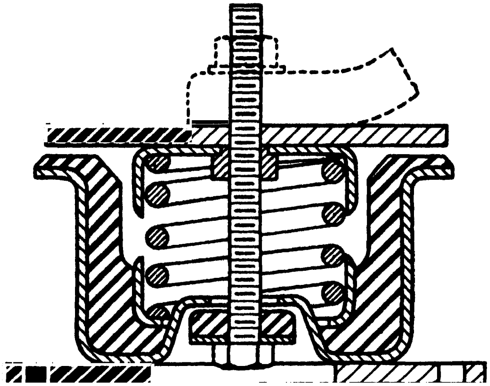

FIGURE 4.43. Isolator embodying (1) metal spring to isolate vibration and low-frequency components of sound and (2) rubber member to isolate high-frequency components of sound.

BIBLIOGRAPHY

ABBOTT, E. J., "New Technique for Noise Reduction," *S.A.E. Jour. (Trans)*, Vol. 42, No. 4, April 1938.

CRANDALL, I. B., *Theory of Vibrating Systems and Sound*, D. Van Nostrand Co., New York, 1927.

DEN HARTOG, J. P., "Forced Vibrations With Combined Coulomb and Viscous Friction," *Trans. A.S.M.E.*, Vol. 53 (APM-53-9), 1931.

DEN HARTOG, J. P., and R. M. HEILES, "Forced Vibration in Nonlinear Systems With Various Combinations of Linear Springs," *Trans. A.S.M.E. (Jour. App. Mech.*, Vol. 3, No. 4), December 1936.

DEN HARTOG, J. P., and S. J. MIKINA, "Forced Vibrations With Non-Linear Spring Constants," *Trans. A.S.M.E.*, Vol. 54 (APM-54-15), 1932.

HARDY, H. C., "Acoustical Factors in the Design of Motion Picture Equipment," *Soc. Motion Picture Eng. Jour.*, Vol. 50, No. 2, February 1948.

HARDY, H. C., "Fundamentals of Noise," *Prod. Eng.*, Vol. 19, No. 2, February 1948.

HARDY, H. C., "Sources of Machine Noise," *Prod. Eng.*, Vol. 19, No. 3, March 1948.

HARDY, H. C., "Analyzing Machine Noise," *Prod. Eng.*, Vol. 19, No. 4, April 1948.

JACOBSEN, L. S., "Steady Forced Vibration As Influenced by Damping," *Trans. A.S.M.E.*, Vol. 52 (APM-52-15), 1930.

LUDEKE, C. A., "An Experimental Investigation of Forced Vibrations in a Mechanical System Having a Non-Linear Restoring Force," *Jour. App. Phys.*, Vol. 17, No. 7, July 1946.

OLSON, H. F., *Elements of Acoustical Engineering*, McGraw-Hill Book Co., New York, 1947.

PETERSON, J. B., "Damping Characteristics of Dashpots," *NACA Tech. Note* No. 830, 1941.

SABINE, P. E., *Acoustics and Architecture*, McGraw-Hill Book Co., New York, 1932.

SLOCUM, S. E., *Noise and Vibration Engineering*, D. Van Nostrand Co., New York, 1931.

WOHLBERG, G., "Gear Noise," *Mach. Des.*, Vol. 20, No. 8, August 1948.

WYLIE, C. R., JR., "On the Forced Vibrations of Non-Linear Springs," *Jour. Frank. Inst.*, Vol. 236, No. 3, September 1943.

CHAPTER FIVE

Properties of Materials and Design of Isolators

This chapter sets forth engineering data on materials that are in common use as the resilient media in vibration and shock isolators. The data include useful properties of the materials, and their effect upon the characteristics of typical isolators that embody the respective materials. Natural and synthetic rubbers are discussed in considerable detail, because the information is not otherwise available in a form conveniently useful to the design engineer. Metal springs are discussed in less detail, as the designer has ready access to excellent reference material. Other materials are discussed briefly, the brevity being due at least partially to the scarcity of authentic engineering information.

A. NATURAL AND SYNTHETIC RUBBERS

5·1 General Properties

Before World War II, practically all vibration and shock isolators were made of natural rubber. With the start of the war, the natural rubber supply was interrupted and the embryonic synthetic rubber industry had not yet developed to such an extent that the synthetic rubbers had come into extensive use. Many types of synthetic rubber were then used in isolators with varying success. Natural rubber again became available at the end of the war and constitutes the material used in the majority of isolators, although special properties of certain synthetic rubbers established during the war have proved useful in many applications. Buna N (known by the trade names Perbunan, Hycar, Chemigum, Thiokol RD, and others) and Neoprene are used where oil resistance or operation at high temperature is required. Buna S is used to a limited extent, whereas Butyl and Thiokol A, B, and FA find little application in isolators.

It is beyond the scope of this treatise to consider all of the many properties of natural and synthetic rubber. Rubber technology remains an art rather than a science and, although a large mass of information has been published in the technical literature, the available data are not sufficiently established so that they may be applied with absolute confidence in the solution of engineering problems. The important properties of rubber vary greatly, and sometimes unpredictably, with variations in the compound, the method of curing, and the shape of the part. It is possible in this book to indicate only a few of the important general properties. Many exceptions can be found to a summary of properties because materials can be compounded to obtain predominantly favorable properties for a particular purpose, with a resulting deterioration of other properties. Important properties of natural and synthetic rubber for vibration and shock isolators are indicated in the following paragraphs:

HIGH-TEMPERATURE OPERATION

Natural and synthetic rubber tend to deteriorate rapidly at elevated temperatures. When subjected to temperatures higher than 150°, rubber slowly develops surface cracks which gradually deepen and ultimately impair the strength of the material. Both Neoprene and Buna N deteriorate less rapidly at elevated temperatures and are giving reasonably satisfactory service in some applications at temperatures as high as 250° F.

LOW-TEMPERATURE OPERATION

Natural rubber exhibits only a moderate increase in stiffness at temperatures as low as −50° F and is superior to most synthetics at low temperatures. Many compounds can be made "freeze resistant" by the addition of the proper ingredients, but the increased flexibility at low temperatures usually is gained at the expense of tensile strength and ease of molding.

OIL RESISTANCE

Natural rubber and Buna S deteriorate rapidly when exposed to mineral oil and its derivatives. Buna N shows excellent resistance not only to oil and gasoline but also to many commercially used solvents. Neoprene is second only to Buna N in ability to withstand oil and gasoline but has a tendency to swell when immersed in water.

DRIFT

Natural rubber exhibits superior ability at room temperature to withstand a static load without excessive drift or creep; i.e., without experiencing excessive permanent deformation. Neoprene, when compounded for this purpose, also shows low drift at room temperature. Buna N has notable ability to withstand a load at elevated temperatures with but relatively moderate drift.

AGING

A continuance of the vulcanization process, known as aging, contributes to a gradual increase in the hardness of rubber. Surface oxidation, accelerated by direct sunlight, also takes place. Both Neoprene and Buna N show better aging properties than rubber, particularly at elevated temperatures, and are more resistant to the effects of direct sunlight and ozone.

Silicone rubber is a synthetic material which shows promise in applications involving very high or low temperatures, for which no suitable rubber-like material has heretofore been available. This material shows a remarkable stability in important properties over a very wide temperature range, both above and below room temperature. It is still in its early development stage, and presently available information is tenative and preliminary. It has been established, however, that Silicone rubber retains its flexibility at temperatures of −70° F, or lower, and is undamaged by temperatures as high as 400° F. The compression set tends to become relatively great at elevated temperature. The stiffness of the material appears to change but little, however, after exposure to high temperatures for a considerable time. Tear and abrasion resistance usually are relatively low. The characteristically low tensile strength and high drift rate introduce limitations on this material for general use in vibration and shock isolators, except where the material is loaded very lightly. A bumper or snubber that is not required to support a dead-weight load continually, and which is not subjected to stress or abrasion, apparently constitutes a more suitable application. The rapid developments which have taken place in this field give promise that more suitable materials will be available in the future.

5·2 Methods of Use

The most important characteristic of an isolator is its stiffness. Methods for determining the required stiffness for particular applications are considered in preceding chapters. The properties of various available materials are discussed in this chapter, together with methods of applying the materials to utilize their peculiar properties in attaining the desired stiffness. Several typical methods of loading rubber parts are illustrated in Figure 5.1; the designations of the following subparagraphs refer to corresponding designations in Figure 5.1.

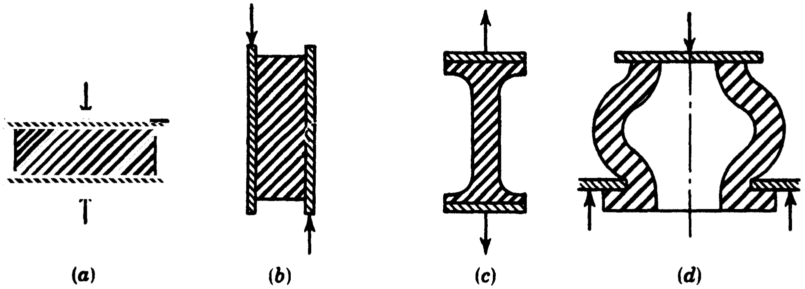

FIGURE 5.1. Typical rubber parts illustrating different types of stress: compression (*a*); shear (*b*); tension (*c*); and flexure (*d*).

(*a*) The rubber may be stressed in compression by placing it between two parallel plates, and loading it by a force acting perpendicular to the plates. The distance between plates decreases in response to the force, and the rubber bulges around the periphery or into holes cut through the assembly perpendicular to the plates.

(*b*) The rubber may be stressed in shear, if placed between and adhered to two parallel plates. The forces then are applied in a direction parallel with the plates, and the resultant deflection is approximately in the direction of the forces.

(*c*) Rubber is capable of carrying a considerable tension load. It is seldom used in this manner, however, because of the difficulty of obtaining suitable end connections and because a rubber member under severe tensile stress may fail if it experiences slight surface damage. It is considered poor engineering practice to load an adhered or bonded joint in tension.

(*d*) Rubber may be stressed in flexure, in which case a portion of the rubber member has a bending moment applied thereto. One surface, therefore, is subjected to tensile stress, and the opposite surface to compressive stress. It is particularly convenient to obtain large deflections in response to very light loads in this manner, and it is relatively easy to control the stiffnesses in various directions.

The art of adhering rubber to metal is known as bonding. The details of the bonding process are not within the scope of this treatise; suffice it to state that natural rubber or practically any synthetic rubber used in isolators may be successfully bonded to any common metal. Bond strengths as high as several hundred pounds per square inch are commonly and consistently obtained in quantity production. It is conservative design practice to limit the bond stress in shear to approximately 50 psi, although this stress may be increased somewhat if it is assured that the bonded region will not be subjected to elevated temperatures, mineral oils, or direct sunlight.

5·3 *Rubber Stiffness*

The stiffness of a rubber member is a function generally of (1) the rubber compound and method of curing and (2) the size and shape of the member. The compound and method of curing determine a property that bears some similarity to Young's modulus for metals. This "modulus" is measured indirectly by determining the resistance of the material to indentation. The most common instrument for this purpose is a Shore Durometer. The indenting needle is a truncated cone having a flat end approximately $\frac{1}{32}$ inch in diameter. The instrument is constructed with an internal spring which presses the end of the truncated cone against the surface of the rubber with an average pressure of 2,500 psi. The durometer reading is indicated on an arbitrary scale by the depth of the indentation, the reading being taken almost immediately upon the application of the load. Correlation of this reading with structural properties of the rubber is discussed in later sections of this chapter.

Durometer readings tend to be somewhat inconsistent, partly because some rubber compounds drift perceptibly when subjected to the force of the needle and thereby introduce a time factor which may appreciably affect the reading. Furthermore, the thickness of the rubber part and its surface contour influence the durometer reading and cause uncertainties in comparisons between members of different shape. Finally, some variation in readings results from differences in the force by which the instrument is pressed against the rubber, and the reading consequently is not entirely independent of the technique of the operator.

A large indentation such as occurs in soft rubber is indicated by a low durometer number. The softest rubber that has been found generally useful as the resilient medium of isolators is approximately 30 durometer; the hardest commonly used is approximately 70 durometer. Although the stiffness of an isolator is a function of the entire volume of the rubber, a reasonably good indication of this stiffness is obtained from the surface hardness, or resistance to indentation, as measured by the durometer. The relation between stiffness and durometer is most conveniently demonstrated by reference to the shear sandwich illustrated in Figure 5.1(*b*). The shear modulus, defined in Section 5·5 below, is plotted as a function of durometer reading in Figure 5.2. Mean values of modulus are shown, from which the modulus of any particular compound may differ as much as 15 percent.

Another peculiarity that introduces considerable uncertainty into calculations of the stiffness of rubber members is the relatively high

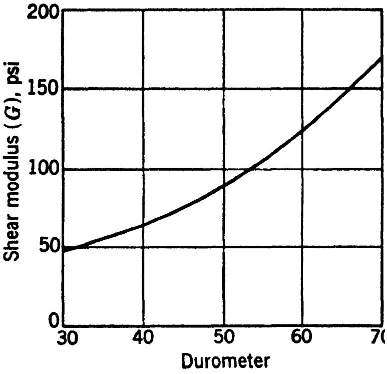

FIGURE 5.2.

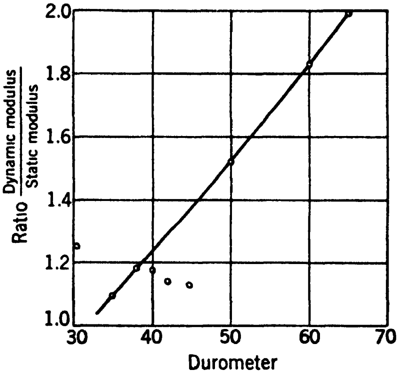

FIGURE 5.3.

FIGURE 5.2. Shear modulus of rubber for small deflections, as a function of durometer. This curve indicates the slope at the origin of the curves given in Figure 5.9.

FIGURE 5.3. Relation between dynamic and static moduli of rubber, as a function of rubber durometer. The plotted points show the range of experimentally determined values.

value of dynamic modulus as compared with static modulus. The natural frequency computed from equation 2.16, using the stiffness k determined from a static force-deflection test, almost invariably gives a value lower than that experienced during vibration. The reason for this discrepancy is not entirely clear. It has been observed that the ratio of dynamic to static modulus appears to be independent of the velocity of strain. The numerical value of this ratio generally falls between one and two, being higher for harder rubber compounds. The general nature of the relation is indicated by Figure 5.3, which shows the ratio of moduli as a function of durometer. These data were determined from a number of representative isolators selected at random. The scatter of the points may be ascribed to the several different types of isolator employed, to the many different rubber compounds represented, and to discrepancies in determining the durometer of rubber molded in irregular shapes. The experimental points thus indicate not only the numerical value of the ratio of moduli but also the scatter that may be expected in the results.

The engineer who is confronted with the task of designing a rubber member having prescribed stiffnesses in several directions has a difficult problem. The difficulties arise, first, from the fact that the member usually has a more or less complex shape in order to be easily adaptable mechanically and structurally. If the member can be separated into mutually independent component parts, the procedures available for calculating the stiffnesses of the parts usually yield results that are reasonable first approximations. Rubber members of various regular shapes subjected to typical methods of loading are considered in the following paragraphs.

5·4 Compression Pad

Rubber may be considered an incompressible substance, since its bulk modulus is very large compared with its compression and shear moduli. As a consequence, a rubber member may be deflected by a compressive force only if it is permitted to expand laterally; in the absence of lateral expansion space, such deflection becomes nearly impossible. It thus follows that any condition that restricts lateral expansion also tends to restrict deflection in response to compressive forces, with a resultant increase in stiffness. Two very important factors in this respect are:

(*a*) The conditions at the interface over which the compressive force is applied to rubber. If this interface is perfectly lubricated, lateral expansion of the rubber occurs uniformly from one loading face to the other, as indicated by the dotted lines in Figure 5.4 (*a*). Lateral restraint, and consequently the stiffness in compression, are then a minimum. On the other hand, if the rubber is adhered to a rigid member at the interface, lateral expansion cannot take place adjacent to the rigid member, and the rubber bulges as shown by the dotted lines in Figure 5.4 (*b*). The stiffness in compression is increased by this restriction of lateral expansion.

(*b*) The free area available for lateral expansion. A rubber member to which a compressive force is applied has the greatest stiffness per unit of load-carrying area when the ratio of free lateral area to load-carrying area is a minimum. The free lateral area may be increased by providing holes through the rubber parallel to the direction of the compressive force, or by selecting a shape whose peripheral area is large. The member shown in Figure 5.4 (*c*) is stiffer than that shown in Figure 5.4 (*d*), although of the same load-carrying area, because the lateral area of the latter has been increased by the central hole and by the increased periphery.

Some work has been done in deriving equations for the force-deflection relations of an incompressible solid subjected to large strains.* These analyses are in good agreement with experimental results for special shapes of rubber members to which the theory is applicable. The analyses make no provision, however, for various conditions at the loading face or for the effect of lateral expansion area. As pointed out above, these conditions are of primary importance and must be considered in the design of rubber members for isolators.

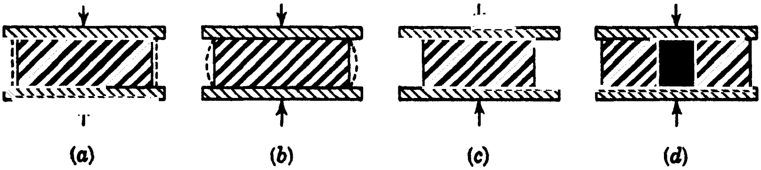
(*a*) (*b*) (*c*) (*d*)

FIGURE 5.4. Factors that affect the stiffness of rubber pads loaded in compression. Pad *a* is unbonded, and pad *b* is bonded. Pads *c* and *d* have same loaded area, but pad *d* is less stiff because its lateral area is increased by the central hole.

In the absence of a suitable theory, empirical data must be employed to determine the stiffness characteristics of rubber members loaded in compression. One of the early investigations in this field was carried out by Keys.† He conducted extensive tests on rubber pads of square load-carrying area made of identical rubber. Keys defined the area ratio of the pads as the ratio of the load-carrying area to the lateral expansion area and observed that pads whose area ratios are equal deflect the same percentage of their thicknesses when supporting equal unit loads. As a result of this work, a series of force-deflection curves has been made available, as reproduced in Figure 5.5. A family of curves is presented for each of several rubber durometers, the parameter of each family being the ratio of load-carrying area to lateral expansion area. These curves are substantially straight lines in the region of the origin, and the stiffness of the pad is thus constant for small deflections.

---

* See H. Henkey, "Elastic Behavior of Vulcanized Rubber," *Trans. A.S.M.E.*, Vol. 55 (APM-55-8), 1933; and E. G. Chilton, "Large Deformations of an Elastic Solid," *Trans. A.S.M.E.* (*Jour. App. Mech.*, Vol. 15, No. 4), December 1948.

† W. C. Keys, (United States Rubber Co.), "Rubber Springs," *Mech. Eng.*, Vol. 59, No. 5, May 1937.

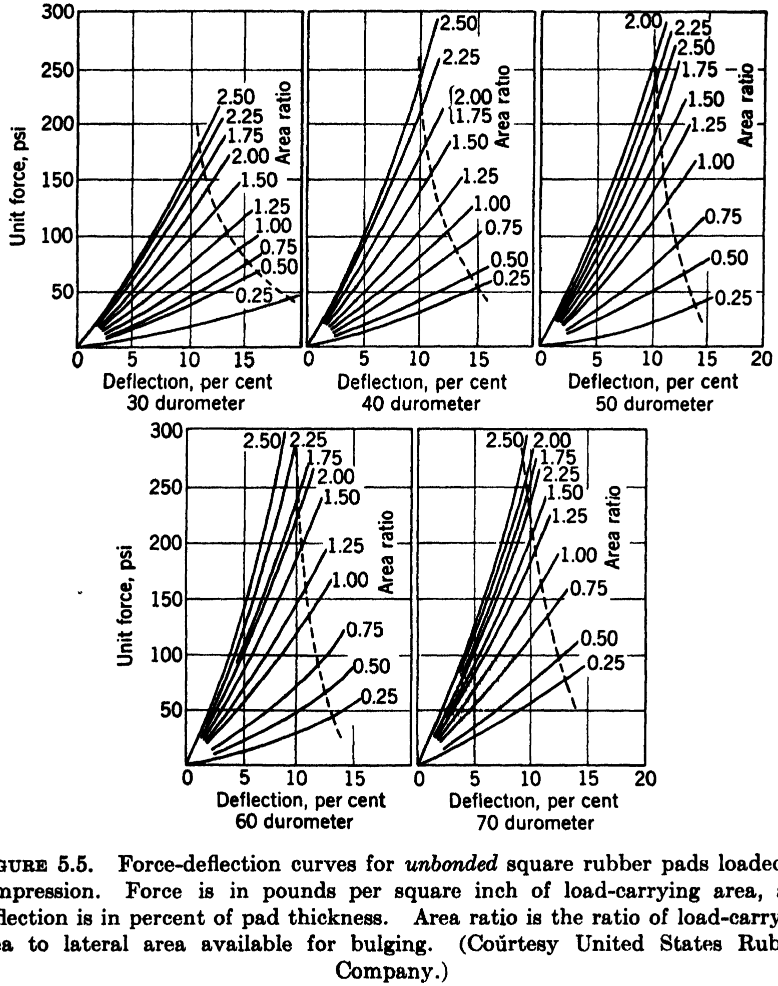

FIGURE 5.5. Force-deflection curves for *unbonded* square rubber pads loaded in compression. Force is in pounds per square inch of load-carrying area, and deflection is in percent of pad thickness. Area ratio is the ratio of load-carrying area to lateral area available for bulging. (Courtesy United States Rubber Company.)

The curves of Figure 5.5 refer to rubber pads in which the interface between the rubber and the rigid loading member is *unlubricated and non-adhered;* the stiffnesses should therefore fall between the extremes obtained with perfectly lubricated and adhered interfaces. These curves were obtained from rubber pads whose load-carrying faces were square in each instance. The stiffness apparently decreases as the load-carrying face deviates from a square; some later work by Hirshfeld and Piron* show 15 percent lower stiffness, for the same area ratio, when the length of the pad is twice its width, and 40 percent lower stiffness when the length is ten times the width.

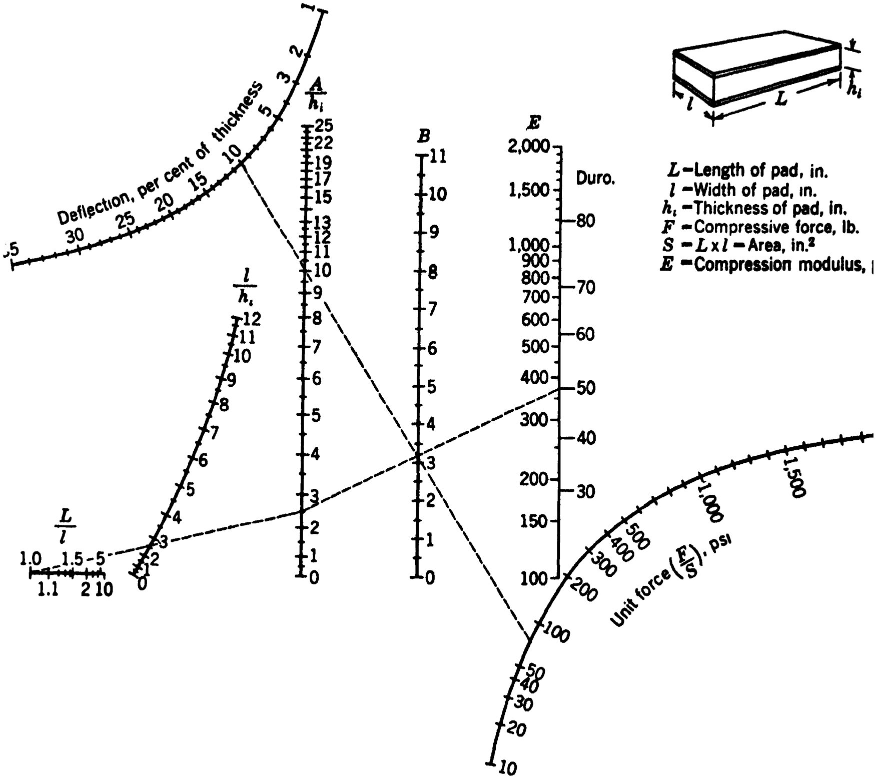

FIGURE 5.6. Nomograph for determining relation of force and deflection for *bonded* rectangular rubber pads loaded in compression. A straight line is drawn intersecting the L/l and l/h_i scales at appropriate values. This determines a value of A/h_i, from which a second straight line is drawn to the E scale. To determine the deflection resulting from any unit force, a straight line is drawn from the force scale to the deflection scale, intersecting the B scale at the same point as the line from A/h_i to E. (Courtesy United States Rubber Company.)

Compression pads that are bonded to the rigid members by which the load is applied usually are stiffer than the non-adhered pads tested by Keys. Research work by the United States Rubber Company has resulted in a nomograph for determining force-deflection relations of

---

* C. F. Hirshfeld and E. H. Piron, "Rubber Cushioning Devices," *Trans. A.S.M.E.*, Vol. 59, No. 6, August 1937, page 471.

bonded pads. This nomograph is reproduced here as Figure 5.6. The deflection is expressed in percentage of pad thickness, resulting from a unit force expressed in pounds per square inch. Ratios of length to width and width to thickness are first determined from the dimensions of the pad. A straight line establishes a point on the A/h_t scale, from which another straight line to the appropriate durometer number or modulus determines a point on the B scale. Every straight line through this point establishes a relation between force and deflection.

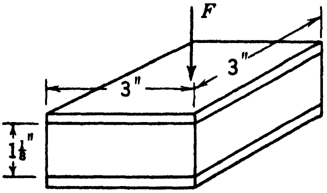

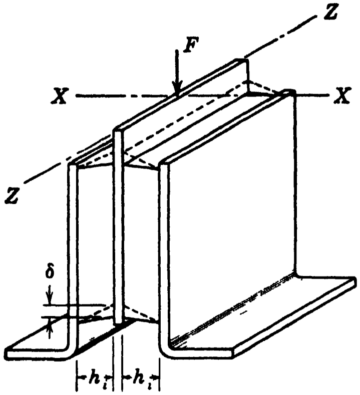

FIGURE 5.7. FIGURE 5.8.

FIGURE 5.7. Rectangular rubber pad bonded between two metal plates and adapted to be loaded in compression by the force F.

FIGURE 5.8. Double shear sandwich, in which two rectangular rubber pads are stressed in shear by the vertical force F. The solid lines indicate the position in response to the force F; the dotted lines indicate the outline of the rubber in its free position.

Example 5.1. The method of using the nomograph, Figure 5.6, is illustrated by computing the stiffness of the compression pad shown in Figure 5.7. From the dimensions of the pad, the following ratios are established:

$$\frac{L}{l} = \frac{3 \text{ inches}}{3 \text{ inches}} = 1,$$

$$\frac{l}{h_t} = \frac{3 \text{ inches}}{1.125 \text{ inches}} = 2.67.$$

A straight line through these two values intersects the A/h_t scale at 2.5. Assuming the pad to be made of 50-durometer rubber, another straight line is drawn from $A/h_t = 2.5$ to the 50 index on the durometer scale. The intersection of this line with the B coordinate scale determines the value $B = 3.2$, through which a straight line is drawn connecting the force and deflection scales. For a deflection of ten percent of the thickness, a force of 80 psi is required. The stiffness of the pad is the total force divided by the deflection:

$$\text{Stiffness} = \frac{80 \times 3 \times 3}{1.125 \times 0.10} = 6{,}400 \text{ lb/in.}$$

The experimentally determined stiffness of the pad is 5,700 lb/in. This difference between actual and calculated stiffness indicates the accuracy that may be anticipated in design calculations of a relatively simple element.

5·5 Shear Sandwich

The stiffness of a rubber sandwich stressed in shear is subject to fewer uncertainties in calculation than that of a pad loaded in compression. Adhering of the rubber to metal is essential under these circumstances in order to carry the load to the rubber. For the simple sandwiches to which the following analysis applies, the bonded interfaces usually are parallel and remain parallel throughout the deflection range. A typical shear sandwich is illustrated in Figure 5.8. This sandwich embodies two rubber members and three metal plates bonded thereto. The outermost plates are secured to a rigid support; the mounted load is supported by the central plate. The dotted lines indicate the outline of the rubber in its unloaded condition, and the solid lines show its outline under load.

The shear stress is the total force divided by the area in shear; and the shear strain is the deflection of one plate relative to the other, divided by the distance between plates. Typical stress-strain curves in shear for rubber of several different durometers are shown in Figure 5.9. These curves are approximately linear for small strains but exhibit a slope which decreases as the strain increases. The slope of the curves at the origin gives the modulus for small deflections; it is plotted in Figure 5.2 as a function of durometer. The shape of the rubber piece and the area available for lateral expansion apparently have little influence on the stiffness in shear. Deflection in shear is usually accompanied by compression or tension in a lateral direction, but the stiffness in shear appears to be substantially unaffected by either the initial value or variations in the incidental compression or tension.

The expression that applies to the force-deflection characteristics of the shear sandwich shown in Figure 5.8 for small deflections is

$$\frac{F}{S} = G\frac{\delta}{h_i}, \tag{5.1}$$

where F = applied force, lb.

S = area of rubber in shear, in.^{2} (This is total area of both pads in Figure 5.8 because they share the load.)

G = modulus of elasticity in shear, as indicated by slope of curves of Figure 5.9 in the region of the origin, psi (see Figure 5.2).

δ = deflection, in.

h_i = rubber thickness, in.

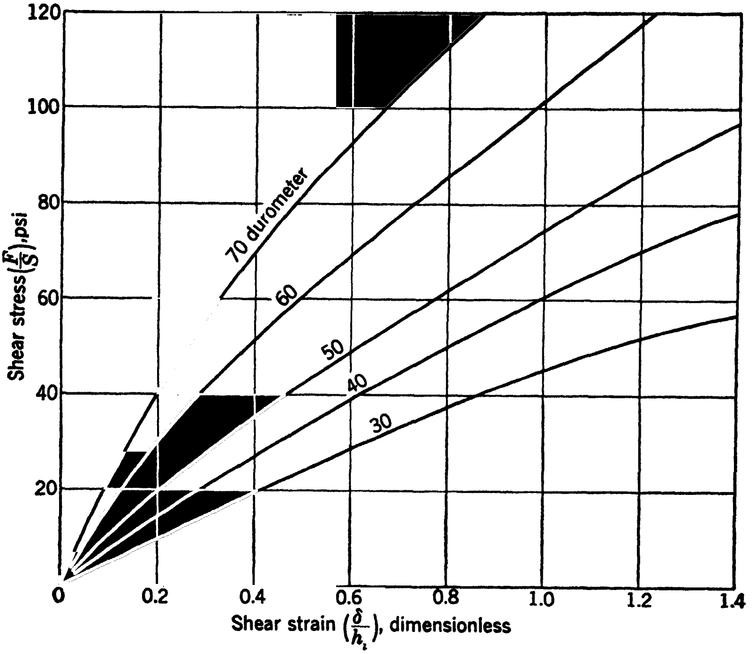

FIGURE 5.9. Stress-strain curves for rubber in shear. (Courtesy United States Rubber Company.)

For large values of shear strain δ/h_i, the shear modulus G is not constant but decreases with an increasing strain. Equation 5.1 then is not applicable, but the deflection resulting from the applied force is readily determined from Figure 5.9.

Example 5.2. It is desired to determine the deflection of the double shear sandwich, Figure 5.8, as a result of an applied force of 500 lb. Each pad is 3 in. square and $\frac{3}{4}$ in. thick. The area of rubber in shear is $S = 2 \times 3 \times 3 = 18$ in.^{2}, where the two rubber members share the load. The shear stress is then:

$$\frac{F}{S} = \frac{500}{18} = 27.8 \text{ psi.}$$

If the sandwich is made of 40-durometer rubber, the shear strain resulting from a shear stress of 27.8 psi is found from Figure 5.9 to be 0.4. The overall deflection of the sandwich is then the product of strain and rubber thickness:

$$\delta = \frac{\delta}{h_i} \times h_i = 0.4 \times 0.75 = 0.3 \text{ in.}$$

5·6 Bushing

A hollow rubber cylinder bonded or otherwise confined between concentric metal cylinders is used under various types of loading. It is applied with the load either parallel with or perpendicular to the axis of symmetry, or with a couple which deflects the cylinder in torsion about the axis of symmetry. The first type of loading is illustrated in Figure 5.10, in which the force F is applied to the inner cylinder, and an equal and opposite reaction is distributed about the periphery of the outer cylinder. The initial position of the rubber bushing is indicated by the dotted lines, and the deflected position by the solid lines.

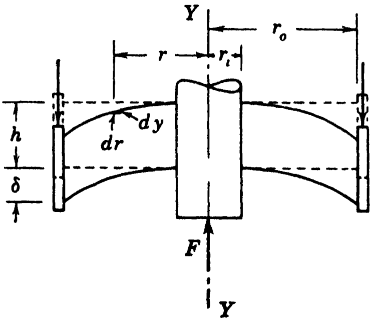

FIGURE 5.10.

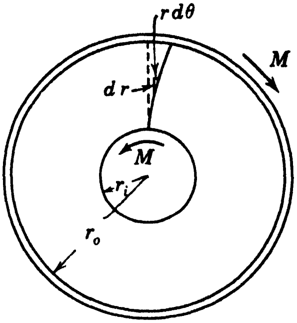

FIGURE 5.11.

FIGURE 5.10. Bonded rubber bushing subjected to axial force. The solid lines indicate the deflected position in response to the force F; the dotted lines indicate the free position.

FIGURE 5.11. Bonded rubber bushing subjected to couple. The solid line indicates the deflected position in response to the couple M; the dotted line indicates the free position.

The relation between shear stress and shear strain is given by equation 5.1 of Section 5·5. This equation is made applicable to a rubber bushing subjected to an axial force by setting up the following relations:

$$S = 2\pi rh = \text{Area subjected to shear force,}$$

$$\frac{\delta}{h_i} = \frac{dy}{dr} = \text{Shear strain.}$$

Substituting these expressions in equation 5.1, and integrating between appropriate limits:

$$\int_0^\delta dy = \frac{F}{2\pi hG} \int_{r_i}^{r_o} \frac{dr}{r}. \tag{5.2}$$

Performing the indicated integration, the following expression for the deflection δ resulting from the force F is obtained:

$$\delta = \frac{F}{2\pi hG} \log_e \frac{r_o}{r_i}, \tag{5.3}$$

where δ = axial deflection of bushing, in.
F = axial force applied to bushing, lb.
h = length of bushing, in.
G = modulus of elasticity of rubber in shear, as given by Figure 5.2, psi.
r_o = outer radius of rubber element, in.
r_i = inner radius of rubber element, in.

Equation 5.3 applies only to small deflections for which the shear modulus G may be considered a constant.

The characteristics of an identical bushing deflected in torsion may be investigated by a similar analysis. Referring to Figure 5.11, the initially straight dotted line extending in a radial direction assumes the curved position of the solid line when the bushing is deflected torsionally. The relation between shear stress and shear strain, in terms of the shear modulus, is given by equation 5.1. Designating the applied couple by M, it is evident from the geometry of Figure 5.11 that:

$$\frac{\delta}{h_i} = \frac{r\,d\theta}{dr} = \text{Shear strain},$$

$$F = \frac{M}{r} = \text{Force applied to area in shear},$$

$$S = 2\pi rh = \text{Area subjected to shear force}.$$

Substituting these expressions in equation 5.1, and integrating between the appropriate limits:

$$\int^\theta d\theta = \frac{M}{2\pi hG} \int_{r_i}^{r_o} \frac{dr}{r^3}. \tag{5.4}$$

Performing the indicated integration, the following expression is obtained for angular deflection θ resulting from the couple M:

$$\theta = \frac{M}{4\pi hG}\left(\frac{1}{r_i^2} - \frac{1}{r_o^2}\right), \tag{5.5}$$

where θ = torsional deflection of bushing, rad.
M = couple applied to bushing, in. lb.
h = length of bushing, in.
G = modulus of elasticity of rubber in shear, as given by Figure 5.2, psi.
r_o = outer radius of rubber element, in.
r_i = inner radius of rubber element, in.

A bushing of the type illustrated in Figure 5.11 often experiences large torsional deflections, and equation 5.5 then does not apply. J. F. D. Smith has derived equations* that apply for large deflections and finds that equation 5.5 is the first term of a series equation. Smith's equation for large deflections is:

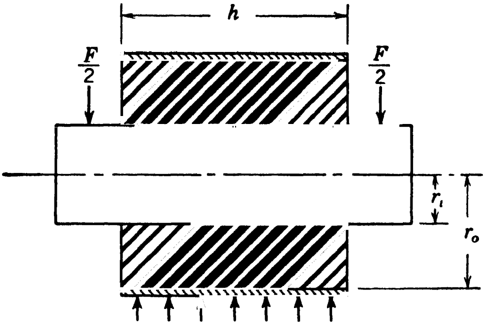

FIGURE 5.12. Bonded rubber bushing subjected to radial force. (Courtesy United States Rubber Company.)

$$\theta = \frac{M}{4\pi hG}\left[\left(\frac{1}{r_i^2} - \frac{1}{r_o^2}\right) + \frac{1}{9}\left(\frac{M}{2\pi hG}\right)^2\left(\frac{1}{r_i^6} - \frac{1}{r_o^6}\right) + \cdots\right]. \quad (5.6)$$

When a force is applied to a rubber bushing in a direction perpendicular to the axis of symmetry, the strain of the rubber is a complicated combination of compression and shear which is not well adapted to analysis. It then becomes necessary to rely upon an empirical relation to determine the stiffness.† This involves creating a hypothetical bonded compression pad whose stiffness is equivalent to the stiffness of the bushing, Figure 5.12, when loaded by the force F. The length L of the hypothetical pad is either h or $r_o + r_i$, whichever is larger; the width l is the smaller of h and $r_o + r_i$. The thickness h_i of the hypothetical pad is the difference between the outer and the inner radii of the bushing, $r_o - r_i$. The deflection of the hypothetical pad is determined from the nomograph, Figure 5.6, in terms of percentage of the thickness h_i. The radial deflection of the rubber bushing, Figure 5.12, is the same percentage of the radial difference $r_o - r_i$.

---

* J. F. D. Smith, "Rubber Springs—Shear Loading—II," *Trans. A.S.M.E.*, Vol. 70, No. 3, April 1948, pages 227–32.

† United States Rubber Co., *Absorbing Vibration, Noise, Impact*, New York, 1942, page 101.

Example 5.3. Use of the above equations and procedures to calculate the stiffness of a rubber bushing for several types of loading will be illustrated by calculating the various stiffnesses of the following bushing:

$$\begin{aligned} \text{length } h &= 1 \text{ in.} \\ \text{outer radius } r_o &= \tfrac{11}{16}\ (0.687) \text{ in.} \\ \text{inner radius } r_i &= \tfrac{7}{16}\ (0.437) \text{ in.} \\ \text{rubber durometer} &= 40. \end{aligned}$$

The stiffness in shear parallel with the axis of symmetry is obtained from equation 5.3 as follows, using the shear modulus, $G = 65$ psi, given by Figure 5.2:

$$\frac{F}{\delta} = \frac{2\pi hG}{\log_e (r_o/r_i)} = \frac{2\pi \times 1 \times 65}{\log_e (0.687/0.437)} = 905 \text{ lb/in.}$$

The stiffness in torsion about the axis of symmetry is obtained from equation 5.5 as follows:

$$\frac{M}{\theta} = \frac{4\pi hG}{(1/r_i)^2 - (1/r_o)^2} = \frac{4\pi \times 1 \times 65}{(1/0.437)^2 - (1/0.687)^2} = 263 \text{ in. lb/rad.}$$

The radial stiffness of the bushing, i.e., the stiffness when deflected by a force normal to the axis of symmetry, is determined by constructing a hypothetical compression pad as described above The length L is the sum of the radii ($\frac{11}{16} + \frac{7}{16} = 1.12$), the width l is the dimension $h = 1$, and the thickness h_i is the radial difference ($\frac{11}{16} - \frac{7}{16} = 0.25$). Drawing a straight line on the nomograph, Figure 5.6, through the points $L/l = 1.12$ and $l/h_i = 4$ determines the point $A/h_i = 4.2$. Another straight line from $A/h_i = 4.2$ to 40 on the durometer scale determines the point $B = 3.5$. A third straight line through $B = 3.5$ and a deflection of 10 percent of the thickness determines a unit force of 94 psi, or a total force of $94 \times 1.12 \times 1 = 106$ lb. The radial stiffness is the radial force divided by the radial deflection:

$$\frac{F}{\delta} = \frac{106}{0.10 \times 0.25} = 4{,}230 \text{ lb/in.}$$

5·7 Application of Stiffness Data

The graphs and equations given in the above sections are useful for calculating, to a fair first approximation, the stiffnesses of simple rubber elements stressed in compression and shear. Such elements are used in many applications. A given rubber element has different stiffnesses when deflected in different directions, and the ratios of those stiffnesses determine, in many cases, the effectiveness of an application.

A rubber pad that is deflected in compression as a result of the dead-weight load experiences a shear strain when deflected laterally. The ratio of compression to shear stiffness varies somewhat with the shape factor of the rubber element. An approximate numerical value which applies generally may be obtained from the rubber pad shown in Figure 5.7. The compression stiffness is calculated in Example 5.1 to be 6,400 lb/in. for 50-durometer rubber. The shear stiffness is calculated from the area subjected to shear and the modulus $G = 90$ psi as obtained from Figure 5.2:

$$\text{Shear stiffness} = \frac{90 \times 3 \times 3}{1.125} = 720 \text{ lb/in.}$$

The ratio of compression to shear stiffness is thus:

$$\frac{6{,}400}{720} = 8.89.$$

When a rubber pad or sandwich is applied so that it experiences shear stress as a result of the dead-weight load, as shown in Figure 5.8, the shear stiffness is effective for deflection in the lateral direction of the Z axis, as well as in the vertical direction. The compression stiffness is effective for deflection in the lateral direction of the X axis. The ratio of lateral to vertical stiffness is therefore different along the two coordinate axes. The designer is thus given some freedom in selecting the design and orientation of an isolator in such a manner as to provide the stiffnesses and stiffness ratios indicated by the analyses of resiliently mounted systems which are set forth in preceding chapters.

One who has critically examined the various isolators currently being used in many applications is impressed by the fact that the rubber members of the isolators do not, in general, fall within the scope of the elemental shapes considered in the preceding sections. The engineer who has the task of designing an isolator frequently discovers that, for practical mechanical and structural reasons, a complex shape is more suitable than a simple shape for which a stiffness equation is available. By separating the isolator into components that resemble as closely as possible the simple shapes for which equations have been derived, it is sometimes possible to estimate at least the order of magnitude of the stiffness. The next step in accurately determining the stiffness is to fabricate by the most expedient means a sample isolator, or the rubber member for the isolator. Tests of the samples usually will indicate the nature of the modifications required.

5·8 *Maximum Loads*

Opinion differs greatly on the maximum permissible loads for rubber members of isolators. A vibration isolator is subjected to many cycles of stress, but the range between extreme values is small; furthermore, the deflection under dead-weight load is relatively great, and the nature of the stress is usually not changed during vibration. A shock isolator, on the other hand, is generally subjected to relatively few cycles of stress involving large numerical values and reversals of direction. Both shock and vibration isolators are generally required to support a dead-weight load continuously. All compounds of natural and synthetic rubber exhibit as an undesirable property a constantly increasing deflection when they are required to support a load continuously. This increasing deflection is known as drift, or creep. In many isolator applications, the drift must be maintained within reasonable limits, in order to preserve the alignment of component parts and the clearances required for proper functioning of the isolators. To make most effective use of space and material without introducing excessive drift requires some discrimination in design.

Although maximum stress has been suggested as a criterion to determine maximum permissible load, maximum strain seems preferable because the criterion is then substantially independent of the modulus of the rubber. For rubber loaded in compression, there is fair agreement that the strain resulting from the dead-weight load should be limited to approximately 10 percent. Low-durometer compounds usually exhibit superior drift characteristics, and the permissible strain consequently may be taken as somewhat greater than 10 percent. There is little agreement with regard to a maximum permissible shear strain for continuous loading. A conservative criterion is a strain of 25 percent, although it has been suggested that strains as great as 100 percent are permissible. The shear strain is often limited by the bond stress. A bond stress in shear of 50 psi is conservative; some designers tolerate a somewhat higher stress for applications where the bond will not be subjected to elevated temperatures, mineral oils, or direct sunlight.

Drift is defined by the following expression:

$$\text{Drift} = \frac{\text{Final deflection} - \text{Initial deflection}}{\text{Initial deflection}}$$

where initial deflection is variously defined as the deflection immediately upon application of load, five minutes after application of load, or one day after application of load. The exact definition is of little importance. The drift rate for natural and synthetic rubber is very sensitive to changes in the compound, the curing cycle, and test conditions. Consequently, numerical values for drift are difficult to establish on an absolute basis. The relative merits of various materials and isolators may be evaluated by arbitrarily choosing appropriate definitions; where a specific design is being investigated, the definitions may be chosen to emphasize critical aspects of the design.

Drift test results usually follow the pattern illustrated by the curve of Figure 5.13. The drift is expressed here as a percentage of the deflection which occurs immediately upon application of the load.

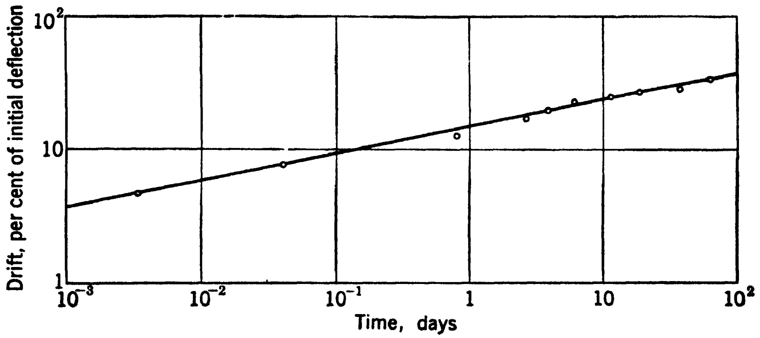

FIGURE 5.13. Typical drift-time curve for rubber.

When the drift, expressed as a percentage of the initial deflection, is plotted as a function of time to double logarithmic coordinates, the result is a straight line extending from a very small part of a day to several hundred days. Data extending to almost four years show no apparent deviation from a straight line. The magnitude of the drift and the slope of the drift curve vary widely with different compounds, with the degree of strain, and with the test temperature. Figure 5.13 was actually obtained from the test of the rather complicated rubber element illustrated in Figure 5.1 (*d*), in which flexure of the rubber sphere-like element occurs as a result of deflection. The order of magnitude of the numerical values is fairly typical, however, of good grades of natural and synthetic rubber loaded in compression or shear to a strain of 10 to 20 percent.

5·9 *Minimum Natural Frequencies*

As there is a natural tendency to attempt to attain increasingly effective isolation by continuing to reduce the natural frequency of the isolator, it is important to know the minimum natural frequency that can be attained with a given type and size of isolator. The static deflection varies inversely as the square of the natural frequency, according to equation 2.18, and may be increased to such an extent that deterioration of the rubber becomes likely as a result of excessive strain. An additional factor that must be considered with rubber loaded in compression is the increase in stiffness as the deflection increases. Curve *B* in Figure 4.4 is a typical force-deflection curve for rubber in compression, and Figure 4.5 shows that the resulting natural frequency increases if the deflection of the isolator becomes excessively great. The magnitude of this effect varies considerably with the stiffness and shape of the rubber member, but the stiffness at a deflection of 10 percent of the thickness seldom exceeds 150 percent of the stiffness at a very small deflection. Taking the maximum permissible static deflection as 10 percent of the thickness of the pad in compression, in accordance with Section 5·8 above, and applying the maximum expected stiffness increase of 150 percent, equation 2.18 above may be written as follows:

$$f_c = 3.13\sqrt{\frac{1.5}{h_i/10}} = 12.1\sqrt{\frac{1}{h_i}}, \qquad (5.7)$$

where h_i = thickness of rubber pad in compression, in.
f_c = minimum attainable natural frequency with rubber loaded in compression, cps.

A similar equation can be obtained for rubber in shear. The shear modulus of rubber decreases somewhat as deflection increases, in contrast to the increasing compression modulus. This factor is not pronounced, however, and its omission produces a result that tends to be conservative. Using a maximum permissible static deflection of 25 percent of the rubber thickness in shear, an equation for minimum attainable natural frequency f_s is derived from equation 2.18 as follows:

$$f_s = 3.13\sqrt{\frac{1}{h_i/4}} = 6.16\sqrt{\frac{1}{h_i}}, \qquad (5.8)$$

where h_i = thickness of rubber sandwich in shear, in.
f_s = minimum attainable natural frequency with rubber loaded in shear, cps.

The relations given by equations 5.7 and 5.8 are shown graphically in Figure 5.14 for ready reference.

When unbonded compression pads are used, it is necessary that the mounted equipment, or some integral part thereof, be confined between two pads that are initially compressed in order to position the equipment. This is illustrated schematically in Figure 5.15 (*a*). Some confusion frequently arises with respect to the stiffness of this com-

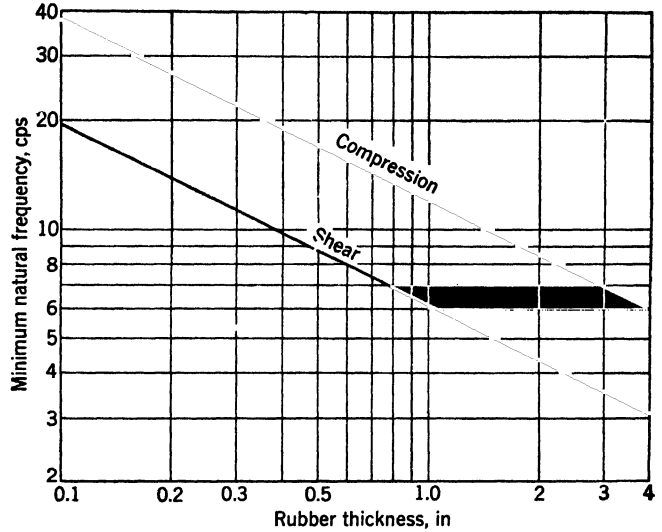

FIGURE 5.14. Minimum recommended natural frequency for rubber members loaded in compression and in shear.

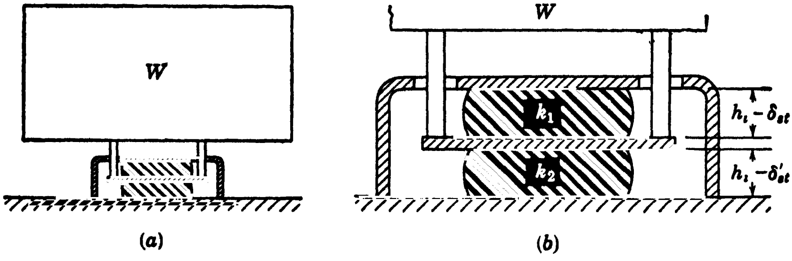

FIGURE 5.15. Schematic illustration of method for employing unbonded rubber pads in opposition for compression loading. The detail *b* is an enlargement of the assembly shown in *a*.

bination of pads, shown to an enlarged scale in Figure 5.15 (*b*). Designating the uncompressed thickness of each pad by h_i, the equation of static equilibrium for the system is:

$$k_1\delta_{st} + W = k_2\delta_{st}', \tag{5.9}$$

where k_1, k_2 = stiffnesses of upper and lower pads, respectively, lb/in.

δ_{st}, δ_{st}' = deflection of upper and lower pads, respectively, in.

W = weight of mounted body, lb.

If a downward-directed force F is now applied to the mounted equipment, and a deflection δ results therefrom, a new equation of static equilibrium may be written:

$$F + k_1\delta_{st} + W - k_1\delta = k\delta_{st}' + k_2\delta. \tag{5.10}$$

Subtracting equation 5.9 from equation 5.10, and solving the remainder for the effective stiffness F/δ of the system:

$$\frac{F}{\delta} = k_1 + k_2. \tag{5.11}$$

The effective stiffness of the rubber pad arrangement illustrated in Figure 5.15 is thus the sum of the individual pad stiffnesses.

5·10 Damping

An important factor in many aspects of vibration and shock isolation is the degree of damping embodied in the isolator. The influence of damping on the effectiveness of isolation is discussed in detail in Chapter 4. In recapitulation, damping is important in the following respects:

(*a*) In a vibration isolator required to operate for a short period at or near its resonant frequency, as during the speeding up or slowing down of a machine, a considerable amount of damping is desirable to prevent excessive excursion of the mounted equipment.

(*b*) In a shock isolator employed to protect equipment containing some elements of relatively low rigidity, damping in the isolator is desirable to prevent excessive excursion of these elements as a result of resonance with the isolator.

Rubber, in comparison with most structural materials, is a highly damped substance. The extent of the damping is indicated by the logarithmic decrement, where a highly damped substance exhibits a numerically large decrement. The decrement may be evaluated by observing the transmissibility at resonance of a system that is executing forced vibration, or by noting the rate of decay of free vibration of the system. The logarithmic decrement is calculated from these experimental data as follows:

(*a*) For a viscously damped, single-degree-of-freedom system executing forced vibration, the relation between the logarithmic decrement and the maximum transmissibility may be found by combining equations 4.37 and 4.69:

$$\Delta \approx \frac{T_0}{\pi}, \tag{5.12}$$

where Δ = logarithmic decrement, dimensionless.
T_0 = maximum transmissibility, dimensionless.

(*b*) In free vibration, the relation between the maximum amplitude at two successive cycles of a viscously damped single-degree-of-freedom system and the logarithmic decrement is given by equation 4.35.

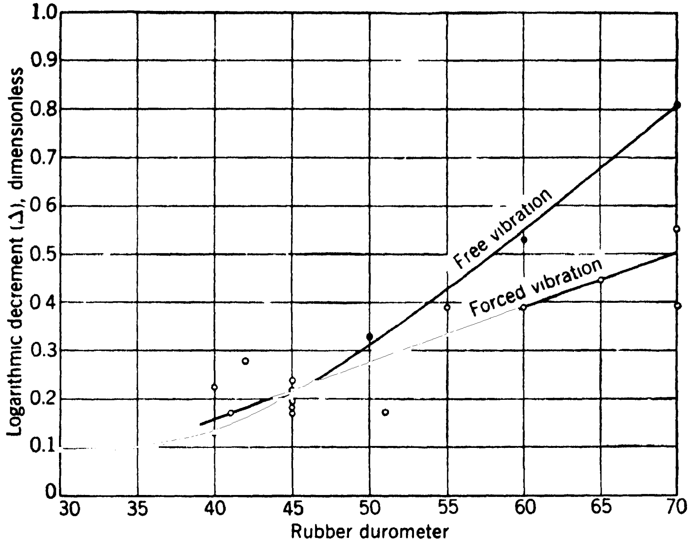

FIGURE 5.16. Logarithmic decrement for rubber as a function of durometer. The curve marked free vibration is calculated from the decay rate, using equation 4.35; the curve marked forced vibration is calculated from the maximum transmissibility, using equation 5.12.

Values of the logarithmic decrement Δ are shown in Figure 5.16 for a number of typical isolators. The discrepancy between the curves for free and for forced vibration may be ascribed to the fact that the damping is not viscous, as assumed by the theory. The general scatter of the experimentally determined points may be the result of including data from different types of isolator, and of the discrepancies involved in determining the durometer of rubber molded in irregular shapes.

It is evident from Figure 5.16 that the logarithmic decrement, i.e., the damping capacity of rubber, increases very appreciably as the durometer increases. The logarithmic decrement tends to decrease somewhat as the temperature increases. The numerical values given in Figure 5.16 apply at room temperature and become approximately one-third lower at 180° F.

5·11 Effect of Temperature

Isolators made of natural and synthetic rubber are not suitable for use at excessively high or low temperatures. The principal difficulty at high temperature is deterioration. Natural rubber shows a tendency to harden, to develop surface cracks, and to drift excessively when subjected to temperatures higher than approximately 150° F. Some of the synthetic rubbers show better properties at elevated temperatures. Certain compounds of Neoprene and Hycar, for example, have been used with reasonable success at temperatures as high as 250° F. Variation in the stiffness of an isolator as a result of elevated temperature is generally not of sufficient magnitude to be of practical importance.

Operation of natural and synthetic rubber isolators at extremely low temperatures poses an entirely different problem. There is a pronounced tendency for the isolators to exhibit increased stiffness almost immediately upon exposure to the low temperature. The degree of stiffness increase varies with the compound and the temperature. At moderately low temperature, some increase in stiffness occurs; at lower temperatures, the stiffness becomes greater and may approach complete rigidity. The stiffness increase of several typical compounds of natural and synthetic rubber is shown in Figure 5.17 as a function of temperature. These data represent practically instantaneous values; additional stiffening may occur after long exposure to the low temperatures. Curves *A* and *B* are representative of good-quality compounds of natural rubber and Neoprene suitable for general-purpose applications. The remaining curves, *C*, *D*, and *E*, refer to materials that have been specially compounded to retain their flexibility at extremely low temperatures. Any beneficial effects that derive from low-temperature flexibility are at least partially counteracted by other detrimental effects. The tensile strength of the material is often appreciably reduced, the material is more difficult to handle in the molding process, and effective adherence to metal is more difficult to attain. These shortcomings are often justifiable, however, for applications where satisfactory operation at low temperatures is of paramount importance.

5·12 Practical Design Considerations

After the general type of isolator has been determined, and the size and stiffness are known, certain practical factors must be considered in the design so that manufacture is feasible. Rubber parts are molded by vulcanizing compounded, uncured rubber in a metal mold which is subjected to heat and pressure. The mold usually has many identical cavities, the number depending on the required production rate. Correct mold design requires specialized experience, and the designer of rubber parts is advised to consult an experienced mold designer during the course of designing the rubber part. A few general remarks here, however, may assist in avoiding major pitfalls.

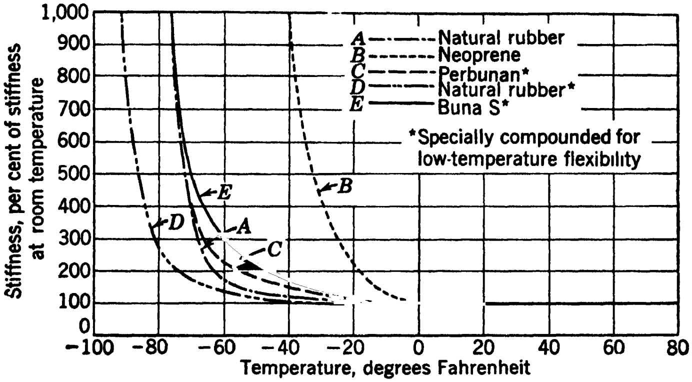

FIGURE 5.17. Change in stiffness of typical natural and synthetic rubbers as a function of temperature.

The rubber parts should be kept relatively thin. Rubber is not a good conductor of heat, and the rubber at the center of a large member can be cured only by heat conducted through the outer layers of the rubber. In order to cure the rubber properly at the center of relatively thick members, it becomes necessary to overcure the rubber at the surface with a consequent loss of strength and resilience. A similar condition exists when a single rubber member has portions of greatly different thicknesses. The preferable maximum thickness is approximately one inch, although a thickness as great as two inches may be tolerated in extreme cases.

It is unwise to place a continuous stress in tension on a rubber-to-metal bond. Shear sandwiches can be designed as illustrated by the dotted lines in Figure 5.8, with initially inclined free faces which tend to become horizontal when deflected. The application of a shear force thus subjects the bond to compressive stress. An equivalent and equally satisfactory method is to space the outer metal plates, referring again to Figure 5.8, so that the dimension h_i is slightly less than the thickness of the rubber part in its free state. Failure of a bond often starts at the periphery of the bonded interface. The likelihood of such a failure may be reduced by molding a fillet in the rubber part at its juncture with the metal. The thickness of a shear sandwich should be not more than 25 percent of the smaller of the other two dimensions to assure that deflection occurs in shear. If the sandwich is too thick, it will deflect in flexure and apply a tensile stress to the bond.

It should be kept in mind that the mold must be parted to remove the molded rubber parts. The design should have a minimum of undercut portions to avoid complexities, both in the manufacture of the mold and in the molding operation. Complete elimination of undercuts is not necessary because the flexibility of rubber enables it to deform within limits to permit removal from the mold. Bonding of rubber to metal is done during the vulcanization process; the metal parts, therefore, must fit the mold, and provision must be made for their removal after the completion of vulcanization. The metal parts should be as small as possible. Large metal parts require a large mold with consequent high cost of handling and molding. A preferred design embodies a rubber member bonded to a relatively small metal part, which is then attached after molding to a larger metal member.

Rubber shrinks perceptibly during the molding process. Molding is done at a temperature of approximately 300° F, at which temperature the size and shape of the rubber member is determined. The member then shrinks upon cooling to room temperature. The shrinkage is approximately two percent in linear dimensions for 30- to 40-durometer rubber, and 1½ percent for 60- to 70- durometer rubber. Shrinkage of Silicone rubber may be as great as eight percent. The mold designer usually compensates for this shrinkage by providing a slightly oversize cavity, but distortions of the rubber occur where the tendency to shrink is prevented by bonded metal parts. This result should be anticipated if any disadvantage will derive therefrom.

B. METAL SPRINGS

5·13 General Properties

Metal springs play a definite and important role as vibration and shock isolators. They are superior to rubber isolators for certain applications, and inferior for other applications. The niche occupied by metal springs in the field of vibration and shock isolation is indicated by a consideration of their important properties:

(*a*) Metal springs are readily designed with ability to partake of large deflections without exceeding the safe working stress for the spring material. In contrast, a rubber isolator capable of sustaining large deflections is generally required to have large dimensions to attain a low unit strain. The result is a bulky isolator which is well adapted to support only relatively large loads.

(*b*) Where wide extremes of temperature are encountered, metal springs are advantageous. Special alloys are available for high-temperature operation and show little or no deterioration when subjected to temperatures of several hundred degrees Fahrenheit for long periods. At very low temperatures, metal does not show an appreciable increase in stiffness.

(*c*) Metal springs have little tendency to drift under continuous dead-weight load, provided that the material is not overstressed. This is a definite advantage obtainable with metal springs when compared with the continuously increasing deflection of rubber isolators.

(*d*) The cost of metal springs may be either relatively high or relatively low, depending on the application. The unit cost of metal springs manufactured in quantity is low. Where the springs can be made an integral part of a structure by utilizing existing members for spring seats, retainers, and attaching means, the cost of isolators may be relatively modest. Where the metal springs are embodied in detachable isolators, the cost can become high because the necessary spring seats, retainers, attaching means, and limiting means often are more costly than corresponding parts of isolators that employ rubber as the resilient material.

(*e*) Sound is transmitted relatively well through metal. An isolator that embodies a metal spring as the load-carrying element is not an effective sound isolator unless it includes sound-isolating material in series with the metal spring.

(*f*) A metal spring exhibits very little damping. Auxiliary damping means is thus required in conjunction with a metal spring where the service conditions demand a damped isolator.

(*g*) Calculation of the characteristics of metal springs has become much more of an exact science than the calculation of the properties of rubber isolators.

5·14 *Stiffness of Helical Compression Springs*

Metal springs are such commonly used components of mechanical devices that a detailed description here would seem trite. An excellent discussion of the many types of springs and their characteristics is contained in a book by A. M. Wahl,* to which the reader is referred for design data. Some of these data and formulae are correlated and presented in the following paragraphs for ready reference in the design of isolators. Certain specialized aspects of spring design which are of interest to the designer of isolators, notably stiffnesses and stability, are discussed in considerable detail. The subject of stress is not discussed, because an adequate treatment is included in available references.

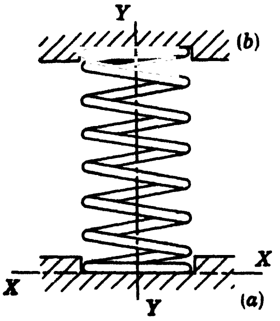

FIGURE 5.18.

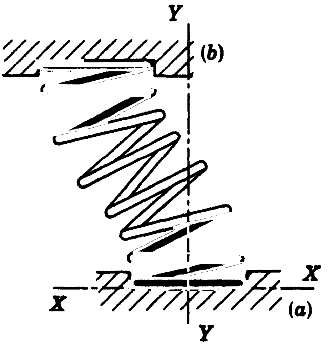

FIGURE 5.19.

FIGURE 5.18. Typical application of helical compression spring as a vibration isolator.

FIGURE 5.19. Lateral deflection of helical compression spring illustrated in Figure 5.18.

A typical application of a helical compression spring to an isolator is illustrated in Figure 5.18. The spring has squared and ground ends. It is placed between the support *a* and the mounted equipment *b*, often with no positive attachment but with cavities or other equivalent means to locate the spring. The springs constitute the sole support, vertically and laterally, for the mounted equipment. It is essential, therefore, that the springs have proper stiffnesses in both vertical and lateral directions, as determined by the analysis included in Chapter 2.

The stiffness of a helical spring in the direction of its axis, i.e., in the direction of the Y axis in Figure 5.18, is given by the following equation:

$$k_y = \frac{F_y}{\delta_y} = \frac{Gd^4}{8nD^3}, \tag{5.13}$$†

---

* A. M. Wahl, *Mechanical Springs*, Penton Publishing Co., Cleveland, 1944.

† This equation is derived by A. M. Wahl and presented on page 29 of *Mechanical Springs*.

where k_y = axial stiffness, lb/in.
F_y = applied axial force, lb.
δ_y = axial deflection resulting from force F_y, in.
G = modulus of elasticity of spring material in shear, psi.
d = diameter of spring wire, in.
n = number of active coils.
D = mean coil diameter, in.

The deflection of a helical spring in the direction of the Y axis results preponderantly from torsional strain of the spring wire. Lateral deflection of the spring in the direction of the X axis in Figure 5.19 embodies strain of the wire in both torsion and flexure. The analysis of lateral deflection becomes rather complicated; it has been carried out* for applications where the ends of the spring are constrained to remain parallel during deflection. The results of this analysis may be simplified by introducing the limitations that the spring be made of steel and that the cross section of the spring wire be circular. These limitations make possible the substitution of specific numerical values for the moduli of steel, and known relations for the cross section of the wire. It is assumed, for the moment, that the axial force F_y is zero. The following expression is then obtained for the stiffness in the direction of the X axis:

$$k_x = \frac{F_x}{\delta_x} = \frac{10^6 d^4}{nD(0.204h_s^2 + 0.256D^2)}, \tag{5.14}$$

where k_x = lateral stiffness, lb/in.
F_x = applied force normal to the spring axis, lb.
δ_x = deflection normal to axis in response to force F_x, in.
d = wire diameter, in.
n = number of active coils.
D = mean coil diameter, in.
h_s = working height of spring, in.

A definite relation thus exists between the stiffnesses of the spring in the directions of the X and the Y axes. This relation can be evaluated by dividing equation 5.13 by equation 5.14:

$$\frac{k_y}{k_x} = \frac{G(0.204h_s^2 + 0.256D^2)}{8 \times 10^6 D^2} \tag{5.15}$$

---

* A. M. Wahl, *Mechanical Springs*, Penton Publishing Co., Cleveland, 1944, page 179. Also see W. E. Burdick, F. S. Chaplin, and W. L. Sheppard, "Deflection of Helical Springs under Transverse Loadings," *Trans. A.S.M.E.*, Vol. 61, No. 7, October 1939, page 623.

Substituting the numerical value, $G = 11.5 \times 10^6$ psi, for the modulus of elasticity in shear, the following expression is obtained involving dimensionless ratios:

$$\frac{k_y}{k_x} = 1.44\left(0.204\frac{h_s^2}{D^2} + 0.256\right). \tag{5.16}$$

Equation 5.14 gives an expression for the lateral stiffness of a helical spring that neglects the influence of an axial load. The effect of an axial load is to increase the lateral deflection δ_x; i.e., to decrease the lateral stiffness k_x. The stiffness ratio k_y/k_x consequently is increased. Of the various corrections that have been proposed to compensate for axial load, the most suitable for present purposes appears to be the correction factor derived by Rausch.* The Rausch factor, designated by α, is a number always greater than unity by which equation 5.16 is multiplied as follows:

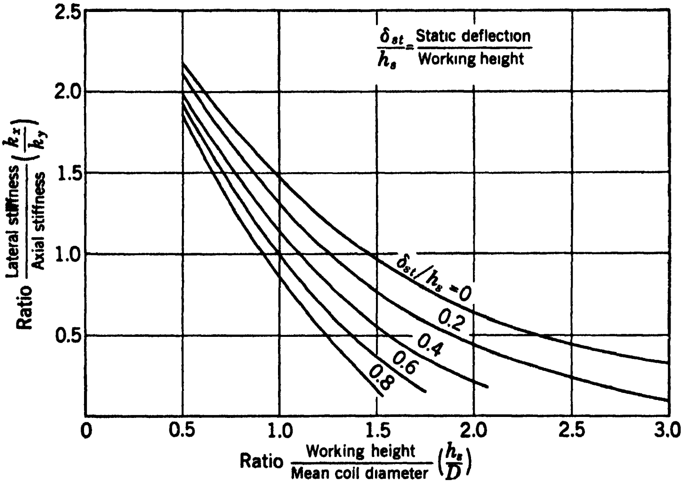

FIGURE 5.20. Ratio of lateral to axial stiffness for helical compression springs, as a function of the ratio of working height to mean coil diameter and the ratio of static deflection to working height. (*Journal of Applied Mechanics*, Vol. 14, No. 1, March 1947.)

$$\left(\frac{k_y}{k_x}\right)_c = 1.44\alpha\left[0.204\left(\frac{h_s}{D}\right)^2 + 0.256\right], \tag{5.17}$$

where the stiffness ratio is written $(k_y/k_x)_c$ to indicate the correction for axial load. The correction factor α is a function of the ratio h_s/D, working height to mean coil diameter, and of the ratio δ_{st}/h_s,* static deflection to working height. Equation 5.17 has been evaluated numerically, and the results are given in Figure 5.20. It should be noted that the stiffness ratio used as the ordinate parameter of this family of curves is the reciprocal of that given by equation 5.17; this is done in order to preserve correlation with the analysis given in Chapter 2.

---

* E. Rausch, "Die Steifigkeit von Schraubenfedern senkrecht zur Federachse," *Zeit. V.D.I.*, Vol. 78, No. 12, March 24, 1934.

5·15 Stability of Helical Compression Springs

One of the predominant applications of helical springs is for the isolation of low-frequency vibration. The natural frequency, and consequently the stiffness, of the mounting system must be low. With springs of low stiffness deflected as shown in Figure 5.19, the lateral stiffness of the springs may be insufficient to restore the mounted equipment to its initial position. The mounted equipment will then fall sideways as a result of instability of the springs. The necessary conditions to assure stability in such an installation have been investigated and are outlined briefly in the following paragraphs.

The stability of a system is determined by the energy relations existing within the system. Stable equilibrium exists when a system is in a condition of minimum potential energy. The stability of the system now being discussed is, therefore, analyzed by writing the equation for the change of potential energy as a function of horizontal deflection, and noting the conditions for which the energy increases and decreases as horizontal movement of the mounted equipment takes place. During horizontal deflection of the spring illustrated in Figure 5.19, the vertical stiffness decreases as a result of the eccentric load. The mounted equipment therefore is lowered, and its potential energy is reduced. If stability is to be maintained, this loss of potential energy must be at least balanced by an increase in strain energy in the spring. Increased strain energy in the spring results from (1) its horizontal deflection and (2) its increased vertical deflection. From this energy relation, it is found that the system is stable when

$$\frac{k_x}{k_y} \geq 1.20\left(\frac{\delta_{st}}{h_s}\right), \qquad (5.18)\dagger$$

---

* The static deflection δ_{st} is the deflection in the direction of the Y axis resulting from the weight of the equipment. In other words, $\delta_{st} = \delta_y$ when $W = F_y$.

† Details of the analysis leading to this equation are given by C. E. Crede and J. P. Walsh, "The Design of Vibration Isolating Bases for Machinery," *Trans. A.S.M.E.* (*Jour. App. Mech.*, Vol. 14, No. 1), March 1947.

where k_x = horizontal spring stiffness, lb/in.
k_y = vertical spring stiffness, lb/in.
δ_{st} = static deflection, in.
h_s = working height of spring, in.

Equation 5.18 is represented by a straight line which separates stable from unstable conditions, as shown graphically in Figure 5.21. The condition of stability is above, that of instability below, the line. The analysis indicates that a system that embodies stability in accordance with the criterion of Figure 5.21 is stable not only for small lateral displacements but also for displacements as great as 10 to 20 percent of the spring height.

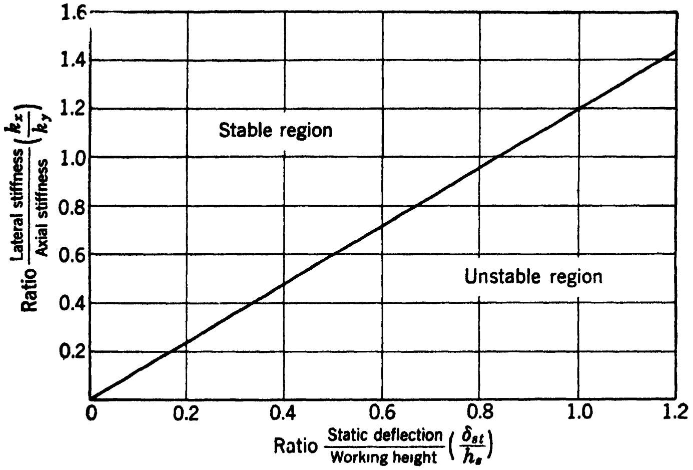

FIGURE 5.21. Curve that separates stable and unstable regions for a system whose sole support is comprised of helical springs loaded in compression. (*Journal of Applied Mechanics*, Vol. 14, No. 1, March 1947.)

Example 5.4. The above spring-design data are best illustrated by an example. Assume that it is desired to design a spring whose lateral stiffness is 50 percent of its vertical stiffness, and which is capable of sustaining a static deflection of two inches. In a cut-and-try procedure, several springs are selected, and the stability of each is investigated by use of Figure 5.21. Pertinent data on the springs are tabulated in Table 5.1.

Arbitrary values for the ratio δ_{st}/h_s, static deflection to working height, are assumed first; numerical values for the working height h_s are next calculated from these assumed ratios and from the desired static deflection, $\delta_{st} = 2$ in. The corresponding ratios h_s/D, working height to mean coil diameter, are then found from Figure 5.20 for the stiffness ratio $k_x/k_y = 0.5$. Values of mean coil diameter D are next calculated from the relation $D = h_s \div (h_s/D)$. The stability of each spring is noted from Figure 5.21. Two stable springs of different heights and diameters are thus available from which to choose. The free height is found by adding the working height h_s and the static deflection $\delta_{st} = 2$ in.

TABLE 5.1

DATA FOR SELECTING SUITABLE SPRING

$\dfrac{\delta_{st}}{h_s}$	h_s	$\dfrac{h_s}{D}$	D	Stability	Free Height
0.2	10	1.87	5.35	Stable	12
0.4	5	1.65	3.03	Stable	7
0.6	3.33	1.37	2.43	Unstable	5.33
0.8	2.5	1.23	2.03	Unstable	4.5

5·16 Stiffness of Helical Tension Springs

Helical springs are used in tension as well as in compression. Tension springs are more suitable than compression springs for some types of service, whereas the reverse is true for other types of service. The following factors should be considered in weighing the relative merits of the two methods of application:

(*a*) Tension springs may be less expensive for small and medium-size applications, particularly when an overhead support is available, because of the simplicity and convenience in attaching the end loops. On the other hand, a compression spring is often less expensive for mounting large and massive equipment where an overhead support is not used.

(*b*) A tension-spring application is always stable, in contrast to a compression-spring application having a large static deflection.

(*c*) Compression springs are much better adapted to control of the stiffnesses in various directions and should be used where the natural frequencies in the several modes of vibration are important.

(*d*) An excessive load is less likely to damage a compression spring, because the spring can be designed in such a manner that the coils close before the safe stress is exceeded. A tension spring, on the other hand, may yield when subjected to excessive load, unless auxiliary means are provided to restrict deflection of the spring.

A typical tension spring is illustrated in Figure 5.22. The half-loop ends are inserted through apertures in the attaching members. The expression for the axial stiffness of a helical compression spring, equation 5.13, also applies to the stiffness of a helical tension spring. Tension springs are often wound in such a manner that a certain tension load must be applied to the ends of the spring before the coils begin to separate. The magnitude of the force required to separate the coils is called initial tension. Equation 5.13 applies to all tension springs, with or without initial tension, provided that the applied force is greater than the initial tension.

When an equipment supported by tension springs is deflected laterally a distance x, the axis of the spring experiences a rotational displacement ϕ, as shown in Figure 5.22. If the weight of the supported body is designated as W, the horizontal force F_x required to maintain the displacement x is the horizontal component of the axial force in the spring:

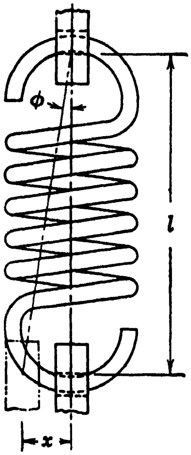

FIGURE 5.22.

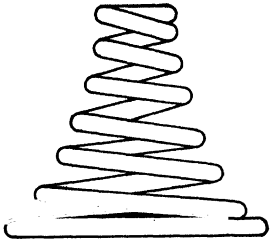

FIGURE 5.23.

FIGURE 5.22. Helical tension spring.
FIGURE 5.23. Conical compression spring.

$$F_x = W \tan \phi.$$

For a small horizontal displacement, $\tan \phi \approx \phi \approx x/l$, and the above equation becomes

$$F_x = \frac{Wx}{l}, \tag{5.19}$$

where l is the working length of the spring.

The horizontal stiffness k_x is the quotient obtained by dividing the restoring force F_x by the displacement x; the following expression for horizontal stiffness is then obtained from equation 5.19:

$$k_x = \frac{F_x}{x} = \frac{W}{l}. \tag{5.20}$$

The axial stiffness k_y, for a spring without initial tension, is obtained from the equation of static equilibrium:

$$k_y = \frac{W}{\delta_{st}}, \tag{5.21}$$

where δ_{st} is the static deflection of the spring resulting from the load W. The ratio of horizontal to vertical stiffness for a spring without initial tension is now obtained by dividing equation 5.20 by equation 5.21:

$$\frac{k_x}{k_y} = \frac{\delta_{st}}{l}. \tag{5.22}$$

For a spring with initial tension F_i, the equation of static equilibrium for a load W greater than the initial tension is:

$$W = F_i + k_y \delta_{st}', \tag{5.23}$$

where δ_{st}' is the deflection of the spring under the static load, measured from the closed position. An expression for the stiffness ratio k_x/k_y for a tension spring with initial tension is now written, using the expression for k_x given by equation 5.20 and an expression for k_y obtained from equation 5.23:

$$\frac{k_x}{k_y} = \frac{\delta_{st}'}{l}\left(\frac{W}{W - F_i}\right). \tag{5.24}$$

When there is no initial tension, $F_i = 0$ and $\delta_{st}' = \delta_{st}$. Equation 5.24 then becomes identical to equation 5.22.

It should be noted that the horizontal stiffness of a spring without initial tension is always less than the vertical stiffness, because the static deflection must always be less than the length of the spring under load. It is interesting to observe, also, that the stiffness ratio k_x/k_y can be influenced somewhat by changing the initial tension F_i. The stiffness ratio k_x/k_y is always small, however, for a tension spring; when k_x/k_y is required to approach unity, a compression spring should be used.

5·17 Constant Frequency Springs

It is pointed out in Section 4·2 that an isolator whose stiffness varies in proportion to the applied force has a natural frequency that remains constant, independently of the load. Such a stiffness characteristic is easy to attain with a metal spring. One type of spring that has been successfully used in this manner is the conical spring illustrated in Figure 5.23. The radii of the spring coils decrease continually as the height of the spring increases. It is characteristic of a coil spring that the stiffness increases as the coil radius decreases, and as the number of coils decreases. The application of a vertical load to the conical spring shown in Figure 5.23 causes a vertical deflection which is initially comprised largely of deflection of the outer coils. The outer coils thus become inactive because the clearance between the coils is closed, and the coils rest upon the supporting surface. The spring is now effectively comprised of fewer active coils of smaller diameter, and consequently it is stiffer. Further application of load causes additional coils to become inactive, with further stiffening of the spring. The several outermost coils are made to telescope so that they seat firmly upon the supporting surface. By careful design, a spring of the type illustrated in Figure 5.23 can be made to exhibit a constant natural frequency over a considerable load range.

C. OTHER MATERIALS

Isolators that utilize rubber or metal springs as the resilient media are more adaptable to analysis and rational design than isolators that employ other resilient materials. Felt, cork, and sponge rubber, for example, are used to a considerable extent, but reliable engineering data on these materials are difficult to obtain. Such information as is available is included in the following sections.

5·18 *Felt*

Felt is defined by the Felt Association as "a fabric built up by the interlocking of fibers by a suitable combination of mechanical work, chemical action, moisture, and heat, without spinning, weaving, or knitting. Felt may consist of one or more classes of wool fibers, with or without admixture with animal, vegetable, and synthetic fibers."* A distinction is thus made from textile products in which the fibers are drawn into parallelism, spun into yarns, and then interlaced by weaving. The felting process, on the other hand, induces the movement of individual fibers throughout the mass and utilizes the natural crimp and interlocking characteristics of the wool fiber. The result is a well-compacted fibrous material made in a range of thicknesses from $\frac{1}{32}$ inch to three inches, and in widths as great as 72 inches.

Felt usually is applied for isolation purposes by cutting small pads of the desired area and placing them under the equipment to be supported. This is done in such a manner that the felt is loaded in compression. Accepted methods of applying the felt are (1) cementing the felt to the mounted machine and to the floor or (2) lagging the machine to the floor, using felt washers to isolate the lag screws from the machine. The cement application has many advantages since adhesives are available that have great strength but are readily dissolved when desired by an available solvent. The consequent elimination of bolts and lag screws is a desirable feature in that there are no marred floors upon removal of the equipment, and no labor is expended in installing the bolts. The latter factor is a pronounced advantage, particularly on concrete floors.

---

* Private correspondence from American Felt Company to the author, November 30, 1948.

The property of felt that is most relevant to the isolation of vibration and shock is its behavior when subjected to a compressive force.

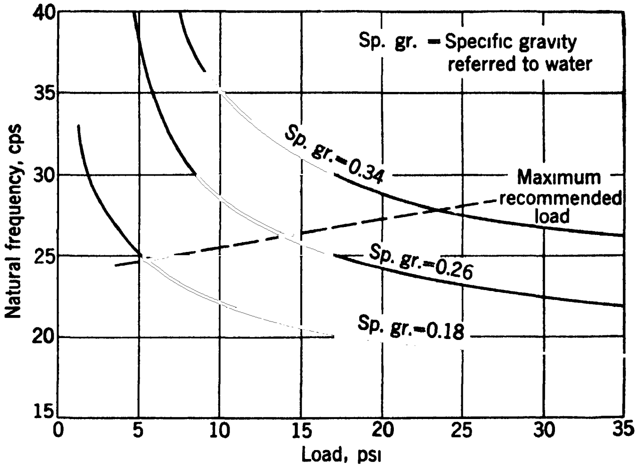

FIGURE 5.24. Natural frequency as a function of load for several weights of felt *one inch thick.* For other thicknesses, see Figure 5.25. (Courtesy American Felt Company.)

The force-deflection curve for a felt pad in compression is fairly linear for deflections as great as 25 percent of the thickness, but thereafter the stiffness increases rapidly, and at 50 percent deflection is approximately ten times as great as at 25 percent deflection. This stiffness increase at deflections greater than 25 percent shows the necessity of exercising care to avoid overloading the felt.

In the application of felt as isolators, the natural frequency of the mounted equipment when supported by the felt is significant. Figure 5.24 shows the natural frequency as a function of load for three densities of felt which are recommended for isolation purposes. The natural frequencies are for a felt pad one inch thick. When the thickness of the felt is greater or less than one inch, the natural frequencies given by Figure 5.24 must be modified by the factor given in Figure

5.25.* It is evident that the decrease in natural frequency as the felt thickness increases is not as pronounced as with rubber, whose stiffness is inversely proportional to its thickness. For example, an increase in felt thickness from one inch to four inches causes a reduction in natural frequency to only 0.66 times the original natural frequency. A decrease to 0.50 times the original natural frequency would be expected.

Available engineering information on the dynamic properties of felt is limited largely to natural-frequency data of the type shown in

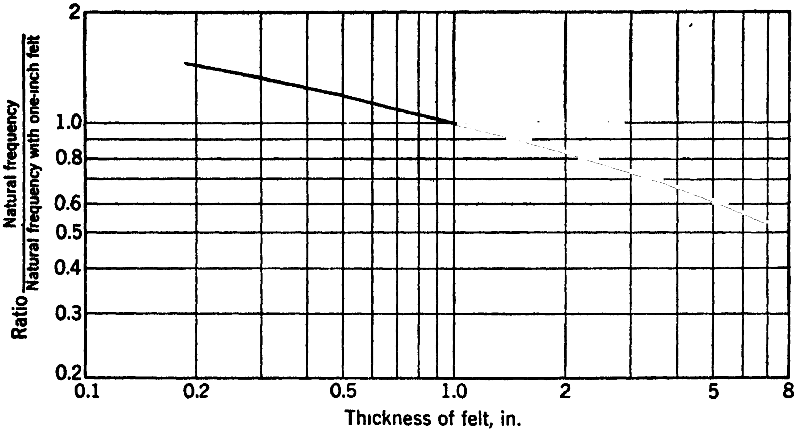

FIGURE 5.25. Ratio of natural frequency with felt of different thicknesses to natural frequency with felt one inch thick. Numerical values for natural frequencies with felt one inch thick are given in Figure 5.24.

Figures 5.24 and 5.25. It is difficult to interpret such data, because it has not been established that the relations between natural frequency and transmissibility developed in Chapter 2 are applicable to felt. There is some evidence that they are not, and caution should be exercised in predicting the transmissibility on the basis of natural frequency alone. There seems little question, however, that available natural-frequency data may be employed to estimate the minimum vibration frequency for which isolation may be achieved.

The curves in Figure 5.24 appear to be substantially horizontal in the extreme right-hand region. A condition thus exists in which the natural frequency cannot be further reduced by an increase in load. The minimum attainable natural frequency is approximately 19 to 26 cps, depending on the density; but the minimum natural frequency corresponding to maximum recommended loading is 25 to 28 cps. This is based on a felt thickness of one inch; minimum natural frequencies for other thicknesses of felt are obtained by multiplying these values by the factor given in Figure 5.25. For a felt thickness of ½ inch, the minimum usable natural frequency is 25 × 1.2 = 30 cps. As shown in Section 2·1 of Chapter 2, isolation is obtained only for frequencies greater than 1.41 times the natural frequency. Felt of ½-inch thickness may thus be considered useful only for isolating vibration whose frequency is greater than 30 × 1.41 = 42.3 cps.

---

* The curve given in Figure 5.25 was calculated from data on dynamic compliance given by F. G. Tyzzer and H. C. Hardy, "The Properties of Felt in the Reduction of Noise and Vibration," *Jour. Acous. Soc. Am.*, Vol. 19, No. 5, September 1947.

The properties of felt would seem reasonably well adapted to the isolation of shock and sound, although no information is available in the technical literature to prove the effectiveness of felt for such applications. The general requirements for shock and sound isolators are discussed in Chapter 3, and in Section 4·12 of Chapter 4, respectively.

5·19 Cork

Cork is often used with considerable success for the isolation of vibration, shock, and sound. It is generally used in the form of slabs which are made by compressing cork particles under high pressure and subsequently baking them by means of superheated steam. Cork differs from rubber in that the particles contain many minute air cells which become reduced in volume as the cork is deflected. Furthermore, the air spaces between the particles are reduced in size as a load is applied to the cork. The material is thus not an incompressible solid but, on the contrary, has been deflected in compression as much as 24 percent without exhibiting noticeable lateral expansion. Its application as an isolating material has been limited largely to the mounting of industrial machinery, some of which has been of relatively large size. It is applied as slabs loaded in compression by placing the slabs directly under the base of the machine or, if additional floating mass is required, under a concrete foundation to which the machine is rigidly mounted. An arrangement of the latter type is shown in Figure 6.14 of Chapter 6.

The stiffness of cork is relatively great, and most applications require the area of the cork to be only a fraction of the base area of the machine or floating foundation that is to be supported. Consequently, the cork is commonly applied in the form of spaced pads. Several conventional procedures are in common use for attaining this result:

(*a*) Where the cork is used directly under a machine or under a preformed concrete foundation, pads of the required area and thickness are located in such a manner as to facilitate the installation and to provide the necessary stability for the machine.

(*b*) Where a concrete foundation is poured subsequent to the placing of the cork, the pads may be set in position and a sheet-metal tank, which is to constitute a permanent form for the concrete foundation, may then be set upon the pads. Upon filling the tank with concrete, a floating foundation has become fabricated and rests upon spaced pads of cork.

(*c*) The result attained by the procedure outlined in (*b*) above can be accomplished by setting the cork pads in position and filling the space between the pads with sand to the level of the upper faces of the pads. The concrete is then poured directly upon the cork and sand; after the concrete has set, the sand is flushed out and the concrete foundation is left supported by the spaced cork pads.

Cork exhibits the same properties as most other resilient materials when loaded in compression and subjected to a great deflection. The stiffness is characterized by a continuing increase as the deflection increases, and a limit is consequently placed upon the minimum natural frequency that is attainable. From a practical standpoint, the maximum load is that which the cork can safely support without being overstressed, and the point of minimum natural frequency is never reached. Quantitative data on the isolating properties of cork are difficult to find in the technical literature. The following data on Vibracork, a cork board made by compressing cork particles one-half inch in diameter, was made available through the courtesy of the Armstrong Cork Company.

The natural frequency of Vibracork as a function of supported load is shown by the curves of Figure 5.26. These curves are for thicknesses of two and four inches, and for densities ranging from 1.11 to 1.66 pounds per board foot.* It is characteristic of many engineering materials used in compression that the stiffness varies inversely as the thickness, and that the natural frequency varies directly as the square root of the stiffness. (See equation 2.16.) The curves of Figure 5.26 show a ratio of only approximately 1.2 to 1 for the natural frequencies of cork of two- and four-inch thicknesses. It thus appears that the anticipated advantage of a lower natural frequency obtained from cork of greater thickness is only partially achieved.

---

* A board foot is the volume of a solid one foot square and one inch thick. A slab of cork 6 inches square and 4 inches thick is thus one board foot.

Cork appears to exhibit peculiar properties that tend to make it less effective as an isolation medium than indicated by the natural frequencies shown in Figure 5.26. To determine the transmissibility under steady-state vibration of a system that employs cork as the resilient element, the natural frequencies indicated by Figure 5.26 should first be multiplied by 1.5. The transmissibility at frequencies higher than the natural frequency may then be determined from equation 2.15 or Figure 2.2, using the corrected natural frequency. It is desired to determine, for example, the transmissibility of four-inch-thick Vibracork of 1.66 pounds per board foot density, when loaded with 40 psi and subjected to vibration at a frequency of 40 cps. From Figure 5.26, it is determined that the natural frequency of the system is 14.0 cps. The corrected natural frequency is then 14.0 × 1.5 = 21.0 cps, and the ratio of forcing frequency to corrected natural frequency is 40 ÷ 21 = 1.90. The transmissibility, as obtained from Figure 2.2 for a frequency ratio of 1.90, is 0.38. This is in good agreement with the transmissibility of the cork as determined experimentally.

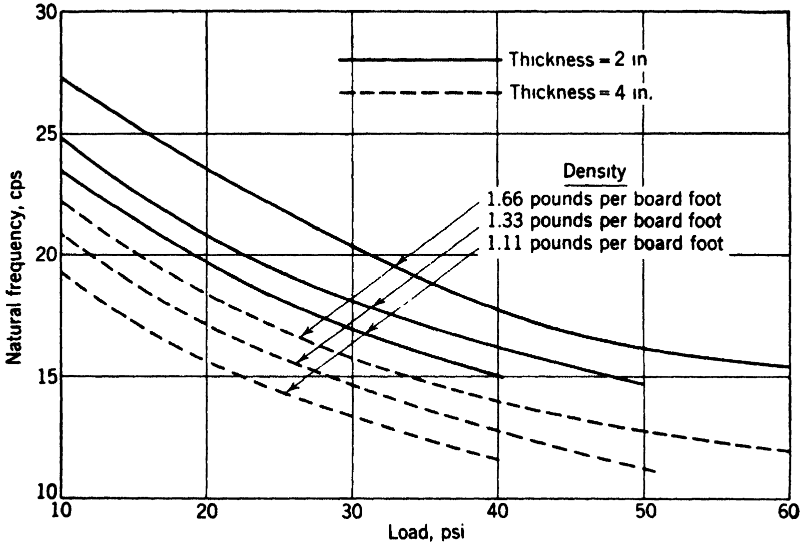

FIGURE 5.26. Natural frequencies of several densities of Vibracork as a function of load. The solid lines refer to material 2 inches thick, and the dotted lines to material 4 inches thick. (Courtesy Armstrong Cork Company.)

The logarithmic decrement Δ for cork loaded in compression is approximately 0.40, independently of the density. This corresponds to a damping ratio c/c_c of 0.064, and a transmissibility at resonance of approximately eight times. The damping of cork is thus equivalent to that of rubber in the range of 50 to 60 durometer.

Available data on the drift of cork subjected to a continuous deadweight load are summarized in Figure 5.27. The drift characteristics of cork appear similar to those of rubber, in that the deflection-time curve is a substantially straight line when plotted to double logarithmic coordinates. The available drift data for cork do not extend beyond 100 days, in contrast to corresponding data for rubber extending over a period of years. Deflection-time curves are shown in Figure 5.27 for two-inch thick Vibracork of 1.11 pounds per board foot density subjected to several different loading pressures. The similarity between the curves of Figures 5.13 and 5.27 is evident.

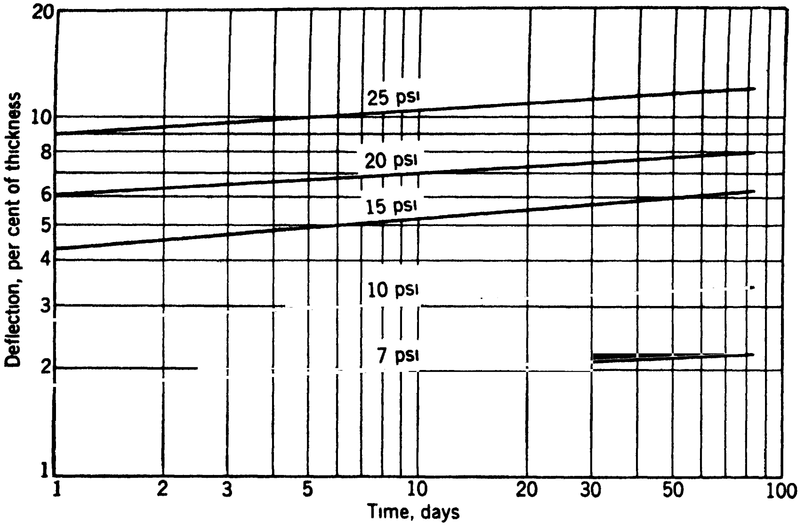

FIGURE 5.27. Deflection as a function of time for Vibracork of 2-inch thickness and 1.11 pounds per board-foot density, loaded at several different unit loads. (Courtesy Armstrong Cork Company.)

The principal limitations of cork as compared with rubber for isolation purposes are (1) a rather small range of available stiffnesses and (2) a lack of adaptability from an application standpoint. Whereas rubber can be molded in many complex shapes and can be loaded in compression, shear, or flexure, cork is available only in slab form and is capable of carrying a load only in compression. Vibracork is classified as light, which includes densities from 1.0 to 1.4 pounds per board foot, and heavy, which includes densities from 1.4 to 1.7 pounds per board foot. Maximum recommended loading is 30 psi for light-density and 60 psi for heavy-density Vibracork.

5·20 *Sponge Rubber*

Rubber in its conventional vulcanized state is a substantially incompressible though flexible solid with considerable stiffness. To reduce the stiffness and to introduce certain advantages derived from compressibility, rubber is made with a multiplicity of minute air or gas pockets. Upon application of load, the air or gas is compressed, and the overall stiffness of the material is thus relatively low. Sponge rubber is molded generally in the form of slabs of constant thickness and large area, which can be cut into pads of the required area. It is also occasionally molded in the form of intricate shapes for use in isolators. Possible variations, not only in the stiffness of the rubber used but also in the percentage of the volume devoted to voids, create problems in quality control which detract from the usefulness of the molded material as a component of isolators.

Although the use of specially molded sponge rubber parts is not to be particularly encouraged, sponge rubber in slab form is a satisfactory material for many applications. It is available in a wide range of stiffnesses as indicated in Table 5.2.*

TABLE 5.2

STIFFNESS DATA FOR SPONGE RUBBER

Designation	Compression Load for 25 Percent Deflection, psi
10	1 ± 1
11	3.5 ± 1.5
12	7 ± 2
13	11 ± 2
14	15 ± 2
15	20½ ± 3½

The designation numerals in Table 5.2 are prefixed by RN to indicate natural rubber, by RS to indicate a non-oil-resistant synthetic rubber, and by SC to indicate an oil-resistant synthetic rubber.

BIBLIOGRAPHY

AMERICAN FELT CO., "Vibration Isolation with Felt and Vibramounts," *Data Sheet* No. 10, September 1947.

ASTM Tentative Specification for Cellular Rubber Products, Designation D 798-46aT, issued 1944.

BROWN R. W., "Engineering Properties of Rubber in Compression," *S.A.E. Jour.* (*Trans.*), Vol. 47, No. 4, October 1940.

---

* Data in the table are taken from *ASTM Tentative Specification for Cellular Rubber Products*, Designation D 798-46aT, issued 1944.

BURDICK, W. E., F. S. CHAPLIN, and W. L. SHEPPARD, "Deflection of Helical Springs Under Transverse Loadings," *Trans. A.S.M.E.*, Vol. 61, No. 7, October 1939.

CHILTON, E. G., "Large Deformations of an Elastic Solid," *Trans. A.S.M.E.* (*Jour. App. Mech.*, Vol. 15, No. 4), December 1948.

COOK, W. J., and P. C. CLARKE, "The Negative Spring—A Basic New Elastic Member," *Prod. Eng.*, Vol. 20, No. 7, July, 1949.

CREDE, C. E., and J. P. WALSH, "The Design of Vibration-Isolating Bases for Machinery," *Trans. A.S.M.E.* (*Jour. App. Mech.*, Vol. 14, No. 1) March 1947.

EISENHOUR, B. E., and F. G. TYZZER, "Elastic Properties of Various Materials and Their Effect on the Transmission of Vibrations," *Jour. Frank. Inst.*, Vol. 214, No. 6, December 1932.

HARINGX, J. A., "The Practical Construction of Vibration-Free Mountings with Auxiliary Mass," *Philips Tech Rev.*, Vol. 9, No. 3, March 1947.

HAUSHALTER, F. L., "The Mechanical Characteristics of Rubber," *Trans. A.S.M.E.*, Vol. 61, No. 2, February, 1939.

HENKEY, H., "Elastic Behavior of Vulcanized Rubber," *Trans. A.S.M.E.*, Vol. 55 (APM-55-8), 1933.

HIRSHFELD, C. F., and E. H. PIRON, "Rubber Cushioning Devices," *Trans. A.S.M.E.*, Vol. 59, No. 6, August 1937.

HOLLAND, C. J., "Volute Spring Formulas," *Trans. A.S.M.E.*, Vol. 65, No. 5, July, 1943.

JACK, W., and J. S. PARKINSON, "A Method for Evaluating Compliant Materials in Terms of Their Ability to Isolate Vibrations," *Jour. Acous. Soc. Am.*, Vol. 9, No. 2, October, 1937.

KEYS, W. C., "Vibration and Rubber Springs," *Mech. Eng.*, Vol. 64, No. 3, March 1942.

KEYS, W. C., "Rubber Springs," *Mech. Eng.*, Vol. 59, No. 5, May 1937.

KOSTEN, C. W., "Static and Dynamic Properties of Rubber Under Compression," *Proc. Rubber Tech. Conf.*, London, 1938.

KROTZ, A. S., and W. B. FAGEOL, "Torsion Rubber Spring Design With Automotive Applications," *Prod. Eng.*, Vol. 17, No. 7, July 1946.

LEHMBERG, W. H., "Mechanical Properties and Uses of Wool Felt," *Mech. Eng.*, Vol. 67, No. 2, February 1945.

MADDEN, B. C., "Effectiveness of Shear-Stressed Rubber Compounds in Isolating Machinery Vibration," *Trans. A.S.M.E.*, Vol. 65, No. 6, August 1943.

MCWHORTER, J. F., "Comparing Rubbers," *Mach. Des.*, Vol. 20, No. 2, February 1948.

MOFFITT, J. A., and A. PANAGROSSI, "Silicone Rubbers," *Machine Design*, Vol. 18, No. 9, September 1946.

MOONEY, M., W. E. WOLSTENHOLME, and D. S. VILLARS, "Drift and Relaxation of Rubber," *Jour. App. Phys.*, Vol. 15, No. 4, April 1944.

RAUSCH, E., "Die Steifigkeit von Schraubenfedern senkrecht zur Federachse," *Zeit. V. D. I.*, Vol. 78, No. 12, March 24, 1934.

ROELY, H., "Dynamic Evaluation of Damping and Durability of Rubber Compounds," *Proc. Rubber Tech. Conf.*, London, 1938.

SAUER, C., and J. F. MCWHORTER, "Molded Rubber Parts—Factors in Their Design," *Mach. Des.* Vol. 17, No. 7, July 1945.

SERVAIS, P. C., "Silastic—The Heat Stable Silicone Rubber," *Rubber Age*, Vol. 58, No. 5, February 1946.

SMITH, J. F. D., "Rubber Mountings," *Trans. A.S.M.E.* (*Jour. App. Mech.*, Vol. 5, No. 1), March 1938.

SMITH, J. F. D., "Rubber Springs—Shear Loading," *Trans. A.S.M.E.* (*Jour. App. Mech.*, Vol. 6, No. 4), December 1939.

SMITH, J. F. D., "Rubber Springs Under Compression Loading," *Mech. Eng.*, Vol. 63, No. 4, April 1941.

SMITH, J. F. D., "Rubber Springs—Shear Loading—II," *Trans. A.S.M.E.*, Vol. 70, No. 3, April 1948.

TYZZER, F. G., and H. C. HARDY, "The Properties of Felt in the Reduction of Noise and Vibration," *Jour. Acoust. Soc. Am.*, Vol. 19, No. 5, September 1947.

UNITED STATES RUBBER CO., *Absorbing Vibration, Noise, Impact*, New York, 1942.

UNITED STATES RUBBER CO., *Some Physical Properties of Rubber*, New York, 1941.

WAHL, A. M., *Mechanical Springs*, Penton Publishing Co., Cleveland, Ohio, 1944.

CHAPTER SIX

Particular Applications of Isolators

This chapter is comprised primarily of a practical discussion of isolators as applied to particular types of equipment. The operation of the equipment is analyzed where necessary to establish a basis for the discussion of isolator application. The minimum of the theory of isolation is included, but frequent reference is made to the analyses set forth in preceding chapters to establish the basic validity of the proposed applications. The equipment and machines discussed in this chapter are arbitrarily grouped for expediency, but pertinent information on a particular application may be found in two or more sections. Cross references to related discussions are included.

6·1 Low-Speed Machinery

The design of isolators for low-speed machinery requires special attention to avoid the pitfall of a system that is either unstable or too unsteady for practical use. The meaning of the term "low speed" is somewhat indefinite, because it depends on the required steadiness of the machine and on the feasibility of decoupling the natural modes of vibration. Many common types of machines may be in the low-speed category, including pumps, compressors, fans, and large diesel engines. The forces created by the operation of such machines are sometimes of a harmonic* nature, as with reciprocating or unbalanced rotating members, and sometimes involve irregular forces of a periodic nature, as the gas pressure in internal combustion engines or the force on the dies of metal-working machinery. Regardless of the exact nature of the forces, if the period is constant and of relatively long-time duration, the machine falls in the low-speed category.

---

* See Section 1·2 of Chapter 1 for a definition of harmonic motion.

Assuming that the forces occurring at the low frequency are to be isolated, a primary limitation on the design of isolators is readily established. It is a necessary but not a sufficient condition that the static deflection indicated in Figure 2.5 be attained. The relation between static deflection and natural frequency is simple only for vibration in the vertical translatory mode. At least one of the other natural frequencies is usually higher than the natural frequency in the vertical translatory mode unless decoupling of natural modes of vibration* can be attained by locating the isolators in a plane that includes the center of gravity of the machine. The curves of Figure 2.5 therefore indicate a minimum static deflection. Assuming, for example, a forcing frequency of 8 cps and a desired transmissibility of 0.2, it is seen that a static deflection of at least 0.9 in. is required. This corresponds to a maximum natural frequency of 3.3 cps in the vertical translatory mode, as obtained from Figure 2.4.

Machinery is commonly designed to rest upon a floor or other horizontal member, and the only convenient location for isolators is under the machine. The nature of the relation among the several natural frequencies for this type of installation is indicated by Figure 2.11. One of the natural frequencies is usually greater than the natural frequency in vertical translation, and it tends to increase as the ratio of horizontal to vertical stiffness of the isolators increases. It may be assumed that the maximum desirable natural frequency in any mode is generally equal to the natural frequency of 3.3 cps as determined above. This may not always be true, because the relations indicated by Figure 2.5 do not apply to vibration in coupled modes. The contribution of coupled modes to force transmissibility is shown in Figures 2.13 and 2.14 for two special cases. The natural frequency in vertical translation, however, must be lower than 3.3 cps, and the static deflection therefore must be greater than 0.9 in.

Care should be exercised in designing isolators for a large static deflection to ensure that the resulting system is stable. When the static deflection is of the order of one inch, metal springs constitute the preferred resilient medium. Helical compression springs are convenient to design and manufacture and can be adapted to a wide range of applications. Data on the stability of a body supported on helical compression springs are given in graphical form in Figures 5.20 and 5.21. A large static deflection tends toward instability, and a low ratio k_x/k_y, horizontal to vertical stiffness, shows the same tendency. If the ratio k_x/k_y is increased in an attempt to gain stability, the maximum coupled natural frequency indicated by Figure 2.11 is increased relative to the vertical natural frequency. To avoid increasing the maximum natural frequency, the vertical natural frequency must be decreased and the static deflection correspondingly increased. Thus the step taken toward stability by increasing the stiffness ratio k_x/k_y results in a step toward instability as a result of the increase in static deflection. The difficulty of breaking this vicious circle suggests a different approach.

---

* See Section 2·10 of Chapter 2 for a discussion of decoupled modes of vibration and equal natural frequencies.

The dilemma described in the preceding paragraph arises partly from the fact that one of the coupled natural frequencies is greater than the natural frequency in the vertical translatory mode. The necessary conditions for attaining equality among the several natural frequencies are indicated by Figure 2.8. It is shown in Section 2·10 of Chapter 2 that such equality is achieved if the various parameters are arranged so that the system is defined by the intersection of the two lines designated $a/\rho = 0$. It is thus required that (1) $a/\rho = 0$, (2) $k_x/k_y = 1$, and (3) $\rho/b = 1$. This is a special case in which vibration in the horizontal and the vertical translatory modes and in the rotational mode in the plane perpendicular to the Z axis are mutually decoupled. The physical significance of these conditions is that the isolators be located in a horizontal plane passing through the center of gravity of the mounted equipment; that the distance between isolators be twice the radius of gyration of the equipment; and that the stiffness of the isolators be equal for a displacement in either the horizontal or the vertical direction.

Possible methods of achieving this arrangement depend on the nature of the machine to be mounted. A method that may be satisfactorily adapted to a wide range of machines is illustrated in Figure 6.1.* The machine is securely attached to a concrete foundation supported by helical springs. The cross section of the foundation is T-shaped, and the downward-extending mass of concrete in the center lowers the center of gravity of the machine-and-foundation assembly to a plane passing through the mid-height† of the helical springs. The shape of the foundation is such that the horizontal distance between springs, measured both crosswise and lengthwise, may be made equal to twice the radii of gyration in the respective planes. It is usually possible to design a helical spring with a stiffness ratio k_x/k_y = unity. All natural frequencies in modes that involve motion in planes perpendicular to the horizontal principal axes of inertia are now equal, and an optimum compromise between stability and performance results.*

---

* A detailed discussion of methods used in designing this type of base is given by C. E. Crede and J. P. Walsh, "Design of Vibration Isolating Bases for Machinery," *Trans. A.S.M.E.* (*Jour. App. Mech.*, Vol. 14, No. 1), March 1947. Also see United States Patent 2,468,043 for "Article Supporting Structure," granted to C. E. Crede and J. P. Walsh on April 26, 1949.

† Refer to the comment following equation 2.22 in Chapter 2 for a brief discussion of this.

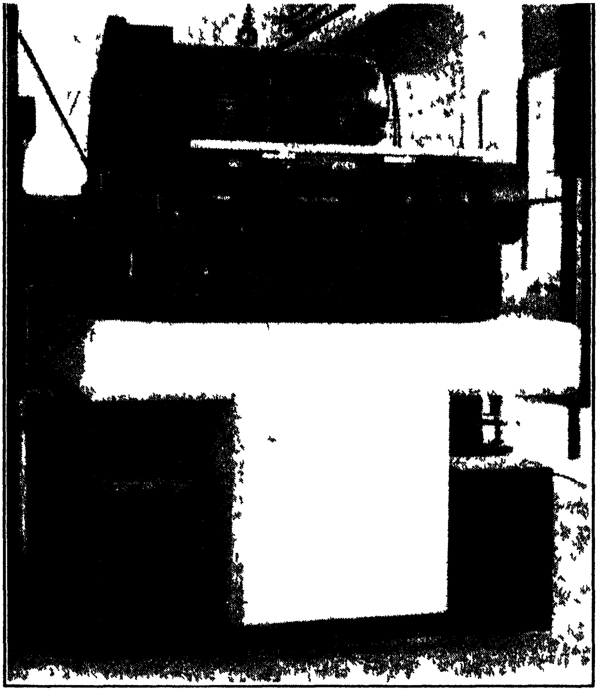

FIGURE 6 1. Machinery support comprised of floating concrete foundation and helical springs located in horizontal plane which passes through center of gravity of machine-and-foundation assembly (Official United States Navy photograph *Journal of Applied Mechanics*, Vol. 14, No. 1, March 1947.)

The mounting arrangement illustrated in Figure 6.1 requires that the machine be mounted upon a floating concrete foundation; that substantial mass be otherwise added to the machine in such a manner as to lower the center of gravity; or that the isolators be located near the mid-height of the machine (see Figure 6.6). This is not always feasible or desirable. An arrangement that can be made to operate satisfactorily under certain conditions is discussed in Example 2.1 of Chapter 2 and illustrated in Figure 2.12. The mounted machine is supported by relatively long beams which span the distance between isolators. This arrangement achieves the basic advantage of the T-shaped foundation, in that the required static deflection of the isolators may be held to a minimum. The distance between isolators is made so great that one of the coupled natural frequencies in the plane perpendicular to the Z axis, referring to Figure 2.12, is substantially greater than the operating frequency; the other coupled natural frequency and the vertical natural frequency are less than the operating frequency.

---

* Another design of concrete base is shown by S Rosenzweig, "Theory of Elastic Engine Supports," *Trans. A S M.E.*, Vol. 61, No. 1, January 1939.

The mechanics of operation may be envisioned in a physical sense by noting that the isolators are located at the ends of relatively long arms. The position of the axis of rotation is indicated by Figure 2.15. The axis of rotation, for motion in a plane perpendicular to the Z axis, is a small distance above the center of gravity when the frequency ratio ω/Ω_y is between three and four. The force F is thus applied close to the axis of rotation. The system is analogous to a bell crank pivoted at the axis of rotation; the force is applied at the shorter arm, and the isolator, being at the end of the longer arm, applies a smaller force to the support. Force reduction in one of the coupled modes may thus be considered to be attained through an arrangement of levers; the natural frequencies in the other coupled mode and in the vertical translatory mode are lower than the operating frequency, and force reduction is obtained by the conventional process of vibration isolation.

The limitations embodied in the arrangement of spaced isolators illustrated in Figure 2.12 must be recognized. Force reduction by means of lever arms is limited by attainable ratios of arm lengths. A definite limit is thus placed on transmissibility, as contrasted to conventional isolation wherein transmissibility decreases almost without limit as the natural frequency is decreased. This may not be a serious disadvantage where the forces resulting from operation of the machine are small. In reciprocating machinery, for example, major forces are predominantly in the direction of piston motion; transverse forces are relatively minor. An arrangement that employs spaced isolators may be used for the reduction of minor forces, and conventional isolation methods may be used where major forces are involved. It is significant to note that spaced isolators may be useful in avoiding a resonant condition, even though no force reduction is attained.

Another disadvantage of the arrangement of spaced isolators shown in Figure 2.12 is its lack of adaptability to variations in operating speed. It is difficult to formulate a general rule in this respect, but the principle is illustrated by Figure 2.13. A minimum transmissibility is attained in this instance at a forcing frequency of approximately three times the vertical natural frequency. For higher and lower forcing frequencies, the transmissibility increases. This method of force reduction is thus useful only for machines of substantially constant speed, in contrast to the arrangement of Figure 6.1 whose effectiveness continues to increase as the operating speed increases. A further possible disadvantage of spaced isolators is the excessive floor area required for the installation.

In conclusion, vibration isolators for low-speed machinery generally embody features that are often considered unattractive for one reason or another. The peculiar difficulties of the problem should be recognized, and the various advantages and disadvantages associated with the several available mounting arrangements should be carefully considered.

6·2 *Kinematics of Reciprocating Machines*

The machines considered in this section are of the type that effect a transformation of rotational motion to, or from, reciprocating motion. The machine may be driven by the reciprocating motion, as an internal combustion engine, or by the rotational motion, as an air compressor. The essential moving elements of such a machine are a piston, a crank, and a connecting rod. Vibration of the machine may result from the gas pressure applied periodically to the piston, and from the inertia forces associated with the moving parts. It will be shown that the inertia forces and couples may be substantially balanced in certain types of multi-cylinder machines, but inherently unbalanced in one- or two-cylinder machines. The gas pressure acting upon the piston reacts on the chassis of the machine in the form of a couple which is transmitted to its support. The nature of these various forces and couples is considered in subsequent paragraphs.

The forces and couples resulting from the gas pressure are illustrated by reference to the single-cylinder, internal combustion engine shown in Figure 6.2 (*a*). The engine is driven by the expanding gas confined between the piston and cylinder head. The resultant force acting on the piston is the product of the unit pressure and the area of the piston; it is indicated by F. Referring to Figure 6.2 (*b*), the reaction to the force F may be resolved into a force $F/\cos\theta$ applied along the line of the connecting rod and a horizontal force $F\tan\theta$. The force $F/\cos\theta$

is applied to the crank pin and combines with the crank arm to form a couple

$$M_s = \frac{Fr \cos \phi}{\cos \theta}, \tag{6.1}$$

which tends to rotate the crankshaft. The force $F/\cos \theta$ at the crankshaft bearing is resolved into a vertical component F and a horizontal component $F \tan \theta$.

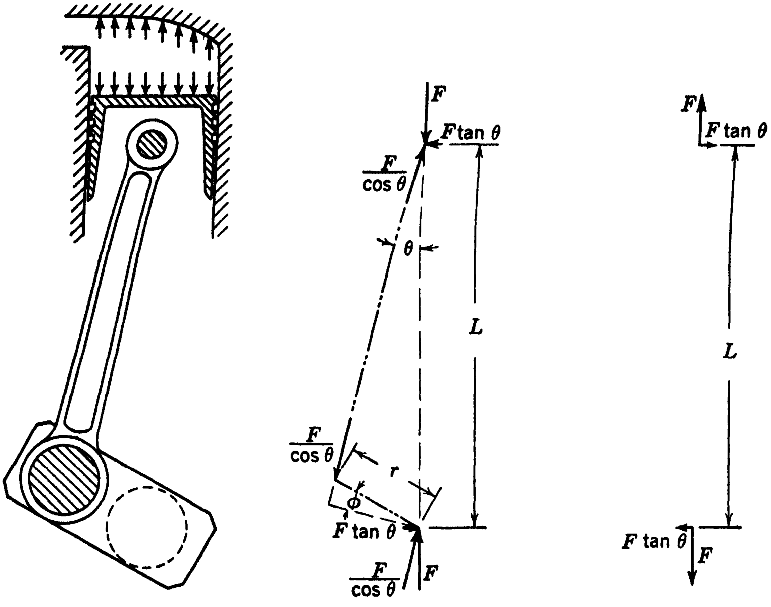

(a) (b) (c)

FIGURE 6.2. Cross section through a cylinder of an internal combustion engine, and diagrams showing forces resulting from gas pressure in the engine.

The resultant forces applied to the engine chassis are shown in Figure 6.2 (*c*). The force F acting upwardly on the cylinder head is balanced by a numerically equal, downward-directed force acting on the crankshaft bearing. The summation of vertical forces for a single cylinder is thus zero. The rightward-directed horizontal force $F \tan \theta$ applied to the cylinder wall is numerically equal to the leftward-directed force applied to the crankshaft bearing. These forces are spaced a vertical distance L apart, and thereby they exert a couple upon the engine chassis defined by

$$M_f = FL \tan \theta. \tag{6.2}$$

From the geometry of the system, Figure 6.2 (*b*), it is apparent that $L = r \cos \phi / \sin \theta$. Substituting this expression for L in equation 6.2 above, the couple M_f is given by

$$M_f = \frac{Fr \cos \phi}{\cos \theta}. \tag{6.3}$$

This is identical to the expression for the couple M_s, equation 6.1, showing that each fluctuation in the magnitude of the couple applied to the crankshaft is reflected at the support for the engine.

The magnitude of the couple M_f varies with time in the manner prescribed by the time variation of the force F. This force periodically reaches a maximum at a frequency governed by the rotating speed of the engine, the number of cylinders, and the nature of the operating cycle. The so-called two-cycle internal combustion engine, more properly a two-stroke-cycle engine, has a power stroke once for each cylinder per revolution. The couple M_f reaches a maximum at each power stroke. The four-cycle, or four-stroke-cycle, engine has a power stroke for each cylinder once during each two revolutions. An air compressor or vacuum pump generally has a power stroke for each cylinder once per revolution of the shaft. The couple applied to the crankshaft of a typical six-cylinder, four-stroke-cycle gasoline engine running at 2,500 rpm is shown by the curves of Figure 6.3. The couple resulting from the gas pressure in each pair of cylinders is indicated by a line of distinct character, from which it is evident that each pair of cylinders produces a couple once in two revolutions. The resultant couple acting on the shaft is the summation of the couples from the individual cylinders, as indicated by the heavy line in Figure 6.3. The peaks of the resultant curve occur at the firing frequency;

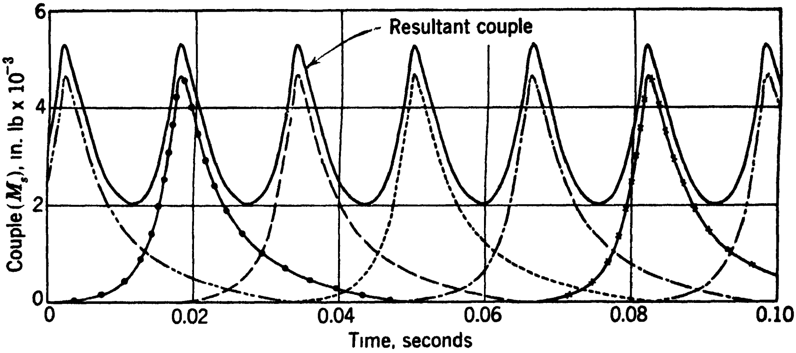

FIGURE 6.3. Time history of couple applied to crankshaft of typical six-cylinder, four-stroke-cycle gasoline engine running at 2,500 rpm.

i.e., at the product of rotational frequency and total number of power strokes per revolution.

The kinematics of the mechanism being considered is illustrated by Figure 6.4. The crank rotates in a counterclockwise direction with constant angular velocity ω. The piston is constrained to move along a vertical line in a manner determined by the crank r and connecting rod l. The uppermost position of the piston is taken as the coordinate reference, and downward displacement y_p of the piston from the reference is considered as positive. The piston displacement is then given by the following expression:

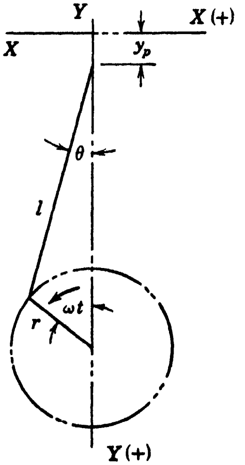

FIGURE 6.4. Kinematics of piston, crank, and connecting rod motion.

$$y_p = r + l - r \cos \omega t - l \cos \theta. \quad (6.4)$$

The last term on the right side of equation 6.4 may be expressed in terms of sin θ by writing

$$l \cos \theta = l \sqrt{1 - \sin^2 \theta}. \quad (6.5)$$

It is evident from the geometry of Figure 6.4 that

$$\sin \theta = \frac{r}{l} \sin \omega t. \quad (6.6)$$

Combining equations 6.5 and 6.6, the last term in equation 6.4 may be written:

$$l \cos \theta = l \sqrt{1 - \left(\frac{r}{l}\right)^2 \sin^2 \omega t}. \quad (6.7)$$

Expanding equation 6.7 by the binomial theorem, and dropping all powers of r/l greater than the second:

$$l \cos \theta = l \left[1 - \frac{1}{2} \left(\frac{r}{l}\right)^2 \sin^2 \omega t \right]. \quad (6.8)$$

The expression involving $\sin^2 \omega t$ may be replaced by a function of the double angle $2\omega t$ as follows:

$$\sin^2 \omega t = \tfrac{1}{2}[1 - \cos 2\omega t]. \quad (6.9)$$

Substituting from equation 6.9 in equation 6.8, and then substituting the resulting expression for $l \cos \theta$ in equation 6.4, the following expression for the displacement y_p of the piston is obtained:

$$y_p = r\left(1 + \frac{r}{4l}\right) - r\left(\cos \omega t + \frac{r}{4l} \cos 2\omega t\right). \quad (6.10)$$

Expressions for the velocity $\dot{y}_p$ and acceleration $\ddot{y}_p$ of the piston are obtained by single and double differentiation of equation 6.10 with respect to time:

$$\dot{y}_p = r\omega\left(\sin\omega t + \frac{r}{2l}\sin 2\omega t\right), \qquad (6.11)$$

$$\ddot{y}_p = r\omega^2\left(\cos\omega t + \frac{r}{l}\cos 2\omega t\right). \qquad (6.12)$$

The crank pin moves in a circular path with the axis of the crankshaft as a center. Taking the center of coordinates through the uppermost position of the piston, equations that define the vertical and the horizontal components of the crank-pin motion are readily written as follows:

$$y_c = l + r(1 - \cos\omega t);\ \dot{y}_c = r\omega\sin\omega t;\ \ddot{y}_c = r\omega^2\cos\omega t; \qquad (6.13)$$

$$x_c = r\sin\omega t;\ \dot{x}_c = r\omega\cos\omega t;\ \ddot{x}_c = -r\omega^2\sin\omega t; \qquad (6.14)$$

where y_c and x_c are vertical and horizontal components, respectively, of the crank-pin displacement taken with respect to the coordinate reference indicated in Figure 6.4. The corresponding velocities and accelerations are indicated by the usual notation.

The motion of the connecting rod is rather complicated. A simplification which is adequate for present purposes is obtained by assuming the connecting rod to consist of (1) a concentrated mass whose motion corresponds to that of the piston and (2) a second concentrated mass, joined to the first mass by a massless strut, whose motion corresponds to that of the crank pin. Designating the mass of the piston and crank pin (including the connecting rod) by m_p and m_c, respectively, the vertical component F_y of the inertia force is obtained from the product of these masses and their respective accelerations as given by equations 6.12 and 6.13:

$$F_y = m_p\ddot{y}_p + m_c\ddot{y}_c. \qquad (6.15)$$

Substituting for $\ddot{y}_p$ and $\ddot{y}_c$ from equations 6.12 and 6.13:

$$F_y = (m_p + m_c)r\omega^2\cos\omega t + m_p r\left(\frac{r}{l}\right)\omega^2\cos 2\omega t. \qquad (6.16)$$

The horizontal component F_x of the inertia force results only from the rotating mass m_c:

$$F_x = m_c\ddot{x}_c = -m_c r\omega^2\sin\omega t. \qquad (6.17)$$

The vertical component of the inertia force thus consists of a part having a frequency equal to the rotational frequency ω and a part having a frequency equal to twice the rotational frequency. Higher harmonics, which usually are of negligible magnitude, were excluded when equation 6.7 was expanded by the binomial theorem, and powers of r/l greater than the second were neglected.

An attempt is made in the modern internal combustion engine to balance the inertia forces. In a single-cylinder engine, little can be accomplished. The crankshaft can be counterbalanced so that the mass m_c is substantially zero. The horizontal component of the inertia force is thus eliminated, but the vertical force resulting from the single reciprocating piston is a source of severe unbalance. In a multi-cylinder engine, some or all of the inertia forces, and the couples resulting therefrom, may be balanced by proper arrangement of cranks. The conditions necessary for such balancing are indicated by reference to Figure 6.5. The cranks are numbered, and the angular position of each is indicated by the angle ϕ_n referred to the position of crank 0. The position of each crank along the shaft is indicated by the distance L_n from crank 0. The vertical and horizontal components of the inertia forces for a single cylinder are given by equations 6.16 and 6.17. The total inertia force for an entire engine is the summation of equations 6.16 and 6.17 over the number of cylinders. If the reciprocating and rotating masses m_p, m_c for each cylinder are respectively equal, the following conditions for balance of inertia forces are obtained from equations 6.16 and 6.17:

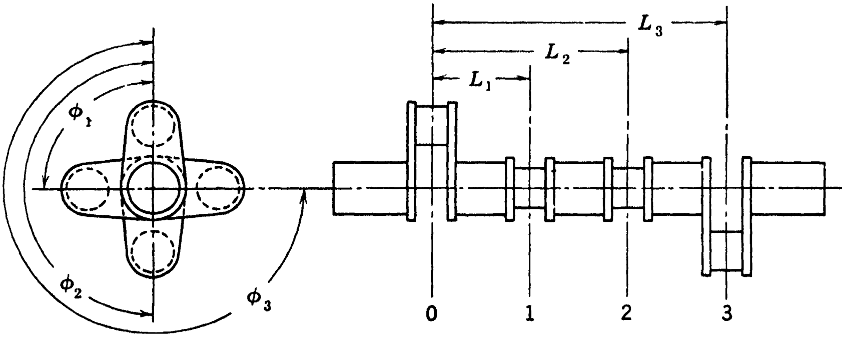

Figure 6.5. Positions of the cranks on the crankshaft of a multi-cylinder engine.

$$\Sigma F_y = 0, \qquad \Sigma \cos \phi_n = 0 \text{ and } \Sigma \cos 2\phi_n = 0;$$
$$\Sigma F_x = 0, \qquad \Sigma \sin \phi_n = 0. \qquad (6.18)^*$$

---

* The instantaneous position of crank 0 in Figure 6.5 may be considered as

In a multi-cylinder engine, the inertia forces defined by equations 6.16 and 6.17 create couples about horizontal and vertical transverse axes. For convenience, the couples are taken with respect to axes through the 0 crank, as indicated in Figure 6.5. Assuming again that the piston and crank masses of each cylinder are respectively equal, the following conditions for balance of inertia couples are obtained from equations 6.16 and 6.17:

$$\begin{aligned} \Sigma L_n F_y &= 0, \quad \Sigma L_n \cos \phi_n = 0 \text{ and } \Sigma L_n \cos 2\phi_n = 0; \\ \Sigma L_n F_x &= 0, \quad \Sigma L_n \sin \phi_n = 0. \end{aligned} \tag{6.19}$$

The inertia forces and couples associated with the frequency ω are referred to as primary forces and couples; those associated with the frequency 2ω are referred to as secondary forces and couples.

For example, consider a four-cylinder engine whose crank angles, starting at one end, are 0, 90, 270, 180 degrees; and whose cranks are spaced apart equal distances L along the shaft. Table 6.1 is now established in accordance with equations 6.18 and 6.19. It is evident from the table that the primary and secondary forces are balanced because $\Sigma \cos \phi = \Sigma \cos 2\phi = \Sigma \sin \phi = 0$. Furthermore, the secondary couples are balanced because $\Sigma L \cos 2\phi = 0$. However, $\Sigma L \cos \phi \neq 0$ and $\Sigma L \sin \phi \neq 0$; the primary couples therefore are not balanced. The engine will thus tend to vibrate in a rotational mode about a transverse axis.

TABLE 6.1

SUMMARY OF INERTIA FORCES AND COUPLES IN FOUR-CYLINDER ENGINE

Crank	ϕ	2ϕ	$\cos \phi$	$\cos 2\phi$	$\sin \phi$	$L \cos \phi$	$L \cos 2\phi$	$L \sin \phi$
0	0	0	1	1	1	0	0	0
1	90	180	0	−1	0	0	$-L$	0
2	270	540	0	−1	−1	0	$-2L$	$-2L$
3	180	360	−1	1	0	$-3L$	$3L$	0
Summation			0	0	0	$-3L$	0	$-2L$

6·3 Application of Isolators to Reciprocating Machines

The forces and couples developed by the operation of reciprocating machinery, as shown by the preceding analysis, may be summarized as follows for ready reference in applying isolators:

(*a*) The gas pressure imposes a force upon the piston, and the reaction upon the chassis of the machine takes the form of a couple that

---

$\phi_0 = \omega t$, as indicated in Figure 6.4. The angles ϕ_n in Figure 6.5 are actually $\phi_0 + \phi_n$; the expressions given by equations 6.18 are then obtained by letting $\phi_0 = 0$.

tends to rotate the machine about an axis parallel to the crankshaft. The couple is periodic, as determined by the frequency of working strokes. This frequency is a function of the speed of the machine, number of cylinders, and nature of the operating cycle, as discussed on page 269.

(*b*) A reciprocating machine includes unbalanced rotating and reciprocating members, and relatively large inertia forces result. These forces act in planes perpendicular to the crankshaft, and they have components both parallel with and normal to the direction of piston motion. The frequencies are the rotational frequency and harmonics thereof.

(*c*) The couple resulting from the gas pressure is a reaction to the torque delivered by or to the machine, and it is present when that torque is present. Some or all of the inertia forces and couples are usually balanced in multi-cylinder machines. In machines having but few cylinders, it is not feasible to balance completely the inertia forces and the couples resulting therefrom.

A number of general rules may be stated as a guide for the design and application of isolators for reciprocating machinery. These rules will first be stated somewhat abstractly, and then followed by additional suggestions directed to specific applications:

(*a*) The natural frequencies of the machine-and-isolator system should be substantially lower than the frequency of the working strokes; i.e., the firing frequency in internal combustion engines. This applies particularly when the machine is operating at rated speed. Internal combustion engines frequently idle at low speed, and vibration isolation at the idling frequency may not be feasible* or necessary because the torque under idling conditions is relatively low. Care should be exercised to employ a damped isolator, if any natural frequency of the isolator system is encountered in changing from idling to running speed. Rubber commonly embodies adequate damping for this purpose.

(*b*) Since unbalanced inertia forces and couples occur at the rotational frequency and harmonics thereof, the isolators should have natural frequencies designed to isolate vibration at the rotational frequency of the machine. Rotational and firing frequencies are not equal, in general.

(*c*) In multi-cylinder machines that have nominal balance of primary and secondary forces and couples, residual unbalances always exist and must be considered. The forces and couples associated with such unbalances are small, but they may cause vibration of high amplitude at resonance unless the isolator embodies appreciable damping.

---

* For a discussion of the problems encountered in applying isolators to machines which operate at low speed, see Section 6·1.

The methods used in applying isolators to reciprocating machinery are governed by the type of machine and by limitations on the location of the isolators. Various possibilities are discussed in a general and descriptive manner in the following paragraphs. One common type of internal combustion engine is the multi-cylinder engine having the cylinders arranged in one or more lines extending parallel to the crankshaft. A typical engine of this type is illustrated in Figure 6.6. Powered by gasoline or diesel oil, it is used in automobiles, airplanes, trucks, buses, farm machinery, and many other applications. Predominant inertia forces and couples are often balanced, but the pulsating torque originating from the gas pressure is capable of causing considerable vibration in the engine support. The great riding comfort of the modern automobile, characterized by a minimum of vibration transmitted from the powerful engine, is testimony to the effectiveness of properly designed vibration isolators for this type of engine.

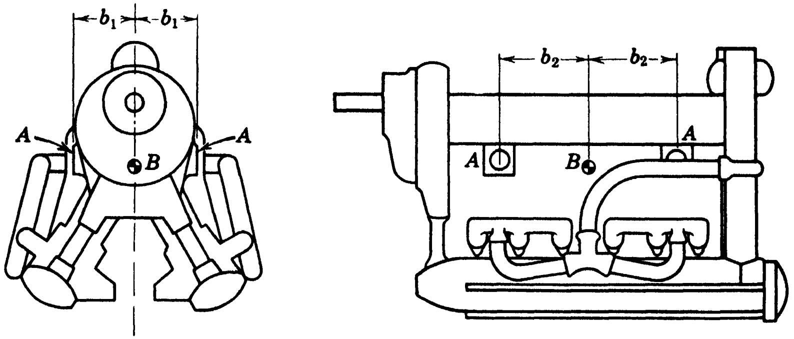

FIGURE 6.6. Typical internal combustion engine having twelve cylinders arranged in two banks of six each. The center of gravity of the engine is at B, and the isolators are attached at A.

The requirements of vibration isolators for supporting engines in vehicles or other conveyances are particularly stringent. The isolator must have substantial stiffness to afford steadiness when subjected to the random motion of the conveyance; it must, at the same time, have sufficient compliance to function as a vibration isolator. This compromise is best attained if the isolators have equal stiffnesses in the directions of the several axes, and if they are positioned with respect to the engine in such a manner that all natural frequencies are equal.* An ideal arrangement is illustrated in Figure 6.6. The center of gravity of the engine is indicated by B, and abutments for attachment of the isolators are shown at A.

Comparison of the end view of the engine, shown at the left of Figure 6.6, with the rectangular shape shown in Figure 1.14 (*d*) of Chapter 1 is significant. There is some geometrical similarity, which indicates that the radius of gyration with respect to an axis parallel to the crankshaft may be expected to approximate the dimension b_1 in Figure 6.6. By placing points A and B in the same horizontal plane and employing isolators with equal horizontal and vertical stiffnesses, the three natural frequencies associated with vibration in a plane perpendicular to the crankshaft may be decoupled and made approximately equal. Furthermore, the dimension b_2 may be selected equal to the radius of gyration with respect to a horizontal axis through the center of gravity and perpendicular to the crankshaft. The natural frequencies associated with vibration in a vertical longitudinal plane thus are decoupled and made equal. This method of mounting engines leads to optimum results and should be followed whenever conditions permit.

Many types of reciprocating machines that cannot be supported in the manner illustrated in Figure 6.6 are mounted to good advantage upon floating concrete foundations. In this type of installation, the machine is securely attached to a heavy concrete block which is supported by isolators. The following important advantages are derived from such an arrangement:

(*a*) By using a floating foundation, it is feasible to place the isolators in the same horizontal plane as the center of gravity of the machine-and-foundation assembly. The advantages of decoupled and equal natural frequencies, as pointed out in connection with Figure 6.6, may be attained in this manner. Suitable forms of concrete foundation are described in various other sections of this book.†

(*b*) The machine gains a rigid support to help maintain alignment of the various component parts thereof. This is of particular advantage with a large, fabricated machine which, if supported at several points by flexible means, is subject to distortions which may impair its operation.

---

* For a more detailed discussion of this requirement, see Sections 2·10 and 6·1.

† Concrete foundations suitable for low-speed machines are shown in Figure 6.1 and in the reference cited in the footnote on page 265. For machines operating at higher speeds, where control of natural frequencies is not critical, suitable foundations are shown in Figures 6.13 and 6.14. A detailed discussion of isolators and materials that are adaptable to such foundations is included in Chapter 5.

(*c*) The overall motion of the machine is held to a minimum. As shown by equation 2.5 of Chapter 2, the inertia of moving members causes overall motion of a mounted machine which is inversely proportional to its mass. The unbalanced inertia forces and couples can become relatively large, particularly in one- or two-cylinder machines, and a concrete foundation may decrease an otherwise objectionably large motion of the machine.

The principal difficulties associated with the application of isolators to reciprocating machinery are derived from (1) the large forces involved, from both inertia and gas-pressure sources, and (2) the characteristically low operating speed of many types of machine. Furthermore, such machines are commonly supported at the bottom, so that it becomes difficult to attain optimum steadiness and transmissibility by decoupling natural modes of vibration and equalizing natural frequencies. Where it is not possible to employ any of the methods set forth in preceding paragraphs of this section, a satisfactory application of isolators becomes exceedingly difficult to accomplish if the operating speed is lower than approximately 1,200 rpm. In order to maintain the maximum natural frequency lower than the operating speed, one of the natural frequencies becomes very low and introduces an objectionable tendency to sway laterally. One method of avoiding this trouble is to space the isolators, as illustrated in Figure 2.12 and described from a practical viewpoint in Section 6·1 of this chapter. This method is feasible only for supporting machines whose operating speed is substantially constant.

6·4 Punch Presses

Machinery used for forming metal by shearing, drawing, or punching is a frequent source of disturbance in industrial plants. Probably the machine most commonly used for these operations is the punch press, as illustrated by the outline drawing of Figure 3.26 and the photograph of Figure 6.7. Such a machine generally embodies a relatively heavy, rigid lower portion carrying the stationary platen and a vertically reciprocating head carrying the moving platen. Various types of dies are placed on the platens for performing the metalworking operations. The moving platen is usually driven by a crank and connecting rod, and in some types of presses it moves in a line inclined to the vertical for convenience of operation. The force applied to the dies creates a condition that may be alleviated by isolators.

A punch press, as pointed out in Section 3·11, is a machine of conservative momentum. There is no addition of momentum from an external source, and the machine cannot permanently acquire a velocity, although it may acquire a displacement. In other words, if the press were supported by some means that offered no constraint to its movement, it would move intermittently with a short step at each cycle of operation. If supported by a rigid foundation which prevents appreciable movement, the forces that tend to cause this stepwise displacement are transmitted directly to the foundation. A shock isolator, on the other hand, permits the press to experience an initial displacement in response to the force on the dies; and it functions to restore the press subsequently to its original position before inception of the next cycle of operation.

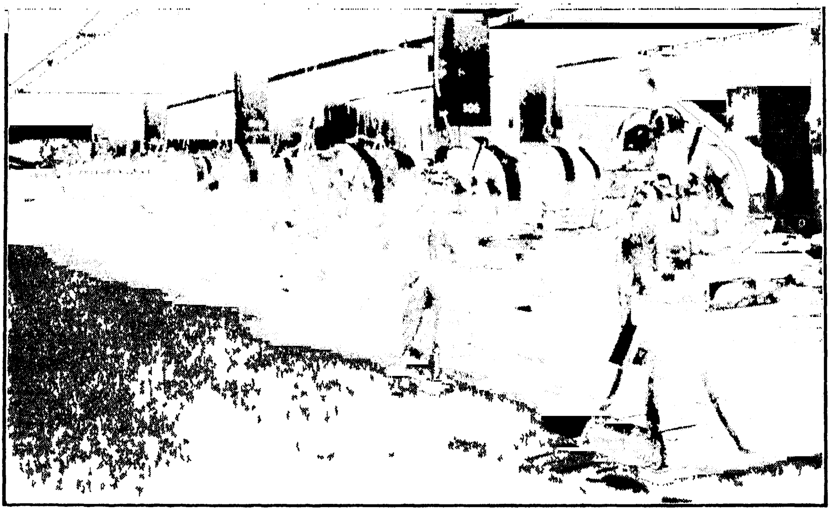

FIGURE 6.7. Battery of small punch presses mounted upon shock isolators. The presses are positioned only by friction between isolators and floor.

That the press tends to experience only a limited displacement during one complete cycle of operation is of considerable significance. This is illustrated in Figure 3.29, which shows that the press becomes stationary but displaced from its initial position as the cycle of operation approaches completion. At this stage, the shock isolator applies a force that acts to restore the press to its initial position. The press thus experiences its maximum displacement once during each cycle of operation; the isolators must be of such design that they are enabled to partake of at least the maximum displacement of the press. This displacement depends on the type of press and the nature of the work being done; usually it would not exceed a fraction of an inch. If the resilient medium of the isolator is made one inch thick, adequate deflection is available in the isolator to afford optimum performance.

A punch press characteristically creates large forces during only a small portion of the operating cycle. Work is not usually done on the upstroke of the moving platen, and a substantial part of the downstroke finds the dies free in order to permit the work to be successively ejected and loaded. The large forces required in the metal-working operation are therefore applied during a very short time interval, but they occur with regular periodicity in a continuously operating machine. Two concepts of operating frequency are thus introduced as follows:

(*a*) The force associated with the metal-working operation is suddenly applied and endures for only a relatively short period of time. If the press is mounted upon isolators, the response to this force may be evaluated from the analysis given in Chapter 3. The applicable system is shown schematically in Figure 3.21, and the results are shown graphically in Figure 3.25. It is evident that the disturbance in the support for the machine is low if Ω_y/ω is low; i.e., if the natural period of the isolators is large compared with the time duration of the force.

(*b*) The force occurs at equal time intervals, even though it is actually applied but for a fractional part of the interval. The entire press experiences vibration of large amplitude if the time interval between successive strokes of the press becomes equal to the natural period, in any mode of vibration, of the press-and-isolator system. This is a condition of resonance, even though the exciting force is not harmonic, and it must be avoided to obtain satisfactory operation of the press.

Methods of attaining the required natural frequencies to isolate the force associated with the metal-working operation and to prevent resonance are considered in later paragraphs of this section.

Numerous benefits are derived from the mounting of punch presses upon isolators. These benefits may be outlined as follows:

(*a*) The vibration and shock transmitted to the building structure is greatly decreased. This results in reduced maintenance costs for the building, in reduced disturbance to other machinery occupying the same building, and in improved working conditions for personnel.

The improvement is very noticeable when the presses are mounted upon an upper floor of the building, and it manifests itself particularly in the greatly reduced noise level in the space immediately below the floor that supports the presses.

(*b*) It usually is not necessary to secure the press to the floor, for reasons explained in Section 3·13. Isolators are secured to the feet of the press and rest upon the floor with only friction as the positioning means. The entire battery of presses shown in Figure 6.7 is mounted in this manner. This makes it possible to transport the press readily to the tool room for maintenance and setting of dies, and to arrange the entire complement of presses in a manner that assures the greatest operating efficiency. The cost and inconveniences occasioned by securing the press to the floor are eliminated.

In the application of isolators to a punch press, much of the information needed to calculate the natural frequencies is difficult to obtain. The total weight of the press is usually known, and the location of the mounting feet for attaching the isolators can be readily determined. The height of the center of gravity and the radii of gyration with respect to the several axes through the center of gravity are generally not known. Fortunately, the design of punch presses follows a common pattern. By taking mean values of the above parameters, the methods set forth in Chapter 2 for determining natural frequencies become applicable to punch presses.

The curves of Figure 2.8 are applicable to a punch press supported by isolators. They require that the radius of gyration of the press and the height of its center of gravity be known. The height of the center of gravity is seldom less than one-half or more than one-and-one-half times the distance between mounting feet; i.e., $1 < a/b < 3$. It is estimated that the ratio a/ρ, height of center of gravity to radius of gyration, usually falls between 0.75 and 1.25. It remains now to select an appropriate value for the stiffness ratio k_x/k_y. Rubber loaded in compression by the dead-weight load of the press is well adapted to this application, and a representative value for the stiffness ratio is $k_x/k_y = 0.15$.* Sufficient information is now available to plot the curves of Figure 6.8. The ratio Ω_c/Ω_y, coupled to vertical natural frequencies, is taken from Figure 2.8 for the range of the parameters a/ρ and a/b indicated above. The term ρ/b which appears in Figure 2.8 is evaluated from the relation $\rho/b = (a/b)(\rho/a)$.

Two ranges of coupled natural frequencies for the press supported by isolators are thus established, as indicated by the spread of the solid

* This characteristic is discussed in some detail in Section 5·7 of Chapter 5.

lines in Figure 6.8. These ranges, together with the marginal areas at their edges, must not coincide with the operating frequency of the press. This leaves certain other regions, shown shaded in Figure 6.8, in which the operating frequency is not likely to become resonant with a natural frequency. The design objective is to operate in these shaded regions. The exact limits of the shaded regions are somewhat arbitrary, but satisfactory results may be expected if the natural frequencies are chosen so that the transmissibility never exceeds a

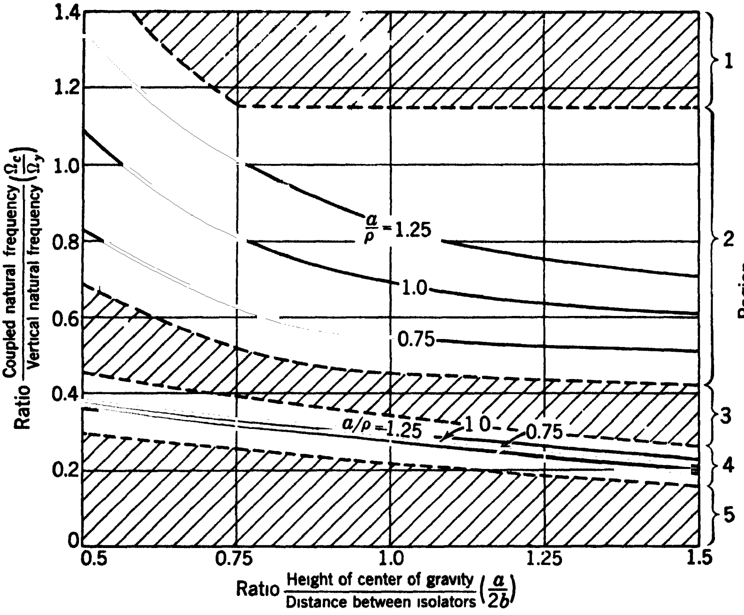

FIGURE 6.8. Probable coupled natural frequencies of a representative group of punch presses, as indicated by solid curves. Shaded areas indicate safe operating conditions, as determined by the requirement that the difference between a shaded region and a solid line should be not less than 15 percent of the solid-line value.

value of three. This condition is obtained, as indicated in Figure 2.2, when $0.82 > \omega/\Omega > 1.15$. The shaded regions are thus located so that their limits and the outermost curves of each family of solid curves are in the ratio 0.82 or 1.15. A further limitation imposed on the uppermost shaded region is that its lower boundary must not be less than 1.15 times the vertical natural frequency Ω_y.

Means to assure that the operating frequency of the press falls within one of the shaded regions may now be devised. As indicated in Figure 6.8, the frequency ratio Ω_c/Ω_y varies as the ratio a/b varies. The height of the center of gravity is often less than the distance between isolators; a typical value for the ratio of these dimensions is $a/b = 1.5$ ($a/2b = 0.75$). A chart, Figure 6.9, is now constructed simply by noting the boundary frequencies, with respect to the vertical natural frequency, of the shaded and the unshaded regions in Figure 6.8. These frequencies are set forth in Table 6.2. The regions are designated at the right of Figure 6.8; the upper and lower limits of each region, in terms of the ratio Ω_c/Ω_v, are set forth in the second and third columns of Table 6.2. The boundary frequencies, expressed in cycles per minute, are tabulated in the last four columns for vertical natural frequencies of 5 and 15 cps.* These boundary frequencies establish the limits, as functions of the vertical natural frequency, of the various "acceptable" and "avoid" regions plotted in Figure 6.9.

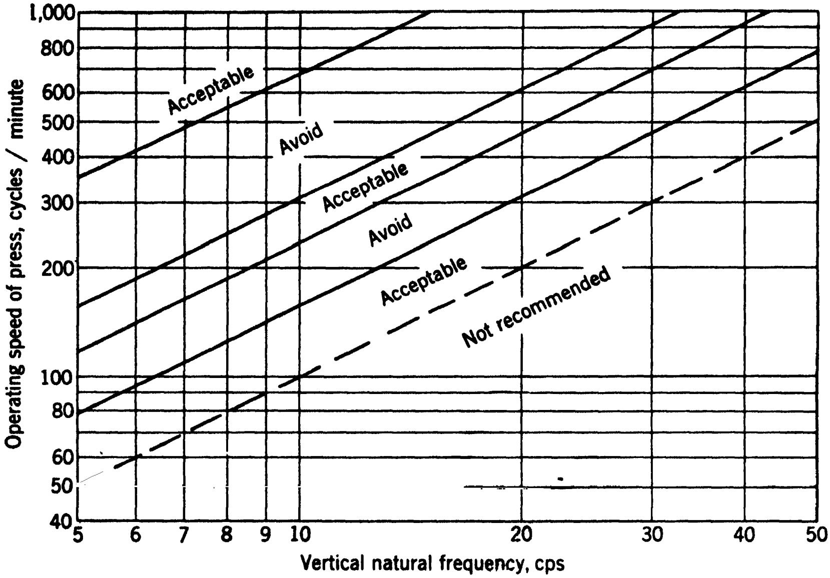

FIGURE 6.9. Chart showing acceptable and non-acceptable natural frequencies for punch-press isolators, as derived from Figure 6.8. Isolators are comprised of rubber members loaded in compression.

The foregoing analysis has for its objective only to assure that a natural period of the punch press, supported by isolators, does not coincide with the period between operating strokes of the press.

---

* Inconsistent units for boundary frequency and for vertical natural frequency are used here, because the former is associated with operating speed of the press, commonly designated in revolutions per minute, whereas the latter is expressed in cycles per second throughout this book.

Additional consideration must be given to isolation of the forces created by operation of the press. In the latter respect, the significant characteristic is the period of time during which forces are acting upon the dies. This is a function of the operating frequency of the press, and of the length of the working stroke. Presses designed for punching, blanking, and shallow drawing generally operate at high speed, and the working stroke is short. The time duration of the work force is short, i.e., the effective frequency is high, and isolators with a relatively high natural frequency may be effectively employed.* Presses used for deep-drawing operations, on the other hand, operate at relatively low speed and with a long working stroke. As a result, the force is applied over a long period; i.e., with a low frequency. Consequently, isolators of low natural frequency are required. This leads to the general proposition that low-speed presses require isolators of low natural frequency. The dotted lines in Figure 6.9 define this condition graphically. The "not recommended" region is satisfactory from the standpoint of avoiding resonance, but generally it does not call for a natural frequency that is sufficiently low for effective isolation.

TABLE 6.2

DATA USED IN CONSTRUCTING FIGURE 6.9

(For a/b = 1.5 in Figure 6.8)

	Boundary Expressed as Frequency Ratio Ω_c/Ω_y		Boundary Expressed as Operating Frequency, rpm (Vertical Natural Frequency = 5 cps)		Boundary Expressed as Operating Frequency, rpm (Vertical Natural Frequency = 15 cps)	
Region	Upper	Lower	Upper	Lower	Upper	Lower
1	....	1.15	...	345	....	1035
2	1.15	0.52	345	156	1035	468
3	0.52	0.39	156	117	468	351
4	0.39	0.26	117	78	351	234
5	0.26	....	78	...	234	....

In applying the chart, Figure 6.9, the known operating frequency of the press is taken on the ordinate; a value for vertical natural frequency of the isolator is selected from the abscissa scale for one of the "acceptable" regions. Appropriate isolators are then selected, of the stiffness required to afford the desired vertical natural frequency when the isolators are supporting the known weight of the press. If the weight of the press is not uniformly distributed among the several isolators, the stiffness of each isolator should be made proportional to the dead-weight load that it supports.*

---

* For a detailed analysis of this problem, see Section 3·10 of Chapter 3.

It is interesting to note that the operating frequency falls between the natural frequencies of the press in two coupled modes if the vertical natural frequency of the isolator is such as to locate a point in the intermediate of the three "acceptable" regions. This results in a reasonable isolator natural frequency only for relatively high-speed presses. For presses that operate at frequencies lower than 200 to 300 cycles per minute, the lower "acceptable" region is more feasible. The operating frequency is then lower than the natural frequency in either coupled mode of vibration. For very high-speed presses, all natural frequencies can be made lower than the operating frequency by selecting the upper "acceptable" region.

6·5 *Looms*

One of the most troublesome machines extant with regard to vibration and shock is the cloth-weaving loom. The principal features that cause vibration and shock are illustrated schematically in Figure 6.10.

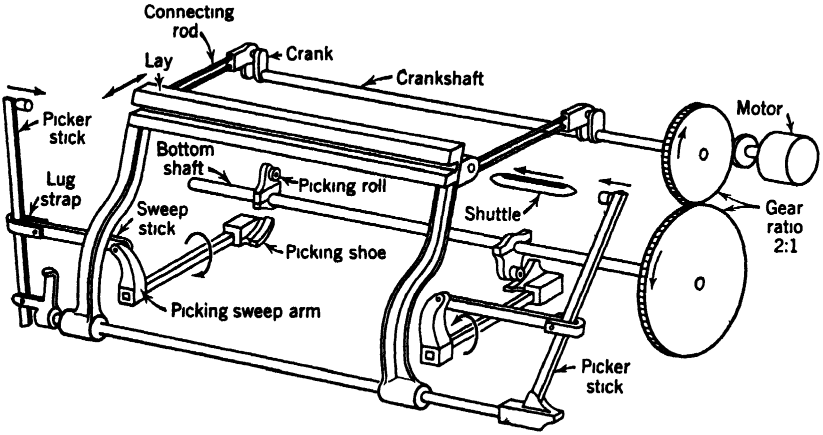

FIGURE 6.10. Schematic diagram of cloth-weaving loom showing principal features that cause shock and vibration. (Courtesy Crompton & Knowles Loom Works.)

The lay, a relatively heavy member, is driven with a horizontally reciprocating motion by a pair of cranks and connecting rods. The lay carries a shuttle box, not shown in Figure 6.10, at each end. A shuttle is caused, by a mechanism to be described later, to travel alternately in opposite directions, across the lay, from one shuttle box to the other. The longitudinally extending warp thread is fed continuously in many parallel strands extending in the direction of the lay movement. Combinations of warp thread are alternately raised and lowered at each cycle of the lay by a harness not shown in the diagram. The shuttle carries the cross or filling thread between the raised and lowered strands of warp thread. After each passage of the shuttle, the lay presses or lays the last-woven filling thread against the previously woven threads.

---

* A method of determining the stiffnesses of the isolators in order to comply with this requirement is set forth in Section 4·10 of Chapter 4.

The shuttle, before it begins to move, rests in contact with a picker attached to the upper end of a picker stick. A picking roll mounted upon an arm carried by the bottom shaft strikes a picking shoe and causes the shaft that carries this shoe to rotate about its longitudinal axis. The resultant sudden angular movement of the picking sweep arm is transmitted to the picker stick through the sweep stick and lug strap. The sudden movement of the picker stick propels the shuttle toward the opposite shuttle box. Upon arriving at the opposite shuttle box, the shuttle is brought to rest and then propelled in the opposite direction to continue the cycle of operation.

The two principal sources of vibration and shock resulting from loom operation are:

(*a*) The inertia force created by the reciprocating motion of the lay is substantial. This is almost a pure harmonic force acting in a horizontal direction, and the reaction upon the frame of the loom is at the crankshaft. When looms are installed on the upper floors of mills, the entire building may sway at the frequency of the lay motion. It is characteristic of textile mills that the amplitude of sway continually increases and decreases as the many looms, operating nominally at the same but actually at slightly different speeds, change phase relations. There is some evidence that the magnitude of the sway is occasionally increased by resonance of the building with the looms. The floors that support the looms are caused to weave or bend under the influence of the moment resulting from the lay force acting upon the loom frame at the height of the crankshaft above the floor.

(*b*) The force that propels the shuttle is in the nature of an impact. The complexity of the mechanism employed for this purpose makes the exact nature and direction of this impact uncertain. As in the punch presses considered earlier, it is necessary to distinguish between the various concepts of frequency. Although the picking action occurs with the same periodicity as the lay movement, the actual force endures for only a small fraction of this period. Since the period of application of the picking force is smaller than the period of the lay force, the associated frequencies are higher.

The difficulty of effectively isolating the inertia force resulting from lay movement is best illustrated by a numerical example. The total weight of a typical box loom is 4,000 lb, and the effective weight of the lay is approximately 400 lb. The lay reciprocates at a frequency of 3 cps, and the amplitude may be taken as 3 in. (total travel of 6 in.). The minimum static deflection required to achieve a stated transmissibility in steady-state vibration is indicated by Figure 2.5. It becomes apparent that a static deflection considerably in excess of 2 in. is necessary in a vibration isolator to obtain transmissibility of 0.5 when the frequency of the forcing vibration is 3 cps. If the frequency of the forcing vibration is lower, or a lower transmissibility is desired, the static deflection must be correspondingly greater. The difficulties with a static deflection of this magnitude become evident when the vibration amplitude of the loom body under the influence of the lay inertia force is computed.

The vibration amplitude of the entire loom, when the operating frequency is high relative to the natural frequency of the isolator, may be estimated from equation 2.5 as follows:

$$y_0 \approx -\frac{\epsilon W_\epsilon}{W}, \tag{6.20}$$

where y_0 = maximum vibration amplitude of entire loom, in.
ϵ = amplitude of lay movement, in.
W_ϵ = weight of lay, lb.
W = total weight of loom, exclusive of lay, lb.

The negative sign indicates that the loom moves at all times in a direction opposite to that of the lay. Substituting the above typical numerical values into equation 6.20:

$$y_0 = \frac{-3 \times 400}{4{,}000 - 400} = \frac{1}{3}\text{ in.}$$

The necessary careful adjustment required of the modern loom cannot be obtained if the entire loom is moving with a vibration amplitude of $\frac{1}{3}$ in.; i.e., a total travel of $\frac{2}{3}$ in. The basic principles of vibration isolation expounded in Chapter 2 show that this motion is essential to attaining isolation. In other words, the only method of preventing the transmission of the force to the building is to permit the loom to move in relation to the building. Equation 6.20 indicates that the loom movement y_0 can be reduced by decreasing the weight W_e of the lay or by increasing the weight W of the loom. It is not practicable to effect a sufficiently great change in either of these weights to reduce the overall movement of the loom to an acceptable value. The practical solution to the problem appears to be either to strengthen the mill building so that it will be enabled to withstand the forces, or to synchronize adjacent looms out of phase so that the inertia forces oppose one another.

A somewhat different condition exists with regard to the force that propels the shuttle. A loom, as explained in Section 3·11, is a machine of conservative momentum, and the isolator is required only to accommodate a definite displacement of the loom. The law that relates the force acting on the shuttle with the velocity acquired by the shuttle, equation 3.63, may be written:

$$\int F\,dt = m_s(\Delta V_s) = -m_l(\Delta V_l), \tag{6.21}$$

where F = force applied to shuttle (also reactive force on loom), lb.
m_s = mass of shuttle, lb sec^2/in.
m_l = mass of loom, lb sec^2/in.
ΔV_s = velocity change of shuttle under influence of force F, in./sec.
ΔV_l = velocity change of loom under influence of force F, in./sec.

Equation 6.21 shows that, if the loom were suspended in space free of all external constraints, it would move to the right with a velocity V_l while the shuttle moves to the left with a velocity V_s. When the shuttle moves to the right, the loom moves to the left. Minimum force is thus transmitted by an isolator that is capable of sustaining adequate deflection to accommodate this loom movement and has the least possible stiffness compatible with the required steadiness.

The order of magnitude of the loom motion under the influence of forces acting on the shuttle may be determined by substituting typical values in equation 6.21. A typical shuttle weighs one pound and travels with an average velocity of 360 in./sec over a 60-in. travel. The weight of a typical box loom as given above is 4,000 lb. Substituting these values in equation 6.21 and solving for ΔV_l:

$$\Delta V_l = -360\left[\frac{1/386}{4{,}000/386}\right] = -0.09 \text{ in./sec.}$$

The time required for the shuttle to travel 60 in. at an average velocity of 360 in./sec is $\frac{1}{6}$ sec. During this same time interval, the loom moves in the opposite direction a distance of $\frac{1}{6} \times 0.09 = 0.015$ in. The maximum displacement of the loom as a result of the picking action thus is not great, and the isolator should freely sustain this deflection.

A definite recommendation for the mounting of looms is difficult to formulate. The isolation of the inertia force resulting from the motion of the lay should not be attempted. The isolators should be sufficiently stiff for the natural frequencies in all natural modes of vibration to be substantially greater than the lay frequency, so that the movement of the loom is not increased by a resonant condition. Figure 2.11 shows that the minimum coupled natural frequency of a body having the geometrical configuration of a loom may be as low as $\frac{1}{3}$ times the vertical natural frequency. If this minimum natural frequency is to be maintained at least twice as great as the operating frequency of 3 cps, a vertical natural frequency of 18 cps or greater is called for.

Felt, described in Section 5·18 of Chapter 5, is used extensively for mounting looms. It is generally considered by the textile industry to be superior to rubber and other materials for this purpose. Natural frequencies attainable with felt of one-inch thickness are indicated in Figure 5.24, and with felt of other thicknesses in Figure 5.25. It is apparent that the minimum suitable vertical natural frequency of 18 cps would always be attained with felt of less than two-inch thickness loaded within the maximum recommended loading. Felt with a thickness of a fraction of an inch appears adequate to accommodate the maximum displacement of 0.015 inch calculated above; it is known to be giving satisfactory service in many textile mills.

The isolator mentioned in the above paragraph is intended to restrain the loom from moving excessively under the influence of the lay inertia force, and to permit the loom to move freely in response to the forces associated with the picking action. This gives no consideration to the ability of such isolators to reduce the magnitude of the forces transmitted to the floor. The full potentialities of an isolator in reducing the shock generated by the picking action seem unattainable unless the floor is very rigid. Concrete floors are well adapted to isolators under looms and are known to experience substantially less disturbance from shock when the looms are mounted upon felt. Little or no improvement may result from the installation of isolators in a building having the wooden floors that are typical of many textile mill buildings. Benefits in ease of installation and reduction of maintenance expense may justify the installation of isolators, even though no reduction of force is achieved.

6·6 Electric Motors

An electric motor is comprised of two principal parts, a stator and a rotor. The torque delivered by the motor results from the attraction of a magnetic field on current-carrying conductors of the rotor. The magnetic field is created by electric current flowing through the windings of the stator. Any variation in the current is reflected in the strength of the field and, consequently, in the torque. In a single-phase 60-cycle alternating-current motor, for example, the current in the windings of the stator passes through zero 120 times per second. There is thus a variation in torque at a frequency of 120 cps, which can be shown to consist of a steady torque with superimposed ripple.

The vibration created by the operation of an electric motor may result from (*a*) the periodic variation in the strength of the magnetic field and (*b*) inertia forces associated with unbalanced rotating parts. The former will be considered first. The power output of a motor is manifested in a torque applied to the motor shaft, and an equal and opposite torque reaction is exerted upon the stator. The motor support thus experiences, in the form of vibration, the periodic fluctuation in the strength of the magnetic field. This disturbance is fundamentally torsional in nature and can be isolated by mounting the stator upon isolators in such a manner that the stator has freedom of motion in rotation about the shaft center. The natural frequency of the stator in rotation should be lower than the frequency associated with the torque fluctuation. The transmissibility in rotation of a system that embodies a torsional spring is given by equation 2.12 of Chapter 2.

Several methods are employed to achieve the required torsional flexibility of the isolator. One of these is illustrated in Figure 6.11. The isolator comprises a rubber ring *a* which encircles the hub *b* of the stator and is attached at its periphery to the motor support *c*. The modulus of elasticity of rubber strained in shear is relatively low. The low modulus, together with the disposition of the rubber adjacent to the axis of rotation, makes possible the attainment of the desired low natural frequency in the rotational mode. An equivalent result is obtained from the arrangement of flat metal springs illustrated in Figure 6.12. The two legs *d* of the spring form an included angle of 90° which has its apex at the shaft axis *e*. The stator is free to rotate about the shaft axis with but little restraint, since the springs embody a characteristically low stiffness when deflected in flexure.

The isolators illustrated in Figures 6.11 and 6.12 are relatively stiff when subjected to forces applied perpendicular to the shaft, because, in the former, rubber has a much higher modulus when strained in compression than when strained in shear,* and, in the latter, any force perpendicular to the shaft can be resolved into components directed along the line of at least one spring. The springs are relatively stiff when loaded in this manner. The isolators are thus adapted to withstand the forces applied by belt drives without sacrificing the torsional flexibility necessary to isolation of torque fluctuations.

Vibration resulting from the unbalance of rotating parts should be treated in the same manner as the vibration of any rotating machine. This problem is discussed comprehensively in Chapter 2, where it is shown that, in general, effective isolation can be attained only when the natural frequencies in the several natural modes of vibration are made substantially lower than the frequency of rotation. The isolators are therefore required to be flexible in radial directions and, except for relatively high-speed motors, are not well adapted to withstand the forces applied by gear, belt, and chain drives.

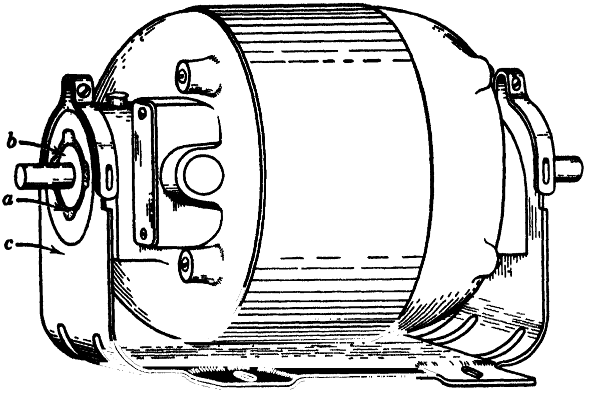

FIGURE 6.11. Electric motor with rubber-ring type isolators. (General Electric Company.)

Electric motors are used in diversified types of equipment, and different isolation requirements apply in the various instances. These various applications are referred to below by the arbitrarily chosen designations of industrial, household, and laboratory applications:

(*a*) *Industrial.* This designation includes a wide variety of machinery used under manufacturing or equivalent conditions. Vibration and noise are commonly prevalent in such circumstances, and the electric motor is looked upon as an inoffensive adjunct to the machine that it drives.

---

* The stiffnesses of a rubber bushing subjected to various types of loading are calculated in Example 5.3, page 232.

(*b*) *Household.* The large increase in use of home appliances driven by fractional-horsepower electric motors has emphasized the need for quiet operation. The vibration resulting from torque fluctuations should be isolated because vibration at the commonly encountered frequency, 120 cps, is audible. It can be very annoying, particularly when amplified as a result of resonance with the metal panels of large area found in home applicances.* Vibration from unbalanced rotating parts seldom causes annoyance because the forces involved are usually small, and because the frequency is unobjectionable from an acoustic viewpoint. Isolators of the types illustrated in Figures 6.11 and 6.12 are commonly employed in home appliances and similar equipment.

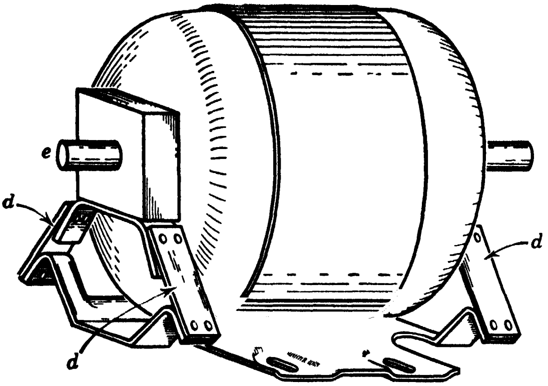

FIGURE 6.12. Electric motor with metal-spring type isolators. (Holtzer-Cabot.)

(*c*) *Laboratory.* This class designates equipment, such as electronic and similarly sensitive equipment, which is adversely affected by the small forces caused by unbalanced rotating members. Isolators of relatively low natural frequency are required here. Alignment of the motor with the driven apparatus can be maintained by mounting both motor and machine upon a common chassis, and in turn mounting the chassis upon isolators. Another possible solution involves independent mounting of the motor, and flexible couplings to permit misalignment of the motor with the driven machine.

6·7 Miscellaneous Industrial Equipment

This section deals with various types of industrial equipment and equipment components. Most of the vibration and shock problems associated with such equipment fall within the scope of the analyses set forth in preceding chapters, or in preceding sections of this chapter. This section serves to point out the pertinent features of the several types of equipment and to suggest methods of applying the preceding analyses in the design and application of isolators.

---

* This is explained in more detail in the discussion of sound isolation, Section 4·12 of Chapter 4.

(a) GEARS, BEARINGS, AND CAMS

Vibration resulting from the operation of bearings and gears usually has its source in friction between sliding members and in turbulent action of lubricating fluids in bearings and gear boxes. Unbalance of rotating members is generally not an important factor in this source of vibration. Where gears are the major source of noise, the predominant frequency is the tooth frequency; i.e., the product of the rotational frequency of the gear and the number of teeth on its periphery. Higher harmonics of the tooth frequency are often present, but subharmonics are seldom encountered. The vibration caused by bearings and fluid turbulence tends to lack defined frequencies.

The method used to isolate the vibration originating in gears and bearings is of a non-critical nature. Adequate isolation generally can be attained with an isolator having a natural frequency as high as 25 cps. The forces, both from tooth contact and from unbalance of rotating members, are small and cause no appreciable overall motion of the mounted machine, provided that the isolators have a moderate degree of damping. The internal damping of rubber is adequate for this purpose. Care should be taken, if undamped isolators are used, to avoid resonance with any predominant frequency, such as rotational or tooth frequency. Since the vibration frequencies originating in the action of gears and bearings extend to relatively high levels, it is important also to observe the principles of sound isolation set forth in Section 4·12 of Chapter 4 to assure that a quiet installation results.

The operation of cams may involve either continuous sliding or rolling contact, or momentary contact in the nature of an impact. In the former case, the vibration resulting from cam action is very similar to that resulting from the operation of gears and bearings. Impact forces are different, and the required treatment depends on the magnitude of the forces involved. In a loom, for example, the force exerted by the cam may be sufficiently great to displace the entire machine. The isolator then should be capable of experiencing a deflection at least equal to this displacement. In other instances, the impacts associated with cam action are small and tend to cause but negligible displacement. When this condition exists, isolators designed in accordance with the principles of isolating gear and bearing vibration will usually give satisfactory results.

(b) TRANSFORMERS

The principal source of vibration in a transformer is the fluctuation in the magnetic force resulting from variations in the voltage. A transformer is used exclusively with alternating current whose frequency is generally constant. The vibration frequency is therefore constant and substantially pure; i.e., it includes few harmonics. Since all the magnetic forces in a transformer are opposed by members that are structurally an integral part of the transformer, the forces transmitted externally of the transformer are small. This is in contrast to a motor, for example, which delivers a torque and exerts an equal reaction upon the motor support.

The technique for isolating the vibration that originates within a transformer is relatively simple. The natural frequency should be sufficiently low, as determined by the methods set forth in Chapter 2, to isolate the vibration induced by the fluctuating voltage. Since this frequency usually is high enough to be audible, the isolator should also be designed in accordance with the principles of sound isolation explained in Section 4·12 of Chapter 4.

(c) MAGNETICALLY ACTUATED DEVICES

This class of equipment includes relays, contactors, circuit breakers, and the like. Devices in this class commonly embody an armature which is caused to move as a result of magnetic forces originating in a solenoid. If the solenoid is energized by alternating current, an alternating force similar to that created by a transformer exists and the same principles of isolation apply. A direct-current solenoid, on the other hand, is characterized by a constant force, and there is no problem in isolating the forces resulting from voltage fluctuation. In either event, however, there is a problem resulting from the movement of the armature.

A magnetically actuated device of the class being considered here is a machine of conservative momentum, similar to the punch press and the loom. (See Section 3·11 of Chapter 3.) It resembles a loom in that the armature is propelled by the solenoid and arrested by a bumper placed in its path of motion. Since the propelling and arresting impulses are generally different in nature, the entire body of the device tends to experience a resultant displacement, as illustrated in Figure 3.29, and must be restored by the isolator. The magnitude of the displacement varies from one device to another, and the isolator is required to accommodate such displacement in order to attain optimum performance.

(d) FANS AND BLOWERS

The term fan is used here to designate a machine having a rotor with several blades arranged to cause a flow of air or gas axially of the fan; the term blower designates the so-called squirrel-cage blower in which the air flows into the blower in an axial direction and out in a radial direction. Machines of these types operate at many different speeds, depending on the size and the type of service. In general, the operating speed decreases as the size of the fan or blower increases. Predominant sources of vibration are rotor unbalance; bearing, gear, and belt forces; motor impulses; and aero-dynamic forces resulting from turbulent flow of air through and around structural members.

In the application of isolators to fans, the method to be pursued depends to a large extent on the rotor speed. Fans and blowers often exhibit evidence of crude workmanship, and rotor unbalances of appreciable magnitude are not uncommon. If the rotor speed is 1,200 rpm or greater, there is a reasonable opportunity to isolate the vibration resulting from rotor unbalance, provided that the isolators can be applied in a plane extending reasonably close to the center of gravity of the machine. Such an application often proves advantageous. If the rotor speed is appreciably lower than 1,200 rpm, isolation of the unbalances should not be undertaken unless one of the relatively elaborate methods described in Section 6·1 on low-speed machinery seems justifiable. In many instances, it is preferable to balance the rotor and thereby eliminate the need for isolation of the forces resulting from the unbalanced condition. Other sources of vibration in a fan or blower are similar to those described above under gears and bearings; any isolator used on a fan or blower should therefore embody the characteristics recommended for isolation of gear and bearing vibration. This is in addition to any requirement for isolation of forces resulting from rotor unbalance.

(e) PUMPS

This class of equipment is comprised of both centrifugal and reciprocating pumps. The former usually includes a multi-vane rotor which operates at a relatively high speed. Vibration may be expected at the rotational frequency, as a result of mass unbalance of the rotor; at the vane frequency, because the moving vanes pass in close proximity to the fixed vanes; and at random frequencies, usually relatively high, as a result of forces created by turbulent flow of liquid within the pump. Centrifugal pumps are quite adaptable to the application of vibration isolators. The principles set forth in Chapter 2 should be followed, care being taken to have the natural frequency of the pump-and-isolator system in all natural modes of vibration substantially lower than the rotational frequency of the pump. This natural frequency will also be lower than the vane frequency. Such an application usually is satisfactory because the operating speed is sufficiently high to justify a relatively stiff isolator, and the oscillating forces are so small that overall vibration of the pump body is not appreciable.

Reciprocating pumps are used for causing a flow of liquid, for compressing air and gas, and for creating a vacuum. These are characteristically low-speed machines, and the number of cylinders usually is small. The discussion in Sections 6·2 and 6·3 of this chapter is generally applicable to reciprocating pumps. Unbalanced rotating and reciprocating parts and torque impulses associated with the work being done on the fluid are predominant sources of vibration. Minor sources of vibration are gears and bearings, motor impulses, and aerodynamic or hydrodynamic forces resulting from turbulent flow of fluids through and around structural members. The isolation of forces resulting from the operation of reciprocating pumps presents many problems. Often the speed is low, and the forces are large. A relatively elaborate arrangement of isolators, as discussed in detail in Sections 6·1 to 6·3 of this chapter, is then necessary in order to obtain satisfactory results. If this is not justifiable, isolation of the major forces should not be attempted. In such instances, the isolator should be designed to be relatively stiff, and thereby prevent excessive movement of the pump. It should, however, embody the characteristics necessary to isolate the vibration originating in gears, bearings, and other similar sources.

(f) PRINTING PRESSES

Printing presses may be of the rotary or the reciprocating type. In the former, the principal rotating parts are quite massive, but the unbalance usually is not great and the rotational frequency is relatively low. An attempt to isolate the vibration from this source should be made only in exceptional cases. If isolation of this vibration is necessary, the methods suggested in Section 6·1 may usually be adapted. In general, however, there is greater need to isolate the vibration originating in the action of gears, bearings, and cams. A relatively stiff isolator whose requirements are set forth in preceding paragraphs of this section is suitable.

A large reciprocating printing press presents a more difficult problem. Characteristic features of such a press are:

(1) Relatively large inertia forces at low frequencies, as a result of the reciprocating motion of massive members. These forces may become sufficiently great to cause objectionable swaying of the building that houses the press.

(2) Miscellaneous vibration and impacts resulting from the operation of gears, cams, bearings, and similar mechanisms. The magnitudes are usually small, but the number of occurrences is large and the cumulative effect may be considerable.

(3) A relatively non-rigid framework for supporting the mechanism. Many machines are fabricated from light and loosely joined structural members and require a rigid mounting base for proper operation.

A printing press presents an unusual problem in that appreciable overall movement of the press often cannot be tolerated because it interferes with the register of the paper moving through the press. Two alternatives are presented: (1) installing relatively stiff isolators which prevent appreciable movement of the press and transmit large forces to the building structure or (2) adding mass to the press in the form of a concrete foundation and employing the methods described in Section 6·1 of this chapter for isolating low-speed machinery. The latter method is feasible only if the operating frequency of the press is approximately 250 cycles per minute or higher. For a lower operating frequency, the isolator must have a natural frequency that is so low that special consideration must be given to maintaining the stability of the system. Some large presses operate at frequencies as low as 50 cycles per minute. In such instances, isolation of the inertia forces resulting from the reciprocating motion of principal members of the press is not feasible.

The most successful method of mounting large printing presses, in locations where the building is able to withstand the inertia forces involved in press operation, is to secure the press rigidly to a concrete foundation which is, in turn, supported by isolators. Two principal advantages of this type of installation are: (1) the press acquires the rigid foundation that is required to maintain the alignment of structural members and (2) mass is provided whose inertia tends to oppose the forces created by operation of the press.

Two typical designs of floating concrete foundation which have been successfully adapted to the mounting of heavy printing presses are shown in Figures 6.13 and 6.14. Where the entire installation must be above floor level, it is desirable to hold the overall height of the foundation to the minimum. The foundation shown in Figure 6.13 meets these requirements. It is encased in a steel frame *a* several inches deep with a steel plate *b* secured to the lower side thereof. The foundation is most conveniently installed by first securing the frame to rubber isolators *c*, setting it in the desired location, and filling it with concrete to the level of the top of the frame. The printing press is then secured to this floating foundation, either by means of anchor bolts embedded in the concrete or by bolts extending through the top flange of the steel frame.

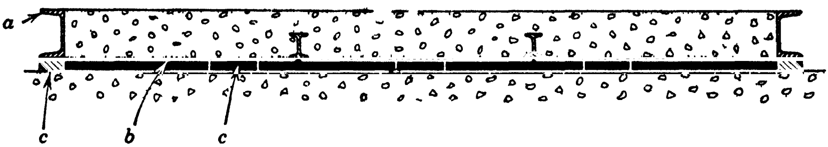

Figure 6.13. Floating concrete foundation supported by rubber isolators and adapted to installation above floor level.

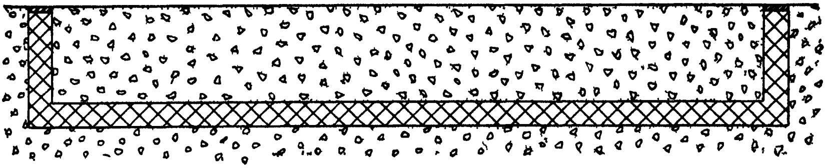

Figure 6.14. Floating concrete foundation supported by cork and adapted to installation flush with floor

The alternate type of foundation shown in Figure 6.14 is preferable when installed on the ground floor because it maintains the base of the machine at floor level, thereby eliminating the increase in height that is inherent with the design illustrated in Figure 6.13. It becomes necessary, however, to provide a pit to receive the foundation block. The pit is lined with concrete so that all inside dimensions are several inches larger than the overall dimensions of the floating foundation. Cork is commonly used for this type of installation; it is arranged at the bottom and sides of the pit before pouring the concrete. If the weights of the foundation and printing press are such that the full plan area is not required for load-carrying purposes, cork pads of the required area are provided and the voids are filled with sand which may be washed out after the concrete has set. Characteristics of cork are given in Section 5·19 of Chapter 5.

(g) FORGING HAMMERS

The term forging hammer is used here to designate a machine in which a relatively heavy hammer is caused to fall freely against an anvil. The metal being forged is placed upon the anvil and struck by the falling hammer. The principal problem from the standpoint of shock arises from the fact that the momentum of the falling hammer is transferred to the body of the machine. The machine thus tends to acquire a downward velocity, and to carry its foundation with it. The shock arising from this condition may be alleviated by any of the following procedures:

(1) The machine may be secured to a massive block of concrete. Such a block is conveniently constructed in a pit used as a mold in which to cast the concrete. The inertia of the concrete mass opposes downward movement of the machine, and reduces the magnitude of the disturbance.

(2) The machine may be supported by isolators placed directly under the machine. The isolators permit the machine to move in response to the momentum transfer and transmit but a relatively small force to the floor. This type of installation is often considered unsatisfactory in operation, however, because the anvil moves away from the hammer and prevents the attainment of a sufficiently great metal-working force. Furthermore, the resultant movement of the machine contributes to excessive operator fatigue.

(3) A combination of methods (*a*) and (*b*) above constitutes a preferred installation. The machine is secured rigidly to a concrete foundation which is, in turn, supported by isolators. The design shown in Figure 6.14 is suitable for this purpose. The concrete foundation adds mass to the machine; it thereby makes possible a large force between hammer and anvil and limits the overall motion of the machine. The isolators limit the magnitude of the force transmitted to the floor.

The theory underlying the application of isolators to forging machines is discussed in detail in Sections 3·8 to 3·10 of Chapter 3. The method of applying this theory to the design of isolators in a particular instance is illustrated by Example 3.3, page 133.

(h) MACHINE TOOLS

Advantageous results may frequently be attained by mounting certain types of machine tools upon isolators. Isolators under surface grinders have been notably successful, but the technique also proves of value with any machine tool that requires that accurate alignment of structural members be maintained. A common source of trouble with such a machine results from impulsive forces applied to the floor that supports the machine. These forces may originate in adjacent machinery, or in the passage of vehicles either inside or outside the building.

The nature of the problem is best explained by reference to Figure 3.33 of Chapter 3. The body of the machine is indicated by m_y, and the abrasive wheel of the surface grinder, for example, is simulated by m_z. The spring k_z represents the arbor and other structure that support the abrasive wheel. In a surface grinder, the spring k_z is designed to be very stiff in order to restrict relative motion between the wheel and the work being ground. It has the characteristics of a spring, nevertheless, in that it deflects elastically if a force is applied to it.

The crucial relation here is the ratio of the natural frequency Ω_z of the arbor assembly to the natural frequency Ω_s of the support or floor. If the latter is equal to or greater than the former, $\Omega_z/\Omega_s \leq 1$ and the deflection δ_{sz} of the spring k_z becomes relatively large when the support is subjected to an impulsively applied force. This is shown in Figure 3.34. In other words, the abrasive wheel moves relatively to the material being ground, and imperfections appear in the ground surface. It is important to note that this relative motion of the abrasive wheel is appreciably reduced by increasing the ratio Ω_z/Ω_s; i.e., by making the support less rigid. This may be accomplished by placing isolators under the base of the machine.

The choice of a natural frequency for the isolators is not critical. Machine tools are designed to be relatively rigid, and the isolator, therefore, is not required to have a low natural frequency to attain a satisfactory frequency ratio Ω_z/Ω_s. A natural frequency of 20 to 25 cps in the vertical translatory mode has been found from experience to give eminently satisfactory results with many types of surface grinder. The same recommendation would seem to be in order for machine tools in general.

6·8 Train and Road-Vehicle Installations

The advent of two-way radio telephone equipment in railroad trains, police cruisers, taxicabs, and other vehicles opened a new field for shock isolators. Experience with such installations is presently quite limited, and but few data are available to indicate the nature of the shock that is encountered. Although the general principles are clear, the quantitative data presented in the following paragraphs are taken from the results of initial experiences only. The concepts probably will be modified somewhat as experience is accumulated.

The principal conditions of vibration and shock significant in railroad-train installations may be outlined as follows:

(*a*) Shock motions of the type described in Chapter 3 as velocity shock occur during coupling of cars and in starting long trains. Coupling often involves impact between two cars, as a result of which an initially stationary car may acquire a velocity or an initially moving car may experience a change in velocity. In starting long trains, common practice calls for suddenly starting one car at a time as the lost motion in the coupling devices is successively taken up from the front to the rear of the train. Although a velocity change of 100 in./sec or greater may occur occasionally, a suggested value for design purposes in connection with equipment mounted in cars and locomotives is 50 in./sec.

(*b*) A principal reason for equipment failure in this type of service arises as a result of resonance of elements of the equipment with the structure of the car or locomotive. Many components of electronic equipment include moderately stiff, lightly damped elastic members. The structure of the vehicle is excited to vibrate in a transient manner by minor impacts and vibration. When the natural frequencies of such structural and electronic components coincide, the vibration amplitude of the latter may be increased by resonant effects; the life of the component is correspondingly reduced. Theoretical aspects of this condition are discussed in Section 3·14 of Chapter 3.

The following recommendation for the design of isolators for electronic equipment to be installed in railroad trains is predicated on the successful experience of Bendix Radio Division of Bendix Aviation Corporation. The recommended design objective is a natural frequency of 20 cps. As in many other applications of shock isolators, it is desirable to maintain this natural frequency as nearly uniform as possible in all modes of vibration.

A linear isolator having a natural frequency of 20 cps experiences a deflection considerably more than one inch when subjected to a velocity shock of 50 in./sec. (see Figure 3.9). Space is limited in railroad trains, and such a deflection would be considered excessive. This application calls for rubber in compression, to limit the deflection to a reasonable value without snubbing. The maximum deflection of the isolator and the maximum acceleration of the mounted equipment are then determined from Figure 4.11. Arbitrarily selecting the isolator thickness $h_i = \frac{3}{8}$ in., and substituting $V_y = 50$ in./sec and $f_t = 20$ cps, the abscissa parameter is calculated to be 6.67. The ordinate as determined by the solid line is 0.00613, from which the maximum acceleration $\ddot{y}_0/g$ is 41 g. The maximum deflection of the isolator, as indicated by the dotted line in Figure 4.11, is $0.7 \times h_i$, or slightly more than $\frac{1}{4}$ inch.

The particular physical arrangement of the isolators with respect to the equipment is not of critical importance. An optimum arrangement calls for the isolators to be located in a plane passing through the center of gravity of the equipment, although installations of isolators only at the four lower corners have been successful. The predominant shock is in a direction longitudinally of the train, and this direction should be favored where a compromise is necessary. Equipment mounted in railroad trains characteristically receives rough treatment, and vulnerable assemblies consequently should be mounted within rugged enclosures. Isolators should preferably be within the enclosure; if external to the enclosure, they afford protection only against shock transmitted through the structure of the vehicle and not against impacts of foreign bodies with the enclosure. Isolators located within the enclosure are protected from prevailing atmospheric conditions and can usually be better applied.

The conditions encountered in road vehicles of the passenger type, such as police cruisers and taxicabs, differ considerably from railroad-service conditions. The most notable difference is the absence of the severe velocity shock that is characteristic of railroad service. The predominant motion in road vehicles is a transient vibration having many frequency components combined in an irregular pattern. The numerical values of the frequencies are largely determined by the characteristic natural frequencies of certain sub-assemblies of the vehicle, whereas the amplitude of the resulting motion is a function of the road surface and the speed of the vehicle. The following frequency components are important:

(*a*) The natural frequency of the vehicle chassis supported by its springs is of the order of one cycle per second. The amplitude associated with motion at this frequency commonly reaches a maximum of several inches but, with modern hydraulic shock absorbers, decreases rapidly to a negligible value.

(*b*) The natural frequency of the unsprung weight is approximately 8 to 12 cps in passenger vehicles. The unsprung weight includes wheels, axles, brakes, gears, and other structure not normally supported by the main springs of the vehicle. Upward and downward motion of the unsprung weight involves elastic extension and compression of the main springs and the tires. This system thus has a characteristic natural frequency. The vibration of the unsprung weight is sometimes referred to as wheelhop, and the amplitudes are so great that substantial force is transmitted through the main springs and shock absorbers to the chassis.

(*c*) The chassis and vehicle body vibrate at the natural frequencies of local structures, but these frequencies vary greatly throughout the vehicle and no typical value can be given.

The principal cause of damage to electronic equipment installed in road vehicles is believed to be resonance of equipment components with structural members of the vehicle, as explained above in connection with railroad service and in Section 3·14 of Chapter 3. As indicated in Section 3·15, the effectiveness of isolators increases as their natural frequency decreases. A minimum natural frequency is established by the necessity of preventing excessive transient motion of the mounted equipment, and of avoiding resonance with vibration of the unsprung weight. A recommended design objective for the isolator natural frequency is 25 cps, although a somewhat lower frequency may be preferable if the wheel hop frequency tends to be low and if the precautions explained in the next paragraph are taken.

In installations that embody relatively flexible supports, the natural frequencies of the isolator system cannot be determined independently of the properties of the support. The interdependence of these parameters is illustrated by Figure 4.36. A common method of installation calls for attachment of the equipment to the floor of the trunk compartment, or to the floor at the side of the driver's position. Floor construction at these locations may embody unstiffened panels whose properties detract from the stiffness of the isolators and give lower natural frequencies than anticipated. The floor construction should be sufficiently rigid, and the equipment as attached to the isolators and installed in the vehicle should have the desired natural frequencies.

6·9 Military Equipment—General

The following several sections deal with vibration and shock isolators for military equipment. Included in this category are isolators for equipment installed in aircraft of the Air Force, the Navy, and the commercial air lines; in vessels of the Navy; in combat vehicles of the armed services; and for portable field equipment. Each of the services has its own particular requirements which are dictated both by the type of equipment to be protected and by the nature of the service to which it is subjected. Although the isolators used by the various branches of the military establishment have many differences, they also have much in common as follows:

(*a*) They are often subjected to much more stringent service conditions than commercial equipment. The shock is more intense; severe vibration is more prevalent; temperatures tend to higher or lower extremes; and atmospheric conditions are more corrosive.

(*b*) The military establishment seeks at all times the most suitable design for the purpose. Any improvement whatsoever, small though it may be, is considered worthwhile on the theory that there is no actual limit to severity during conditions of war and any slight incremental improvement may represent the difference between success and failure. The test for suitability includes not only performance but also size and weight. The services show a reluctance to adopt a complicated design because the time required for fabrication and possible difficulty in obtaining materials would tend to impede procurement in large quantities.

(*c*) Isolators for the military services are usually required to conform to applicable specifications, or to successfully withstand controlled laboratory tests. This is generally the sole test for suitability, in contrast to the usual commercial practice of designing and testing isolators to give adequate performance under actual service conditions. Commercial practice is, of course, impractical for military equipment because service conditions often constitute warfare. Specifications also assure that isolators procured for a certain application will be dimensionally interchangeable with other isolators used for the same application, to permit ready replacement in the field.

The specifications for vibration and shock isolators usually refer to both the durability of the isolators and their ability to protect the equipment that they support. Durability must, of necessity, be determined from accelerated tests whose interpretation requires considerable judgment. Performance is evaluated by several methods. Vibration isolators are sometimes considered an integral part of the equipment which they serve. Their suitability is then judged by the performance of the equipment when the equipment-and-isolator assembly is subjected to a vibration test which is intended to simulate service conditions. Vibration isolators are often evaluated without regard to the operation of specific equipment. The test for suitability is then their ability to limit the magnitude of vibration transmitted to an equipment mock-up.

With regard to shock isolators, past custom has been to consider the isolators integral components of a particular equipment, and to judge their suitability by their ability to protect the equipment when subjected to the accepted standard conditions of shock. Present trends are toward the establishment of absolute performance standards, whereby the adequacy of isolators would be established without regard to the requirements of the particular equipment. In spite of many shortcomings, existing specifications that apply to vibration and shock isolators for military purposes are usually successful in rejecting non-suitable devices. Results that have appeared unsatisfactory in this respect are more likely to have been caused by waiver and non-observance than by inadequacy of the specifications.

6·10 Military Equipment—Aircraft

The requirements for isolators as set forth by the Air Force, the Navy, and the commercial air lines differ only in minor details. Isolators find many applications in modern aircraft. All reciprocating power plants are supported by isolators, for the purpose of reducing the severity of vibration transmitted to the aircraft structure from the power plant. Instrument panels employ vibration isolators to protect panel-mounted instruments from the vibration that is prevalent in the aircraft. Much of the accessory equipment, such as radio, radar, bombsights, and navigational aids, is usually in the form of small individual units, attached to the aircraft structure by isolators. In a few applications, several such devices are secured directly to a large rack, which is then supported by isolators.

The predominant vibration in aircraft results from the propulsion system. Where the power plant is of the reciprocating type, the principal fundamental vibration frequencies and sources of excitation are as follows:

(*a*) Fluctuation in the driving torque is a principal source of excitation. It results from (1) the gas-pressure cycle, considered identical in each cylinder, which gives rise to a predominant vibration at engine firing frequency; (2) variation in the gas-pressure cycle from cylinder to cylinder, which gives rise to a frequency at predominantly one-half engine speed; and (3) the inertia torque of the engine, which gives rise to frequencies depending on the nature of the rotating system of the engine.

(*b*) Mass unbalance of the engine, consisting of inertia forces and couples, occurs primarily at the rotational frequency and secondarily at twice the rotational frequency. Frequencies of higher order are also present, but their importance decreases as the order increases.

(*c*) Residual propeller unbalances, resulting from mass unbalance of the propeller and from failure to obtain accurate centering on the propeller shaft, induce vibration at the rotational frequency of the propeller. This differs from the frequency of engine unbalance in systems with a geared drive from engine to propeller.

(*d*) Aerodynamic forces from the propeller occur at both the rotational frequency and the blade frequency. The latter is the product of the rotational frequency and the number of blades per propeller. Harmonics up to several orders are present in varying degrees, depending on the nature of the excitation and the response of individual local structures to aerodynamic forces. These forces result from the action of the airstream upon exposed surfaces of the aircraft. The numerical values of these frequencies cover a wide range, as they are dependent on the air velocity, the surface characteristics of the aircraft, and the natural frequencies of various structural components.

Different conditions of vibration arise upon the introduction of gas-turbine and jet-propulsion systems. In the so-called turbo-prop system, the conventional propeller is driven by a gas turbine which operates at a very high rotational speed. Vibration induced by aerodynamic action of the propeller or by its mass unbalance is therefore similar to that encountered with reciprocating power plants. Mass unbalance of the high-speed rotating parts of the turbine induces vibration at a relatively high frequency in place of the lower frequency associated with mass unbalance and torque variation of the reciprocating engine. In the turbo-jet system, the propeller is eliminated and only the vibration induced by unbalance of the turbine remains. In both systems, the aircraft exhibits low-frequency vibration, especially at high speeds, owing to aerodynamic buffeting.

The vibration frequencies may be predicted to a large extent from the type of propulsion system, but the prediction of vibration amplitudes is extremely difficult. The latter is almost impossible except on a statistical basis which presupposes extensive test data. A vibration amplitude of a few thousandths of an inch would generally be considered severe, although substantially greater amplitudes have been measured sufficiently often to indicate the possibility of their being encountered in service.

The lowest vibration frequency characteristically occurs during warm-up periods on the ground. This frequency may be so low as to be resonant with vibration isolators for equipment, and the equipment supported by such isolators may vibrate with considerable amplitude. Little harm is likely to occur in such instances, because vibration at low frequencies does not in general cause damage to equipment and because the duration of such vibration is limited to warm-up periods. Damping or other means associated with the isolator to limit the vibration amplitude at low frequencies is desirable. During flight, the vibration frequency is substantially higher and enters the range in which isolators provide appreciable protection.

The shock to which the equipment in aircraft is subjected can hardly be designated by the term shock as it refers to many other applications, both military and non-military. The greatest shock usually occurs during landing. This may be the result of an excessive downward velocity of the aircraft at moment of contact with the ground, or of the action of the arresting gear used on Naval aircraft carriers to bring the aircraft to a stop. In either event, a force is applied to the aircraft by means of a relatively flexible device. The conventional landing gear has a capacity for experiencing a very large deflection. Similarly, the arresting cable on carriers permits the aircraft to travel a considerable distance, after contact with the cable, before being brought to a halt. The landing gear and arresting cable thus function as shock isolators for the aircraft as a whole. They perform the characteristic function of shock isolators by storing a large quantity of energy, which is subsequently released at a much lower time rate. The displacements of these isolators are measured in feet, and the natural frequencies are one cycle per second and lower. The force exerted by the landing gear or arresting cable is relatively small, and the maximum deceleration of the aircraft is not excessive during normal operation.

The optimum natural frequency of isolators for supporting equipment in aircraft is substantially greater than one cycle per second. Figure 3.10 may be adapted to an analysis of this condition. The landing gear of the aircraft is considered as the isolator, with a natural frequency Ω_y; and the equipment-and-isolator assembly is considered as the element, with a natural frequency Ω_z. Then $\Omega_z/\Omega_y \gg 1$, and the extreme right-hand region of Figure 3.10 becomes applicable. The maximum acceleration experienced by the mounted equipment, when the landing gear embodies but little damping, is thus approximately equal to the maximum acceleration embodied in the rigid body motion of the aircraft.

A compromise between mutually opposing considerations must be effected in selecting the optimum natural frequency for the isolators.

The natural frequency should be relatively low, to afford effective vibration isolation at the lower forcing frequency. It should not be too low, however, because excessive motion of the mounted equipment occurs as a result of shock. The static deflection of an isolator, as indicated in Figure 2.4, varies inversely as the square of the natural frequency. For example, the static deflection corresponding to a natural frequency of 10 cps is 0.1 inch. Inasmuch as the right-hand region of Figure 3.10 applies, as explained in the above paragraph, the maximum excursion of the mounted equipment relative to the aircraft is given approximately by the product of static deflection of the isolator and maximum acceleration of the aircraft. For example, an isolator whose natural frequency is 10 cps thus deflects as much as 0.5 inch when the acceleration of the aircraft is $5g$.

Space for installation of equipment in aircraft is limited and means must be adopted to prevent excessive excursion as a result of shock. Two alternate means are available. The first is to provide snubbers that allow adequate clearance for effective vibration isolation but restrict movement of the mounted equipment beyond a designated position. The second is to increase the natural frequency, thereby decreasing the static deflection, to such an extent that snubbers are not necessary during normal operation of the aircraft. There are certain disadvantages to both of the above means. Snubber engagement tends to increase the destructive effects of a shock, as explained in detail in Section 3·6 of Chapter 3, and should be avoided if possible. On the other hand, a high natural frequency is not capable of isolating vibration that occurs at low frequency, as during warm-up periods. There is reason to believe that the higher natural frequency may provide adequate vibration isolation for many types of equipment and that some applications embodying isolators of low natural frequency have suffered as a result of snubber engagement.

A certain degree of damping in the isolator is desirable, provided that the damping is not sufficiently great to increase the transmissibility when the forcing vibration is of high frequency. In rough air and during landing, the mounted equipment tends to experience large excursions as the direction of motion or the velocity of the aircraft is suddenly altered. The equipment is thus forced against the snubber. In the absence of damping, the resultant transient vibration may continue for a long period, during which the equipment rebounds from one snubber to the other. The presence of damping counteracts this tendency. Damping also prevents excessive vibration amplitude of the mounted equipment during warm-up periods on the ground, when the forcing vibration of relatively low frequency may be resonant with the isolators. These factors are taken into consideration in specifications for laboratory vibration testing that require that contact with the snubbers should not continue substantially beyond the resonant frequency, as the test frequency is increased through the specified frequency range. An isolator without adequate damping fails to meet this requirement, and a pseudo-resonance continues to a high frequency.

An outstanding example of optimum isolator arrangement is found on the instrument panels in many types of aircraft. Such panels usually contain many small, directly mounted instruments. One form of instrument panel is a cuboid comprised of an open framework; the isolators are located within the panel in a plane passing through its center of gravity. In another type of construction, the instrument panel is in the form of a single plate arranged in a vertical plane. The instruments represent the principal mass, and they project rearward from the plate. The isolators are also placed at the rear of the plate in a vertical plane through its center of gravity. It is preferable that isolators located in this manner exhibit equal stiffnesses in all directions. The natural frequencies in all translatory modes of vibration thus become equal. If the isolators are located so that their distances from axes through the center of gravity of the panel are equal to the respective radii of gyration, the natural frequencies in rotational modes then become equal to the natural frequencies in translatory modes.*

The ever-increasing quantity of accessory equipment in modern aircraft is mounted to assure maximum convenience of installation and maintenance. Accepted maintenance procedures call for removal and replacement of complete units of equipment. The equipment is secured, by a readily detachable means, to a mounting base which includes vibration isolators that can be permanently secured to the structure of the aircraft. A typical mounting base, as illustrated in Figure 6.15, is comprised of a fabricated frame with a unit isolator at each of the four corners. The equipment is secured to the mounting base by sliding it in a front-to-rear direction against spring-loaded pins at the rear of the mounting base. The pins engage apertures in the rear face of the equipment. The mounting base is provided with thumb nuts at the front edge, which are tightened against projections on the front panel of the equipment. The mounting base sometimes embodies a wiring harness, which includes a receptacle positioned to engage a plug on the rear of the equipment as the equipment is assembled onto the mounting base. Flexible bonding straps commonly by-pass the isolators to provide a connection of high electrical conductivity between the mounted equipment and the structure of the aircraft.

---

* For a detailed analysis of this condition, see Section 2·10 of Chapter 2.

Standardization of methods for mounting aircraft accessory equipment has been formulated as standard dimensions and weights for the equipment, largely as a result of the efforts of the Armed Services Electro Standards Agency. Several discrete lengths, widths, and heights are established, the various combinations of which establish standard equipment sizes. One or two weight ranges are assigned to each size. It is contemplated that mounting bases standardized as to size and weight of equipment will be available for each of the standard equipments. This objective has not yet been attained, however, and the mounting base usually is tailored to the size and weight of the particular equipment involved. Although many odd sizes of equipment are in use, standard dimensions predominate. Little apparent attempt is made to maintain standard weights, however, and the isolator stiffness is adjusted to accommodate the weight of the particular equipment.

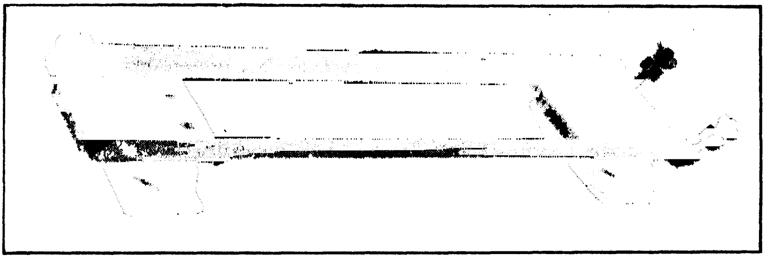

FIGURE 6.15. Typical mounting base with isolators as used with air-borne electronic equipment (Courtesy The Barry Corporation.)

Necessary information for determining the required stiffnesses of the isolators in the various directions is obtained from Figures 2.3 and 2.11. The dimensions of the standard equipments are such that the height-to-width ratio is always greater than approximately 0.5, and always less than approximately 1.5 If the ratio k_x/k_y, horizontal to vertical stiffness of the isolators, is maintained between 0.25 and 0.50, the maximum coupled natural frequency is between 1.25 and 1.65 times the vertical natural frequency. The minimum coupled natural frequency is then between 0.40 and 0.65 times the vertical natural frequency. Isolators having a large stiffness ratio k_x/k_y should be avoided with the type of mounting base illustrated in Figure 6.15. It becomes evident from Figure 2.11 that the maximum coupled natural frequency has a relatively high value when $k_x/k_y = 1.0$, and a very high value when $k_x/k_y = 2.0$. The ability of such isolators to withstand inclination of the aircraft without excessive lateral excursion is not sufficient compensation for the deterioration in isolation effectiveness resulting from the high natural frequencies.

6·11 *Military Equipment—Vehicles*

Extensive investigations have been conducted by agencies of the U. S. Army, principally the Signal Corps, Frankfort Arsenal, and Aberdeen Proving Grounds, to determine the nature of the shock and vibration that exists in wheeled and track-laying vehicles. The shock motion experienced by such vehicles is an irregular transient vibration characterized by relatively large amplitudes and many frequency components. The sudden velocity change that characterizes the severe shock encountered in many military applications does not normally occur as a result of movement of the vehicle on the traveled surface. The following principal frequency components and representative amplitudes have been found typical of shock conditions in a 2½-ton cargo truck:

(*a*) The most prominent vibration involves the motion of the entire vehicle chassis upon the supporting springs. The displacement amplitude of this vibration may be as great as five inches (ten inches peak-to-peak amplitude) at frequencies between one and four cycles per second.

(*b*) The unsprung weight of the vehicle, comprised of wheels, axles, and portions of the driving mechanism, combines with the tires and springs to form an elastic system which is excited by road irregularities to vibrate at its natural frequency. This vibration is transmitted in part to the vehicle chassis. Its characteristic frequencies are between 10 and 20 cps, and the resultant displacement amplitude of parts of the vehicle chassis may be as great as 0.05 inch (0.10 inch peak-to-peak amplitude).

(*c*) The structural members of the vehicle chassis are excited to vibrate in a transient manner at their natural frequencies, as a result of forces transmitted through the springing system of the vehicle. The frequencies cover a wide range, depending on the type of vehicle structure. The displacement amplitudes are almost invariably low, seldom exceeding 0.005 inch (0.01 inch peak-to-peak amplitude).

Data bearing a marked similarity to the above have been obtained from road tests on a medium tank. The natural frequency of the tank body-spring system is between one and three cycles per second, and the maximum displacement amplitude of the body during road travel is approximately two inches. The structures are somewhat more rigid than truck structures. The minimum structural natural frequency is of the order of 100 cps, and a displacement amplitude of 0.001 inch represents a relatively high value for normal operation.

The predominant forced or steady-state vibration in a wheeled vehicle results from the engine and therefore depends on the operating speed of the vehicle. In wheeled and track-laying vehicles, vibration from the engine occurs at a frequency always greater than 30 cps, except at very low speeds and when the engine is idling. The amplitudes associated with these vibrations are usually small compared with the amplitudes of the transient vibration noted above. In track-laying vehicles, the predominant forced vibration occurs at the track frequency. The speed of such vehicles ranges up to 30 miles per hour, and a typical track pitch is six inches. The track frequency is then calculated:

$$f_t = \frac{5280 \times 12 \times V_h}{60 \times 60 \times 6} = 2.93V_h,$$

where f_t = track frequency, cps.
V_h = traveling speed of vehicle, miles per hour.

The frequency f_t is lower than 30 cps only when the vehicle is moving at a speed less than approximately ten miles per hour.

The transient vibration in a vehicle is composed of several principal components. Two of these components, vibration of the vehicle body upon the springs and vibration of the unsprung weight, exhibit frequencies that are relatively low. Isolation of the vibration occurring at these frequencies should not be attempted. The low frequency of the vibration would require isolators of such low stiffness that the resultant system would be too unsteady for vehicular service. Furthermore, the amplitudes are large, and an isolator capable of sustaining the deflection required to accommodate such an amplitude would be too large for vehicular use. A different condition often exists, however, with respect to the transient structural vibration and the forced vibration resulting from the engine. Vibration from these sources is characterized by low amplitudes and relatively high frequencies. Isolation of the vibration at these frequencies is often feasible and contributes to decreasing the possibility of damage being sustained by equipment mounted in vehicles. The principles of isolation of the forced vibration are discussed in Chapter 2; isolation of the vibration resulting from the transient excitation of structural members is considered in Sections 3·14 and 3·15 of Chapter 3.

The following characteristics are recommended for isolators mounted in vehicles of the Armed Forces:

(*a*) Resonance with any predominant vibration of the vehicle as noted above should be avoided. Inasmuch as space limitations preclude isolators with very low natural frequencies, the design objective should be set so that the minimum natural frequency is slightly greater than the frequency caused by vibration of the unsprung weight. The natural frequency of the unsprung weight may occasionally be as great as 20 cps, and a minimum natural frequency of 25 cps for the isolators is thus indicated. This frequency is suggested for general purposes, but it may be adjusted downward if the natural frequency of the unsprung weight is known to be substantially less than 20 cps.

(*b*) The force-deflection characteristic of the isolators should exhibit gradual stiffening, and lack of hard bottoming, for deflections as great as 75 percent of available clearance. A convenient method of attaining this characteristic is to employ rubber in compression for all possible directions of motion. The mounted equipment should be made captive by the metal parts, in event of failure of the resilient element.

(*c*) In order to conserve valuable space, the overall size of the isolators should be made as small as possible, consistent with effective operation. Since the size increases with the required maximum deflection, it is of interest to determine the maximum deflection of isolators in vehicular service. Pertinent data are set forth in Table 6.3. The difference between the vehicle and the equipment amplitudes in Table 6.3 represents the greatest possible deflection of the isolators.

TABLE 6.3

Maximum Vibration Frequencies and Amplitudes in Vehicular Service

Source of Vibration	Frequency, cps	Vehicle Amplitude, in.	Equipment Amplitude,* in.
Body-spring system	4	5.0	$1.04 \times 5 = 5.20$
Unsprung weight	20	0.05	$2.2 \times 0.05 = 0.11$
Structure	75	0.005	$-0.2 \times 0.005 = -0.001$

* The equipment amplitude is calculated from Figure 2.2, on the assumed basis of steady-state vibration and an isolator natural frequency of 25 cps. It thus tends to be extreme because the vibration is actually in the nature of a decaying transient, and the equipment amplitude does not have an opportunity to build up to the equivalent steady-state value indicated by Figure 2.2.

It will be noted that the maximum deflection is 0.20 in. at the frequency of the body-spring system; 0.06 in. at the frequency of the unsprung weight; and 0.006 in. at the frequency of structural vibration. The negative sign of the equipment amplitude in the case of structural vibration indicates phase difference; the deflection of the isolator is thus obtained from addition of numerical values. These maximum deflections may at times become superimposed with a resultant isolator deflection slightly in excess of ¼ inch. On the basis of limiting the maximum deflection to 50 or 65 percent of the rubber thickness, isolators with a rubber thickness of ⅜ to ½ inch satisfy performance requirements; these are usually considered to occupy an acceptable amount of space in the vehicle.

(*d*) The presence of damping to an appreciable degree is a definite attribute in isolators for vehicular service. As pointed out above, the excitation in vehicular applications is usually transient in nature. The vibration of the mounted equipment is thus also transient and tends to die out rapidly if the isolator embodies substantial damping. It is not desirable to employ a complicated mechanical damper. Damping to the extent of 10 or 15 percent of critical ($c/c_c = 0.10$ or 0.15) is obtainable from internal hysteresis of some compounds of natural or synthetic rubber; this is considered suitable for preventing vibration of excessive amplitude when the structural vibration of the vehicle has components of low frequency.

(*e*) Isolators should be located where they can be conveniently installed and maintained. This usually calls for isolators at each of the four lower corners. Coupled natural modes of vibration are then introduced, and at least one of the natural frequencies becomes lower than the vertical natural frequency. The relation between these natural frequencies is indicated by Figure 2.11. The minimum coupled natural frequency may be as low as 50 percent of the vertical natural frequency, when the height-to-width ratio for the equipment is large. The vertical natural frequency is then required to be as high as 50 cps, in order to maintain the minimum coupled natural frequency above 25 cps. This represents an extreme condition, however, and a lower vertical natural frequency usually will suffice to maintain the minimum higher than 25 cps.

Land vehicles are sometimes subjected to ballistic impacts, and isolators must afford shock protection to equipment mounted within the vehicles. The maximum severity of this shock is estimated as equivalent to the maximum encountered in Naval shipboard service. The problems in isolating shock of this severity are discussed in Section 6·12, and the conclusions are generally applicable to ballistic shock in vehicles. Space in a vehicle is usually more restricted than aboard ship, and the sizes of isolators must therefore tend to the minimum. The consequent limitations in performance pointed out in Section 6·12 must be recognized.

6·12 Military Equipment—Naval Vessels

The design of isolators for use on Naval vessels is difficult because both vibration and shock of a troublesome nature exist concurrently. Naval vessels are subjected to a relatively small number of severe shocks, and these usually occur at a time when the vessel can least afford to be even momentarily immobilized. In addition to these severe shocks, many shocks of relatively small magnitude subject the equipment to a type of fatigue. The steady-state vibration of a Naval vessel occurs at a frequency that is generally too low to permit effective vibration isolation. The frequency range extends from practically zero to a maximum which varies from one type of vessel to another. The general philosophy in the design of isolators for Naval shipboard service is to design for protection against severe shock and, at the same time, to avoid excessive amplification of the steady-state vibration.

To define the nature and magnitude of the shock to which Naval vessels are subjected is difficult. The shocks are usually due to explosions of some type. They include contact explosions of torpedoes, bombs, and shells; non-contact underwater explosions of bombs and mines; and, finally, explosions resulting from the operation of the ship's own armament which cause an air blast to impinge upon exposed surfaces of the vessel. The many sources and magnitudes of shock and the many types of structures introduce almost infinite permutations of cause and result. Each shock therefore differs in some respect from every other shock. As a general definition of shock, certain structural members of the vessel suddenly acquire velocities that continue for a sufficient time to result in substantial displacements. These displacements and velocities usually have transient vibrations of the structural members superimposed upon them.

An exact specification of this shock does not appear possible. The general nature and maximum probable severity have been tentatively established and are indicated, to the extent required for isolator design, by the shock motions of the High Impact shock-testing machines in current use for testing Naval equipment. Such a machine includes a mounting plate and a large hammer arranged to strike the plate. As a result of the hammer impact, the plate suddenly acquires a velocity as great as approximately 100 in./sec, and a displacement as great as several inches. The equipment under test is attached to the mounting plate by an adapter whose structure is intended to simulate the structure normally employed for mounting the particular equipment aboard Naval vessels.

Although the shock created by the operation of this shock-testing machine represents the maximum probable severity, it should be expected that a few shocks of greater severity and many shocks of less severity will be encountered. Since there is no positive maximum for the severity of shock likely to be encountered, the force-deflection characteristic of the isolator should exhibit gradual stiffening in order to prevent hard bottoming during excessive shock. The required characteristic is attainable if rubber in compression is the resilient element. The response of an isolator employing rubber in compression, subjected to velocity shock, is analyzed in Section 4·4. The results of the analysis are presented graphically in Figure 4.11, which indicates the magnitude of the maximum transmitted acceleration in terms of shock velocity change, thickness of rubber, and natural frequency. The general data included in Figure 4.11 are transformed into data that are particularly adapted to Naval service, as indicated in Figure 6.16. These data indicate maximum transmitted acceleration as a function of isolator natural frequency, for the accepted velocity change of 100 in./sec, and for several discrete values of rubber

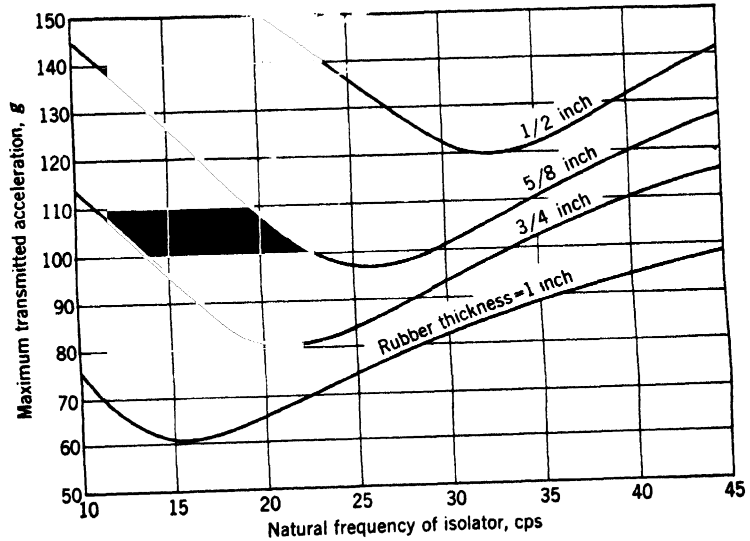

FIGURE 6.16. Maximum acceleration transmitted by shock isolator employing rubber in compression, as a function of isolator natural frequency. This refers to the maximum probable severity of shock encountered in Naval service, as represented by a velocity change of 100 in./sec.

thickness. The application of these curves to the design of isolators for Naval shipboard service is discussed in later paragraphs.

The predominant steady-state vibration of the structural members of a Naval vessel is caused by the propeller action. The vibration frequency is the propeller-blade frequency; i.e., the product of the tail shaft speed and the number of blades on the propeller. This frequency differs from one type of vessel to another. Major combat vessels are usually equipped with propellers having three or four blades, and the maximum tail shaft speed usually does not exceed 300 to 325 rpm. The maximum vibration frequency generally encountered is thus 1,200 cpm, or 20 cps. Frequencies as high as 22.5 cps are encountered in exceptional circumstances on some classes of vessels. The amplitude of the vibration varies within wide limits, depending on the location on the vessel. The vibration amplitude is usually relatively great at the stern, but equally great amplitudes may be encountered at almost any location where a local structure is resonant at the propeller-blade frequency. A displacement amplitude of 0.01 in. (0.02 in. peak-to-peak amplitude) is considered moderately severe on vessels of the Navy; the vibration amplitude of major structural members is usually much lower.

Isolators should be designed so that the shipboard vibration, at its maximum frequency of 20 cps, is not amplified more than three times. Such an amplification generally is not troublesome because the frequency of the forced vibration is low, and there is little danger of resonance with the components of the equipment. Experience indicates that equipment that is sufficiently rugged to meet Naval requirements successfully with respect to shock can be expected to withstand the normal shipboard vibration, even when amplified as much as three times by the shock isolator. Two alternate methods are suggested below for determining the requirements of isolators:

(*a*) A system with a minimum isolator natural frequency of 25 to 30 cps is not likely to become resonant with the highest forcing frequency. Maximum amplification of the forced vibration then does not exceed three times, and no special precautions need be taken to assure adequate damping in the isolator.

(*b*) The isolator natural frequency may be less than 25 cps, if adequate damping is available to maintain the amplitude within the prescribed limits. Such an isolator would operate, at least occasionally, at or near resonance. The damping required, as indicated by Figure 4.23, is then approximately 19 percent of critical damping ($c/c_c = 0.19$) to limit amplification at resonance to three times.

Alternative *a* above, indicating a natural frequency of 25 to 30 cps, represents the currently accepted standard for Naval applications. This is considered preferable to alternative *b* for practical reasons. At the present stage of the art, an isolator that embodies 19 percent of critical damping and is otherwise suitable for Naval service is a relatively elaborate device. It is costly to manufacture and requires appreciable space for installation. In this respect, it compares unfavorably with the currently used "shock mount," a simple, inexpensive device which employs rubber in compression and occupies a minimum of space. However, a highly damped isolator of lower natural frequency would offer better protection than the present "shock mount." This may be deduced from the shock transmissibility curves of Figure 3.8, which show the benefits to be derived from a damped isolator. The lower natural frequency of the isolator is also advantageous, because an isolator provides no protection to elements of equipment whose natural frequencies are less than two times the isolator natural frequency.

It is evident from Figure 6.16 that the currently used shock mount, employing rubber in compression and embodying only moderate damping, exhibits a relatively low value of maximum transmitted acceleration when the rubber thickness is $\frac{5}{8}$ inch and the natural frequency is 25 cps. A lower maximum acceleration is transmitted by an isolator having greater rubber thickness, but the percentage deflection of the rubber is not so great and the space, therefore, is not utilized so efficiently. If the rubber thickness is less than $\frac{5}{8}$ inch and the natural frequency is 25 cps, a large acceleration is transmitted because the rubber is deflected excessively. The overall dimensions of an isolator required to accommodate a rubber thickness of $\frac{5}{8}$ inch are usually acceptable where the supported equipment occupies a large space, because the space occupied by the isolators is a relatively small part of the total. Isolators of the same size are frowned upon for smaller equipment, however, because they occupy a space that is a much larger part of the total. If the isolators are required to be of small overall size, the rubber thickness is necessarily small. This practice is followed to a large extent in current installations, and smaller equipment receives less protection from shock isolators.

It is important to note that the requirements as formulated in alternative *a* above call for (1) a natural frequency of approximately 25 cps to attain favorable shock transmissibility and (2) a minimum natural frequency in any natural mode of vibration of 25 cps to avoid a resonant condition with the forced vibration on the vessel. The first-mentioned requirement can be readily interpreted as a maximum natural frequency of approximately 25 cps, because it is desirable to maintain the transmitted acceleration at a minimum. This is not strictly true, because a shock motion is predominantly translatory in nature, and no disadvantages would result from higher natural frequencies in rotational modes. It is thus more correct to state that all natural frequencies in translatory modes should be 25 cps, and that no natural frequency should be lower than 25 cps.

The most satisfactory arrangement for obtaining optimum conditions is one that decouples all natural modes of vibration. This is accomplished if a plane that passes through the isolators also passes through the center of gravity of the equipment.* Figure 6.17 shows a preferred type of installation, in which the isolators are disposed along two diagonally opposite edges which lie in an oblique plane passing through the center of gravity of the equipment. Similar results may be obtained by attaching the isolators to opposite parallel faces of the equipment. It is not always possible or desirable, however, to provide suitable supports in the vessel for these types of application. A satisfactory alternative for equipment whose height is great relative to its minimum width employs load-carrying isolators

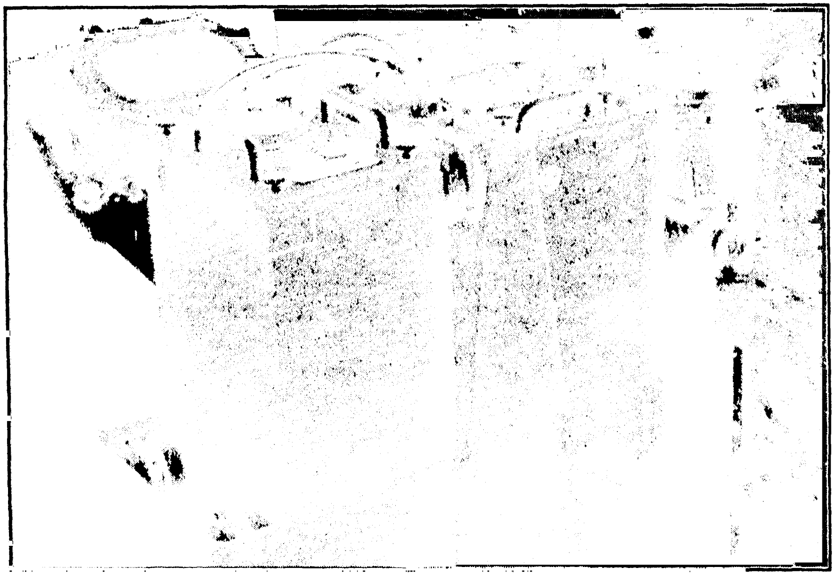

FIGURE 6.17. Naval shipboard application with shock isolators located in oblique plane which passes through center of gravity of equipment. (Official United States Navy photograph.)

---

* See Section 2·10 of Chapter 2 for a detailed discussion of this condition.

at the base of the equipment, and stabilizing isolators near the top. Installation troubles occasionally arise with this arrangement because a sufficiently rigid structure for attachment of the stabilizing isolators is difficult to obtain. The detrimental results obtained in some instances from employing flexible structures for this purpose has created prejudice against stabilizing isolators.

The most common, and sometimes the most satisfactory, arrangement for mounting shipboard equipment employs isolators at each of

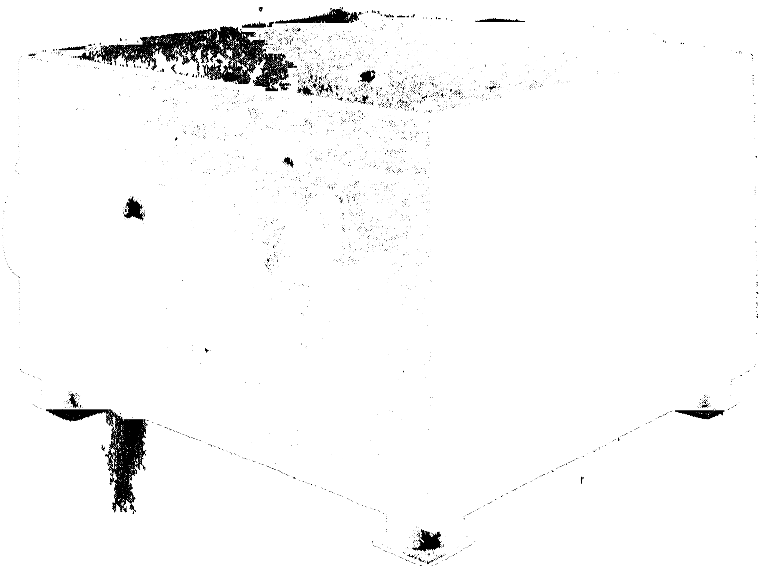

FIGURE 6.18. Naval shipboard application with shock isolators located at lower corners of equipment. (Official United States Navy photograph.)

the four lower corners of the equipment. A typical equipment with this mounting arrangement is shown in Figure 6.18. There are many obvious advantages in using isolators only at the four lower corners. The determining factor is the height of the equipment relative to its horizontal dimensions. It is readily apparent from Figure 2.11 that, when the ratio of height to width is greater than unity, one of the coupled natural frequencies is 75 percent or less of the vertical natural frequency. As a consequence, all natural frequencies can be maintained above 25 cps only by raising the decoupled vertical natural frequency to 33 cps or higher. The effectiveness of the isolators in isolating shock is thus reduced, and the reduction becomes more pronounced as the height of the equipment increases. The usefulness of such an arrangement depends to a large extent on the sacrifice in shock protection that is acceptable. As a general rule, equipment whose height exceeds the minimum horizontal distance between isolators cannot be adequately mounted upon bottom isolators alone.

6·13 *Military Equipment—Portable*

The term portable equipment is applied to a large class of equipment intended for use in the field. Such equipment is transported to its ultimate site by aircraft, land vehicle, or Naval vessel; or by various combinations of these conveyances. It is thus subjected to all the conditions of vibration and shock to which equipment normally installed in these conveyances is subjected, and to many others in addition. It may be transported, carried, and set up by men working under combat conditions; it may be dropped from a truck or a vessel upon a very hard surface or into the water; or it may be dropped from aircraft by parachute. Equipment not strictly of a portable nature by the above definition but destined to be permanently installed may be subjected to certain of these abuses en route to its destination.

Although portable equipment is subjected to many types of rough treatment, the most severe shock is generally that which occurs when it is dropped upon a more or less rigid surface. This may be expected when the equipment is dropped freely from a truck, or by parachute from an aircraft. When loosely transported in land vehicles, it may be thrown into the air each time its upward acceleration exceeds the acceleration due to gravity. It then falls freely upon the vehicle, and its downward velocity is suddenly arrested. The height to which it is thrown is usually relatively small, but the many repetitions that occur in a long trip may prove more damaging than one drop from a greater height. Portable equipment must be capable of withstanding a "drop test," which simulates the above described conditions. The height of free fall is often taken as five feet, which causes a velocity change of 216 in./sec if the downward motion of the equipment is arrested without rebound. The ability to withstand this drop is required, in addition to ability to withstand the type of vibration and shock discussed in preceding sections in connection with applications in aircraft, vehicles, and Naval vessels.

The principal difficulty encountered in designing isolators for portable equipment is that of providing protection against shock that is more severe than that encountered in Naval shipboard service, and of simultaneously withstanding the vibration experienced in aircraft. As pointed out in the preceding section, a shock isolator employing rubber in compression and having a natural frequency of approximately 25 cps affords satisfactory protection against shock as encountered in Naval service. · If this same isolator is subjected to the vibration experienced in aircraft, which includes the frequency range of 10 to 50 cps, the mounted equipment vibrates with excessive amplitude at the resonant frequency unless the isolator is highly damped. Isolators with appreciable damping have not been applied aboard ship because of limitations in space and cost; the same limitations would seem to apply to portable equipment. As a result, most current applications use substantially undamped isolators whose natural frequency is relatively high; this leaves something to be desired when the equipment is subjected to a vibration test.

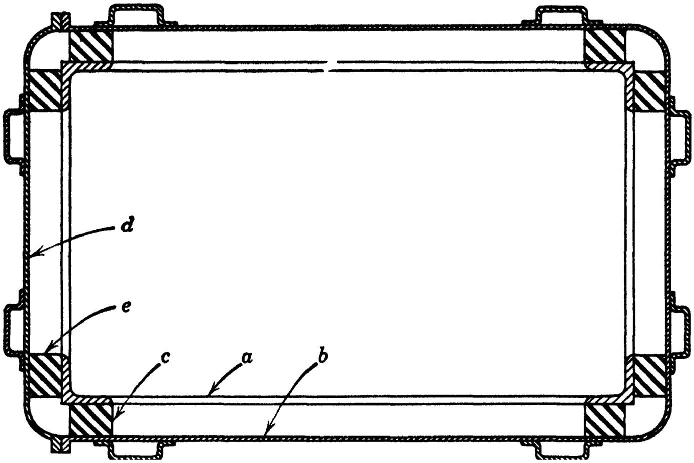

FIGURE 6.19. Schematic diagram of transit case with shock isolators interposed on six faces between equipment chassis and transit case.

The requirements that apply to equipment of this type usually call for a transit case to afford protection for the equipment during shipment. Such a case is designed to be rugged and watertight, with the minimum possible weight. In some instances, the transit case is an integral part of the equipment and is removed only for servicing purposes. In other instances, the transit case is for shipping purposes only and is discarded upon reaching its destination. A typical transit case is illustrated schematically in Figure 6.19. The components of the equipment are mounted upon a chassis *a*, which is supported within the transit case *b* by means of shock isolators indicated schematically at *c*. The isolators are located along each of the six faces of the case and are thus subjected to a compressive stress, regardless of the direction of the shock motion. In the design illustrated in Figure 6.19, the cover *d* carries additional isolators *e*; the chassis *a* is thus readily removable for servicing purposes upon detaching the cover *d*.

An alternate method of applying isolators to a transit case is illustrated in Figure 6.20. In this application, the shock isolators *a* are located along one face *b* of the transit case and are attached to a tray *c* to which the chassis *d* of the equipment is also attached. Isolators used for this application must be of a type that is capable of withstanding a force in any direction. This is in contrast to the design illustrated in Figure 6.19, in which the isolators are required to withstand only compressive forces. Both types of application have been used successfully and extensively. Each has its peculiar advantages and disadvantages, which may be compared as follows:

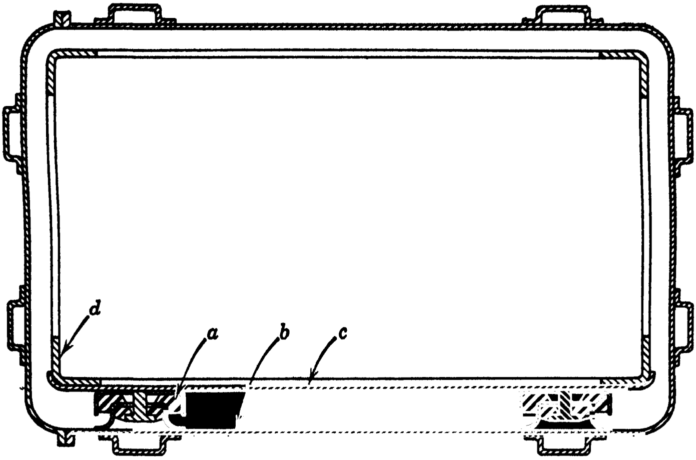

FIGURE 6.20. Schematic diagram of transit case with shock isolators interposed on a single face between equipment chassis and transit case.

(*a*) The isolator arrangement illustrated in Figure 6.19 may be expected to afford better protection against shock because the available space is more effectively employed. The importance of selecting rubber of substantial thickness was pointed out in connection with Figure 6.16. All the space between the equipment chassis and the transit case in Figure 6.19 is utilized to attain rubber of maximum thickness, whereas only a portion of the space at the bottom of the design shown in Figure 6.20 is utilized in this manner. The remainder makes the isolator effective for motion in the opposite direction.

(*b*) The design illustrated in Figure 6.20 is better adapted to rapid removal of the equipment, because the equipment may be attached to the tray by a conveniently operable means. An equivalent result can be attained in the type of construction shown in Figure 6.19 only by maintaining extraordinarily close tolerances in the construction so that the isolators form a guide for the equipment, or by constructing a separate inner framework for connecting the isolators to the equipment. Finally, removal of the transit case cover in Figure 6.20 does not affect the means by which the equipment is secured.

(*c*) The forces on the equipment and the transit case are more evenly distributed in the design shown in Figure 6.19. The isolators shown schematically at *c* are sometimes in the form of long rails whose cross section is shown in Figure 3.18 of Chapter 3. The forces are thus distributed over a large area and on several faces, as contrasted with the localized forces on one face which result from the arrangement shown in Figure 6.20.

(*d*) The arrangement shown in Figure 6.20 usually is less costly because a single set of isolators is arranged to withstand forces in any of six directions, whereas separate isolators are employed for each direction in the design illustrated in Figure 6.19. The difference is more marked if an inner framework is constructed in the latter instance to facilitate removal and replacement of the equipment.

The problem of selecting the size and stiffness for the isolators poses a difficult question. Probably the drop test requirements are the most severe, and equipment that withstands the drop test will also withstand other specified shock tests. Methods for analyzing this problem are set forth in detail in Chapter 3. The methods call for determining the velocity at completion of a free fall, based on the height of drop. The kinetic energy immediately before contact with the ground is equated to the potential energy stored in the isolator to obtain maximum deflection of the isolator. Maximum acceleration experienced by the equipment is determined from the maximum deflection of the isolator. An example that illustrates the application of this analysis to a transit case having non-linear isolators is given in Example 4.1, page 166.

The calculation given in Example 4.1 assumes that both the equipment chassis and transit case are infinitely rigid. The results calculated in this manner are modified by deflection of both the chassis and the case, in response to the forces exerted by the isolators. This flexibility of chassis and case tends to decrease the effective stiffness of the isolators, as illustrated by Figure 4.35. The net result is to increase the relative motion which occurs between the components of the equipment and the point of impact, and thereby to reduce the maximum acceleration imparted to these components. The complexity of the structures involved makes this effect difficult to evaluate, but some exploratory tests by the Army Signal Corps indicate that the energy stored in elastic deflection of structural members may equal the energy stored in the shock isolators. Conservatively, it would appear that satisfactory results would be obtained by reducing the height of drop, for calculation purposes, by one-third of the actual height.

BIBLIOGRAPHY

BALDWIN, M. F., "Reducing Effects of Vibration With Isolating Material," *Inland Printer*, Vol. 88, Nos. 2–3, November–December 1931.

CAIN, B. S., *Vibration of Rail and Road Vehicles*, Pitman Publ. Corp., New York, 1940.

CREDE, C. E. and J. P. WALSH, "Design of Vibration Isolating Bases for Machinery," *Trans. A.S.M.E.* (*Jour. App. Mech.*, Vol. 14, No. 1), March 1947.

HAMMOND, R., "Springs Control Forging Hammer Vibration," *Am. Mach.*, Vol. 93, No. 11, June 2, 1949.

LARKIN, K. H., "Design of Diesel-Engine Foundations," *Trans. A.S.M.E.*, Vol. 64, No. 4, May 1942.

MULLER, L. E., "Vibration Control of Engines," *Prod. Eng.*, Vol. 20, No. 4, April 1949.

ROSENZWEIG, S., "Theory of Elastic Engine Supports," *Trans. A.S.M.E.*, Vol. 61, No. 1, January 1939.

WILSON, T. E., JR., "Isolating Diesel Engines Against Vibration," *Diesel Power*, Vol. 9, No. 11, November 1931.

Index

Acceleration, maximum transmitted,
  - Naval applications, 315
  - rubber in compression, 166
  - tangent isolator, 161
  - undamped linear isolator, 101
  - viscously damped linear isolator, 189

Acceleration in harmonic motion, 12
Acoustical impedance, 206, 210
Acoustical materials, properties of, 206
Aging of rubber, 218
Air damper, 191
Aircraft applications, 304
Amplification factor, 97, 109
Amplitude of harmonic motion, 7
Angle, phase, 179, 183
Angular momentum, 138
Axis, elastic, 75, 84
  - imaginary, 10
  - real, 10

Axis of rotation, 49, 53

Beams, 124
Bearings, vibration of, 292
Blowers, vibration of, 294
Bonded compression pad, 225
Bonding of rubber, 220, 242
Buckling isolator, 120
Buna N, 217, 218
Buna S, 217
Bushing, rubber, 229

Cams, vibration of, 292
Center of gravity, determination of, 16
Chemigum, 217
Compensating spring, 195
Complex notation, 10, 177
Complex plane, 10
Compression pad, 222, 237
Concrete foundation, 127, 132
  - floating, 265, 276, 297

Conical spring, 250
Connecting rod, 270
Conservative momentum, 135
Constant natural frequency, 157
  - springs of, 251

Cork, 255
Coupled modes of vibration, 41
Coupled natural frequencies, 54, 80
Crank motion, 270
Crankshaft, 272
Critical damping, 171

Damped natural frequency, 173
Damper design, 190
Damping, critical, 171
  - effect of change in, 186
  - importance of, in isolators, 238
  - internal, 100, 193
  - viscous, 170, 176

Damping ratio, 173
Dashpot, 190
Decoupled modes of vibration, 42, 83
Decoupled natural frequencies, 84, 264
Decrement, logarithmic, 175, 239
Deflection, maximum, resulting from velocity shock, linear isolator, 102, 104
    - rubber in compression, 166
    - tangent isolator, 162
  - static, 38, 197

Density of acoustical material, 206
Design of dampers, 190
Design of isolators, 241
Displacement in harmonic motion, 12
Drift, 218
  - cork, 258
  - rubber, 234

Drop forging machine, 133, 298
Durometer, 220
Dynamic modulus, 158, 221

Elastic axis, 75, 84
Elastic properties of inclined isolators, 74
Electric motors, isolators for, 289
  - types of application, 290

Electronic equipment, aircraft, 309
Ellipse of stiffness, 26
Ellipsoid, momental, 15
Energy, 105, 159, 163
  - acoustical, 211
  - kinetic, 105, 159, 163
  - potential, 105, 159, 163

Equipment, lack of stiffness in, 201
Equivalent viscous damping ratio, 194

Fans, vibration of, 294
Felt, 252
Floating concrete foundation, 265, 276, 297
Force, gravitational, 101
Force-deflection curve, buckling isolator, 120
  linear isolator, 155
  non-linear isolator, 155
  preloaded isolator, 115
  rubber, compression, 167
    shear, 228
    unbonded square rubber pad, 224
Forging hammer, 133, 298
Free vibration with viscous damping, 170, 173
Frequency, 12
  impulse, 131
  natural, 33
Friction damper, 192

Gas turbine, aircraft, 305
Gears, vibration of, 292
Gravitational force, 101
Grinder, surface, 298

Hammer, forging, 133, 298
Harmonic motion, 7, 12
Helical spring, 243
High-temperature operation, 217
Hycar, 217
Hysteresis, internal, 193

Imaginary axis, 10
Impact of a moving body, 93
Impedance, acoustical, 206, 210
Impulse frequency, 131
Impulse of a force, 123
Inclined isolators, 73
Industrial equipment, 291
Inertia, moment of, calculation, 17
    definition, 12
    experimental determination, 16
    estimated, 21
    of representative bodies, 22
  principal axes of, 12
  principal plane of, 15
Inertia forces, 105
Initial tension in helical springs, 251
Instrument panel, aircraft, 308
Internal combustion engine, 4, 268, 275
Internal hysteresis, 193
Isolation, definition, 2, 37
  shock, 88, 158, 162
  sound, 203
  vibration, 32
Isolator, application of, 58
  buckling, 120
  ellipse of stiffness, 26
  inclined, 73
  natural frequency of, 95
  non-linear, *see* Non-linear isolator
  preloaded, 115
  principal elastic axes, 23
  sound, 204, 214
  tangent, 159

Kinetic energy, 105, 159, 163

Lack of stiffness in equipment, 201
Load, maximum for rubber, 234
  non-uniform distribution, 197
  superimposed, 195
Logarithmic decrement, 175, 239
Loom, application of isolators, 288
  description, 284
  shuttle motion, 140
Low-speed machinery, 262
Low-temperature operation, 217, 240

Machine tools, 298
Magnetically actuated devices, 293
Maximum permissible load, 234
Military equipment, 302
  aircraft, 304
  Naval vessels, 314
  portable, 320
  tanks, 311
  vehicles, 310
Minimum natural frequencies, 235
Modes of vibration, 41
  coupled, 42
  decoupled, 42
  uncoupled, 78
Modulus of rubber, shear, 221
  dynamic, 221
Moment of inertia, calculation of, 17
  definition, 12
  experimental determination of, 16
  of representative bodies, 22

Momental ellipsoid, 15
Momentum, angular, 138
  conservative, 135
  transfer of, 123, 125
Motor, electric, 289
Multi-degree-of-freedom system, 41, 43, 50
  one plane of symmetry, 68
  two planes of symmetry, 53

Natural frequency, beams, 124
  cork, 257
  coupled, 54, 80
  damped, 173
  decoupled, 84, 264
  higher order, 100
  minimum, with rubber, 235
  multi-degree-of-freedom, one plane of symmetry, 68
    two planes of symmetry, 53
  rotational, 56
  single-degree-of-freedom, 33
  snubber, 113
  uncoupled, 78
Naval vessels, 314
Neoprene, 217, 218
Non-linear isolator, 151
  constant natural frequency, 157
  natural frequency, 154, 157
  resonant frequency, 154
  shock transmissibility, 158, 162
  vibration transmissibility, 152
Non-symmetrical weight distribution, 195
  center of gravity determination, 16
  isolator loading, 197

Oil resistance of rubber, 217

Perbunan, 217
Period, 7
Phase angle, 179, 183
Phase relation, 7
Portable equipment, 320
Positioning means, 143
Potential energy, 105, 159, 163
  rubber in compression, 169
  tangent isolator, 159
Preloaded isolator, 115
Press, printing, 295
Press, punch, 136, 277
Principal axes of inertia, 12
Principal elastic axis, 23
Principal plane of inertia, 43
Printing press, 295
  concrete foundation for, 297
Pumps, vibration of, 294
Punch press, 136, 277

Radius of gyration, definition, 14
  of representative bodies, 22
Railroad train, 105, 299
Real axis, 10
Reciprocating machine, 267
  application of isolators, 273
Resonant frequency, 154
Rigid body, dynamics of, 28
  equations of motion for, 30
  rotation of, 29, 42
  translation of, 28, 42
Road vehicle, 299
Rotation, axis of, 49, 53
  of rigid body, 29, 42
Rotational stiffness, 77
Rubber, aging, 218
  bonding, 220, 242
  bushing, 229
  compression pad, 222
    bonded, 225
    unbonded, 224, 237
  damping, 194, 238
  oil resistance, 217
  shear sandwich, 227
  silicone, 218
  sponge, 259
  stiffness, 220

Shear sandwich, 227
Shock, definition of, 5
  velocity, *see* Velocity shock
Shock isolation, 88
  non-linear isolators, analytical treatment, 158
    numerical treatment, 162
Shock transmissibility, 96, 97
Shore durometer, 220
Shuttle, 140, 284
Silicone rubber, 218
Single-degree-of-freedom system, 32, 37, 41

Sinusoidal motion, 5
Snubber natural frequency, 113
Snubbing, 112
Sound, energy, 211
  isolation, 203
  isolator, 204, 214
  velocity, 205
  wavelength, 205
Spectrum, vibration, 209
Sponge rubber, 259
Spring, compensating, 195
  constant natural frequency, 251
  metal, 242
    conical, 250
    constant frequency, 251
    helical, compression, 243
        stability, 247
        stiffness, 243
      tension, 249
Static deflection, 38
  of isolators supporting a rigid body, 197
Steady-state vibration, 4
Stiffness, dynamic, 158, 221
  ellipse of, 26
  lack of, in equipment, 201
  low temperature, 240
  rotational, 77
Stiffness ratio, 233
Superimposed load, 195
Surface grinder, 298

Tangent isolator, 159
  maximum deflection, 162
  maximum transmitted acceleration, 161
Temperature, effect of, 217, 240
Thiokol, 217
Time constant, 176
Train, railroad, 105, 299
Transformer, vibration of, 293
Transient vibration, 1, 33
Translation of rigid body, 28, 42
Transmissibility, shock, 96, 97
  vibration, displacement, 37
    force, 35
    linear system, 36
    non-linear system, 152
    undamped system, 36
Turbo-jet aircraft, 305
Turbo-prop aircraft, 305

Unbonded compression pad, 224, 237
Uncoupled modes of vibration, 78
Uncoupled natural frequencies, 78
Uniform mass distribution, 61

Vacuum tube, 2
Vector addition, 9
Vector notation, 5
Vehicle, military, 310
  track-laying, 311
  wheeled, 299, 310
Velocity, harmonic motion, 12
  sound, 205
Velocity shock, 89
  maximum transmitted acceleration, undamped isolator, 101
    viscously damped isolator, 189
  viscously damped isolator, 186
Vibration, definition, 1
  modes of, 41
  steady-state, 4
  transient, 1, 33
Vibration in aircraft, 304
Vibration spectrum at machine foundation, 209
Viscous damping, forced vibration, 176
  free vibration, 170
  velocity shock, 186
Viscous damping ratio, 171, 173
  equivalent, 194

Wavelength of sound, 205